BUCKLING OF LAMINATED COMPOSITE PLATES

By

SUDHAKAR SHARMA

DEPARTMENT OF AERONAUTICAL ENGINEERING

INDIAN INSTITUTE OF TECHNOLOGY KANPUR

JULY, 1979

BUCKLING OF LAMINATED COMPOSITE PLATES

A Thesis Submitted
In Partial Fulfilment of the Requirements
for the Degree of

DOCTOR OF PHILOSOPHY

By

SUDHAKAR SHARMA

to the

DEPARTMENT OF AERONAUTICAL ENGINEERING

INDIAN INSTITUTE OF TECHNOLOGY KANPUR

JULY, 1979

CERTIFICATE

This is to certify that the work BUCKLING OF LAMINATED COMPOSITE PLATES has been carried out under our supervision and has not been submitted elsewhere for a degree

N.G.R. Iyengar

(N.G.R. IYENGAR)
Professor
Department of Aero. Engg.
I.I.T. Kanpur

P. N. Murthy

(P.N. MURTHY)
Professor
Department of Aero. Engg.
I.I.T. Kanpur

ACKNOWLEDGEMENTS

It is with great pleasure that I acknowledge my deep indebtedness to Prof. P.N. Murthy and Prof. N.G.R. Iyengar for their invaluable guidance, critical supervision and constant encouragement throughout the course of this work.

I sincerely thank Dr. P.S. Kushwaha and Mr. M.K. Patra for several fruitful discussions. Thanks are also due to many of my friends for their help in the development and running of computer programmes in the initial stages.

To my wife, Asha, I am indebted for her patience and willingness to make sacrifices so that this work could be completed.

I am grateful to Mr. M.K. Patra for his help during the manuscript stage and to Mr. R.N. Srivastava for his fine typing.

TABLE OF CONTENTS

LIST OF TABLES

LIST OF FIGURES

SYMBOLS AND NOTATIONS

a, b	:	Dimensions of the plate
A_{ij}, B_{ij}, D_{ij}	:	Elastic constants of the laminated composite plate
E_1, E_2, G_{12} and ν_{12}	:	Elastic constants of an orthotropic lamina
g	:	Pasternak foundation stiffness
k	:	Winkler foundation stiffness
G	:	gb^2/D_{11} is the non-dimensional Pasternak shear stiffness
K	:	kb^4/D_{11} is the non-dimensional Winkler foundation stiffness
m	:	Number of buckles in the x-direction
M	:	$\frac{\sum_{\text{odd}} t_k}{\sum_{\text{even}} t_k}$ is the cross-ply ratio
N	:	Number of layers
M_x, M_y, M_{xy}	:	Bending and twisting moments
N_x, N_y, N_{xy}	:	In-plane normal and shear forces
$N_{x_{cr}}$	:	Buckling load per unit width
$\tilde{Q}_{ij}(\theta)$	:	Reduced stiffnesses evaluated at fibre orientation angle, θ
q	:	Lateral loading
R	:	a/b is the plate aspect ratio
R_1	:	t_1/t_2 is the thickness ratio of a four-layered antisymmetric laminate

R_1	:	t_1/t_3 is the thickness ratio of a six-layered antisymmetric laminate
R_2	:	t_2/t_3 is the thickness ratio of a six-layered antisymmetric laminate
t	:	Overall thickness of the laminate
u, v	:	In-plane displacements
u^o, v^o	:	Mid-plane values of in-plane displacements
w	:	Lateral displacement
$(\varepsilon_x^o, \varepsilon_y^o, \varepsilon_{xy}^o)$	:	Mid-plane strain components in the xy plane
$(\varepsilon_x, \varepsilon_y, \varepsilon_{xy})$	:	Strain components in the xy plane
(K_x, K_y, K_{xy})	:	Curvatures in the xy plane defined by Eq. (3.1b)
θ	:	Fibre orientation angle
ϕ	:	Displacement function
λ	:	Roots of Eq. (3.52)
γ	:	Roots of Eq. (3.53)
α	:	Numerical factor in Eq. (7.1)
α_m	:	$m\pi/a$
β	;	$m\pi/R$

SYNOPSIS

SUDHAKAR SHARMA
Ph. D. Thesis
Department of Aeronautical Engineering
Indian Institute of Technology, Kanpur

BUCKLING OF LAMINATED COMPOSITE PLATES

The composite materials by virtue of their high strength-to-weight and stiffness-to-weight ratios are ideal as structural elements in aerospace applications. During the last decade much effort has been directed towards developing and characterising these materials. Until very recently these efforts have been concentrated on the characterization of the basic materials and the development of information on their behaviour. The basic difference between isotropic materials and fibre reinforced composites is the variety of couplings, for example, between in-plane loading and out-of-plane deflection or between applied bending load and twisting response that the latter exhibit. It is well-known that this coupling phenomenon due to lamination asymmetry can result in substantial reduction of effective stiffness of the plate. Consequently some investigators have tried to eliminate the degrading effect of coupling by suggesting various techniques.

Warren and Norris have shown that it is possible to orient the layers of multiple-layer laminates in such a way

that the resulting elastic stretching behaviour is isotropic. This, however, does not remove, in general, bending and stretching-bending coupling. Abrams and Scheying presented numerous configurations for which the elastic behaviour of the laminate is identical to that of a homogeneous orthotropic or isotropic material. Bartholomew has shown that selection of a suitable ply stacking order enables bending, as well as in-plane orthotropy. A review of relevant literature reveals that almost no study has been made if thickness distribution of the laminae constituting a laminate of a given thickness can achieve special orthotropy. This thesis is partly an attempt in this direction.

Use of laminated plates as an important structural element in both the aerospace and electronics industries has intensified the demand for the development of analytical methods for anisotropic structures. Of particular interest are anisotropic or layered composite materials in the form of thin plates subjected to in-plane compressive loads. The primary mode of failure of these plates is buckling.

Considerable amount of information is available on the buckling of orthotropic panels and on infinitely long anisotropic plates under special load conditions. However, the buckling of finite, homogeneous and layered anisotropic composite plates has been receiving serious attention since 1967. Whitney and Leissa presented a closed form solution of

the buckling of a simply supported arbitrarily laminated rectangular plate subjected to biaxial compression. Their results indicate a strong dependence of the buckling load on bending-stretching coupling. Ashton and Waddoups presented Rayleigh-Ritz solution for buckling of arbitrarily laminated rectangular plates subjected to biaxial compression and in-plane shear loads.

The response of arbitrarily laminated plates is governed by three coupled displacement equations of equilibrium. Most of the analyses dealing with such plates assume suitable functions for the three coupled displacement components. However, it is desirable to combine the three displacement equations of equilibrium into a single higher order partial differential equation in terms of a single function. This thesis is concerned with the formulation of this problem and its application to the buckling of laminated cross- and angle-ply plates under various boundary conditions.

The problem of the buckling of laminated composite plates subjected to non-uniform axial loads is another area which has not been investigated so far. Chamis used the Galerkin method to determine the buckling response of simply supported rectangular plates under uniform normal and shear loads. The present study includes the buckling response of laminated plates under non-uniform axial load employing the Galerkin technique together with formulation developed in the present thesis.

The problem of the analysis of composite plates resting on elastic foundation is yet another area wherein practically very little work has been reported. Such solutions may find important applications in analysing the face behaviour of certain types of foam-filled sandwich panels and the structural response of wing panels resting on a cushion of air during flight. Turvey has presented simple exact solutions for uniformly loaded, simply supported antisymmetrically laminated cross- and angle-ply plate strips resting on Winkler-Pasternak foundation. In a recent paper he has extended the static analysis of composite plates resting on Winkler-Pasternak foundation to finite cross- and angle-ply plates. The buckling analysis of composite plates resting on general elastic foundation has not been reported hitherto and the present thesis is partly an attempt to fill this gap.

The thesis is divided into eight Chapters. Chapter 1 is concerned with the review of pertinent literature on the characterization of laminated composites and the stability of rectangular laminated composite plates.

Chapter 2 deals with characterization of laminated composites. Relations between thickness ratios of the laminae constituting a laminate of a given thickness and reduced stiffnesses of an orthotropic lamina are developed and conditions that lead to partial or complete elimination of coupling stiffnesses (special orthotropy) are studied. It is shown that for

antisymmetric angle-ply laminates, unique numerical values of the thickness ratios exist that correspond to special orthotropy of the laminates. These values are further shown to be independent of material properties and fibre orientations. The possibility of partial or complete elimination of coupling effects for more general types of laminates is also discussed.

Chapter 3 is concerned with formulation and method of solution of the plate stability problems. A system of three coupled equations derived from energy approach and governing the behaviour of general unsymmetric laminates is reduced to a single eighth order partial differential equation in terms of a single displacement function. The displacement, force and moment resultants are also expressed in terms of the same function. A closed form solution is then found for antisymmetric cross- and angle-ply laminates.

In the fourth chapter, a specimen problem entitled "Static analysis of an antisymmetrically laminated angle-ply plate subjected to pure bending with two opposite edges simply supported and the remaining two free" is solved and the results thereof in a special case are compared with those available in literature to confirm the validity of the method proposed in Chapter 3. It is shown that the proposed method leads to a faster convergence.

In the fifth chapter, buckling response of antisymmetrically laminated cross- and angle-ply plates with two

loaded edges simply supported and various other combinations of boundary conditions on the remaining two edges is considered. The effect of number of parameters namely thickness ratio of laminae constituting a laminate of a given thickness, cross-ply ratios, number of layers and fibre orientations etc. on the buckling response of plates is discussed.

Chapter 6 is concerned with the buckling response of antisymmetrically laminated cross- and angle-ply plates with two opposite loaded edges simply supported and various other boundary conditions on the remaining edges resting on general elastic (Winkler-Pasternak) foundation. Typical results for a number of different plate lay-ups and Winkler-Pasternak values are presented in dimensionless graphical form. The effect of material coupling and foundation stiffnesses on the buckling response of plates is discussed. It is shown that material coupling and foundation stiffnesses can affect the buckling response of plates significantly.

In the seventh chapter, buckling response of simply supported antisymmetric cross- and angle-ply plates subjected to pure in-plane bending is discussed. The problem is solved using Galerkin method together with the formulation developed in Chapter 3. The results in a special case (with uniform uniaxial loads) are compared with those available in literature.

The thesis concludes with summing up of the major conclusions drawn from these studies together with suggestions for further work.

- o -

CHAPTER 1

INTRODUCTION

1.1 CHARACTERISATION OF LAMINATED PLATES AND LITERATURE SURVEY

Laminated plates constitute an important structural element in both the aerospace and electronics industries. In aerospace applications where weight savings are of paramount importance, the advent of fibre-reinforced composite materials such as carbon/epoxy and graphite/epoxy has resulted in a dynamic increase in the use of laminated fibre-reinforced plates and other structural shapes. The composite materials are typically a combination of a usually light, weak and flexible binding material, with a more dense, strong and stiff reinforcing material in fibrous or whisker form. Hence, high strength-to-weight and stiffness-to-weight ratios are readily obtained. In electronic applications, circuit boards typically have two or more different materials in laminated form.

During the last decade much effort has been directed towards developing and demonstrating the properties of filament-reinforced composite materials. Until very recently these efforts have been concentrated on the characterisation of the basic materials and the development of information on their behaviour. The basic difference between isotropic materials and fibre-reinforced composites is the variety of couplings,

for example, between inplane loading and out-of-plane deflections or between applied bending load and twisting response that the latter exhibit. Thus on application of an inplane load the laminate deflects transversely, while if the pure bending is applied the plate will undergo twisting. The couplings between inplane and out-of-plane effects may also give rise to warping of the laminate when temperature changes take place. The presence of such couplings result in appreciable reduction in stiffness of the laminate in many situations. However, if the plies are arranged symmetrically with respect to the plate middle surface, a 'balanced' laminate is achieved in which this coupling does not occur. Although balanced laminates are common in current designs, it is evident that designs will occur in general in which the laminates are not balanced. For example, exercises in the minimum weight designs of panels could well show thin plates to be desirable, and if these have a fewer number of plies the number of available options may be strictly limited and the balanced laminate may be an impracticable proposition. Situations will also exist where for an efficient structure, a variable skin thickness is desired as, for example, in a wing structure when the wing thickness is reduced towards the tip. A single ply removed from a balanced laminate, may create imbalance and introduce the couplings referred to. Consequently, coupling effects are to be eliminated as far as practicable in applications of composite laminates. Whitney and Leissa[1] observed that the

degrading effect of coupling for an antisymmetrically laminated plate can be minimised by increasing the number of layers in a laminate of a given thickness. Bartholomew[2] showed that selection of suitable ply stacking order enables the elimination of coupling and thus enables orthotropy to be achieved in bending as well as in in-plane loading conditions. This is known as special orthotropy. He assumes each ply to be identical in thickness and material properties and the fibre directions to lie symmetrically about the orthotropy axes for the laminate. Having achieved inplane orthotropy, the remaining requirements for designing a specially orthotropic laminate are obtained by controlling the ply stacking sequence. It is significant to note that thickness distribution of the laminae of a laminate of a given thickness has not been exploited to obtain extensional and bending orthotropies of a laminate and a part of the present study is devoted to fill this gap.

1.2 BUCKLING OF LAMINATED PLATES

Since the mix-sixties the use of anisotropic fibre-reinforced composites as structural members has increased considerably. This increase owes to the fact that the designer can take advantage of the anisotropic properties of the materials and thereby use this material quite efficiently. Of particular interest are anisotropic or layered composite

materials in the form of thin plates subjected to inplane compressive loads. The primary mode of failure of these plates is buckling. Considerable amount of information is available on the buckling of structural panels of isotropic materials,[3,4] the buckling of orthotropic panels[5,6,7] and on infinitely long anisotropic plates under special load conditions.[6,8]

The buckling of finite homogeneous and layered anisotropic composite plates has been receiving serious attention since 1967.[9-12] Chamis[13] used the Galerkin method to determine the buckling response of simply supported rectangular plates under uniform normal and shear loads. The plates were assumed to be orthotropic along the material axes which are oriented at an angle with the load directions. The buckling loads are determined by the power method which is applicable for the determination of dominant eigenvalues. Bending and stretching coupling effects are also discussed. The complexity of the problem is, however, increased with the application of variable load along the edges. To our knowledge, this problem has not been discussed to date and the present study is partly an attempt in this direction.

Chiu[14] employed the energy method to determine the buckling loads for unstiffened orthotropic plates with a variety of boundary conditions and for stiffened plates with supported free boundary conditions. Buckling mode shapes are represented by trigonometric series which, in general, do not satisfy all the boundary conditions. The unsatisfied boundary

conditions are handled through the use of the Lagrange multiplier method.

Massey[15] considered the elastic buckling of orthotropic rectangular plates by using the 'Reduction method' and obtained the elastic buckling coefficients for flat, rectangular, orthotropic plates with uniform inplane loads in one or two directions for various types of edge conditions.

Harris[16] presented a detailed discussion of the influence of elastically restrained inplane displacement on the buckling load of orthotropic rectangular plates subjected to end compression. His analysis was based on well-known equations for elastic buckling of simply supported orthotropic plates subjected to biaxial inplane loading and with no coupling between inplane and bending effects.

Ashton and Waddoups[17] employed the Ritz energy formulation to predict the buckling response of anisotropic rectangular plates with various boundary conditions. The displacements were expanded in terms of beam functions. In this, the moment boundary condition was not exactly satisfied for simply supported or free edges, but the results were found to be acceptable.

Ashton[18] identified the analogy between skewed isotropic and anisotropic plates. This allows direct adaption of solutions for skewed isotropic plates to rectangular anisotropic plates for which D_{16} and D_{26} are not zero.

Wang[19] observed that a separation of variable technique cannot be employed to obtain an exact solution for simply supported anisotropic plates. The exact satisfaction of the moment boundary condition precludes the use of separation of variables, if the Love-Kirchoff hypothesis is accepted.

Holston[20] developed an approximate equation for the buckling load of orthotropic plates with three edges simply supported and the remaining edge free.

Kicher and Mandell[21] have attempted to outline the differences between the buckling behaviour of laminated composite plates and isotropic plates. They derived the governing differential equations utilizing the variational approach and including the effect of coupling between extensional and bending stiffnesses. They have shown that a reduced flexural stiffness method can be used to account for coupling in some types of laminates. However, Reissner and Stavsky[22] were the first to identify the full complexity associated with the analysis of unbalanced angle-ply laminates. They analyzed the response of a two-layered, angle-ply composite plate in terms of a stress function and out of plane displacement.

Whitney and Leissa[23] analyzed the antisymmetrically laminated angle-ply and cross-ply plates in terms of a stress function and out of plane displacement, w. They extended the work of Reissner and Stavsky[22] by presenting solutions for the transverse vibration and buckling analysis of angle-ply

composite plates. The exact solutions for the buckling load of an angle-ply laminate with all edges simply supported and including the effect of coupling were obtained. However, the results for the buckling of cross-ply composites were not presented.

Whitney[24] and Whitney and Leissa[1] formulated the analysis of cross-plied and angle-plied composite plates in terms of three equilibrium equations in terms of displacement variables u, v and w. The stability analysis[1] of simply supported angle-ply plates is cast in terms of the displacements associated with buckling and the loads prior to buckling. The buckling analysis of simply supported cross-ply plate is again omitted.

Turvey[25] determined the buckling response of moderately thick laminated plates simply supported on all sides. He used the concept of reduced plate stiffness along with shear correction factor to obtain an approximate solution for biaxial buckling of simply supported laminated square plates. Design data is generated in the form of buckling load versus thickness ratio curves for angle-ply plates fabricated from a high modulus lamina.

Jones[26] considered the buckling and vibration of unsymmetrically laminated cross-ply rectangular plates simply supported on all sides. The classical laminated plate theory including the Kirchoff hypothesis of non-deformable normals is used for simply supported rectangular plates.

Chamis[27] presented the theoretical results for the buckling of anisotropic plates subjected to simple and combined inplane loading. The plates are made from fibre composite material of boron/aluminium or high modulus graphite/resin. The results are presented in non-dimensional form as buckling load versus fibre orientation angle for various plate aspect ratios. An excellent review of the work done on the mechanics of composite materials has been reported by Bert[28].

A survey of foregoing literature on the buckling aspect of composite materials indicates that practically very little work has been done to study the effect of the following on the buckling response of antisymmetrically laminated angle-ply and cross-ply plates: (i) boundary conditions other than simply supported (ii) thickness ratio of the laminae of a laminate of a given thickness and (iii) cross-ply ratios. The purpose of this thesis is partly to fill this gap by attempting an efficient formulation to yield closed form solutions to predict the buckling response of certain types of laminated composites for various boundary conditions and investigating the effect of the various couplings and thickness ratios of laminae and of cross-ply ratios on the buckling load of laminated composites. These results have been put in the form of design charts.

1.3 BUCKLING OF LAMINATED PLATES UNDER LATERAL LOADS

It is worthwhile studying the effect of transverse load on the buckling of the laminated plates. In effect it is like an elastic foundation on which these plates are resting. The problem of isotropic beams and plates resting on elastic foundations have received extensive treatment in literature.[29-43] However, it appears that only a few solutions[44-45] have been published for the case of anisotropic composite plates on elastic foundation. In this thesis, the Winkler-Pasternak foundation has been chosen for investigating the effect of lateral loads on buckling of laminates.

Turvey[44] obtained a simple exact solution for the static response of a simply supported, antisymmetrically laminated cross- and angle-ply strips resting on Winkler-Pasternak foundation and subjected to a uniform lateral load. The same author in another paper[45] analyzed a uniformly loaded, simply supported antisymmetrically laminated cross- and angle-ply rectangular plate resting on a general (Winkler-Pasternak) elastic foundation. The importance of the material coupling and foundation stiffness on the plate response has been discussed.

A survey of above literature reveals that a study of the influence of Winkler-Pasternak stiffnesses on the buckling response of antisymmetrically laminated cross- and angle-ply composite plates has not been reported so far.

1.4 SCOPE OF THE THESIS

The thesis has eight chapters. In the second chapter, the characterization of the angle-ply laminates with special reference to antisymmetric laminates is considered. It is observed that a suitable choice of a thickness ratio of the laminae of a laminate can lead to special orthotropy with a consequent increase in the overall stiffness of the laminate.

Chapter 3 is concerned with the formulation and method of analysis for the static and buckling response of angle-ply and cross-ply plates. A system of three governing equations derived from energy approach is reduced to an eighth order partial differential equation in terms of a displacement function. The displacements and stress resultants are also expressed in terms of a single displacement function.

In the fourth chapter, a specimen problem entitled "static analysis of an antisymmetrically laminated angle-ply plate subjected to pure bending with two opposite edges simply supported and the other two free" is solved and the results thereof in a limiting case are compared with those available in literature to confirm the validity of the method proposed in Chapter 3. It is shown that the proposed method leads to a faster convergence.

In the fifth chapter, buckling response of antisymmetrically laminated angle-ply and cross-ply plates with two loaded edges simply supported and various boundary conditions on the remaining two edges is discussed in detail.

The analysis of Chapter 5 is extended in Chapter 6 to study the influence of Winkler-Pasternak stiffnesses on the buckling response of composite plates with various boundary conditions. Some of the results presented herein appear to be new and reveal several interesting features.

Chapter 7 is concerned with the buckling response of simply supported antisymmetrically laminated angle-ply plates subjected to pure bending at the two opposite edges. The problem is solved using Galerkin method and the limiting results (with uniform uniaxial loads) are compared with those available in literature.

The thesis concludes with summing up of the major conclusions drawn from these studies together with suggestions for further work.

- o -

CHAPTER 2

CHARACTERISATION OF THE LAMINATED COMPOSITES

2.1 INTRODUCTION

In recent years the use of anisotropic laminated composites as structural members has increased considerably. This is due to the fact that these can be used very efficiently by taking advantage of their anisotropic properties and light weight coupled with high strength. A considerable amount of research work, therefore, is under progress regarding the elastic behaviour of laminated composites. Until very recently these efforts have been concentrated on the characterisation of the basic material properties and the documentation of information on their behaviour in practical applications.

The laminated plates consist of a number of layers of thin orthotropic sheets with the orthotropic axes of symmetry of each lamina oriented at an arbitrary angle to the plate axes. Two of the important types of arrangements are (i) antisymmetrical cross-ply and (ii) antisymmetrical angle-ply laminates. Antisymmetrical cross-ply laminates consist of an even number of layers of equal thickness and same elastic properties with the orthotropic axes of symmetry in each layer alternately oriented at angles of 0° and 90° to the plate axes. Antisymmetrical angle-ply laminates also consist of an even number of

layers having the same thickness and elastic properties but the orthotropic axes in each ply (layer) are alternately oriented at angles at + θ and - θ to the plate axes. It is well-known that antisymmetrical cross-ply and angle-ply laminates exhibit a variety of couplings, for example, between inplane loading and out-of-plane deflection or between applied bending load and twisting response. The presence of such couplings in addition to complicating the analysis of laminated plates, result in an appreciable reduction in overall stiffness of the plate for certain types of laminates. Consequently, it is desirable that coupling effects are eliminated as far as possible in the application of composite laminates.

A laminated plate so designed that the coupling between inplane and bending effects does not occur and which is orthotropic both inplane and in bending is generally referred to as 'specially orthotropic'. The analysis required for such plates is more straightforward than for more general laminated plates.

A few methods have been suggested by various investigators to do away with the degrading effects of couplings. In this chapter, the various methods for eliminating the adverse effects of couplings associated with the general laminated plates are reviewed and a technique is suggested to arrive at the decoupling effect. It is further shown that in the case of angle-ply laminates for a stacking sequence of $(45^\circ \pm \theta)$,

the thickness distribution of laminae at which the decoupling effect is achieved, is independent of material properties.

2.2 REVIEW OF LITERATURE

The effect of coupling between inplane stretching (or membrane action) and plate bending as discussed above was recognized as early as 1953 by Ambartsumyan[46] who was concerned with the study of unsymmetrically laminated orthotropic shells. At about the same time, Reissner[47] also realized the presence of coupling in laminated plates. This coupling effect is the major difference between the macroscopic structural behaviour of an arbitrarily laminated plate (either isotropic, specially orthotropic or anisotropic) and homogeneous plates (either isotropic, specially orthotropic or anisotropic) such as treated in books by Timoshenko and Woinowsky-Krieger[48] and Lekhnitskii[6].

Werren and Norris[49] have shown that it is possible to orient the layers of multiple-layer laminates in such a way that the resulting elastic stretching behaviour is isotropic i.e., it has elastic coefficients which are independent of layer orientations in the plane. According to them, the conditions which must be met by the laminating sequence to achieve this result are (i) the total number of layers must be three or more, (ii) the individual layers (denoted by index k, ranging from one to n) must have identical orthotropic elastic

coefficients and thicknesses and (iii) a typical layer k, must be oriented at an angle $\theta_k = \pi (k - 1)/n$ with respect to a reference direction. However, the laminate made according to the Werren-Norris[49] design is isotropic in regard to stretching and not, in general, in regard to bending and stretching-bending coupling.

Abrams and Scheyhing[50] presented numerous configurations for which the elastic behaviour of the laminate is identical to that of a homogeneous orthotropic or isotropic material. Herein, the constitutive equation of a thin multilayer plate or shell element is derived and compared with its counterparts for homogeneous media in order to determine the mathematical relations which will ensure composite orthotropic and isotropic elastic behaviour. Laminate configurations satisfying these relations are then found by approximate and exact means.

Bartholomew[2] has shown that selection of a suitable ply stacking order for uncoupled, orthotropic laminates enables orthotropy in bending, as well as in-plane, to be achieved. This paper assumes some degree of standardisation of design parameters. Each ply is taken to be identical in thickness and material properties, and the fibre directions lie symmetrically about the orthotropic axes for the laminate. Having achieved in-plane orthotropy, the remaining requirements for designing a specially orthotropic laminate are achieved by controlling ply stacking sequence.

From the above it can be seen that not all the parameters have been considered to achieve uncoupled orthotropic laminates. An attempt is, therefore, made in this thesis to exploit the thickness variation of laminae constituting a laminate of a given overall thickness to achieve complete elimination of coupling effects (special orthotropy) for anti-symmetrically laminated angle-ply plates. An analysis leading to partial reduction of coupling effects for more general types of laminates is also made. It has been further shown that for a stacking sequence given by $(45^\circ \pm \theta)$, the thickness ratios of the laminae at which the complete elimination of coupling terms occurs are independent of the material properties.

2.3 ANALYSIS

Consider a laminate with N layers (Figure 2.1). Each ply of the laminate, made of fibre reinforced material, is assumed to be orthotropic with uniform material properties E_1, E_2, G_{12} and ν_{12}, where 1 and 2 refer to the axes along and perpendicular to the fibre. Following the usual notation as in reference 2, the matrix of elastic stiffness coefficients for such a ply is given by

$$Q = \begin{bmatrix} Q_{11} & Q_{12} & 0 \\ Q_{12} & Q_{22} & 0 \\ 0 & 0 & Q_{66} \end{bmatrix} \qquad (2.1)$$

where

$$Q_{11} = \frac{E_1}{(1 - \nu_{12}\nu_{21})}$$

$$Q_{12} = \frac{\nu_{12}E_2}{(1 - \nu_{12}\nu_{21})} = \frac{\nu_{21}E_1}{(1 - \nu_{12}\nu_{21})}$$

$$Q_{22} = \frac{E_2}{(1 - \nu_{12}\nu_{21})}$$

$$Q_{66} = G_{12}$$

The Poisson's ratio ν_{21} can be obtained from the reciprocal relation

$$\frac{\nu_{12}}{E_1} = \frac{\nu_{21}}{E_2} \tag{2.2}$$

The matrix of elastic stiffness coefficients (2.1) is referred to the orthotropic axes. However, if the fibres of such a ply are taken to lie at an angle θ relative to the x-axis of the reference plane (Figure 2.1), then the transformed ply stiffness matrix $\bar{Q}$ is given by

$$\bar{Q} = \begin{bmatrix} \bar{Q}_{11} & \bar{Q}_{12} & \bar{Q}_{16} \\ \bar{Q}_{12} & \bar{Q}_{22} & \bar{Q}_{26} \\ \bar{Q}_{16} & \bar{Q}_{26} & \bar{Q}_{66} \end{bmatrix} \tag{2.3}$$

where

$$\bar{Q}_{11} = Q_{11}\cos^4\theta + 2(Q_{12} + 2Q_{66})\sin^2\theta\cos^2\theta + Q_{22}\sin^4\theta$$

$$\bar{Q}_{12} = (Q_{11} + Q_{22} - 4Q_{66})\sin^2\theta\cos^2\theta + Q_{12}(\sin^4\theta + \cos^4\theta)$$

$$\bar{Q}_{22} = Q_{11}\sin^4\theta + 2(Q_{12} + 2Q_{66})\sin^2\theta\cos^2\theta + Q_{22}\cos^4\theta$$

$$\bar{Q}_{16} = (Q_{11} - Q_{12} - 2Q_{66})\sin\theta\cos^3\theta + (Q_{12} - Q_{22} + 2Q_{66})\sin^3\theta\cos\theta$$

$$\bar{Q}_{26} = (Q_{11} - Q_{12} - 2Q_{66})\sin^3\theta\cos\theta + (Q_{12} - Q_{22} + 2Q_{66})\sin\theta\cos^3\theta$$

$$\bar{Q}_{66} = (Q_{11} + Q_{22} - 2Q_{12} - 2Q_{66})\sin^2\theta\cos^2\theta + Q_{66}(\sin^4\theta + \cos^4\theta)$$

(2.4)

A ply with fibres at an angle $-\theta$ to the x-axis may be seen to have the same elastic stiffness coefficients as given in relation (2.4) above apart from $\bar{Q}_{16}$ and $\bar{Q}_{26}$ which change sign.

Now, assuming small deformations and following the thin plate theory, it can be shown that the relationship characterising the response of laminates to applied membrane stresses and bending moments is linear.[51] A full 6 x 6 symmetric matrix is required, in general, to describe this elastic behaviour. It is given by[51]

$$\begin{Bmatrix} N \\ M \end{Bmatrix} = \begin{bmatrix} A & B \\ B & D \end{bmatrix} \begin{Bmatrix} \varepsilon^o \\ k \end{Bmatrix} \qquad (2.5)$$

where

$$N = (N_x, N_y, N_{xy})$$

$$M = (M_x, M_y, M_{xy})$$

are membrane and bending stress resultants and

$$\varepsilon^o = (\varepsilon^o_x, \varepsilon^o_y, \varepsilon^o_{xy})$$

$$k = (k_x, k_y, k_{xy})$$

are middle plane strains and curvatures respectively. The matrices A, B and D are defined as follows: Assume the kth ply of the laminate as shown in Figure 2.1, to lie between z_k and z_{k-1}. Then the components of the membrane stiffness matrix A, coupling matrix B and bending stiffness matrix D are given by a summation over the N plies:

$$\begin{aligned} A_{ij} &= \sum_{k=1}^{N} (\bar{Q}_{ij})_k (z_k - z_{k-1}) \\ B_{ij} &= \frac{1}{2} \sum_{k=1}^{N} (\bar{Q}_{ij})_k (z_k^2 - z_{k-1}^2) \\ D_{ij} &= \frac{1}{3} \sum_{k=1}^{N} (\bar{Q}_{ij})_k (z_k^3 - z_{k-1}^3) \end{aligned} \qquad (2.6)$$

It can be shown that $A_{16} = A_{26} = 0$ leads to in-plane orthotropy; $D_{16} = D_{26} = 0$ ensures orthotropy in bending while $B_{ij} = 0$ yields an uncoupled lay-up.

In what follows, the symmetry of the laminate about its middle plane is important since the plies considered herein

are grouped in pairs, symmetrically placed about the mid-plane and numbered outwards from the centre (Figure 2.1). When both plies of a pair have fibres aligned in the same direction, the pair is referred to as symmetric, the term antisymmetric is applied to pairs with fibre directions of + θ and - θ respectively.

In general, it has been noticed that antisymmetric laminates tend to become orthotropic for $N \geq 8$. It should, therefore, be our endeavour now to investigate whether it is possible to obtain orthotropic and uncoupled behaviour even in cases where $N < 8$ by manipulating the thickness distributions of layers. The minimum number of layers in such a case will have to be four and accordingly the analysis is given for 4 and 6 layers in the following sections.

2.3.1 Four-Layered Angle-Ply Laminate

Consider a four-layered laminate with laminae thicknesses t_1 and t_2 on each side of the middle surface and with fibre directions aligned at + θ_1 and - θ_2 to the x-axis of the coordinate system as shown in Figure 2.2.

The first of Eq. (2.6) for the present case is reduced to

$$A_{ij} = 2\bar{Q}_{ij}(\theta_1)\,[t_1 + \alpha_{ij}\, t_2] \qquad (2.7)$$

where

$$\alpha_{ij} = \bar{Q}_{ij}(\theta_2)/\bar{Q}_{ij}(\theta_1)$$

and $\bar{Q}_{ij}(\theta)$ are the reduced stiffnesses evaluated at angle of orientation of the fibre, θ.

For an antisymmetric angle-ply plate, $\alpha_{ij} = 1$ and the extensional stiffnesses A_{ij} reduce to

$$A_{ij} = \bar{Q}_{ij}\, t \qquad \text{for } j \neq 6 \qquad (2.8a)$$

$$= 0 \qquad \text{for } j = 6 \qquad (2.8b)$$

where t is the overall thickness of the laminate.

The relation (2.8a) shows that the extensional stiffnesses A_{ij} are independent of the individual ply thicknesses.

The second of Eq. (2.6) upon substitution of parameters assumed in Figures 2.1 and 2.2 and after simplification reduces to

$$B_{ij} = \frac{1}{2}\bar{Q}_{ij}(\theta_1)\,[(z_1^2 - z_o^2 + z_3^2 - z_4^2) + \alpha_{ij}(z_1^2 - 2z_2^2 + z_3^2)]$$

$$= \frac{1}{2}\bar{Q}_{ij}(\theta_1)\,[2t_2^2 - 2(t_1 + t_2)^2 + 2\alpha_{ij}\, t_2^2]$$

$$= \bar{Q}_{ij}(\theta_1)\,[t_2^2(1 + \alpha_{ij}) - (t_1 + t_2)^2]$$

or

$$B_{ij} = \bar{Q}_{ij}(\theta_1)\, f(t_1, t_2, \alpha_{ij}) \qquad (2.9)$$

The purpose of the present investigation is to reduce B_{ij} to zero in order to obtain uncoupled lay-ups. B_{ij} can be zero, provided $f(t_1, t_2, \alpha_{ij})$ is zero since $\bar{Q}_{ij}(\theta_1)$ cannot be equal to zero. This leads to

$$R_1^2 + 2R_1 - \alpha_{ij} = 0 \qquad (2.10)$$

where

$$R_1 = t_1/t_2$$

Eq. (2.10) is quadratic in R_1 and yields

$$R_1 = -1 \pm \sqrt{1 + \alpha_{ij}} \qquad (2.11)$$

For an antisymmetric angle-ply laminate, $\alpha_{ij} = 1$. Hence

$$R_1 = 0.4142 \qquad (2.12)$$

The bending stiffnesses from the third of Eq. (2.6) can be reduced to

$$D_{ij} = \frac{2}{3} \bar{Q}_{ij}(\theta_1) \left[(\alpha_{ij} - 1)t_2^3 + \frac{t^3}{8}\right] \qquad \text{for } j \neq 6 \qquad (2.13a)$$

$$= 0 \qquad \text{for } j = 6 \qquad (2.13b)$$

which are obviously independent of the thickness of an individual lamina for the antisymmetric angle-ply laminate.

2.3.2 Six-Layered Angle-Ply Laminate

Consider a six layered angle-ply laminate with thickness distribution and laminae orientation as shown in Figure 2.3.

The extensional stiffnesses A_{ij} and bending stiffnesses D_{ij} can be derived as before and are given by

$$A_{ij} = 2\bar{Q}_{ij}(\theta_1)\,[t_1 + \alpha_{ij}t_2 + \beta_{ij}t_3] \quad \text{for } j \neq 6 \tag{2.14a}$$

$$= 0 \quad \text{for } j = 6 \tag{2.14b}$$

$$D_{ij} = \frac{2}{3}\bar{Q}_{ij}(\theta_1)\left[\frac{t^3}{8} - (t_2 + t_3)^3 + \alpha_{ij}\left\{-t_3^3 + (t_2 + t_3)^3\right\} + \beta_{ij}\,t_3^3\right] \quad \text{for } j \neq 6 \tag{2.15a}$$

$$= 0 \quad \text{for } j = 6 \tag{2.15b}$$

where

$$\beta_{ij} = \bar{Q}_{ij}(\theta_3)/\bar{Q}_{ij}(\theta_1)$$

For an antisymmetric angle-ply laminate,

$$\alpha_{ij} = \beta_{ij} = 1$$

and upon substituting these in Eqs. (2.14) and (2.15), we find that

$$A_{ij} = 2\bar{Q}_{ij}(\theta_1)\,(t_1 + t_2 + t_3)$$

$$= \bar{Q}_{ij}(\theta_1)t \quad \text{for } j \neq 6 \tag{2.16a}$$

$$= 0 \quad \text{for } j = 6 \tag{2.16b}$$

$$D_{ij} = \frac{2}{3}\bar{Q}_{ij}(\theta_1) \cdot \frac{t^3}{8}$$

$$= \bar{Q}_{ij}(\theta_1)\,\frac{t^3}{12} \quad \text{for } j \neq 6 \tag{2.17a}$$

$$= 0 \quad \text{for } j = 6 \tag{2.17b}$$

Eqs. (2.16) and (2.17) show that A_{ij} and D_{ij} are independent of the individual ply thicknesses.

The coupling stiffnesses B_{ij} for the six-layered configuration as obtained from the second of Eq. (2.6) are given by

$$B_{ij} = \bar{Q}_{ij}(\theta_1)\,[(t_2 + t_3)^2 - (t_1 + t_2 + t_3)^2 + \alpha_{ij}\{(t_2 + t_3)^2 - t_3^2\} - \beta_{ij}\, t_3^2]$$

$$= \bar{Q}_{ij}(\theta_1)\, f(t_1, t_2, t_3, \alpha_{ij}, \beta_{ij}) \qquad (2.18)$$

$$B_{ij} = 0 \quad \text{if} \quad f(t_1, t_2, t_3, \alpha_{ij}, \beta_{ij}) = 0$$

This gives upon algebraic simplifications

$$\alpha_{ij}\, R_2^2 + 2(\alpha_{ij} - R_1)R_2 - (R_1^2 + 2R_1 + \beta_{ij}) = 0 \qquad (2.19)$$

where

$$R_1 = t_1/t_3$$

$$R_2 = t_2/t_3$$

In terms of R_1, R_2 can be written as

$$R_2 = \frac{(R_1 - \alpha_{ij}) \pm \sqrt{(\alpha_{ij} - R_1)^2 + \alpha_{ij}(R_1^2 + 2R_1 + \beta_{ij})}}{\alpha_{ij}} \qquad (2.20)$$

For an antisymmetric laminate, Eq. (2.20) reduces to

$$R_2 = (R_1 - 1) \pm \sqrt{2R_1^2 + 2} \qquad (2.21)$$

2.4 RESULTS AND DISCUSSION

The variations of coupling stiffnesses B_{16} and B_{26} as a function of thickness ratio, R_1 $(= t_1/t_2)$ of the laminae of a four-layered antisymmetric angle-ply laminate are shown in Figure 2.4 for three different fibre orientations 30°, 45° and 60°. It is seen that in each case B_{16} and B_{26} vanish simultaneously at $R_1 = 0.4142$. For other values of R_1, there exist finite values of B_{16} and B_{26}. The coupling stiffnesses do not exist for extreme fibre orientations of 0° and 90° for obvious reasons. Thus it is possible to eliminate the coupling terms entirely and achieve special orthotropy at any fibre orientation of a four-layered antisymmetric angle-ply laminate. However, if the laminate is not antisymmetric i.e., if the angle of orientation of the fibres in each layer is different ($+\theta_1$, $-\theta_2$, $+\theta_2$, $-\theta_1$ arrangement, for example), it is possible to eliminate one of the coupling stiffnesses B_{16} and B_{26}. Such a choice may be used for the elimination of more predominant coupling stiffness. Table 2.1 gives the values of α_{16} and α_{26} for various stacking sequences for laminates made of different materials. These values can be used in Eq. (2.11) to obtain a thickness ratio which results in the elimination of one of

the coupling stiffnesses (B_{16} or B_{26}). Figures 2.5 and 2.6 show the variations of the coupling stiffnesses B_{16} and B_{26} with R_2 ($= t_2/t_3$) for given values of R_1 ($= t_1/t_3$) of 1.0 and 2.0 respectively for a six-layered antisymmetric angle-ply laminate. Here again, a unique value of thickness ratio exists for which the coupling terms vanish at any fibre orientation. Figure 2.7 shows the plot of R_1 versus R_2 for a six-layered antisymmetric laminate. This is valid for any fibre orientation. A choice of point falling on this curve ensures the absence of coupling terms and consequent achievement of special orthotropy. The intersection of this curve with the R_2-axis ($R_1 = 0$) yields the critical thickness ratio of 0.4142 for a four-layered laminate, since with $R_1 = 0$, the six-layered laminate is analogous to a four-layered one. However the case of $t_3 = 0$ which also corresponds to one of four-layered cannot come out as a limiting case of the above derivation since all the quantities tend to infinity at different rates.

Similar to the case of four-layered laminate, the absence of both the coupling stiffnesses may not, in general, be possible if the fibre orientation in each lamina is different. In such a situation, Table 2.1 may still be used for a particular stacking sequence to obtain a partial reduction in coupling. Consider, for example, a six-ply laminate with stacking sequence: 30°/-45°/60°/-60°/45°/-30°.

The values of α_{ij} and β_{ij} to be used in Eq. (2.20) as obtained from Table 2.1 are:

$$\alpha_{16} = 0.82385, \qquad \beta_{16} = 0.42696$$
$$\alpha_{26} = 1.92957, \qquad \beta_{26} = 2.34212$$

A choice of R_1 and R_2 leading to partial elimination of coupling stiffnesses ($B_{16} = 0$ or $B_{26} = 0$) for a six-layered laminate with the above stacking sequence is given in Figure 2.8 for a carbon-fibre reinforced plastic (CFRP) laminate. The intersection of the two curves which ensures simultaneous elimination of B_{16} and B_{26} is seen to be a peculiar behaviour of this stacking sequence. It is further observed that the point of intersection namely $R_1 = 0.25$ approximately and $R_2 = 0.60$ approximately is independent of material properties as shown by Figures 2.8 to 2.10 for three different materials. A similar behaviour, in general, can be expected for a stacking sequence of $(\pi/4 \pm \theta)$. This peculiar behaviour may not, in general, be expected from an arbitrary stacking sequence. Figures 2.11 and 2.12 drawn for two different materials (GFRP and CFRP) between R_1 and R_2 for a stacking sequence of 45°/-30°/60°/-60°/30°/-45°, for example, do not exhibit any intersection.

2.5 CONCLUSIONS

1. For antisymmetric angle-ply laminates, it is possible to eliminate the coupling effects by a suitable choice of thicknesses of laminae.

2. The coupling effects can be alleviated for general angle-ply laminates by a suitable choice of thickness ratios.
3. It is possible to obtain the orthotropic behaviour of an angle-ply laminate with a fewer number of layers ($4 \leq N \leq 8$) by suitably selecting the laminae thicknesses.

- o -

TABLE 2.1. VALUES OF α_{16} AND α_{26} FOR VARIOUS STACKING SEQUENCES FOR COMMON COMPOSITE MATERIALS

I. Carbon Fibre Reinforced Plastic

($E_1/E_2 = 6.333$; $G_{12}/E_2 = 0.667$; $\nu_{12} = 0.20$)

Sr. No.	Stacking Sequence	α_{16}	α_{26}
1	30°/-45°/45°/-30°	0.8238	1.9295
2	45°/-30°/30°/-45°	1.2138	0.5182
3	30°/-60°/60°/-30°	0.4269	2.3421
4	60°/-30°/30°/-60°	2.3421	0.4269
5	60°/-45°/45°/-60°	1.9295	0.8238
6	45°/-60°/60°/-45°	0.5182	1.2138

II. Graphite Fibre Reinforced Plastics

($E_1/E_2 = 40.0$; $G_{12}/E_2 = 0.50$; $\nu_{12} = 0.25$)

1	30°/-45°/45°/-30°	0.7731	2.2803
2	45°/-30°/30°/-45°	1.2935	0.4385
3	30°/-60°/60°/-30°	0.3390	2.9496
4	60°/-30°/30°/-60°	2.9496	0.3390
5	60°/-45°/45°/-60°	2.2803	0.7731
6	45°/-60°/60°/-45°	0.4385	1.2937

Continued...

TABLE 2.1 (continued)

III. Boron Fibre Reinforced Plastic

($E_1/E_2 = 10.0$; $G_{12}/E_2 = 0.333$; $\nu_{12} = 0.30$)

Sr. No.	Stacking Sequence	α_{16}	α_{26}
1	30°/-45°/45°/-30°	0.7676	2.3298
2	45°/-30°/30°/-45°	1.3028	0.4292
3	30°/-60°/60°/-30°	0.3294	3.0353
4	60°/-30°/30°/-60°	3.0353	0.3294
5	60°/-45°/45°/-60°	2.3298	0.7676
6	45°/-60°/60°/-45°	0.4292	1.3028

IV. Glass Fibre Reinforced Plastic

($E_1/E_2 = 3.0$; $G_{12}/E_2 = 0.50$; $\nu_{12} = 0.25$)

1	30°/-45°/45°/-30°	0.8334	1.8788
2	45°/-30°/30°/-45°	1.9980	0.5322
3	30°/-60°/60°/-30°	0.4436	2.2542
4	60°/-30°/30°/-60°	2.2542	0.4436
5	60°/-45°/45°/-60°	1.8788	0.8334
6	45°/-60°/60°/-45°	0.5322	1.1998

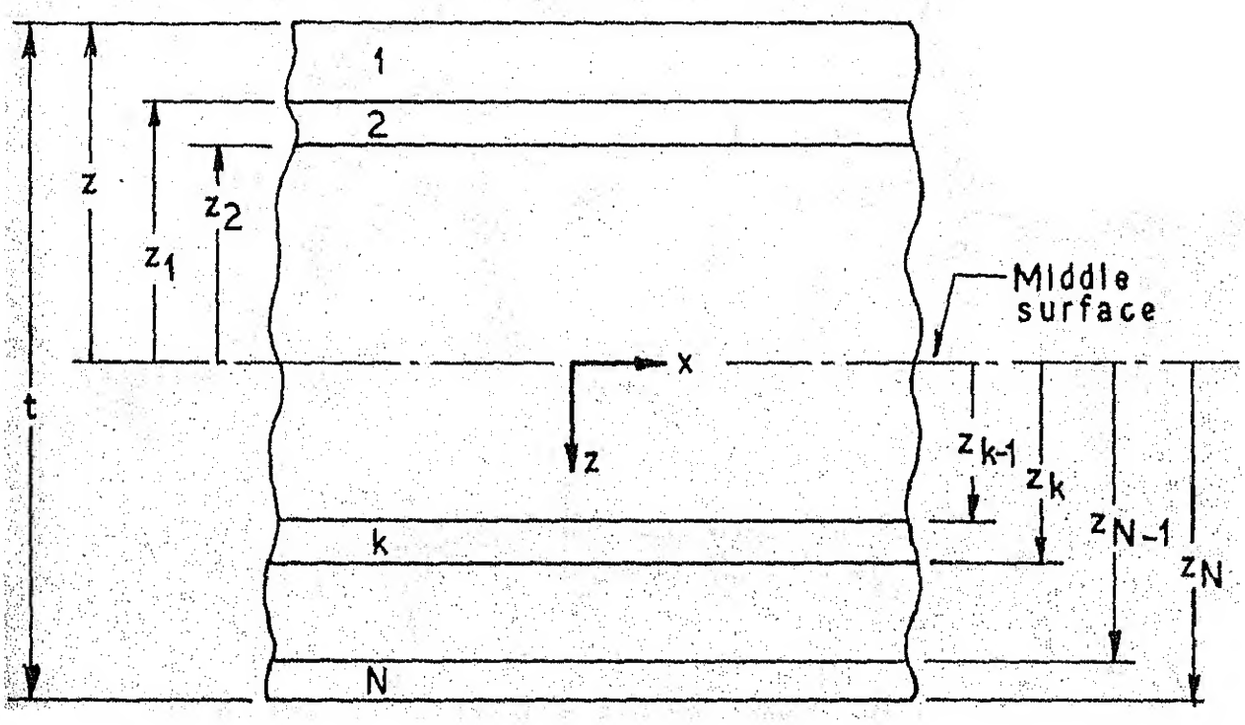

FIG. 2·1: GEOMETRY OF A n – LAYERED LAMINATE.

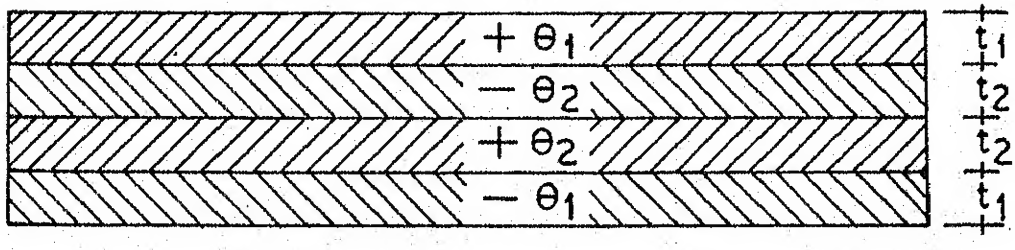

FIG. 2·2: GEOMETRY OF A FOUR LAYERED LAMINATE.

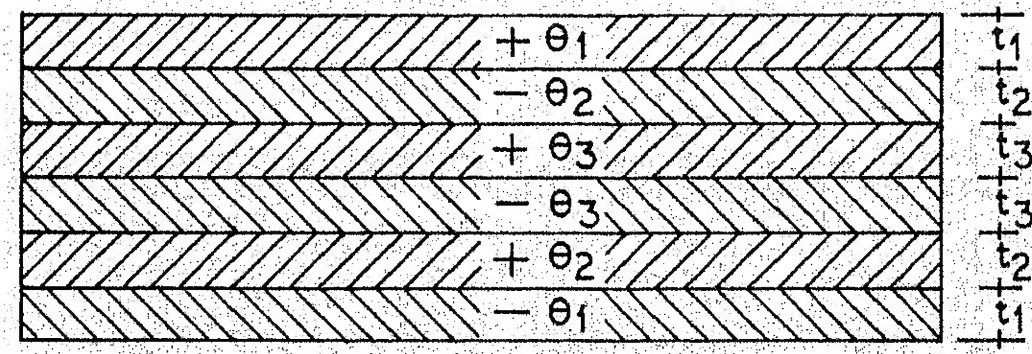

FIG. 2·3: GEOMETRY OF A SIX LAYERED LAMINATE.

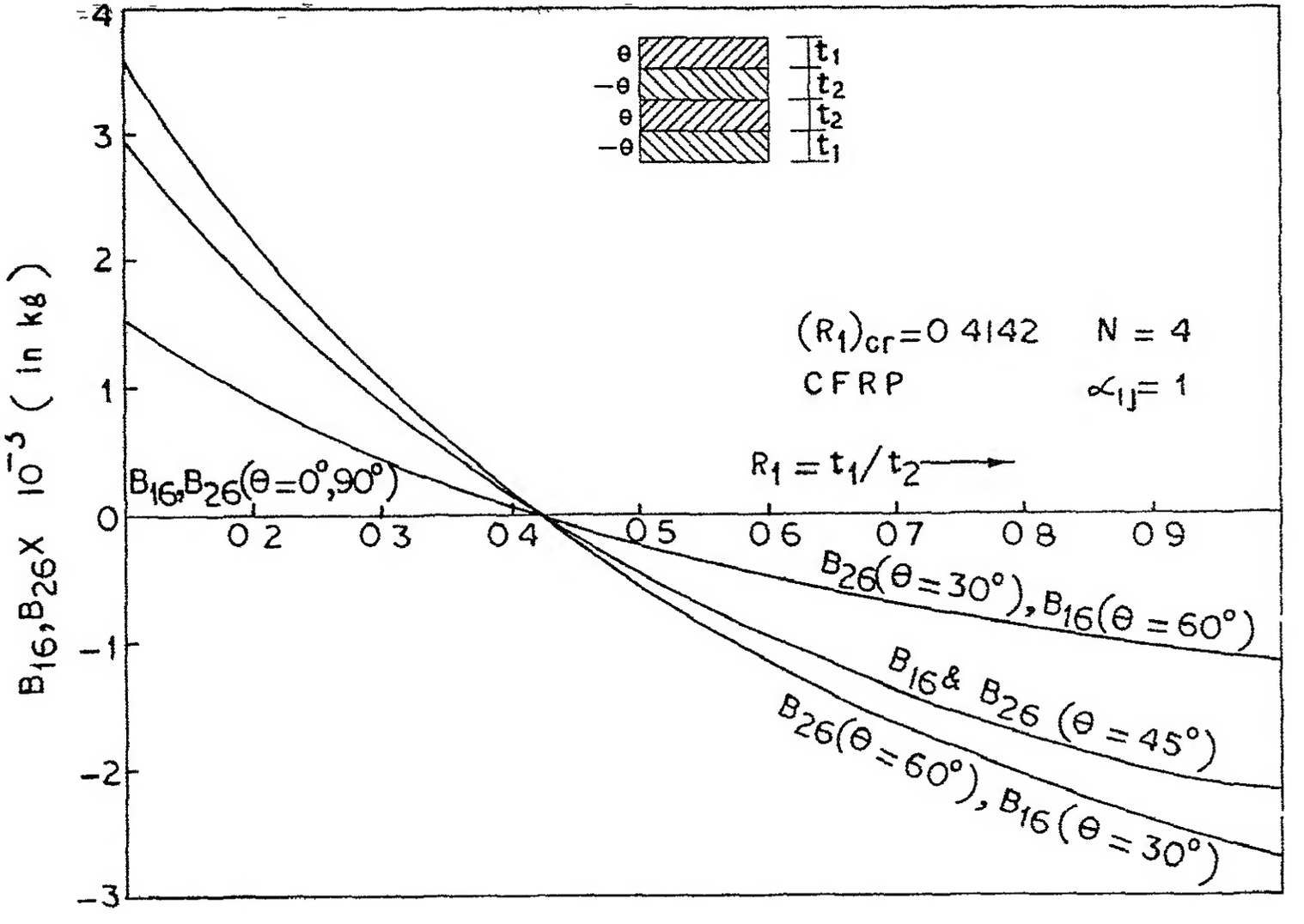

FIG 2-4 VARIATION OF COUPLING STIFFNESSES WITH THICKNESS RATIO FOR A FOUR-LAYERED ANTISYMMETRIC LAMINATE

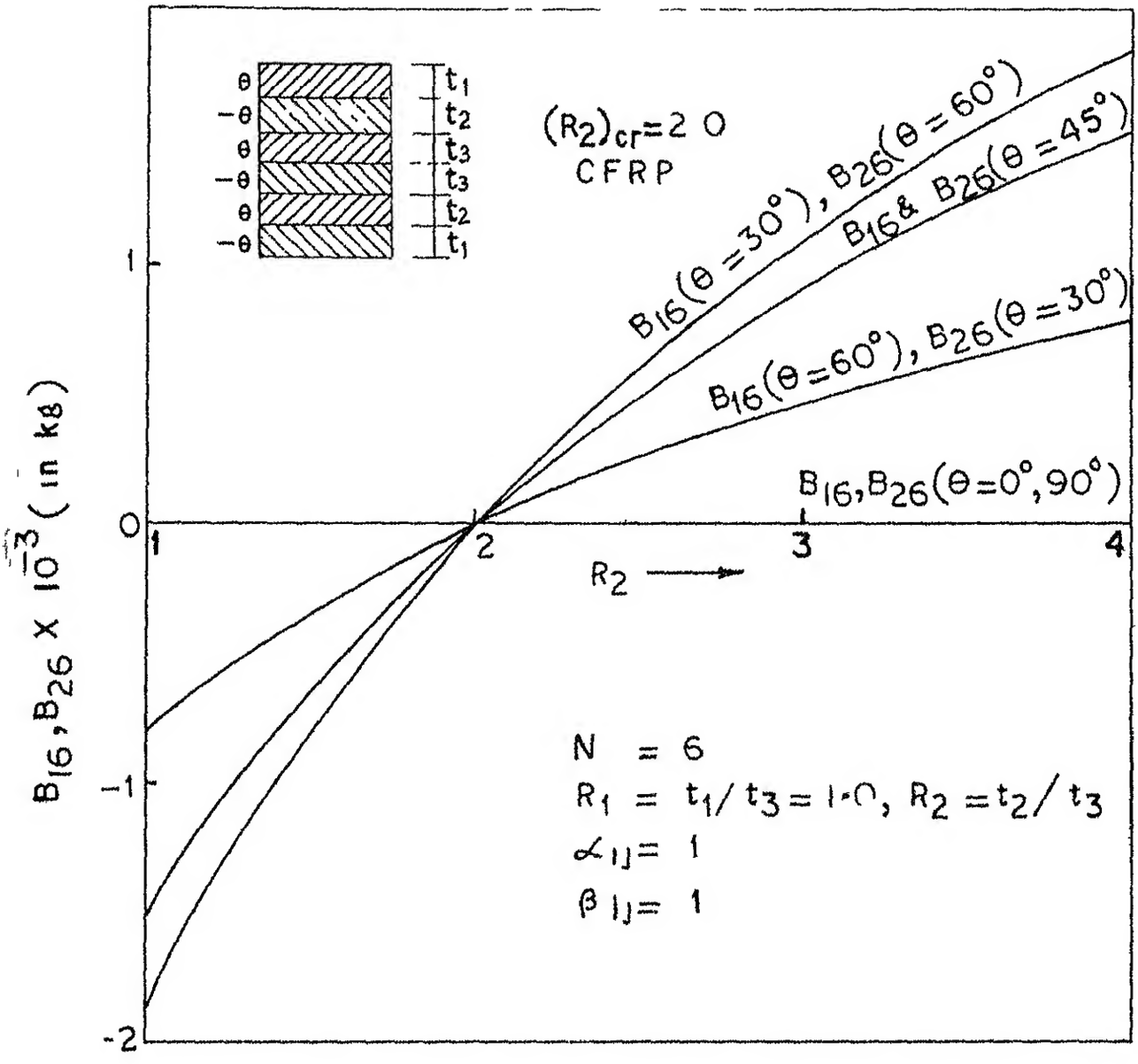

FIG 2 5 VARIATION OF COUPLING STIFFNESSES WITH THICKNESS RATIO FOR A SIX LAYERED ANTISYMMTRIC LAMINATE

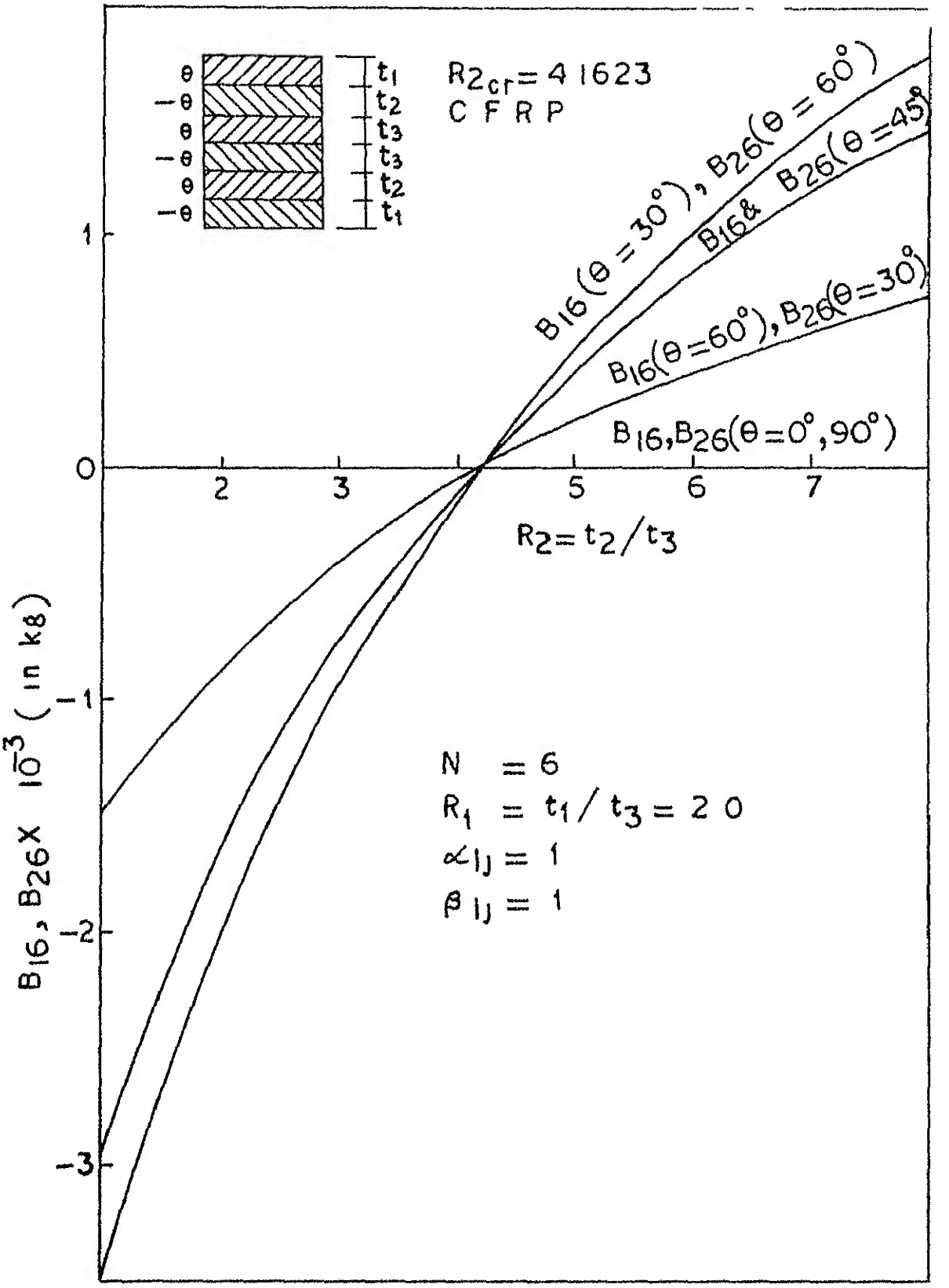

FIG. 2 6 VARIATION OF COUPLING STIFFNESSES WITH THICKNESS RATIO FOR A SIX — LAYERED ANTISYMMETRIC LAMINATE

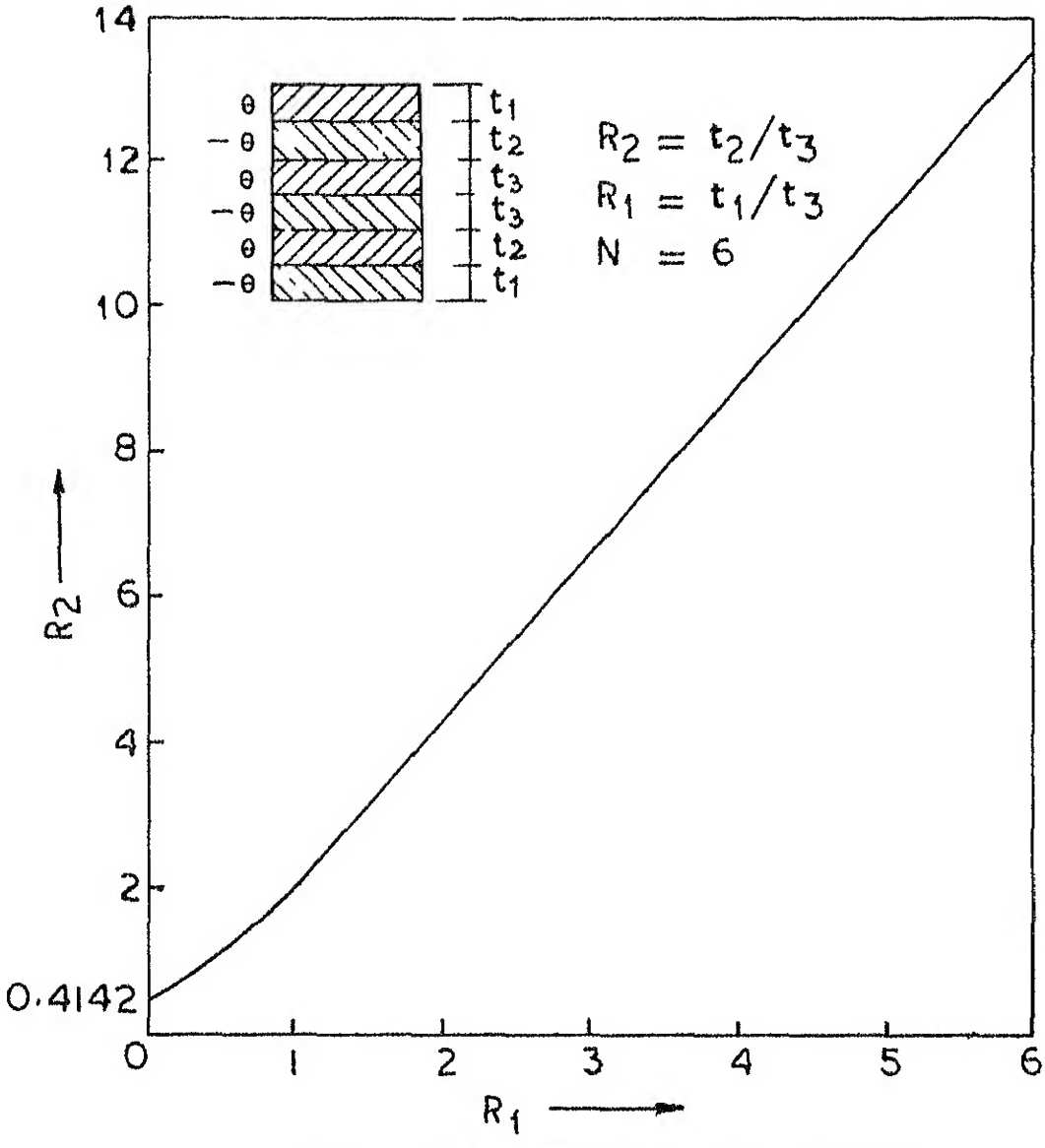

FIG 2 7 LOCUS OF ORTHO-TROPIC THICKNESS RATIOS

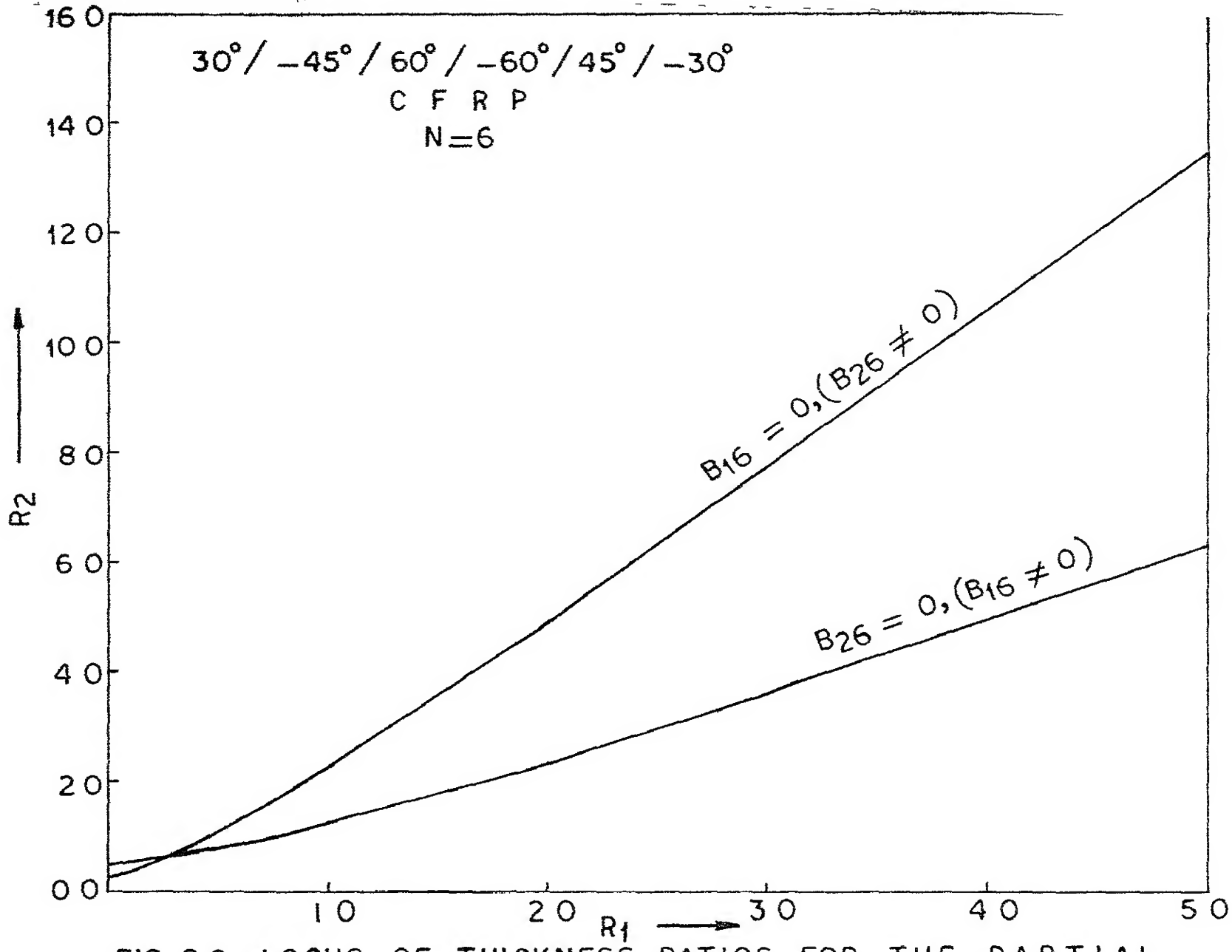

FIG 28 LOCUS OF THICKNESS RATIOS FOR THE PARTIAL ELIMINATION OF COUPLING STIFFNESS

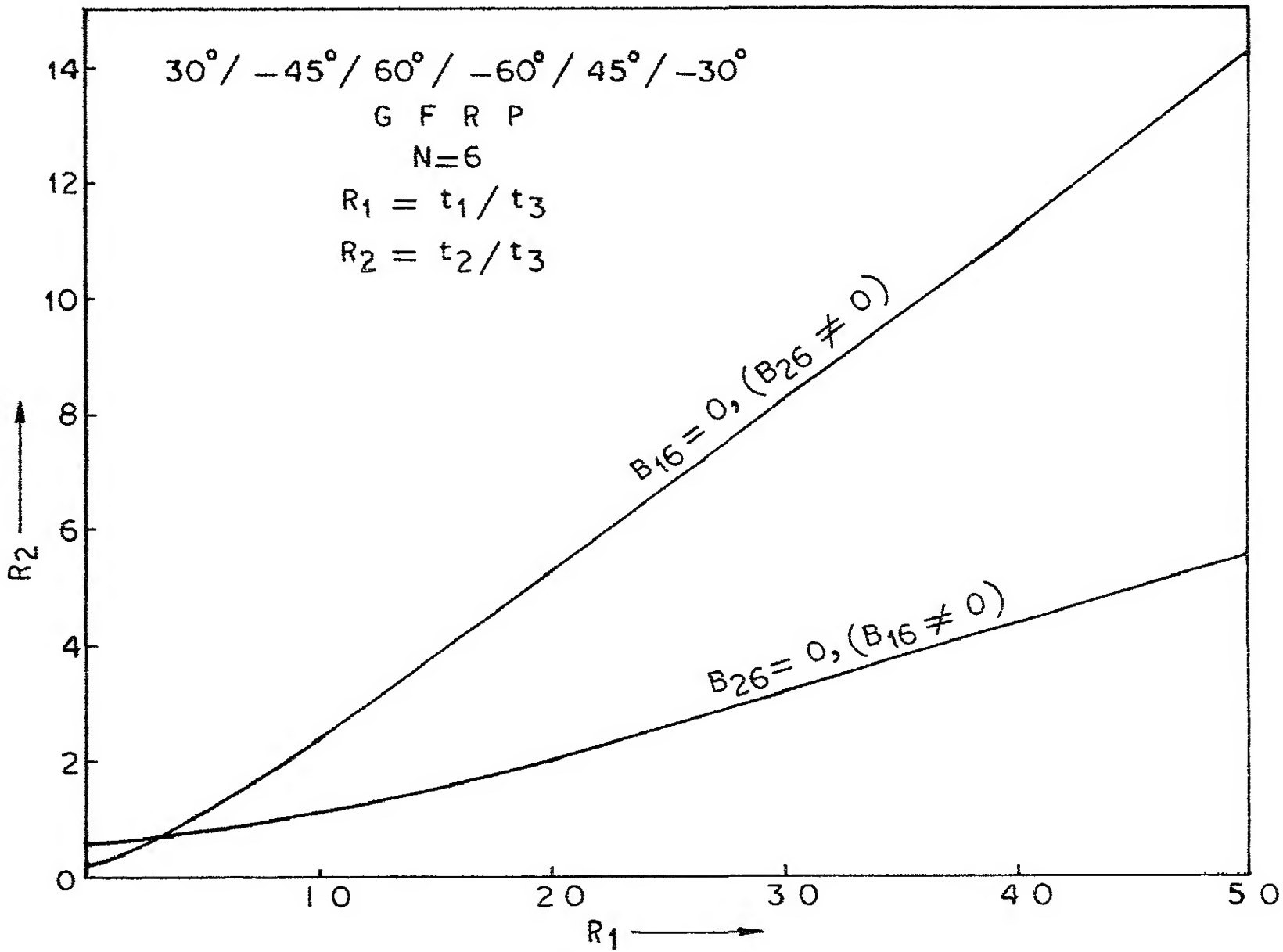

FIG. 29 LOCUS OF THICKNESS RATIOS FOR THE PARTIAL ELIMINATION OF COUPLING STIFFNESS

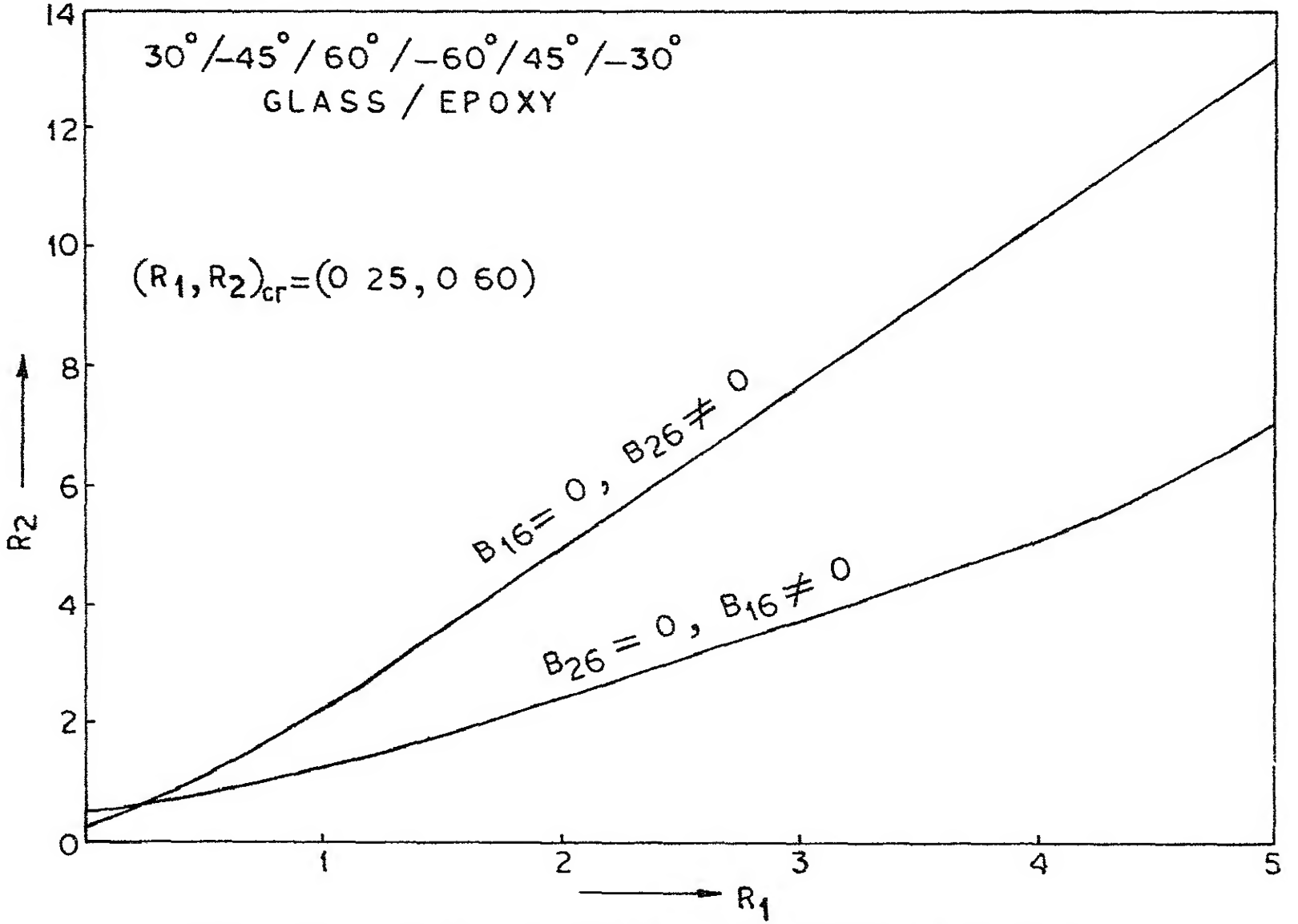

FIG 2 10 LOCUS OF THICKNESS RATIOS FOR THE PARTIAL ELIMINATION OF COUPLING STIFFNESS

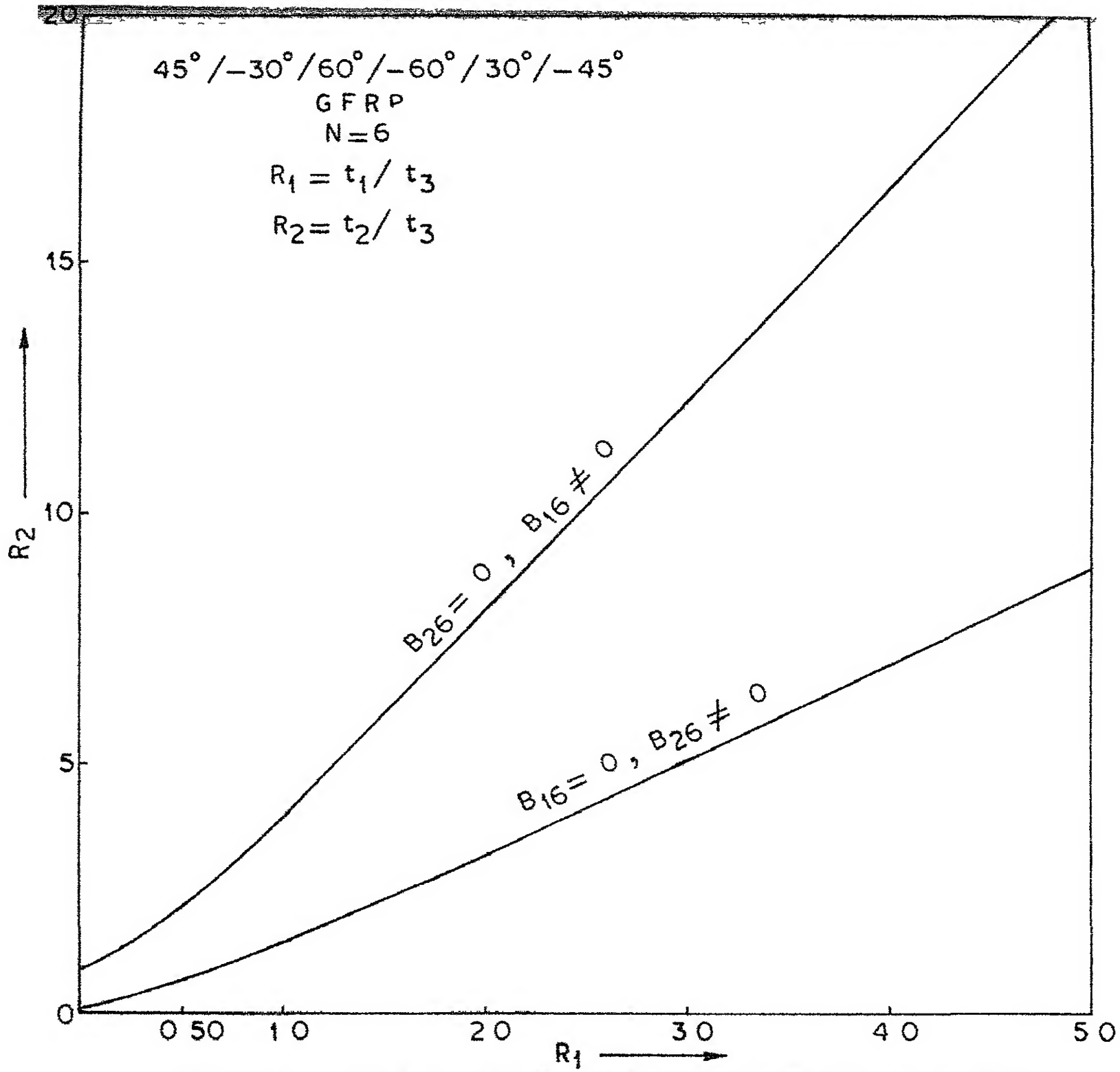

FIG 2.11 LOCUS OF THICKNESS RATIOS FOR THE PARTIAL ELIMINATION OF COUPLING STIFFNESS

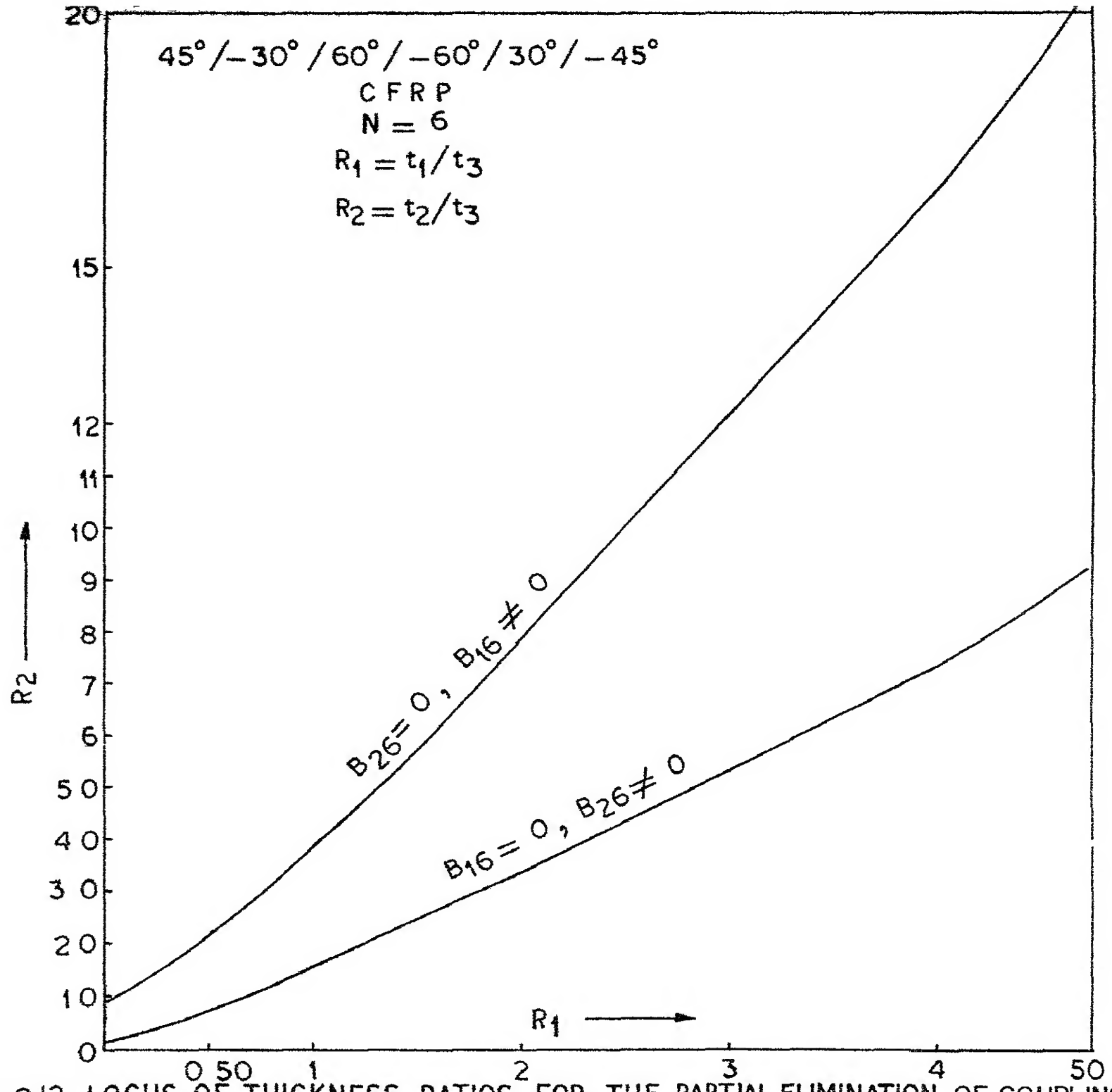

FIG 2.12 LOCUS OF THICKNESS RATIOS FOR THE PARTIAL ELIMINATION OF COUPLING STIFFNESS

CHAPTER 3

FORMULATION OF THE PROBLEM AND METHOD OF SOLUTION

3.1 INTRODUCTION

Laminated plates are one of the simplest and most widely used practical applications of composite laminates. There exist many kinds of theories and levels of sophistication in the theory of laminated plates, both linear and nonlinear. These can be subdivided as: (1) thin plate analysis (2) moderately thick plate analysis including the thickness-shear and thickness-normal deformation (3) classical elasticity analysis applicable to non-homogeneous laminated plates. Owing to simplicity of analysis, thin plate theory has been most popular. The simplified form of this theory has been applied to a plate laminated symmetrically with respect to its middle plane.[52,53] A general form of this theory has been applied to arbitrarily laminated plates including bending-stretching coupling effects.[23,54] A more complete classification of laminated plate problems is found in reference 55.

The response of laminated plates is governed by three coupled displacement equations of equilibrium. The laminated plate analyses have been carried out mostly by assuming suitable functions for the three displacement components separately. However, to obtain a more general solution, it is

desirable to combine the three displacement equations of equilibrium into a single higher order partial differential equation. In what follows, a system of three coupled governing equations for arbitrarily laminated plates is derived by an energy approach and this system of three equations is then reduced to a single eighth order partial differential equation in terms of a single displacement function. A closed form solution to this equation is then found for some types of laminates under various boundary conditions.

3.2 DERIVATION OF EQUILIBRIUM EQUATIONS AND NATURAL BOUNDARY CONDITIONS

3.2.1 Assumptions

(1) Each layer is orthotropic. The principal material directions of each layer are, in general, aligned at an angle θ to the plate axes.

(2) The plate thickness is very small compared to its length and width (plate is assumed to be thin).

(3) The usual assumptions of the small deformation theory of thin plates are valid here also.

(4) Strains ε_x, ε_y and ε_{xy} are small.

(5) No body forces exist.

3.2.2 Strain-Displacement-Curvature Relationships

The rectangular coordinate system considered is shown in Figure 3.1. The assumptions of classical thin plate theory lead to the following displacement relations:

$$\begin{aligned} u &= u^{o}(x, y) - z \frac{\partial w}{\partial x} \\ v &= v^{o}(x, y) - z \frac{\partial w}{\partial y} \\ w &= w(x, y) \end{aligned} \tag{3.1a}$$

The corresponding strain-curvature and the strain-displacement relations are

$$\begin{aligned} \varepsilon_x &= \varepsilon_x^{o} + z\, k_x \\ \varepsilon_y &= \varepsilon_y^{o} + z\, k_y \\ \varepsilon_z &= \varepsilon_{xy}^{o} + z\, k_{xy} \end{aligned} \tag{3.1b}$$

where

$$\varepsilon_x^{o} = \frac{\partial u^{o}}{\partial x} \; ; \qquad \varepsilon_y^{o} = \frac{\partial v^{o}}{\partial y} \; ; \qquad \varepsilon_{xy}^{o} = \frac{\partial u^{o}}{\partial y} + \frac{\partial v^{o}}{\partial x}$$

$$k_x = -\frac{\partial^2 w}{\partial x^2} \; ; \qquad k_y = -\frac{\partial^2 w}{\partial y^2} \; ; \qquad k_{xy} = -2\frac{\partial^2 w}{\partial x\, \partial y}$$

The superscript 'o' refers to the middle plane values.

3.2.3 Derivation of Equilibrium Equations and Boundary Conditions by Energy Approach

A general expression for the elemental strain energy is given by

$$dV = \frac{1}{2}[\sigma_x \varepsilon_x + \sigma_y \varepsilon_y + \sigma_z \varepsilon_z + \tau_{xy} \varepsilon_{xy} + \tau_{yz} \varepsilon_{yz} + \tau_{xz} \varepsilon_{xz}]\, dx\, dy\, dz + q(x, y)\, w\, dx\, dy \qquad (3.2a)$$

Incorporating the general assumptions of classical thin plate theory and integrating over the thickness t, the strain energy of the plate is given by

$$V = \frac{1}{2}\iint [N_x \frac{\partial u^o}{\partial x} + N_y \frac{\partial v^o}{\partial y} + N_{xy} (\frac{\partial u^o}{\partial y} + \frac{\partial v^o}{\partial x}) - M_x \frac{\partial^2 w}{\partial x^2} - M_y \frac{\partial^2 w}{\partial y^2} - 2M_{xy} \frac{\partial^2 w}{\partial x\, \partial y}]\, dx\, dy + \iint q(x, y)\, w\, dx\, dy \qquad (3.2b)$$

where

$$N_x = \int_{-t/2}^{t/2} \sigma_x dz; \quad N_y = \int_{-t/2}^{t/2} \sigma_y dz; \quad N_{xy} = \int_{-t/2}^{t/2} \tau_{xy} dz$$

$$M_x = \int_{-t/2}^{t/2} \sigma_x\, z\, dz; \quad M_y = \int_{-t/2}^{t/2} \sigma_y\, z\, dz; \quad M_{xy} = \int_{-t/2}^{t/2} \tau_{xy}\, z\, dz$$

are the inplane normal and shear forces (N_x, N_y, N_{xy}) and bending and twisting moments (M_x, M_y, M_{xy}) respectively.

The constitutive relation[55] is given by

$$\begin{bmatrix} N_x \\ N_y \\ N_{xy} \\ \hline M_x \\ M_y \\ M_{xy} \end{bmatrix} = \left[\begin{array}{ccc:ccc} A_{11} & A_{12} & A_{16} & B_{11} & B_{12} & B_{16} \\ A_{12} & A_{22} & A_{26} & B_{12} & B_{22} & B_{26} \\ A_{16} & A_{26} & A_{66} & B_{16} & B_{26} & B_{66} \\ \hdashline B_{11} & B_{12} & B_{16} & D_{11} & D_{12} & D_{16} \\ B_{12} & B_{22} & B_{26} & D_{12} & D_{22} & D_{26} \\ B_{16} & B_{26} & B_{66} & D_{16} & D_{26} & D_{66} \end{array}\right] \begin{bmatrix} \varepsilon_x^o \\ \varepsilon_y^o \\ \varepsilon_{xy}^o \\ \hline k_x \\ k_y \\ k_{xy} \end{bmatrix} \qquad (3.2c)$$

where

$$A_{ij},\ B_{ij},\ D_{ij} = \int_{-t/2}^{t/2} \bar{Q}_{ij}^{(k)}\ (1,\ z,\ z^2)\ dz \qquad (3.2d)$$

$\bar{Q}_{ij}^{(k)}$ is the reduced stiffness of the kth lamina. The substitution of relation (3.2c) into Eq. (3.2b) yields

$$\begin{aligned} V = \frac{1}{2}\int\int \Big[& A_{11}\left(\frac{\partial u^o}{\partial x}\right)^2 + 2A_{12}\,\frac{\partial u^o}{\partial x}\,\frac{\partial v^o}{\partial y} + A_{22}\left(\frac{\partial v^o}{\partial y}\right)^2 \\ & + 2A_{16}\left(\frac{\partial u^o}{\partial x}\,\frac{\partial u^o}{\partial y} + \frac{\partial u^o}{\partial x}\,\frac{\partial v^o}{\partial x}\right) + 2A_{26}\left(\frac{\partial v^o}{\partial x}\,\frac{\partial v^o}{\partial y} + \frac{\partial u^o}{\partial y}\,\frac{\partial v^o}{\partial y}\right) \\ & + A_{66}\left(\frac{\partial u^o}{\partial y} + \frac{\partial v^o}{\partial x}\right)^2 - 2B_{11}\,\frac{\partial^2 w}{\partial x^2}\,\frac{\partial u^o}{\partial x} - 2B_{12}\left(\frac{\partial^2 w}{\partial x^2}\,\frac{\partial v^o}{\partial y} + \frac{\partial^2 w}{\partial y^2}\,\frac{\partial u^o}{\partial x}\right) \\ & - 2B_{22}\,\frac{\partial^2 w}{\partial y^2}\,\frac{\partial v^o}{\partial y} - 2B_{16}\left(\frac{\partial^2 w}{\partial x^2}\,\frac{\partial u^o}{\partial y} + \frac{\partial^2 w}{\partial x^2}\,\frac{\partial v^o}{\partial x} + 2\,\frac{\partial^2 w}{\partial x\,\partial y}\,\frac{\partial u^o}{\partial x}\right) \\ & - 2B_{26}\left(\frac{\partial^2 w}{\partial y^2}\,\frac{\partial u^o}{\partial y} + \frac{\partial^2 w}{\partial y^2}\,\frac{\partial v^o}{\partial x} + 2\,\frac{\partial^2 w}{\partial x\,\partial y}\,\frac{\partial v^o}{\partial y}\right) - 4B_{66}\,\frac{\partial^2 w}{\partial x\,\partial y}\cdot\left(\frac{\partial u^o}{\partial y}\right. \\ & \left. + \frac{\partial v^o}{\partial x}\right) + D_{11}\left(\frac{\partial^2 w}{\partial x^2}\right)^2 + 2D_{12}\,\frac{\partial^2 w}{\partial x^2}\,\frac{\partial^2 w}{\partial y^2} + D_{22}\left(\frac{\partial^2 w}{\partial y^2}\right)^2 \\ & + 4D_{16}\,\frac{\partial^2 w}{\partial x^2}\,\frac{\partial^2 w}{\partial x\,\partial y} + 4D_{26}\,\frac{\partial^2 w}{\partial y^2}\,\frac{\partial^2 w}{\partial x\,\partial y} + 4D_{66}\left(\frac{\partial^2 w}{\partial x\,\partial y}\right)^2 \Big]\ dx\ dy \end{aligned} \qquad (3.2e)$$

Considering the variation of each term in Eq. (3.2e) and applying the Principle of Virtual Displacement, the following set of equilibrium equations and the associated boundary conditions are obtained:

Equilibrium Equations

$$A_{11}\frac{\partial^2 u^o}{\partial x^2} + A_{12}\frac{\partial^2 v^o}{\partial x\,\partial y} + A_{16}\left(2\frac{\partial^2 u^o}{\partial x\,\partial y} + \frac{\partial^2 v^o}{\partial x^2}\right) + A_{26}\frac{\partial^2 v^o}{\partial y^2}$$

$$A_{66}\left(\frac{\partial^2 u^o}{\partial y^2} + \frac{\partial^2 v^o}{\partial x\,\partial y}\right) - B_{11}\frac{\partial^3 w}{\partial x^3} - B_{12}\frac{\partial^3 w}{\partial x\,\partial y^2}$$

$$- 3B_{16}\frac{\partial^3 w}{\partial x^2\,\partial y} - B_{26}\frac{\partial^3 w}{\partial y^3} - 2B_{66}\frac{\partial^3 w}{\partial x\,\partial y^2} = 0 \qquad (3.2f)$$

$$A_{12}\frac{\partial^2 u^o}{\partial x\,\partial y} + A_{22}\frac{\partial^2 v^o}{\partial y^2} + A_{16}\frac{\partial^2 u^o}{\partial x^2} + A_{26}\left(2\frac{\partial^2 v^o}{\partial x\,\partial y} + \frac{\partial^2 u^o}{\partial y^2}\right)$$

$$+ A_{66}\left(\frac{\partial^2 v^o}{\partial x^2} + \frac{\partial^2 u^o}{\partial x\,\partial y}\right) - B_{12}\frac{\partial^3 w}{\partial x^2\,\partial y} - B_{22}\frac{\partial^3 w}{\partial y^3} - B_{16}\frac{\partial^3 w}{\partial x^3}$$

$$- 3B_{26}\frac{\partial^3 w}{\partial x\,\partial y^2} - 2B_{66}\frac{\partial^3 w}{\partial x^2\,\partial y} = 0 \qquad (3.2g)$$

$$D_{11}\frac{\partial^4 w}{\partial x^4} + 2D_{12}\frac{\partial^4 w}{\partial x^2\,\partial y^2} + D_{22}\frac{\partial^4 w}{\partial y^4} + 4D_{16}\frac{\partial^4 w}{\partial x^3\,\partial y}$$

$$+ 4D_{26}\frac{\partial^4 w}{\partial x\,\partial y^3} + 4D_{66}\frac{\partial^4 w}{\partial x^2\,\partial y^2} - B_{11}\frac{\partial^3 u^o}{\partial x^3}$$

$$- B_{12}\left(\frac{\partial^3 u^o}{\partial x\,\partial y^2} + \frac{\partial^3 v^o}{\partial x^2\,\partial y}\right) - B_{22}\frac{\partial^3 v^o}{\partial y^3} - 3B_{16}\frac{\partial^3 u^o}{\partial x^2\,\partial y}$$

$$- B_{16}\frac{\partial^3 v^o}{\partial x^3} - B_{26}\left(3\frac{\partial^3 v^o}{\partial x\,\partial y^2} + \frac{\partial^3 u^o}{\partial y^3}\right)$$

$$- 2B_{66}\frac{\partial^3 v^o}{\partial x^2\,\partial y} - 2B_{66}\frac{\partial^3 u^o}{\partial x\,\partial y^2} = q(x, y) \qquad (3.2h)$$

Boundary Conditions

Different types of simply supported and clamped edge boundary conditions are possible for laminated plates. The detailed discussion of these boundary conditions is given in references 56 and 57. The following types of edge boundary conditions (Figure 3.1) are considered in the present thesis:

(a) Simply supported boundary conditions:

(i) Antisymmetric angle-ply laminates

$$\left.\begin{aligned} w &= 0, \quad & M_x &= 0 \\ u^o &= 0, \quad & N_{xy} &= 0 \end{aligned}\right\} \quad x = 0,\ a \qquad (3.2i)$$

(ii) Antisymmetric cross-ply laminates

$$\left.\begin{aligned} w &= 0, \quad & M_x &= 0 \\ v^o &= 0, \quad & N_x &= 0 \end{aligned}\right\} \quad x = 0,\ a \qquad (3.2j)$$

(b) Free edge boundary conditions:

$$\left.\begin{aligned} N_y &= 0, \quad & N_{xy} &= 0 \\ M_y &= 0, \quad & \frac{\partial M_y}{\partial y} + 2\frac{\partial M_{xy}}{\partial x} &= 0 \end{aligned}\right\} \quad y = \pm \frac{b}{2} \qquad (3.2k)$$

(c) Clamped edge boundary conditions:

$$\left.\begin{aligned} u^o &= v^o = 0 \\ w &= \frac{\partial w}{\partial y} = 0 \end{aligned}\right\} \quad y = \pm \frac{b}{2} \qquad (3.2l)$$

$$L_{31} = -B_{11}\frac{\partial^3}{\partial x^3} - B_{12}\frac{\partial^3}{\partial x \partial y^2} - 3B_{16}\frac{\partial^3}{\partial x^2 \partial y} - B_{26}\frac{\partial^3}{\partial y^3} - 2B_{66}\frac{\partial^3}{\partial x \partial y^2}$$

$$L_{32} = -B_{12}\frac{\partial^2}{\partial x^2 \partial y} - B_{22}\frac{\partial^3}{\partial y^3} - B_{16}\frac{\partial^3}{\partial x^3} - 3B_{26}\frac{\partial^3}{\partial x \partial y^2} - 2B_{66}\frac{\partial^3}{\partial x^2 \partial y}$$

$$L_{33} = D_{11}\frac{\partial^4}{\partial x^4} + 2D_{12}\frac{\partial^4}{\partial x^2 \partial y^2} + D_{22}\frac{\partial^4}{\partial y^4} + 4D_{16}\frac{\partial^4}{\partial x^3 \partial y} + 4D_{26}\frac{\partial^4}{\partial x \partial y^3} + 4D_{66}\frac{\partial^4}{\partial x^2 \partial y^2}$$

Assume

$$u^o = -L_{12}\,\eta(x, y) - L_{13}\,\psi(x, y) \tag{3.6}$$

$$v^o = L_{11}\,\eta(x, y) \tag{3.7}$$

$$w = L_{11}\,\psi(x, y) \tag{3.8}$$

where the functions $\eta(x, y)$ and $\psi(x, y)$ are continuous in the domain of the plate. These representations are chosen to satisfy Eq. (3.3) identically.

Substitution of Eqs. (3.6-3.8) into Eq. (3.4) leads to

$$(L_{22}L_{11} - L_{12}L_{21})\,\eta(x, y) + (L_{23}L_{11} - L_{13}L_{21})\,\psi(x, y) = 0$$

This can be rewritten as

$$P\eta + Q\psi = 0 \tag{3.9}$$

If we now choose

$$\eta = -Q\,\Phi(x, y)$$

$$\psi = P\,\Phi(x, y)$$

Eq. (3.9) is identically satisfied.

This enables us to express relations (3.6-3.8) in terms of as

$$u^{o} = (L_{12}L_{23} - L_{13}L_{22})\,\phi(x, y) \tag{3.10}$$

$$v^{o} = (L_{13}L_{21} - L_{23}L_{11})\,\phi(x, y) \tag{3.11}$$

$$w = (L_{11}L_{22} - L_{12}L_{21})\,\phi(x, y) \tag{3.12}$$

where

$$\phi(x, y) = L_{11}\,\Phi(x, y)$$

substitution of expressions (3.10-3.12) into Eq. (3.5) leads to

$$(L_{11}L_{22}L_{33} - L_{21}L_{12}L_{33} - L_{32}L_{23}L_{11} + L_{31}L_{12}L_{23} + L_{32}L_{13}L_{21} - L_{31}L_{13}L_{22})\,\phi(x, y) = q(x, y) \tag{3.13}$$

Expanding the differential operators, the above equation can be written as

$$A_1\frac{\partial^8\phi}{\partial x^8} + A_2\frac{\partial^8\phi}{\partial x^7\partial y} + A_3\frac{\partial^8\phi}{\partial x^6\partial y^2} + A_4\frac{\partial^8\phi}{\partial x^5\partial y^3} + A_5\frac{\partial^8\phi}{\partial x^4\partial y^4} + A_6\frac{\partial^8\phi}{\partial x^3\partial y^5} + A_7\frac{\partial^8\phi}{\partial x^2\partial y^6} + A_8\frac{\partial^8\phi}{\partial x\,\partial y^7} + A_9\frac{\partial^8\phi}{\partial y^8} = q(x, y) \tag{3.14}$$

where

$$A_1 = B_{11}(2A_{16}B_{16} - A_{66}B_{11}) - A_{11}B_{16}^2 + D_{11}(A_{11}A_{66} + A_{16}^2)$$

$$A_2 = 2B_{11}(A_{16}G + E_1B_{16} - 3A_{66}B_{16} - A_{26}B_{11}) + 2B_{16}(2A_{16}B_{16} - A_{11}G) + 2D_{11}(A_{16}A_{66} + A_{11}A_{26} - A_{16}E_1) + 4D_{16}(A_{11}A_{66} - A_{16}^2)$$

$$A_3 = 2B_{11}(3A_{16}B_{26} + E_1G - 5A_{26}B_{16} - A_{66}G) + 2B_{16}(2A_{16}G + 3E_1B_{16} - 5A_{66}B_{16} - 3A_{11}B_{26}) + D_{11}(2A_{16}A_{26} + A_{66}^2 + A_{11}A_{22} - E_1^2) + 8D_{16}(A_{16}A_{66} + A_{11}A_{26} - A_{16}E_1) - A_{22}B_{11}^2 - A_{11}G^2 + 2F(A_{11}A_{66} - A_{16}^2)$$

$$A_4 = 2B_{11}(A_{16}B_{22} + 3E_1B_{26} - A_{66}B_{26} - 3A_{22}B_{16} - A_{26}G) - 2B_{22}B_{16}A_{11} + 4B_{16}(2A_{16}B_{26} + 2E_1G - 3A_{26}B_{16} - 2A_{66}G) - 6B_{26}A_{11}G + 2D_{11}(A_{22}A_{16} + A_{26}A_{66} - A_{26}E_1) + 4D_{16}(A_{66}^2 + A_{11}A_{22} + 2A_{16}A_{26} - E_1^2) + 4D_{26}(A_{11}A_{66} - A_{16}^2) + 4F(A_{16}A_{66} + A_{11}A_{26} - A_{16}E_1)$$

$$A_5 = 2B_{11}(E_1B_{22} + A_{26}B_{26} - A_{22}G) + 2B_{22}(A_{16}B_{16} - A_{11}G) - 4B_{16}A_{26}G - 4B_{26}A_{16}G - 9(A_{22}B_{16}^2 + A_{11}B_{26}^2) + 4B_{16}B_{26}(5E_1 - 3A_{66}) + D_{11}(A_{22}A_{66} - A_{26}^2) + D_{22}(A_{11}A_{66} - A_{16}^2) + 8D_{16}(A_{22}A_{16} + A_{26}A_{66} - A_{26}E_1) + 8D_{26}(A_{16}A_{66} + A_{11}A_{26} - A_{16}E_1) + 2G(E_1^2 - A_{66}G) + 2F(A_{66}^2 + A_{11}A_{22} + 2A_{16}A_{26} - E_1^2)$$

$$
\begin{aligned}
A_6 &= 2B_{11}(A_{26}B_{22} - A_{22}B_{26}) \\
&\quad + 2B_{22}(3E_1B_{16} - A_{16}G - 3A_{11}B_{26} - A_{66}B_{16}) \\
&\quad + 2B_{16}(4A_{26}B_{26} - 3A_{22}G) + 4B_{26}(2E_1G - 2A_{66}G - 3A_{16}B_{26}) \\
&\quad + 2D_{22}(A_{16}A_{66} + A_{11}A_{26} - A_{16}E_1) \\
&\quad + 4D_{16}(A_{22}A_{66} - A_{26}^2) + 4D_{26}(A_{11}A_{22} + 2A_{16}A_{26} + 2A_{66}^2 \\
&\quad - 2E_1^2) + 4F(A_{22}A_{16} + A_{26}A_{66} - A_{26}E_1)
\end{aligned}
$$

$$
\begin{aligned}
A_7 &= B_{22}(6A_{26}B_{16} + 2E_1G - 10A_{16}B_{26} - 2A_{66}G - A_{11}B_{22}) \\
&\quad - 6B_{16}B_{26}A_{22} + 2B_{26}^2(3E_1 - 5A_{66}) \\
&\quad + D_{22}(A_{11}A_{22} + A_{66}^2 - E_1^2 + 2A_{16}A_{26}) \\
&\quad + 8D_{26}(A_{22}A_{16} + A_{26}A_{66} - A_{26}E_1) + 2F(A_{22}A_{66} - A_{26}^2) \\
&\quad + G(4A_{26}B_{26} - A_{22}G)
\end{aligned}
$$

$$
\begin{aligned}
A_8 &= 2B_{22}(A_{26}G + B_{26}E_1 - 3A_{66}B_{26} - A_{16}B_{22}) \\
&\quad + 2B_{26}(2B_{26}A_{26} - GA_{22}) + 2D_{22}(A_{22}A_{16} + A_{26}A_{66} - A_{26}E_1) \\
&\quad + 4D_{26}(A_{66}A_{22} - A_{26}^2)
\end{aligned}
$$

$$
\begin{aligned}
A_9 &= B_{22}(2A_{26}B_{26} - B_{22}A_{66}) - A_{22}B_{26}^2 \\
&\quad + D_{22}(A_{22}A_{66} - A_{26}^2)
\end{aligned}
$$

$$E_1 = A_{12} + A_{66}; \quad F = D_{12} + 2D_{66}; \quad G = B_{12} + 2B_{66}$$

Equation (3.14) is the governing equation for laminated plates. It can be easily verified that this equation reduces to the classical thin plate equation for an isotropic case. In what follows, we discuss two special cases.

3.3.1 Antisymmetric Angle-Ply Plates

It has been shown in Chapter 2 that for an antisymmetric angle-ply laminate

$$A_{16} = A_{26} = B_{11} = B_{12} = B_{22} = B_{66} = D_{16} = D_{26} = 0 \tag{3.15}$$

For such a laminate, the coefficients of the governing Eq. (3.14) assume the following values:

$$A_2 = A_4 = A_6 = A_8 = 0 \tag{3.16}$$

$$A_1 = A_{11}(A_{66}D_{11} - B_{16}^2) \tag{3.17}$$

$$A_3 = 2B_{16}^2(3E_1 - 5A_{66}) + 2A_{11}(A_{66}F - 3B_{16}B_{26}) + D_{11}(A_{11}A_{22} + A_{66}^2 - E_1^2) \tag{3.18}$$

$$A_5 = 4B_{16}B_{26}(5E_1 - 3A_{66}) + 2F(A_{11}A_{22} + A_{66}^2 - E_1^2) - 9(A_{22}B_{16}^2 + A_{11}B_{26}^2) + A_{66}(A_{11}D_{22} + A_{22}D_{11}) \tag{3.19}$$

$$A_7 = 2B_{26}^2(3E_1 - 5A_{66}) + 2A_{22}(A_{66}F - 3B_{16}B_{26}) + D_{22}(A_{11}A_{22} + A_{66}^2 - E_1^2) \tag{3.20}$$

$$A_9 = A_{22}(A_{66}D_{22} - B_{26}^2) \tag{3.21}$$

Thus, the governing Eq. (3.14) for an antisymmetric angle-ply laminate is reduced to

$$A_1 \frac{\partial^8 \phi}{\partial x^8} + A_3 \frac{\partial^8 \phi}{\partial x^6 \partial y^2} + A_5 \frac{\partial^8 \phi}{\partial x^4 \partial y^4} + A_7 \frac{\partial^8 \phi}{\partial x^2 \partial y^6} + A_9 \frac{\partial^8 \phi}{\partial y^8} = q(x,y) \tag{3.22}$$

The displacement components for this type of plate in terms of the displacement function, ϕ can be obtained from Eqs. (3.10-3.12) and are given by

$$u^o = a_1 \frac{\partial^5 \phi}{\partial x^4 \partial y} + a_2 \frac{\partial^5 \phi}{\partial x^2 \partial y^3} + a_3 \frac{\partial^5 \phi}{\partial y^5} \tag{3.23}$$

$$v^o = a_4 \frac{\partial^5 \phi}{\partial x^5} + a_5 \frac{\partial^5 \phi}{\partial x^3 \partial y^2} + a_6 \frac{\partial^5 \phi}{\partial x \partial y^4} \tag{3.24}$$

$$w = a_7 \frac{\partial^4 \phi}{\partial x^4} + a_8 \frac{\partial^4 \phi}{\partial x^2 \partial y^2} + a_9 \frac{\partial^4 \phi}{\partial y^4} \tag{3.25}$$

where

$$a_1 = B_{16}(3A_{66} - E_1)$$

$$a_2 = B_{26}(A_{66} - 3E_1) + 3B_{16}A_{22}$$

$$a_3 = B_{26}A_{22}$$

$$a_4 = B_{16}A_{11}$$

$$a_5 = B_{16}(A_{66} - 3E_1) + 3A_{11}B_{26}$$

$$a_6 = B_{26}(3A_{66} - E_1)$$

$$a_7 = A_{11}A_{66}$$

$$a_8 = A_{11}A_{22} + A_{66}^2 - E_1^2$$

$$a_9 = A_{22}A_{66}$$

The force and moment resultants in terms of the displacement function, ϕ can be obtained from the constitutive relation (3.2c) and Eqs. (3.23-3.25). These are given by

$$N_x = a_{10} \frac{\partial^6 \phi}{\partial x^3 \partial y^3} + a_{11} \frac{\partial^6 \phi}{\partial x \partial y^5} \tag{3.26}$$

$$N_y = a_{12} \frac{\partial^6 \phi}{\partial x^5 \partial y} + a_{13} \frac{\partial^6 \phi}{\partial x^3 \partial y^3} \tag{3.27}$$

$$N_{xy} = a_{14} \frac{\partial^6 \phi}{\partial x^4 \partial y^2} + a_{15} \frac{\partial^6 \phi}{\partial x^2 \partial y^4} \tag{3.28}$$

$$M_x = a_{16} \frac{\partial^6 \phi}{\partial x^6} + a_{17} \frac{\partial^6 \phi}{\partial x^4 \partial y^2} + a_{18} \frac{\partial^6 \phi}{\partial x^2 \partial y^4} + a_{19} \frac{\partial^6 \phi}{\partial y^6} \tag{3.29}$$

$$M_y = a_{20} \frac{\partial^6 \phi}{\partial x^6} + a_{21} \frac{\partial^6 \phi}{\partial x^4 \partial y^2} + a_{22} \frac{\partial^6 \phi}{\partial x^2 \partial y^4} + a_{23} \frac{\partial^6 \phi}{\partial y^6} \tag{3.30}$$

$$M_{xy} = a_{24} \frac{\partial^6 \phi}{\partial x^5 \partial y} + a_{25} \frac{\partial^6 \phi}{\partial x^3 \partial y^3} + a_{26} \frac{\partial^6 \phi}{\partial x \partial y^5} \tag{3.31}$$

where

$$a_{10} = B_{16}(A_{11}A_{22} - 3A_{12}E_1 + A_{12}A_{66} - 2A_{66}^2 + 2E_1^2) + B_{26}A_{11}(A_{66} + 3A_{12} - 3E_1)$$

$$a_{11} = B_{26}(A_{11}A_{22} + 3A_{12}A_{66} - A_{12}E_1) - 2B_{16}A_{22}A_{66}$$

$$a_{12} = B_{16}(3A_{12}A_{66} + A_{11}A_{22} - A_{12}E_1) - 2B_{26}A_{11}A_{66}$$

$$a_{13} = B_{16}A_{22}(3A_{12} - 3E_1 + A_{66}) + B_{26}(-3A_{12}E_1 + A_{12}A_{66} + A_{11}A_{22} - 2A_{66}^2 + 2E_1^2)$$

$$a_{14} = B_{16}(3A_{66}^2 + E_1^2 - A_{11}A_{22} - 4E_1A_{66}) + 2B_{26}A_{11}A_{66}$$

$$a_{15} = 2B_{16}A_{22}A_{66} + B_{26}(E_1^2 + 3A_{66}^2 - A_{11}A_{22} - 4E_1A_{66})$$

$$a_{16} = A_{11}(B_{16}^2 - A_{66}D_{11})$$

$$a_{17} = 3A_{11}B_{16}B_{26} - 4B_{16}^2A_{12} - D_{11}(A_{11}A_{22} + A_{66}^2 - E_1^2) - D_{12}A_{11}A_{66}$$

$$a_{18} = B_{16}(3B_{16}A_{22} - 4B_{26}A_{12}) - D_{11}A_{22}A_{66} - D_{12}(A_{11}A_{22} + A_{66}^2 - E_1^2)$$

$$a_{19} = A_{22}(B_{16}B_{26} - D_{12}A_{66})$$

$$a_{20} = A_{11}(B_{16}B_{26} - A_{66}D_{12})$$

$$a_{21} = A_{11}(3B_{26}^2 - A_{66}D_{22}) - 4B_{16}B_{26}A_{12} - D_{12}(A_{11}A_{22} + A_{66}^2 - E_1^2)$$

$$a_{22} = A_{22}(3B_{16}B_{26} - D_{12}A_{66}) - 4B_{26}^2A_{12} - D_{22}(A_{11}A_{22} + A_{66}^2 - E_1^2)$$

$$a_{23} = A_{22}(B_{26}^2 - D_{22}A_{66})$$

$$a_{24} = A_{11}(B_{16}B_{26} - 2D_{66}A_{66}) + B_{16}^2(2A_{66} - A_{12})$$

$$a_{25} = 3(B_{16}^2A_{22} + B_{26}^2A_{11}) + 2B_{16}B_{26}(A_{66} - 3E_1) - 2D_{66}(A_{11}A_{22} + A_{66}^2 - E_1^2)$$

$$a_{26} = B_{16}B_{26}A_{22} - B_{26}^2(E_1 - 3A_{66}) - 2D_{66}A_{22}A_{66}$$

3.3.2 Antisymmetric Cross-Ply Plates

It has been shown in Chapter 2 that for an antisymmetric cross-ply plate

$$A_{16} = A_{26} = D_{16} = D_{26} = B_{12} = B_{16} = B_{26} = B_{66} = 0 \tag{3.32}$$

and

$$B_{22} = -B_{11} \tag{3.33}$$

This coefficients of the governing Eq. (3.14) for this type of plate are reduced to

$$A_2 = A_4 = A_6 = A_8 = 0 \tag{3.34}$$

$$A_1 = A_{66}(A_{11}D_{11} - B_{11}^2) \tag{3.35}$$

$$A_3 = 2A_{11}A_{66}F - A_{22}B_{11}^2 + D_{11}(A_{11}A_{22} + A_{66}^2 - E_1^2) \tag{3.36}$$

$$A_5 = 2F(A_{11}A_{22} + A_{66}^2 - E_1^2) - 2E_1B_{11}^2 + A_{66}(A_{11}D_{22} + A_{22}D_{11}) \tag{3.37}$$

$$A_7 = 2A_{22}A_{66}F - A_{11}B_{11}^2 + D_{22}(A_{11}A_{22} + A_{66}^2 - E_1^2) \tag{3.38}$$

$$A_9 = A_{66}(A_{22}D_{22} - B_{11}^2) \tag{3.39}$$

The displacement components in terms of ϕ for antisymmetric cross-ply plates can be obtained from Eqs. (3.10-3.12) and are given by

$$u^o = b_1 \frac{\partial^5 \phi}{\partial x^5} + b_2 \frac{\partial^5 \phi}{\partial x^3 \partial y^2} + b_3 \frac{\partial^5 \phi}{\partial x \partial y^4} \tag{3.40}$$

$$v^o = b_4 \frac{\partial^5 \phi}{\partial x^4 \partial y} + b_5 \frac{\partial^5 \phi}{\partial x^2 \partial y^3} + b_6 \frac{\partial^5 \phi}{\partial y^5} \tag{3.41}$$

$$w = b_7 \frac{\partial^4 \phi}{\partial x^4} + b_8 \frac{\partial^4 \phi}{\partial x^2 \partial y^2} + b_9 \frac{\partial^4 \phi}{\partial y^4} \tag{3.42}$$

where

$$b_1 = B_{11}A_{66}; \quad b_2 = B_{11}A_{22}; \quad b_3 = B_{11}E_1; \quad b_4 = -B_{11}E_1$$

$$b_5 = -B_{11}A_{11}; \quad b_6 = -B_{11}A_{66}; \quad b_7 = A_{11}A_{66}$$

$$b_8 = A_{11}A_{22} + A_{66}^2 - E_1^2; \quad b_9 = A_{22}A_{66}$$

The force and moment resultants in terms of ϕ can be obtained from Eq. (3.2c) and Eqs. (3.40-3.42). These are given by

$$N_x = b_{10} \frac{\partial^6 \phi}{\partial x^4 \partial y^2} + b_{11} \frac{\partial^6 \phi}{\partial x^2 \partial y^4} + b_{12} \frac{\partial^6 \phi}{\partial y^6} \tag{3.43}$$

$$N_y = b_{13} \frac{\partial^6 \phi}{\partial x^6} + b_{14} \frac{\partial^6 \phi}{\partial x^4 \partial y^2} + b_{15} \frac{\partial^6 \phi}{\partial x^2 \partial y^4} \tag{3.44}$$

$$N_{xy} = b_{16} \frac{\partial^6 \phi}{\partial x^5 \partial y} + b_{17} \frac{\partial^6 \phi}{\partial x^3 \partial y^3} + b_{18} \frac{\partial^6 \phi}{\partial x \partial y^5} \tag{3.45}$$

$$M_x = b_{19} \frac{\partial^6 \phi}{\partial x^6} + b_{20} \frac{\partial^6 \phi}{\partial x^4 \partial y^2} + b_{21} \frac{\partial^6 \phi}{\partial x^2 \partial y^4} + b_{22} \frac{\partial^6 \phi}{\partial y^6} \tag{3.46}$$

$$M_y = b_{23} \frac{\partial^6 \phi}{\partial x^6} + b_{24} \frac{\partial^6 \phi}{\partial x^4 \partial y^2} + b_{25} \frac{\partial^6 \phi}{\partial x^2 \partial y^4} + b_{26} \frac{\partial^6 \phi}{\partial y^6} \tag{3.47}$$

$$M_{xy} = b_{27} \frac{\partial^6 \phi}{\partial x^5 \partial y} + b_{28} \frac{\partial^6 \phi}{\partial x^3 \partial y^3} + b_{29} \frac{\partial^6 \phi}{\partial x \partial y^5} \qquad (3.48)$$

where

$$b_{10} = A_{12}A_{66}B_{11}$$

$$b_{11} = B_{11}(A_{11}E_1 - A_{11}^2 - A_{22}A_{66})$$

$$b_{12} = - A_{11}A_{66}B_{11}$$

$$b_{13} = A_{12}A_{16}B_{11}$$

$$b_{14} = B_{11}(A_{11}A_{66} - A_{22}A_{66})$$

$$b_{15} = B_{11}(A_{12}E_1 + A_{66}^2 - E_1^2)$$

$$b_{16} = - A_{12}A_{66}B_{11}$$

$$b_{17} = B_{11}A_{66}(A_{22} - A_{11})$$

$$b_{18} = A_{12}A_{66}B_{11}$$

$$b_{19} = A_{66}(B_{11}^2 - A_{11}D_{11})$$

$$b_{20} = B_{11}^2A_{22} - D_{11}(A_{11}A_{22} + A_{66}^2 - E_1) - A_{11}A_{66}D_{12}$$

$$b_{21} = B_{11}^2E_1 - A_{22}A_{66}D_{11} - D_{12}(A_{11}A_{22} + A_{66}^2 - E_1^2)$$

$$b_{22} = - A_{22}A_{66}D_{12}$$

$$b_{23} = - A_{11}A_{66}D_{12}$$

$$b_{24} = B_{11}^2E_1 - D_{12}(A_{11}A_{22} + A_{66}^2 - E_1^2) - D_{22}A_{11}A_{66}$$

$$b_{25} = B_{11}^2A_{11} - D_{12}A_{22}A_{66} - D_{22}(A_{11}A_{22} + A_{66}^2 - E_1)$$

$$b_{26} = A_{66}(B_{11}^2 - A_{22}D_{22})$$

$$b_{27} = - 2A_{11}A_{66}D_{66}$$

$$b_{28} = -2D_{66}(A_{11}A_{22} + A_{66}^2 - E_1^2)$$

$$b_{29} = -2D_{66}A_{22}A_{66}$$

In the chapters to follow, equation (3.22) is applied to buckling and static problems.

3.4 METHOD OF SOLUTION

As stated in Chapter 1, all the problems considered hereafter will have two opposite edges simply supported. Consequently, it will be proper to attempt a solution which will satisfy these boundary conditions identically. The displacement function can, therefore, be written as

$$\phi(x, y) = \phi_m(y) \sin(\alpha_m x) \tag{3.49}$$

where

$$\alpha_m = m\pi/a$$

When this expression is substituted in Eq. (3.22), the resulting equation for $\phi_m(y)$ will be an ordinary differential equation and will have a solution of the type

$$\phi_m(y) = e^{\lambda \alpha_m y} \tag{3.50}$$

The solution of Eq. (3.22) can, therefore, be written in the form

$$\phi_m(x, y) = e^{\lambda \alpha_m y} \sin(\alpha_m x) \tag{3.51}$$

Substituting relation (3.51) into the homogeneous part of Eq. (3.22), we get

$$\lambda^8 + C_1 \lambda^6 + C_2 \lambda^4 + C_3 \lambda^2 + C_4 = 0 \qquad (3.52)$$

where

$$C_1 = A_7/A_9 \; ; \qquad C_2 = A_5/A_9$$

$$C_3 = A_3/A_9 \; ; \qquad C_4 = A_1/A_9$$

Setting

$$\lambda^2 = \gamma$$

Eq. (3.52) becomes

$$\gamma^4 + C_1 \gamma^3 + C_2 \gamma^2 + C_3 \gamma + C_4 = 0 \qquad (3.53)$$

The above equation is a quadratic in γ and can be solved in closed form by the well-known Ferrari's method.[58]

Assuming that the possibility of multiple roots is remote, the following combination of roots of Eq. (3.53) are considered.

(a) All roots real:

Let $\gamma = \gamma_1, \gamma_2, \gamma_3$ and γ_4 be the four real roots of Eq. (3.53). Then

$$\lambda = \pm \sqrt{\gamma_1}; \quad \pm \sqrt{\gamma_2}; \quad \pm \sqrt{\gamma_3} \quad \text{and} \quad \pm \sqrt{\gamma_4}$$

or $$\lambda = \pm \lambda_1; \quad \pm \lambda_2; \quad \pm \lambda_3 \quad \text{and} \quad \pm \lambda_4$$

If all the roots of the characteristic Eq. (3.53) are distinct, then eight linearly independent solutions are possible. Thus we can write

$$\phi_m(y) = d_1 e^{\lambda_1 \alpha_m y} + d_2 e^{\lambda_2 \alpha_m y} + d_3 e^{\lambda_3 \alpha_m y} + d_4 e^{\lambda_4 \alpha_m y}$$
$$+ d_5 e^{-\lambda_1 \alpha_m y} + d_6 e^{-\lambda_2 \alpha_m y} + d_7 e^{-\lambda_3 \alpha_m y} + d_8 e^{-\lambda_4 \alpha_m y}$$

or

$$\phi_m(y) = A_{m_1} \cosh(\lambda_1 \alpha_m y) + A_{m_2} \sinh(\lambda_1 \alpha_m y)$$
$$+ A_{m_3} \cosh(\lambda_2 \alpha_m y) + A_{m_4} \sinh(\lambda_2 \alpha_m y)$$
$$+ A_{m_5} \cosh(\lambda_3 \alpha_m y) + A_{m_6} \sinh(\lambda_3 \alpha_m y)$$
$$+ A_{m_7} \cosh(\lambda_4 \alpha_m y) + A_{m_8} \sinh(\lambda_4 \alpha_m y) \qquad (3.54)$$

(b) Two real and two complex:

Let

$$\lambda = \pm \sqrt{\gamma_1}; \pm \sqrt{\gamma_2}; \pm \sqrt{(\gamma_3 + i\,\gamma_4)}; \pm \sqrt{(\gamma_3 - i\,\gamma_4)}$$

or $\lambda = \pm \lambda_1; \pm \lambda_2; \pm (\lambda_3 + i\lambda_4); \pm (\lambda_3 - i\lambda_4)$

Then the function $\phi_m(y)$ can be written as

$$\phi_m(y) = A_{m_1} \cosh(\lambda_1 \alpha_m y) + A_{m_2} \sinh(\lambda_1 \alpha_m y)$$
$$+ A_{m_3} \cosh(\lambda_2 \alpha_m y) + A_{m_4} \sinh(\lambda_2 \alpha_m y)$$
$$+ A_{m_5} \cosh(\lambda_3 \alpha_m y) \cos(\lambda_4 \alpha_m y)$$
$$+ A_{m_6} \sinh(\lambda_3 \alpha_m y) \cos(\lambda_4 \alpha_m y)$$
$$+ A_{m_7} \cosh(\lambda_3 \alpha_m y) \sin(\lambda_4 \alpha_m y)$$
$$+ A_{m_8} \sinh(\lambda_3 \alpha_m y) \sin(\lambda_4 \alpha_m y) \qquad (3.55)$$

(c) All roots complex:

The case of all roots in complex conjugate pairs follows directly from case (b) and the solution $\phi_m(y)$ can be written as

$$\begin{aligned}\phi_m(y) = {} & A_{m_1} \cosh(\lambda_1 \alpha_m y) \cos(\lambda_2 \alpha_m y) \\ & + A_{m_2} \sinh(\lambda_1 \alpha_m y) \cos(\lambda_2 \alpha_m y) \\ & + A_{m_3} \cosh(\lambda_1 \alpha_m y) \sin(\lambda_2 \alpha_m y) \\ & + A_{m_4} \sinh(\lambda_1 \alpha_m y) \sin(\lambda_2 \alpha_m y) \\ & + A_{m_5} \cosh(\lambda_3 \alpha_m y) \cos(\lambda_4 \alpha_m y) \\ & + A_{m_6} \sinh(\lambda_3 \alpha_m y) \cos(\lambda_4 \alpha_m y) \\ & + A_{m_7} \cosh(\lambda_3 \alpha_m y) \sin(\lambda_4 \alpha_m y) \\ & + A_{m_8} \sinh(\lambda_3 \alpha_m y) \sin(\lambda_4 \alpha_m y) \end{aligned} \tag{3.56}$$

The particular solution of Eq. (3.22) depends upon the nature of the loading function $q(x, y)$.

In subsequent chapters, this method is applied for the solution of static and buckling problems of layered plates.

- o -

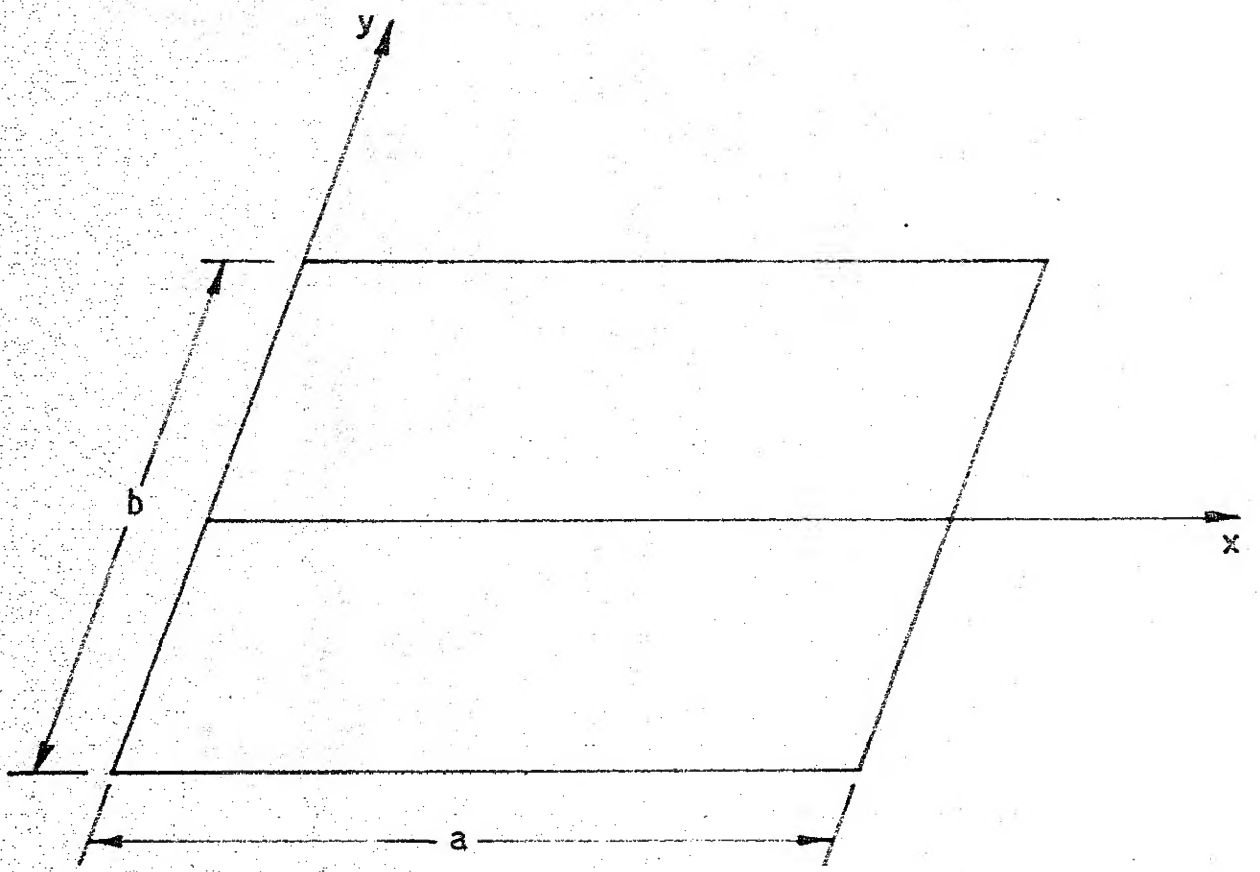

FIG. 3·1: CO-ORDINATE SYSTEM OF THE PLATE.

CHAPTER 4

STATIC ANALYSIS OF ANTISYMMETRIC ANGLE-PLY PLATES

4.1 INTRODUCTION

As pointed out in earlier sections, lamination asymmetry of geometrical and material properties in laminated plates can result in coupling between bending and extension of the laminate. This phenomenon is demonstrated by bending of a laminate that is subjected to only in-plane forces or extension of a laminate that is bent by application of moments only.

Anisotropic composite plates that are simply supported on all sides have been studied extensively.[1,22,24,59] Sun[60] employed the double Fourier series representation for displacement of an anisotropic plate simply supported on all sides. Results for the maximum deflection and bending moments show that bending-twisting coupling decreases the plate stiffness.

Kan and Ito[61] employed the Boussinesq method to obtain integral equilibrium equations of the plate. Single Fourier series used in load and displacements reduces the system of partial differential equations to a system of ordinary differential equations. In conclusion, authors list plate characteristics which influence degree of coupling and estimates of the magnitude of the coupling.

Whitney[62] presented an analysis for bending deflections and buckling loads of a simply supported, square,

single-ply composite plates employing both the Fourier analysis and Ritz method. He observed that the Fourier analysis provides a faster convergence than the Ritz method.

From the available literature, it appears that practically no work has been done to analyse the unsymmetric angle-ply plates with two opposite edges simply supported and the remaining edges free. In this chapter, the static analysis of unsymmetric angle-ply plate is investigated with the above boundary conditions. A particular case of this problem is presented by Keays[63] who analysed an orthotropic plate with two opposite edges simply supported and the other two free. The loading, plate geometry and material properties employed for solving this problem are assumed to be the same as used by Keays[63] with a view to compare the results obtained by this technique with that of Keays[63]. The formulation itself is quite general and can be applied for the analysis of angle-ply laminated plates.

4.2 ANALYSIS

4.2.1 Governing Equations

Consider the case of an antisymmetric angle-ply plate of length a, width b and thickness t with two opposite edges simply supported and the remaining two free (Figure 4.1). The applied load is considered as two line distributions of uniform

intensity across the plate width applied at a fixed distance from either end of the plate as shown in Figure 4.2.

The governing equilibrium equation for a thin angle-ply plate in bending is derived in Chapter 3 and is given by

$$A_1 \frac{\partial^8 \phi}{\partial x^8} + A_3 \frac{\partial^8 \phi}{\partial x^6 \partial y^2} + A_5 \frac{\partial^8 \phi}{\partial x^4 \partial y^4} + A_7 \frac{\partial^8 \phi}{\partial x^2 \partial y^6} + A_9 \frac{\partial^8 \phi}{\partial y^8} = q(x, y) \qquad (3.22)$$

where A_1, A_3, A_5, A_7 and A_9 are defined in Chapter 3 by relations (3.17-3.21). The in-plane forces and moments for this type of plate in terms of ϕ have been derived in Chapter 3 and are given by relations (3.26-3.31).

4.2.2 Boundary Conditions

(a) The boundary conditions at the ends of the plate are those of simply supported edges, namely

(i) In-plane boundary conditions:

$$u^o = N_{xy} = 0; \qquad x = 0, a \qquad (4.1)$$

(ii) Transverse boundary conditions:

$$w = M_x = 0; \qquad x = 0, a \qquad (4.2)$$

(b) The boundary conditions at the free edges are given by

(i) In-plane boundary conditions:

$$N_y = N_{xy} = 0; \qquad y = \pm b/2 \qquad (4.3)$$

(ii) Transverse boundary conditions:

$$M_y = \frac{\partial M_y}{\partial y} + 2\frac{\partial M_{xy}}{\partial x} = 0; \quad y = \pm b/2 \qquad (4.4)$$

4.2.3 Loading

The particular load case considered here is a pair of line loads symmetrically placed one inch from either end as shown in Figure 4.2. The line loads are assumed to be of uniform intensity across the width of the plate. The loading being symmetric with respect to the middle of the plate can be represented by a single Fourier sine series containing odd terms as

$$q = \sum_{m=1,3,5\ldots} Q_m \sin(\alpha_m x) \qquad (4.5)$$

where

$$Q_m = \frac{2}{a}\int_0^a f(x)\sin(\alpha_m x)\,dx \qquad (4.6a)$$

For the present case

$$Q_m = q_o \frac{4}{a}\sin m\pi c/a \qquad (4.6b)$$

where

c = Distance between the line of action of the applied load and either end of the plate = 1 in.

4.2.4 Method of Solution

A solution satisfying the boundary conditions at x = 0, a can be written in the form

$$\phi(x, y) = \sum_{m=1,3,5\ldots} \phi_m(y) \sin(\alpha_m x) \tag{4.7}$$

The solution of homogeneous part of Eq. (3.22) has been presented in Section 3.4 of Chapter 3.

The particular solution can be obtained as follows: substituting a single term from the series given by Eq. (4.7) into Eq. (3.22) gives

$$A_1(\alpha_m)^8 \phi_m(y) - A_3(\alpha_m)^6 \phi_m^{II}(y) + A_5(\alpha_m)^4 \phi_m^{IV}(y)$$

$$- A_7(\alpha_m)^2 \phi_m^{VI}(y) + A_9 \phi_m^{VIII}(y) = Q_m \tag{4.8}$$

where superscripts on ϕ indicate the order of the derivative with respect to y. Substitution of

$$\phi_m = H_m + A_m e^{\alpha_m y}$$

into Eq. (4.8), leads to

$$H_m = Q_m / A_1(\alpha_m)^8 \tag{4.9}$$

Substituting now the value of Q_m from Eq. (4.6b) into Eq. (4.9) yields

$$H_m = \frac{2}{3} \frac{q_o}{A_1(\alpha_m)^8} \sin \alpha_m \tag{4.10}$$

Incorporating the homogeneous solution obtained in Section 3.4, the total solution can be written as

$$\phi(x, y) = \sum_{m=1,3,5\ldots} [H_m + A_{m_1} \cosh(\lambda_1 \alpha_m y) + A_{m_2} \sinh(\lambda_1 \alpha_m y) + A_{m_3} \cosh(\lambda_2 \alpha_m y) + A_{m_4} \sinh(\lambda_2 \alpha_m y) + A_{m_5} \cosh(\lambda_3 \alpha_m y) \cos(\lambda_4 \alpha_m y) + A_{m_6} \sinh(\lambda_3 \alpha_m y) \cos(\lambda_4 \alpha_m y) + A_{m_7} \sinh(\lambda_3 \alpha_m y) \sin(\lambda_4 \alpha_m y) + A_{m_8} \cosh(\lambda_3 \alpha_m y) \sin(\lambda_4 \alpha_m y)] \sin(\alpha_m x) \qquad (4.11)$$

assuming two roots (λ_1, λ_2) real and two in complex conjugate pair $(\lambda_3 \pm i\lambda_4)$.

Since loading and boundary conditions are symmetric with respect to x and y axes, the displacement function $\phi(x, y)$ will also be symmetric. The asymmetric part of the solution is zero and the total solution can then be written as

$$\phi(x, y) = \sum_{m=1,3,5\ldots} [H_m + A_{m_1} \cosh(\lambda_1 \alpha_m y) + A_{m_3} \cosh(\lambda_2 \alpha_m y) + A_{m_5} \cosh(\lambda_3 \alpha_m y) \cos(\lambda_4 \alpha_m y) + A_{m_7} \sinh(\lambda_3 \alpha_m y) \sin(\lambda_4 \alpha_m y)] \sin(\alpha_m x) \qquad (4.12)$$

Because of symmetry it is sufficient to satisfy the boundary conditions at $y = + b/2$. The four boundary conditions (4.3) and (4.4) give four simultaneous equations which can be solved to give A_{m_1}, A_{m_3}, A_{m_5} and A_{m_7}. The in-plane forces and moments can be evaluated from relations (3.26-3.31).

4.3 NUMERICAL COMPUTATIONS

The plate dimensions assumed are[63]

$$a = 6.0 \text{ in.}$$

$$b = 0.75 \text{ in.}$$

$$t = 0.1 \text{ in.}$$

Typical properties for unidirectional carbon-fibre reinforced plastic (CFRP) are

$$E_1 = 19 \times 10^6 \text{ psi}; \qquad E_2 = 3 \times 10^6 \text{ psi}$$

$$G_{12} = 2 \times 10^6 \text{ psi}; \qquad \nu_{12} = 0.20$$

$$\nu_{21} = \nu_{12} E_2/E_1 = 0.0315$$

The stiffness matrices A_{ij}, B_{ij} and D_{ij} for the antisymmetrically laminated angle-ply plate for various fibre orientations are computed by the procedure set out in Chapter 2. The load intensity, q_o is set to unity. A computer programme is written to evaluate the force and moment resultants at various points of the plate. A check on convergence showed that deflection of the plate, force and moment resultants converged to four figure accuracy within about 12 terms. On this basis, thirteen term solution was used throughout this study.

4.4 DISCUSSION AND CONCLUSIONS

The nondimensionalized values of static deflection, w and moment M_y along the centre line of the plate are given in Tables 4.1 and 4.2 respectively. The nondimensionalized values of moment resultants and transverse shear along a free edge of the plate are given in Tables 4.3 and 4.4 respectively. However, for the purpose of comparison with the available literature[63], only the dimensional values of w, M_y, M_{xy} and Q_y are plotted in Figures 4.3, 4.4, 4.5 and 4.6 respectively.

The centre line deflection, w is plotted in Figure 4.3 for three different fibre orientations (0°, 15° and 30°) with number of layers as a parameter. The figure also shows the forty-eight term orthotropic solution given by Keays[63]. It can be seen that the plate deflections increase with increase in fibre orientations. This may be attributed to the general decrease of overall stiffness of the plate with fibre orientation for a plate with free edges. The orthotropic solution merges into the 0° fibre orientation solution which is independent of the number of layers. Further, it may be noted that 0° fibre oriented angle-ply plate is analogous to the orthotropic plate of Keays[63]. It is also observed that the deflection, w tends to be independent of the number of layers when the same is increased beyond N = 4. The difference in maximum deflection between four and six-layered configuration, for example, is of the order of two percent. This corroborates the results of Whitney.[1,22,24]

The variation of moment resultant, M_y along the centre line and that of M_{xy} along the free edge of the plate are shown in Figures 4.4 and 4.5 respectively for three different fibre orientations (0°, 15° and 30°). Again the orthotropic moment resultants[63] shown in the same figures merge into 0° fibre orientation solution. However, the moment resultants unlike the plate deflection, w are found to increase with the increase in the number of layers for a given fibre orientation and tend to become independent of the number of layers beyond N = 4. This may be attributed to the fact that for a given fibre orientation, the effective stiffness of the plate and hence moment resultants increase with the increase in number of layers in a given thickness of the plate.

A study of the Tables 4.2-4.4 show that the moment resultants and transverse shear increase with fibre orientations upto $\theta = 45°$ whereafter the trend is reversed. This may be due to the coupling between bending and extension which increases continuously upto $\theta = 45°$ and falls progressively thereafter.

Figure 4.6 shows the variation of transverse shear along a free edge of the plate. The trend of variation with the number of layers and fibre orientations is the same as for the moment resultants. The sudden increase in the value of the transverse shear at the point of application of the applied load is as expected.

Figures 4.3 to 4.6 show that the orthotropic resultants[63] with 48 terms match closely with those of 0° fibre oriented plate (or anologous orthotropic plate) with 13 terms in the series. The convergence of the present formulation is, therefore, faster.

- o -

TABLE 4.1. VARIATION OF NON-DIMENSIONAL DISPLACEMENT (wE_2t^4/q_0b^4) ALONG THE CENTRE LINE OF AN ANTISYMMETRICALLY LAMINATED ANGLE-PLY PLATE WITH a/b = 8.0

Distance Along the Centre Line, x (in.)	N	θ =15° (10^{-2})	θ =30° (10^{-2})	θ=45° (10^{-2})	θ=60° (10^{-2})	θ=75° (10^{-2})
	2	0.9968	1.6158	1.9532	2.8197	4.1899
0.50	4	0.8638	1.2459	1.2791	2.2490	4.0779
	6	0.8432	1.1994	1.2013	2.1788	4.0609
	2	1.8925	3.0679	3.7044	5.3513	7.9540
1.0	4	1.6393	2.3666	2.4244	4.2676	7.9540
	6	1.6005	2.2784	2.2755	4.1330	7.7054
	2	2.6031	3.9358	5.0821	7.3500	10.9321
1.50	4	2.2556	3.2569	3.3175	5.8576	10.6382
	6	2.2025	3.1365	3.1128	5.6727	10.6003
	2	3.1109	5.0432	6.0615	8.7751	13.0655
2.0	4	2.6965	3.8950	3.9490	6.9897	12.7146
	6	2.6330	3.7509	3.7034	6.7678	12.6673
	2	3.4161	5.5381	6.6484	9.6237	14.3455
2.50	4	2.9611	4.2780	4.3273	7.6686	13.9567
	6	2.8909	4.1206	4.0573	7.4245	13.8999
	2	3.5092	5.7031	6.8447	9.9081	14.7721
3.0	4	3.0492	4.4060	4.4525	7.8952	14.3739
	6	2.9772	4.2439	4.1747	7.6440	14.3170

TABLE 4.2. VARIATION OF NON-DIMENSIONAL MOMENT RESULTANT ($M_y E_2 t/A_{11} q_o b$) ALONG THE CENTRE LINE OF AN ANTISYMMETRICALLY LAMINATED PLATE WITH a/b = 8.0

Distance Along the Centre Line, x (in.)	N	$\theta=15^\circ$ (10^{-2})	$\theta=30^\circ$ (10^{-2})	$\theta=45^\circ$ (10^{-2})	$\theta=60^\circ$ (10^{-2})	$\theta=75^\circ$ (10^{-2})
	2	0.0946	0.3406	0.7941	0.7992	0.2308
0.50	4	0.1428	0.6699	1.7435	1.7498	0.4183
	6	0.1491	0.7180	1.8854	1.8649	0.3933
	2	0.2989	1.0292	2.6867	4.0383	2.8916
1.0	4	0.4168	1.7932	3.1433	7.6640	4.3289
	6	0.4326	1.8986	5.4919	8.1714	4.4724
	2	0.1007	0.3664	0.8355	0.7898	0.1954
1.50	4	0.1583	0.7649	1.9359	1.8528	0.4574
	6	0.1629	0.8117	2.0589	1.8779	0.34108
	2	0.0264	0.1064	0.2005	0.0791	0.0546
2.0	4	0.0523	0.2911	0.6451	0.4213	0.0980
	6	0.0553	0.2977	0.6455	0.4224	0.07158
	2	0.0056	0.0271	0.0320	0.0445	0.0756
2.50	4	0.0195	0.1245	0.2481	0.1568	0.0840
	6	0.0199	0.1250	0.2485	0.1570	0.1125
	2	0.0012	0.0097	0.0017	0.0020	0.0784
3.0	4	0.0128	0.0098	0.1605	0.1181	0.0867
	6	0.0129	0.0099	0.1610	0.1185	0.1172

TABLE 4.3. VARIATION OF NON-DIMENSIONAL TWISTING MOMENT RESULTANT ($M_{xy}E_2t/A_{11}q_ob$) ALONG THE FREE EDGE OF AN ANTISYMMETRICALLY LAMINATED PLATE WITH a/b = 8.0

Distance Along the Edge, x (in.)	N	$\theta=15°$ (-10^{-2})	$\theta=30°$ (-10^{-2})	$\theta=45°$ (-10^{-2})	$\theta=60°$ (-10^{-2})	$\theta=75°$ (-10^{-2})
	2	0.6631	2.3840	5.7063	6.0714	3.8355
0.50	4	0.9669	4.7308	11.9332	13.8008	5.7103
	6	1.0220	4.9612	13.0458	15.0476	6.0569
	2	0.3799	1.3729	3.2410	3.7910	2.0039
1.0	4	0.5647	2.7207	6.9363	7.5636	2.9877
	6	0.5988	2.9675	7.6203	8.2623	3.1701
	2	0.0932	0.3459	0.7421	0.5962	0.1693
1.50	4	0.1553	0.8228	1.8578	1.2944	0.2592
	6	0.1676	0.9206	2.0895	1.4355	0.2764
	2	0.0265	0.1058	0.2035	0.1206	0.0318
2.0	4	0.0490	0.2914	0.5854	0.2835	0.0498
	6	0.0537	0.3326	0.6717	0.3180	0.0532
	2	0.0073	0.0307	0.0545	0.0288	0.0112
2.50	4	0.0144	0.0944	0.1732	0.0687	0.0174
	6	0.0160	0.1095	0.2018	0.0772	0.0185
	2	0.0	0.0	0.0	0.0	0.0
3.0	4	0.0	0.0	0.0	0.0	0.0
	6	0.0	0.0	0.0	0.0	0.0

TABLE 4.4. VARIATION OF NON-DIMENSIONAL TRANSVERSE SHEAR ($Q_y E_2 t^2/A_{11} q_o b$) ALONG THE FREE EDGE OF AN ANTISYMMETRICALLY LAMINATED ANGLE-PLY PLATE WITH a/b = 8.0

Distance Along the Edge, x (in.)	N	$\theta=15°$ (-10^{-2})	$\theta=30°$ (-10^{-2})	$\theta=45°$ (-10^{-2})	$\theta=60°$ (-10^{-2})	$\theta=75°$ (-10^{-2})
	2	0.0215	0.0749	0.1779	0.1871	0.0657
0.50	4	0.0321	0.1505	0.3873	0.3796	0.0979
	6	0.0340	0.1640	0.4262	0.4164	0.1039
	2	0.1116	0.4038	0.9963	1.3688	0.8944
1.0	4	0.1552	0.7113	1.9543	2.6138	1.3437
	6	0.1627	0.7618	2.1130	2.9082	1.4275
	2	0.0243	0.0862	0.2018	0.2096	0.0790
1.50	4	0.0369	0.1770	0.4463	0.4273	0.1183
	6	0.0393	0.1833	0.4924	0.4690	0.1256
	2	0.0087	0.0325	0.0711	0.0642	0.0286
2.0	4	0.0141	0.0736	0.1710	0.1377	0.0443
	6	0.0152	0.0818	0.1911	0.1519	0.0473
	2	0.0047	0.0180	0.0396	0.0434	0.0285
2.50	4	0.0075	0.0406	0.0924	0.0894	0.0442
	6	0.0080	0.0452	0.1031	0.0979	0.0471
	2	0.0039	0.0151	0.0338	0.0414	0.0295
3.0	4	0.0060	0.0328	0.0757	0.0836	0.0457
	6	0.0064	0.0365	0.0840	0.0912	0.0487

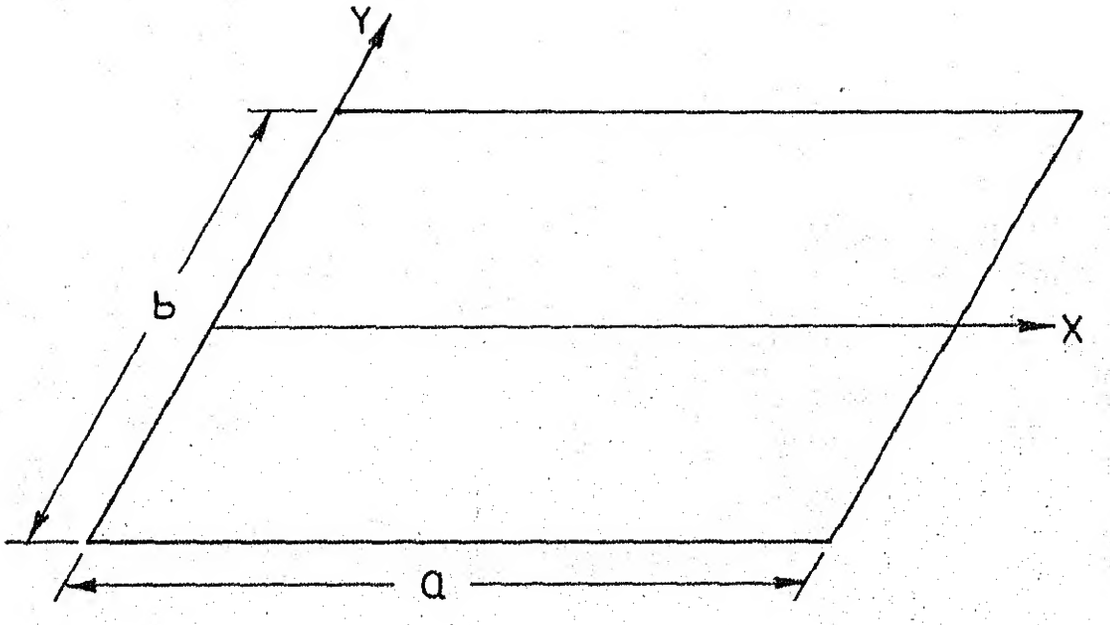

FIG. 4·1: CO-ORDINATE SYSTEM OF THE PLATE

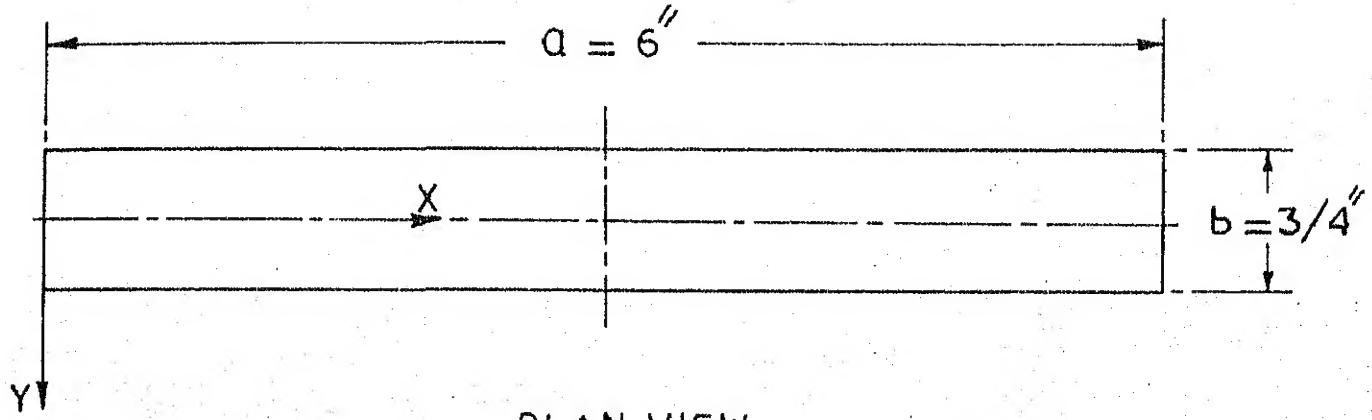

PLAN VIEW

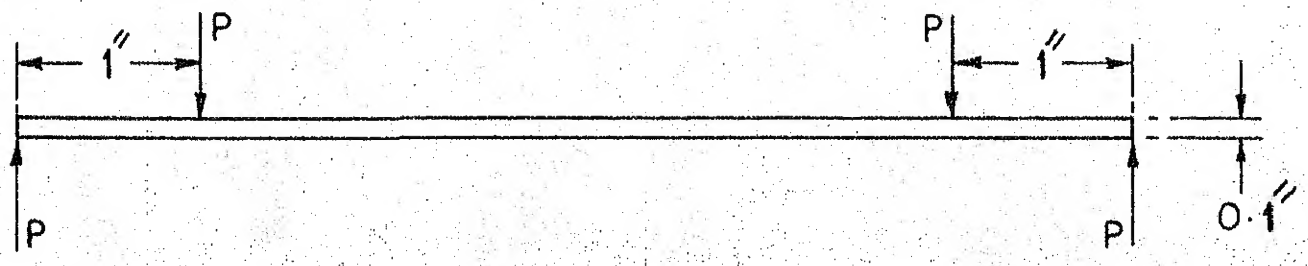

SIDE VIEW

FIG. 4·2: LOADING ARRANGEMENT

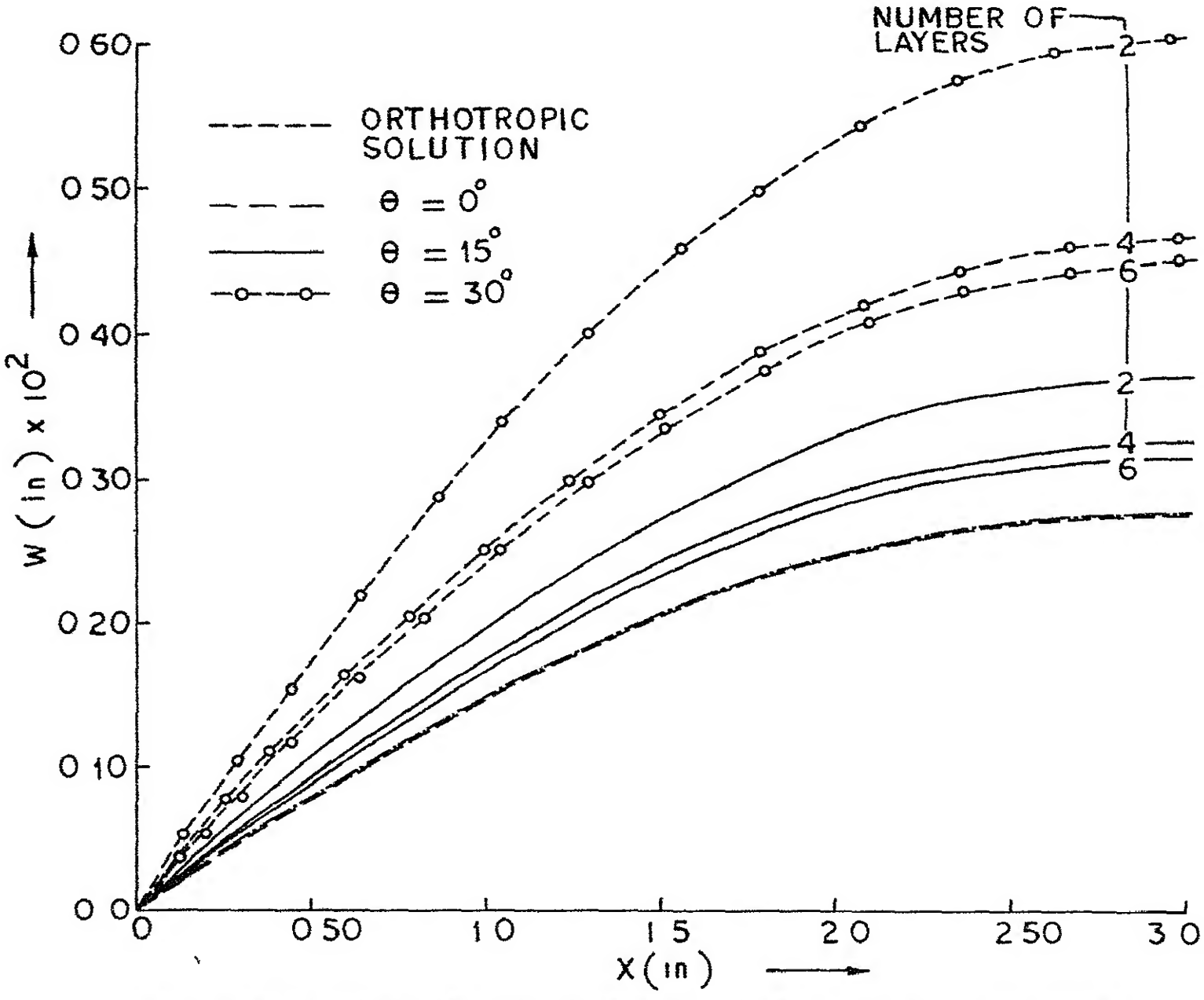

FIG 4 3 VARIATION OF CENTRE - LINE DEFLECTION

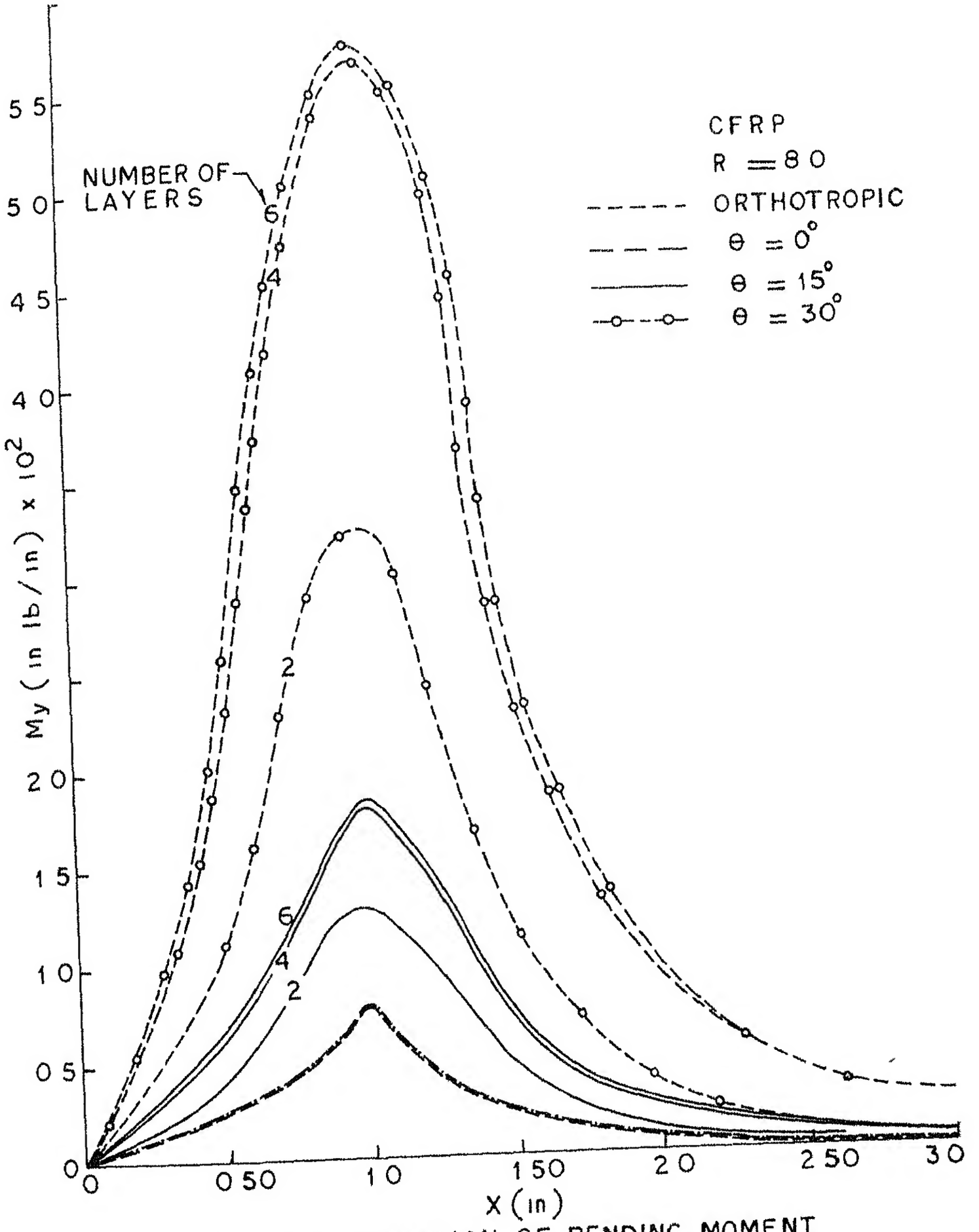

FIG 4 4 VARIATION OF BENDING MOMENT ALONG THE CENTRE LINE

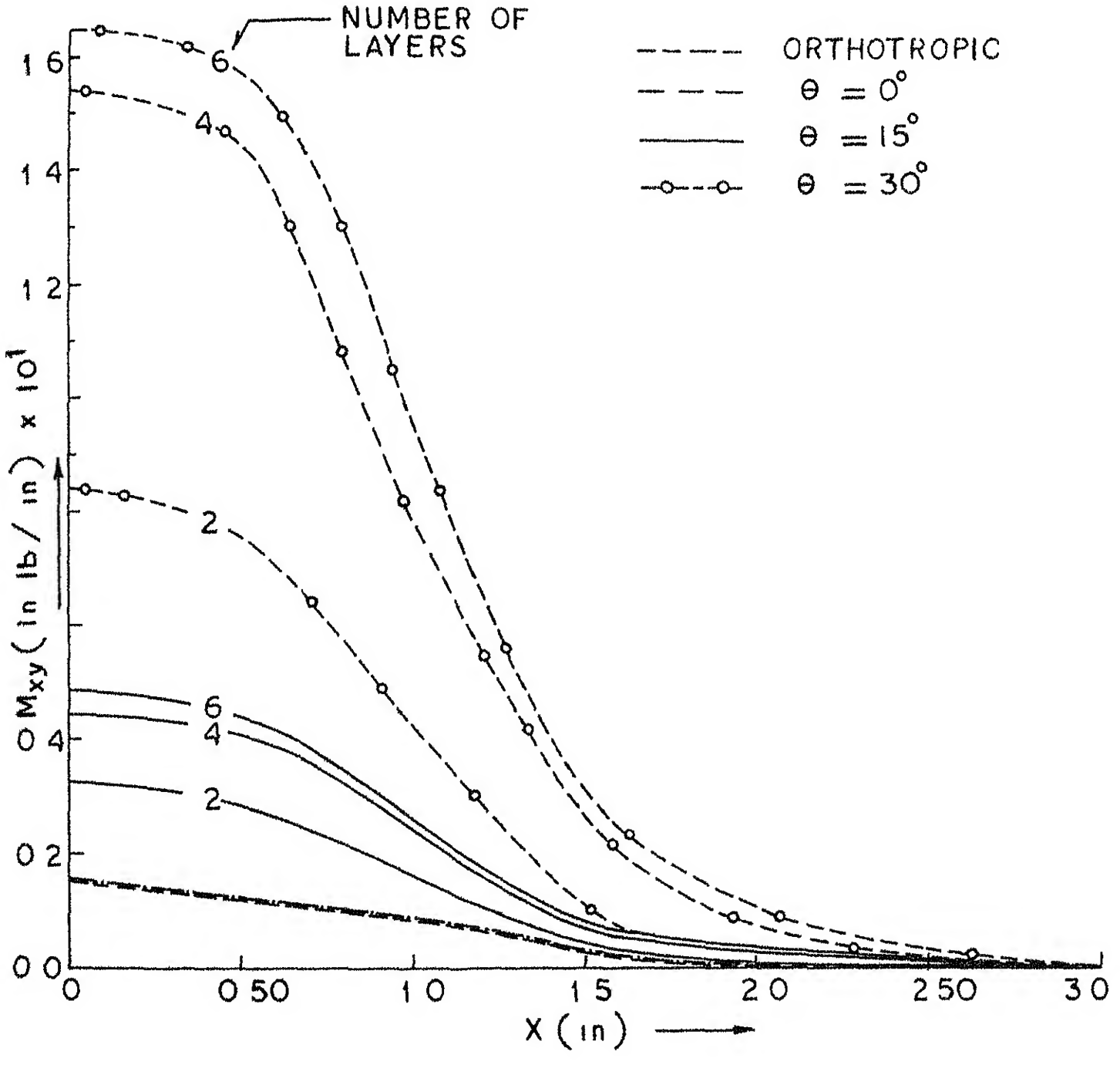

FIG 4 5 VARIATION OF TWISTING MOMENT ALONG A FREE EDGE OF THE PLATE

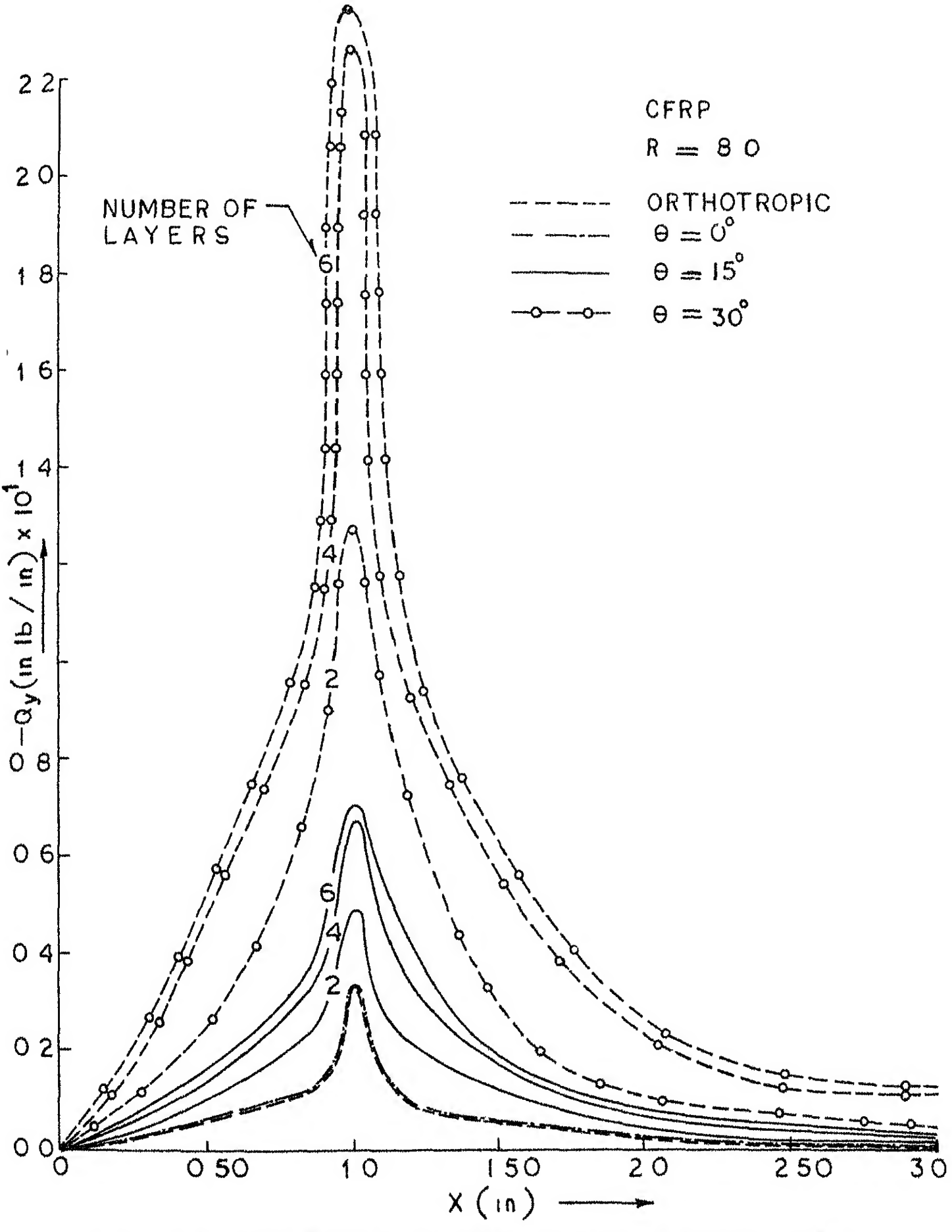

FIG 4 6 VARIATION OF TRANSVERSE SHEAR ALONG A FREE EDGE OF THE PLATE

CHAPTER 5

BUCKLING OF ANTISYMMETRIC CROSS- AND ANGLE-PLY PLATES

5.1 INTRODUCTION

It is well-known that the critical regions of aerospace structures utilizing thin plate construction are prone to buckling. The application of new design concepts and new materials such as fibre reinforced laminated composites in aerospace structures have precipitated the need for corresponding improvements in analysis techniques. A particular characteristics of these laminated plates in contrast to homogeneous plates is the possible coupling between in-plane extension and out-of-plane bending.[23,64] Such couplings can significantly affect the load response characteristics of these plates.[65]

Considerable amount of information is available on the buckling of isotropic[66-71] and orthotropic[3,8,72] plates with various boundary conditions and subjected to various types of loadings. However, buckling of laminated composite plates has been receiving increased attention in the recent past.

Ashton and Waddoups[17] presented a Rayleigh-Ritz solution for buckling of arbitrarily laminated rectangular plates subjected to biaxial compression and in-plane shear

buckling response of antisymmetrically laminated cross- and angle-ply plates for many boundary conditions for which the solutions do not seem to be available.

5.2 BUCKLING ANALYSIS

5.2.1 Derivation of Governing Equation

For an antisymmetric cross-ply or angle-ply plate subjected to an in-plane load N_x per unit width (Figure 5.1), the governing equation (3.22) can be written as

$$A_1 \frac{\partial^8 \phi}{\partial x^8} + A_3 \frac{\partial^8 \phi}{\partial x^6 \partial y^2} + A_5 \frac{\partial^8 \phi}{\partial x^4 \partial y^4} + A_7 \frac{\partial^8 \phi}{\partial x^2 \partial y^6} + A_9 \frac{\partial^8 \phi}{\partial y^8} = q(x, y) \tag{3.22}$$

where $$q(x, y) = - N_x \frac{\partial^2 w}{\partial x^2} \tag{5.1}$$

Substituting the expression for w from Eq. (3.25) for antisymmetric angle-ply plate, Eq. (3.22) can be rewritten as

$$A_1 \frac{\partial^8 \phi}{\partial x^8} + A_3 \frac{\partial^8 \phi}{\partial x^6 \partial y^2} + A_5 \frac{\partial^8 \phi}{\partial x^4 \partial y^4} + A_7 \frac{\partial^8 \phi}{\partial x^2 \partial y^6} + A_9 \frac{\partial^8 \phi}{\partial y^8} + N_x \left(a_7 \frac{\partial^6 \phi}{\partial x^6} + a_8 \frac{\partial^6 \phi}{\partial x^4 \partial y^2} + a_9 \frac{\partial^6 \phi}{\partial x^2 \partial y^4} \right) \tag{5.2}$$

A similar governing equation for an antisymmetric cross-ply plate can be obtained by substituting the expression for w from Eq. (3.42) and is given by

$$A_1 \frac{\partial^8 \phi}{\partial x^8} + A_3 \frac{\partial^8 \phi}{\partial x^6 \partial y^2} + A_5 \frac{\partial^8 \phi}{\partial x^4 \partial y^2} + A_7 \frac{\partial^8 \phi}{\partial x^2 \partial y^6} + A_9 \frac{\partial^8 \phi}{\partial y^8}$$

$$+ N_x\left(b_7 \frac{\partial^6 \phi}{\partial x^6} + b_8 \frac{\partial^6 \phi}{\partial x^4 \partial y^2} + b_9 \frac{\partial^6 \phi}{\partial x^2 \partial y^4}\right) = 0 \qquad (5.3)$$

The coefficients A_1, A_3, A_5, A_7 and A_9 in Eq. (5.3) for an antisymmetric cross-ply plate are given by relations (3.35-3.39).

5.2.2 Method of Solution

The general method of solution is explained in Section (3.4) of Chapter 3. The coefficients of the eighth order polynomial in λ given by Eq. (3.52) take the following values for an antisymmetric angle-ply plate:

$$\begin{aligned} C_1 &= -A_7/A_9 \\ C_2 &= A_5/A_9 - \mu a_9/A_9 \\ C_3 &= -A_3/A_9 + \mu a_8/A_9 \\ C_4 &= A_1/A_9 - \mu a_7/A_9 \\ \mu &= N_x/\alpha_m^2 \end{aligned} \qquad (5.4)$$

The corresponding coefficients C_1 through C_4 for an antisymmetric cross-ply plate are obtained by replacing a_7, a_8 and a_9 in the above expressions by b_7, b_8 and b_9 respectively.

5.2.3 Boundary Conditions

The following sets of boundary conditions are considered on the edges $y = \pm b/2$ whilst the edges $x = 0, a$ are simply supported in each case:

(i) Both edges free

(ii) Both edges clamped

(iii) One edge clamped and the other edge free.

The boundary conditions for all these cases have been derived in terms of the function $\phi(x, y)$ in Chapter 3, which are repeated here for convenience of reference. The coefficients of Eq. (3.53) for the buckling problem contain two unknowns namely N_x and m. The term 'm' can be identified with the number of half waves along x-direction at buckling and take integer values depending on the mode of buckling. As indicated in Chapter 3, the closed form solution of Eq. (3.53) can be readily obtained. Substitution of solution $\phi_m(y)$ given by expressions (3.54), (3.55) or (3.56) in first two of the boundary conditions leads to a set of four algebraic equations in view of the symmetry of the boundary conditions, while for the third set of boundary conditions, a set of eight algebraic equations is obtained. The free edge boundary conditions, namely

$$\left.\begin{aligned} N_y &= 0 \\ N_{xy} &= 0 \\ M_y &= 0 \\ \text{and} \quad \frac{\partial M_y}{\partial y} + 2\frac{\partial M_{xy}}{\partial x} &= 0 \end{aligned}\right\} \quad y = b/2 \qquad (5.5)$$

lead to the following four algebraic equations for an anti-symmetric angle-ply laminate :

$$C_{11}A_{m_1} + C_{12}A_{m_2} + C_{13}A_{m_3} + C_{14}A_{m_4} + C_{15}A_{m_5} + C_{16}A_{m_6} + C_{17}A_{m_7} + C_{18}A_{m_8} = 0 \qquad (5.6)$$

$$C_{21}A_{m_1} + C_{22}A_{m_2} + C_{23}A_{m_3} + C_{24}A_{m_4} + C_{25}A_{m_5} + C_{26}A_{m_6} + C_{27}A_{m_7} + C_{28}A_{m_8} = 0 \qquad (5.7)$$

$$C_{31}A_{m_1} + C_{32}A_{m_2} + C_{33}A_{m_3} + C_{34}A_{m_4} + C_{35}A_{m_5} + C_{36}A_{m_6} + C_{37}A_{m_7} + C_{38}A_{m_8} = 0 \qquad (5.8)$$

$$C_{41}A_{m_1} + C_{42}A_{m_2} + C_{43}A_{m_3} + C_{44}A_{m_4} + C_{45}A_{m_5} + C_{46}A_{m_6} + C_{47}A_{m_7} + C_{48}A_{m_8} = 0 \qquad (5.9)$$

where

$$C_{11} = \lambda_1 \sinh(S_1)\,[1 - a_{123}\lambda_1^2]$$

$$C_{12} = \lambda_1 \cosh(S_1)\,[1 - a_{123}\lambda_1^2]$$

$$C_{13} = \lambda_2 \sinh(S_2)\,[1 - a_{123}\lambda_2^2]$$

$$C_{14} = \lambda_2 \cosh(S_2)\,[1 - a_{123}\lambda_2^2]$$

$$C_{15} = \sinh(S_3)\cos.(S_4)\,[\lambda_3 - a_{123}J_4] - \cosh(S_3)\sin(S_4)\,[\lambda_4 + a_{123}J_3]$$

$$C_{16} = \cosh(S_3)\cos(S_4)[\lambda_3 - a_{123}J_4] - \sinh(S_3)\sin(S_4)[\lambda_4 + a_{123}J_3]$$

$$C_{17} = \cosh(S_3)\cos(S_4)[\lambda_4 + a_{123}J_3] + \sinh(S_3)\sin(S_4)[\lambda_3 - a_{123}J_4]$$

$$C_{18} = \sinh(S_3)\cos(S_4)[\lambda_4 + a_{123}J_3] + \cosh(S_3)\sin(S_4)[\lambda_3 - a_{123}J_4]$$

$$C_{21} = \lambda_1^2 \cosh(S_1)[1 - a_{154}\lambda_1^2]$$

$$C_{22} = \lambda_1^2 \sinh(S_1)[1 - a_{154}\lambda_1^2]$$

$$C_{23} = \lambda_2^2 \cosh(S_2)[1 - a_{154}\lambda_2^2]$$

$$C_{24} = \lambda_2^2 \sinh(S_2)[1 - a_{154}\lambda_2^2]$$

$$C_{25} = \cosh(S_3)\cos(S_4)[J_1 - a_{154}J_5] + \sinh(S_3)\sin(S_4)[J_2 - a_{154}J_6]$$

$$C_{26} = \sinh(S_3)\cos(S_4)[J_1 - a_{154}J_5] + \cosh(S_3)\sin(S_4)[J_2 - a_{154}J_6]$$

$$C_{27} = \cosh(S_3)\sin(S_4)[J_1 - a_{154}J_5] + \sinh(S_3)\cos(S_4)[-J_2 + a_{154}J_6]$$

$$C_{28} = \sinh(S_3)\sin(S_4)\,[J_1 - a_{154}J_5] + \cosh(S_3)\cos(S_4)\,[-J_2 + a_{154}J_6]$$

$$C_{31} = \cosh(S_1)\,[-1 + a_{210}\lambda_1^2 - a_{220}\lambda_1^4 + a_{230}\lambda_1^6]$$

$$C_{32} = \sinh(S_1)\,[-1 + a_{210}\lambda_1^2 - a_{220}\lambda_1^4 + a_{230}\lambda_1^6]$$

$$C_{33} = \cosh(S_2)\,[-1 + a_{210}\lambda_2^2 - a_{220}\lambda_2^4 + a_{230}\lambda_2^6]$$

$$C_{34} = \sinh(S_2)\,[-1 + a_{210}\lambda_2^2 - a_{220}\lambda_2^4 + a_{230}\lambda_2^6]$$

$$C_{35} = \cosh(S_3)\cos(S_4)\,[-1 + a_{210}J_1 - a_{220}J_5 + a_{230}J_9] + \sinh(S_3)\sin(S_4)\,[a_{210}J_2 - a_{220}J_6 + a_{230}J_{10}]$$

$$C_{36} = \sinh(S_3)\cos(S_4)\,[-1 + a_{210}J_1 - a_{220}J_5 + a_{230}J_9] + \cosh(S_3)\sin(S_4)\,[a_{210}J_2 - a_{220}J_6 + a_{230}J_{10}]$$

$$C_{37} = \cosh(S_3)\sin(S_4)\,[-1 + a_{210}J_1 - a_{220}J_5 + a_{230}J_9] + \sinh(S_3)\cos(S_4)\,[-a_{210}J_2 + a_{220}J_6 - a_{230}J_{10}]$$

$$C_{38} = \sinh(S_3)\sin(S_4)\,[-1 + a_{210}J_1 - a_{220}J_5 + a_{230}J_9] + \cosh(S_3)\cos(S_4)\,[-a_{210}J_2 + a_{220}J_6 - a_{230}J_{10}]$$

$$C_{41} = \lambda_1 \sinh(S_1)\,[-1 + a_{240}\lambda_1^2 - a_{250}\lambda_1^4 + a_{260}\lambda_1^6]$$

$$C_{42} = \lambda_1 \cosh(S_1)\,[-1 + a_{240}\lambda_1^2 - a_{250}\lambda_1^4 + a_{260}\lambda_1^6]$$

$$C_{43} = \lambda_2 \sinh(S_2)\left[-1 + a_{240}\lambda_2^2 - a_{250}\lambda_2^4 + a_{260}\lambda_2^6\right]$$

$$C_{44} = \lambda_2 \cosh(S_2)\left[-1 + a_{240}\lambda_2^2 - a_{250}\lambda_2^4 + a_{260}\lambda_2^6\right]$$

$$C_{45} = \cosh(S_3)\sin(S_4)\left[\lambda_4 + a_{240}J_3 - a_{250}J_7 + a_{260}J_{11}\right]$$
$$+ \sinh(S_3)\cos(S_4)\left[-\lambda_3 + a_{240}J_4 - a_{250}J_8 + a_{260}J_{12}\right]$$

$$C_{46} = \sinh(S_3)\sin(S_4)\left[\lambda_4 + a_{240}J_3 - a_{250}J_7 + a_{260}J_{11}\right]$$
$$+ \cosh(S_3)\cos(S_4)\left[-\lambda_3 + a_{240}J_4 - a_{250}J_8 + a_{260}J_{12}\right]$$

$$C_{47} = \cosh(S_3)\cos(S_4)\left[-\lambda_4 - a_{240}J_3 + a_{250}J_7 - a_{260}J_{11}\right]$$
$$+ \sinh(S_3)\sin(S_4)\left[-\lambda_3 + a_{240}J_4 - a_{250}J_8 + a_{260}J_{12}\right]$$

$$C_{48} = \sinh(S_3)\cos(S_4)\left[-\lambda_4 - a_{240}J_3 + a_{250}J_7 - a_{260}J_{11}\right]$$
$$+ \cosh(S_3)\sin(S_4)\left[-\lambda_3 + a_{240}J_4 - a_{250}J_8 + a_{260}J_{12}\right]$$

$$S_1 = 1\,\frac{m\pi}{2R}; \qquad S_2 = 2\,\frac{m\pi}{2R}$$

$$S_3 = 3\,\frac{m\pi}{2R}; \qquad S_4 = 4\,\frac{m\pi}{2R}$$

$R = a/b$ = Plate aspect ratio,

$$a_{123} = \frac{a_{13}}{a_{12}} ; \qquad a_{154} = \frac{a_{15}}{a_{14}}$$

$$a_{210} = \frac{a_{21}}{a_{20}} ; \qquad a_{220} = \frac{a_{22}}{a_{20}}$$

$$a_{230} = \frac{a_{23}}{a_{20}} ; \qquad a_{240} = \frac{(a_{21} + 2a_{25})}{(a_{20} + 2a_{24})}$$

$$a_{250} = \frac{(a_{22} + 2a_{26})}{(a_{20} + 2a_{24})} ; \qquad a_{260} = \frac{a_{23}}{(a_{20} + 2a_{24})}$$

$$J_1 = \lambda_3^2 - \lambda_4^2$$

$$J_2 = -2\lambda_3\lambda_4$$

$$J_3 = \lambda_4(\lambda_4^2 - 3\lambda_3)$$

$$J_4 = \lambda_3(\lambda_3^2 - 3\lambda_4)$$

$$J_5 = \lambda_3^4 + \lambda_4^4 - 6\lambda_3^2\lambda_4^2$$

$$J_6 = 4\lambda_3\lambda_4(\lambda_4^2 - \lambda_3^2)$$

$$J_7 = 5\lambda_3\lambda_4(2\lambda_3\lambda_4^2 - \lambda_3^3) - \lambda_4^5$$

$$J_8 = 5\lambda_3\lambda_4(\lambda_4^3 - 2\lambda_3^2\lambda_4) + \lambda_3^5$$

$$J_9 = 15\lambda_3^2\lambda_4^2(\lambda_4^2 - \lambda_3^2) + \lambda_3^6 - \lambda_4^6$$

$$J_{10} = 2\lambda_3\lambda_4(10\lambda_3^2\lambda_4^2 - 3\lambda_3^4 - 3\lambda_4^4)$$

$$J_{11} = 7\lambda_3\lambda_4(5\lambda_3^3\lambda_4^2 - 3\lambda_3\lambda_4^4 - \lambda_3^5) + \lambda_4^7$$

$$J_{12} = 7\lambda_3\lambda_4(5\lambda_3^2\lambda_4^3 - 3\lambda_3^4\lambda_4 - \lambda_4^5) + \lambda_3^7$$

The fixed edge boundary conditions, namely

$$u^o = v^o = w = \frac{\partial w}{\partial y} = 0 \quad \text{at} \quad y = -b/2 \tag{5.10}$$

lead to the following set of four algebraic equations for an antisymmetric angle-ply laminate:

$$C_{51}A_{m_1} + C_{52}A_{m_2} + C_{53}A_{m_3} + C_{54}A_{m_4} + C_{55}A_{m_5} + C_{56}A_{m_6} + C_{57}A_{m_7} + C_{58}A_{m_8} = 0 \tag{5.11}$$

$$C_{61}A_{m_1} + C_{62}A_{m_2} + C_{63}A_{m_3} + C_{64}A_{m_4} + C_{65}A_{m_5} + C_{66}A_{m_6} + C_{67}A_{m_7} + C_{68}A_{m_8} = 0 \tag{5.12}$$

$$C_{71}A_{m_1} + C_{72}A_{m_2} + C_{73}A_{m_3} + C_{74}A_{m_4} + C_{75}A_{m_5} + C_{76}A_{m_6} + C_{77}A_{m_7} + C_{78}A_{m_8} = 0 \tag{5.13}$$

$$C_{81}A_{m_1} + C_{82}A_{m_2} + C_{83}A_{m_3} + C_{84}A_{m_4} + C_{85}A_{m_5} + C_{86}A_{m_6} + C_{87}A_{m_7} + C_{88}A_{m_8} = 0 \tag{5.14}$$

where

$$C_{51} = \lambda_1 \sinh(S_1) [-1 + a_{21}\lambda_1^2 - a_{31}\lambda_1^4]$$

$$C_{52} = \lambda_1 \cosh(S_1) [1 - a_{21}\lambda_1^2 + a_{31}\lambda_1^4]$$

$$C_{53} = \lambda_2 \sinh(S_2) [-1 + a_{21}\lambda_2^2 - a_{31}\lambda_2^4]$$

$$C_{54} = \lambda_2 \cosh(S_2) [1 - a_{21}\lambda_2^2 + a_{31}\lambda_2^4]$$

$$C_{55} = \cosh(S_3)\sin(S_4)[\lambda_4 + a_{21}J_3 - a_{31}J_7]$$
$$+ \sinh(S_3)\cos(S_4)[-\lambda_3 + a_{21}J_4 - a_{31}J_8]$$

$$C_{56} = \sinh(S_3)\sin(S_4)[-\lambda_4 - a_{21}J_3 + a_{31}J_7]$$
$$+ \cosh(S_3)\cos(S_4)[\lambda_3 - a_{21}J_4 + a_{31}J_8]$$

$$C_{57} = \cosh(S_3)\cos(S_4)[\lambda_4 + a_{21}J_3 - a_{31}J_7]$$
$$+ \sinh(S_3)\sin(S_4)[\lambda_3 - a_{21}J_4 + a_{31}J_8]$$

$$C_{58} = \sinh(S_3)\cos(S_4)[-\lambda_4 - a_{21}J_3 + a_{31}J_7]$$
$$+ \cosh(S_3)\sin(S_4)[-\lambda_3 + a_{21}J_4 - a_{31}J_8]$$

$$C_{61} = \cosh(S_1)[1 - a_{54}\lambda_1^2 + a_{64}\lambda_1^4]$$

$$C_{62} = \sinh(S_1)[-1 + a_{54}\lambda_1^2 - a_{64}\lambda_1^4]$$

$$C_{63} = \cosh(S_2)[1 - a_{54}\lambda_2^2 + a_{64}\lambda_2^4]$$

$$C_{64} = \sinh(S_2)[-1 + a_{54}\lambda_2^2 - a_{64}\lambda_2^4]$$

$$C_{65} = \cosh(S_3)\cos(S_4)[1 - a_{54}J_1 + a_{64}J_5]$$
$$+ \sinh(S_3)\sin(S_4)[-a_{54}J_2 + a_{64}J_6]$$

$$C_{66} = \sinh(S_3)\cos(S_4)[-1 + a_{54}J_1 - a_{64}J_5]$$
$$+ \cosh(S_3)\sin(S_4)[a_{54}J_2 - a_{64}J_6]$$

$$C_{67} = \cosh(S_3)\sin(S_4)\left[-1 + a_{54}J_1 - a_{64}J_5\right] + \sinh(S_3)\cos(S_4)\left[-a_{54}J_2 + a_{64}J_6\right]$$

$$C_{68} = \sinh(S_3)\sin(S_4)\left[-a_{54}J_1 + a_{64}J_5\right] + \cosh(S_3)\cos(S_4)\left[a_{54}J_2 - a_{64}J_6\right]$$

$$C_{71} = \cosh(S_1)\left[1 - a_{87}\lambda_1^2 + a_{97}\lambda_1^4\right]$$

$$C_{72} = \sinh(S_1)\left[-1 + a_{87}\lambda_1^2 - a_{97}\lambda_1^4\right]$$

$$C_{73} = \cosh(S_2)\left[1 - a_{87}\lambda_2^2 + a_{97}\lambda_2^4\right]$$

$$C_{74} = \sinh(S_2)\left[-1 + a_{87}\lambda_2^2 - a_{97}\lambda_2^4\right]$$

$$C_{75} = \cosh(S_3)\cos(S_4)\left[1 - a_{87}J_1 + a_{97}J_5\right] + \sinh(S_3)\sin(S_4)\left[-a_{87}J_2 + a_{97}J_6\right]$$

$$C_{76} = \sinh(S_3)\cos(S_4)\left[-1 + a_{87}J_1 - a_{97}J_5\right] + \cosh(S_3)\sin(S_4)\left[a_{87}J_2 - a_{97}J_6\right]$$

$$C_{77} = \cosh(S_3)\sin(S_4)\left[-1 + a_{87}J_1 - a_{97}J_5\right] + \sinh(S_3)\cos(S_4)\left[-a_{87}J_2 + a_{97}J_6\right]$$

$$C_{78} = \sinh(S_3)\sin(S_4)\left[1 - a_{87}J_1 + a_{97}J_5\right] + \cosh(S_3)\cos(S_4)\left[a_{87}J_2 - a_{97}J_6\right]$$

$$a_{81} = \lambda_1 \sinh(S_1)\left[-1 + a_{87}\lambda_1^2 - a_{97}\lambda_1^4\right]$$

$$a_{82} = \lambda_1 \cosh(S_1)\,[1 - a_{87}\lambda_1^2 + a_{97}\lambda_1^4]$$

$$a_{83} = \lambda_2 \sinh(S_2)\,[-1 + a_{87}\lambda_2^2 - a_{97}\lambda_2^4]$$

$$a_{84} = \lambda_2 \cosh(S_2)\,[1 - a_{87}\lambda_2^2 + a_{97}\lambda_2^4]$$

$$C_{85} = \cosh(S_3)\sin(S_4)[\lambda_4 + a_{87}J_3 - a_{97}J_7]$$
$$+ \sinh(S_3)\cos(S_4)[-\lambda_3 + a_{87}J_4 - a_{97}J_8]$$

$$C_{86} = \sinh(S_3)\sin(S_4)[-\lambda_4 - a_{87}J_3 + a_{97}J_7]$$
$$+ \cosh(S_3)\cos(S_4)[\lambda_3 - a_{87}J_4 + a_{97}J_8]$$

$$C_{87} = \cosh(S_3)\cos(S_4)[\lambda_4 + a_{87}J_3 - a_{97}J_7]$$
$$+ \sinh(S_3)\sin(S_4)[\lambda_3 - a_{87}J_4 + a_{97}J_8]$$

$$C_{88} = \sinh(S_3)\cos(S_4)[-\lambda_4 - a_{87}J_3 + a_{97}J_7]$$
$$+ \cosh(S_3)\sin(S_4)[-\lambda_3 + a_{87}J_4 - a_{97}J_8]$$

$$a_{21} = a_2/a_1 \;; \qquad a_{31} = a_3/a_1$$

$$a_{54} = a_5/a_4 \;; \qquad a_{64} = a_6/a_4$$

$$a_{87} = a_8/a_7 \;; \qquad a_{97} = a_9/a_7$$

It may be noted that the above eight algebraic equations for an antisymmetric angle-ply plate have been derived assuming the most general solution given by relation (3.55).

The corresponding eight algebraic equations for an antisymmetric cross-ply plate can be similarly derived by using relations given by (3.44-3.45), (3.47-3.48) and (3.40-3.42). The determinant of the coefficients of A_{m_1} to A_{m_8} given by

$$\begin{Vmatrix} C_{11} & C_{12} & C_{13} & C_{14} & C_{15} & C_{16} & C_{17} & C_{18} \\ C_{21} & C_{22} & C_{23} & C_{24} & C_{25} & C_{26} & C_{27} & C_{28} \\ C_{31} & C_{32} & C_{33} & C_{34} & C_{35} & C_{36} & C_{37} & C_{38} \\ C_{41} & C_{42} & C_{43} & C_{44} & C_{45} & C_{46} & C_{47} & C_{48} \\ C_{51} & C_{52} & C_{53} & C_{54} & C_{55} & C_{56} & C_{57} & C_{58} \\ C_{61} & C_{62} & C_{63} & C_{64} & C_{65} & C_{66} & C_{67} & C_{68} \\ C_{71} & C_{72} & C_{73} & C_{74} & C_{75} & C_{76} & C_{77} & C_{78} \\ C_{81} & C_{82} & C_{83} & C_{84} & C_{85} & C_{86} & C_{87} & C_{88} \end{Vmatrix}$$

set to zero leads to a transcendental equation in N_x and m. The elements of this determinant contain N_x and m as unknowns. For a given integer value of m, the value of N_x which makes the above determinant zero is obtained by a method of hit and trial. The minimum value of N_x which satisfies this condition is the critical buckling load. A computer programme incorporating the various possible solutions given by Eqs. (3.54), (3.55) and (3.56) is then written to obtain critical values of N_x for antisymmetric cross- and angle-ply plates with various aspect ratios, fibre orientations and different number of layers.

5.3 NUMERICAL COMPUTATIONS

Numerical computations are carried out for the following composite materials:

(a) Carbon fibre reinforced plastics (CFRP)

$E_1/E_2 = 6.33$; $G_{12}/E_2 = 0.667$; $\nu_{12} = 0.20$

(b) Graphite fibre reinforced plastics (GFRP)

$E_1/E_2 = 40$; $G_{12}/E_2 = 0.50$; $\nu_{12} = 0.25$

(c) Boron fibre reinforced plastics (BFRP)

$E_1/E_2 = 10$; $G_{12}/E_2 = 0.33$; $\nu_{12} = 0.30$

The extensional, coupling and bending stiffnesses have been calculated by the method as indicated in Chapter 2.

5.4 RESULTS AND DISCUSSION

5.4.1 Plates With Two Opposite Edges Simply Supported and the Remaining Edges Free

Non-dimensional buckling loads as a function of thickness ratio, t_1/t_2 of the laminae of a four-layered anti-symmetric angle-ply square plate are plotted in Figure 5.2 for three different fibre orientations (30°, 45° and 60°). It is seen that for all the orientations, the buckling load reaches its maximum at the thickness ratio of 0.4142. This is attributed to the fact that the coupling stiffnesses (B_{16} and B_{26}) tend to vanish at this thickness ratio (Refer Chapter 2). It is also observed that the buckling load is more sensitive

to thickness ratios at $\theta = 30^{\circ}$ than at other orientations. This may be due to the existence of maximum coupling effect in the region of $\theta = 30^{\circ}$ (see Table 5.1). The increase in buckling load is, therefore, maximum as the critical thickness ratio of 0.4142 is approached with a corresponding decrease of coupling terms B_{16} and B_{26}. The variations of non-dimensional buckling loads with the thickness ratio for a six-layered antisymmetric angle-ply square plate for two different values of R_1 are shown in Figures 5.3 and 5.4. The buckling load is seen to reach its maximum at thickness ratio, R_2 of 2.0 and 4.1623 at R_1=1 & 2 respectively for all orientations. The coupling stiffnesses B_{16} and B_{26} have been shown to disappear at these thickness ratios for a six-layered laminate (Refer Chapter 2).

The variations of non-dimensional buckling loads as a function of aspect ratio for an antisymmetric angle-ply plate are shown in Figures 5.5, 5.6 and 5.7 respectively for three different fibre orientations (30°, 45° and 60°) with number of layers as a parameter. It can easily be seen that as the number of layers is increased, the buckling load tends to be independent of this parameter (N). This corroborates the results of Whitney and Leissa[1] for antisymmetric types of lay-ups.

The effect of coupling as a percentage reduction in buckling load between four- and two-layered and between six-

and four-layered configurations of a square antisymmetric angle-ply plate as a function of fibre orientations is shown in Table 5.1. The effect is comparatively small at extreme values of fibre orientations because the coupling stiffnesses tend to vanish in these regions. However, the effects of coupling are more pronounced in the regions of fibre orientations of 15°-40° than those of 45°-75°.

The variations of non-dimensional buckling loads with fibre orientation, θ is shown in Figure 5.8 with number of layers as a parameter. The buckling loads tend to be independent of the number of layers faster in the region of 45°-75° than they do in the region of 15°-40° as discussed above.

Figure 5.9 shows the variation of non-dimensional buckling load as a function of aspect ratio for a regular (M = 1) antisymmetric cross-ply laminate for different number of layers in a given thickness. The dependence of buckling load progressively decreases with increase in the number of layers. Similar observation was made even in the case of antisymmetric angle-ply laminates. The variation of buckling load for a square antisymmetric cross-ply plate with cross-ply ratio, M is shown in Figure 5.10 with number of layers, N as a parameter. It is seen that the buckling load increases with M, the increase being maximum between cross-ply ratios of 1 and 3 whereafter the buckling load becomes asymptotic with cross-ply

ratio. The steep rise in the buckling load in the region of M = 1 to 3 could be attributed to the increase in the overall thickness of odd-numbered layers, the fibres of which are aligned in the axial direction. Since the overall thickness of the plate is constant, the buckling load tends to stabilize with increase in odd-numbered layers and hence with increase in cross-ply ratio. For a designer this may indicate the optimal cross-ply ratio beyond which the increase in the ratio becomes unnecessary to achieve a given buckling load.

5.4.2 Plates With Two Opposite Edges Simply Supported and the Remaining Edges Clamped

Figures 5.11 through 5.13 depict the variations of buckling load as a function of fibre orientation, θ for GFRP, BFRP and CFRP square plates respectively. It is seen that the buckling load reaches a maximum in the region of $\theta = 45°$ approximately in each case. It may also be noted here that the buckling mode in the x direction changes from 1 to 2 at $\theta \geq 40°$. This feature is distinct from the other two sets of boundary conditions where the buckling mode always retains the single wave shape. The rising trend for $0° < \theta \leq 45°$ may be due to the result of increasing effect of the clamped edge moments as θ increases, thereby increasing the effective cross stiffness. This is again distinct from the other two cases where such an effect is not present. It may be noted that at $\theta = 0°$, the magnitude of the buckling load is of the

same order of magnitude as in the other two cases. This shows that the edge conditions are not affecting the buckling load as much as at higher orientations. Another point of interest is the different magnitude of the buckling load at $\theta = 90^{\circ}$ compared to that at $\theta = 0^{\circ}$. This may be due to the existence of a higher mode shape i.e., $m = 2$ as compared to $m = 1$ at $\theta = 0^{\circ}$. This again is distinct from the other two edge conditions. The minima of a two-layered solution in the region of $\theta = 20^{\circ}$ and $\theta = 70^{\circ}$ is also worth noting. A composite plate with two loaded edges simply supported and the remaining edges fixed is, therefore, at its minimum buckling strength for a two-layered lay-up in these regions of fibre orientations. As expected, the various solutions tend to be independent of the number of layers at extreme values of fibre orientations owing to the absence of coupling stiffnesses. The results for an infinite number of layers are the same as the orthotropic solution in which all coupling between bending and extension (B_{16} and B_{26}) is ignored. Percentage reduction in buckling loads between four- and two-layered configurations and those between six- and four-layered configurations are shown in Table 5.2 for an antisymmetric carbon/epoxy square plate as a function of fibre orientation. It is seen that maximum reduction in buckling load due to coupling effects occurs at $\theta = 45^{\circ}$. However, as the number of layers increases from 4 to 6, the buckling loads approach

the values for orthotropic plates. This shows that the coupling between bending and extension rapidly dies out as the number of layers is increased.

The variation of buckling load as a function of thickness ratio, t_1/t_2 for a four-layered antisymmetric square plate for three different fibre orientations ($\theta = 30°$, $45°$ and $60°$) is shown in Figure 5.14. At all orientations, the buckling load reaches a maximum at the thickness ratio of 0.4142 (see Chapter 2). The percentage increase in buckling load between an equal thickness ratio laminate ($t_1/t_2 = 1$) and an optimum thickness ratio laminate ($t_1/t_2 = 0.4142$) is of the order of 8 percent for $30°$ and $60°$ fibre oriented plates and 10 percent for a $45°$ oriented plate. This increase in buckling load from the design point of view is quite significant and this can be treated as the optimum thickness ratio for a given design buckling load. Figure 5.15 shows a similar variation of buckling load with thickness ratio for a six-layered antisymmetric square plate for the same fibre orientations. The maximum buckling load occurs at thickness ratios, $R_2 = 2.0$ and 4.1623 at $R_1 = 1.0$ and 2.0 respectively. This may again be attributed to the absence of coupling effects occurring at these thickness ratios (see Chapter 2).

The variations of buckling load with aspect ratio, R for two different fibre orientations of $\theta = 30°$ and $\theta = 45°$ are shown in Figures 5.16 and 5.17 respectively for

graphite/epoxy antisymmetric angle-ply plates with number of layers as a parameter. The cusps in these figures represent the changes in the buckling mode shape as the plate aspect ratio changes. It can be noted that the curves approach the lowest level at each respective curve in the neighbourhood of R = 1.0 as the aspect ratio increases. This behaviour is typical of an isotropic plate as discussed by Timoshenko and Gere[4]. It can also be observed that the coupling between bending and extension has a constant influence of aspect ratio for a given number of layers. Figures 5.18 and 5.19 depict respectively the variations of buckling load of a carbon/epoxy composite plate with aspect ratio for two different fibre orientations, $\theta = 30°$ and $45°$. It is observed from Figures 5.16 through 5.19 that the pattern of cusps is a function of number of layers, angle of fibre orientation and degree of anisotropy of the material (E_1/E_2). The first change in mode shape pattern, for example, for graphite/epoxy plate occurs between aspect ratios 1.25 and 1.50 for all the number of layers (2, 4 and 6) at $\theta = 30°$. For carbon/epoxy plate, this occurs between aspect ratios 1.0 and 1.25. However, the location of cusps moves to the right from two-layered configuration to a six-layered one. The first change in mode shape pattern occurs between aspect ratios 1.50 and 1.75 for a 45° oriented plate both for the graphite/epoxy and carbon/epoxy materials for all the number

of layers considered. This may be attributed to the symmetry of fibre orientation at $\theta = 45°$.

5.4.3 Plates With Two Loaded Edges Simply Supported, One Fixed and the Remaining Free

Figures 5.20 through 5.22 show the variations of buckling loads for square plates of boron/epoxy, glass/epoxy and carbon/epoxy respectively with fibre orientation, θ. It is seen that the buckling load progressively decreases with increase in fibre orientation. This is in contrast with the trend noticed both in the clamped and simply supported edge conditions where the maximum load occurs in the neighbourhood of $\theta = 45°$. However, this trend is similar to the case of two edges free. The reason for this distinct difference can be traced to the conditions on the in-plane displacements imposed at the edges. In the free edge case there is no restriction on the in-plane displacements while these have been restricted completely in both the simply supported and fixed edge cases. The variations of buckling loads for four-layered and six-layered plates are distinctly different from those of two-layered plates. However, all the solutions tend to be independent of the number of layers at extreme values of fibre orientations. The difference between two-layered and four-layered solutions as a function of E_1/E_2 can be clearly noted. The coupling effects, as expected, become more predominant as the ratio E_1/E_2 increases. For

each of the materials considered, however, the coupling effects are observed to be maximum in the region of $\theta = 45°$. Percentage reduction in buckling load between four and two-layered and between six and four-layered configurations of a square antisymmetric carbon/epoxy plate is shown in Table 5.3. as a function of fibre orientation, θ. A cursory study of the Table 5.3 reveals that the coupling effects are more in the fibre orientation range of 15°-45° than in the corresponding range of 45°-75°.

The variations of buckling loads with aspect ratio for a carbon/epoxy antisymmetric angle-ply plate are shown in Figures 5.23, 5.24 and 5.25 for three different fibre orientations, $\theta = 30°$, 45° and 60° respectively with number of layers, N as a parameter. As discussed earlier, the cusps in these figures occur because of changes in the buckle mode shape as the plate aspect ratio is changed. However, the aspect ratio at which changes in mode shapes occur appear to be dependent upon the fibre orientation and number of layers. The first change in mode shape for a 30° oriented plate with N = 4 and 6 occurs between aspect ratios of 2.75 and 3.0 whereas for 45° and 60° oriented plates, the corresponding figures are 2.25 and 1.75 respectively for the same number of layers. Thus with increase of fibre orientation, the cusps move backward with respect to aspect ratio for four- and six-layered plates. The trend for two-layered coupled solution is also similar

though numerically different. It is, however, observed that for symmetrical 45° fibre orientation, the cusps become independent of the number of layers and occur simultaneously at the same aspect ratio. This behaviour which is distinctly different from isotropic one, may be attributed to the different levels of overall stiffnesses at various fibre orientations.

The effect of thickness ratio, t_1/t_2 of a four-layered antisymmetric carbon/epoxy square plate on the buckling load is represented in Figure 5.26 for three different fibre orientations, $\theta = 30°$, 45° and 60°. The buckling load is found to be maximum at the thickness ratio of 0.4142 for all the orientations considered (see Chapter 2). However, the buckling load appears to be more sensitive to thickness ratio at $\theta = 45°$ followed by $\theta = 30°$ and 60° respectively. The percentage increase in buckling load between a laminate of thickness ratio, $t_1/t_2 = 1.0$ and an identical laminate with $t_1/t_2 = 0.4142$ is of the order of 9 percent for a 45° oriented square plate whereas the corresponding figures for 30° and 60° oriented square plates are of the order of 8 and 7 percent respectively. An examination of the Table 5.3 shows that the increase in the buckling load for a given fibre orientation is proportional to the coupling effects which are more predominant at $\theta = 45°$ than elsewhere. At the critical thickness ratio of 0.4142, since the coupling effects

are entirely absent, one can conclude that the increase in buckling load is due to the elimination of coupling. Figure 5.27 depicts the similar variations of buckling loads for a six-layered antisymmetric square plate. The general observations with these types of laminates are similar to those of a four-layered laminate discussed above.

Figures 5.28 and 5.29 depict respectively the variation of buckling load with cross-ply ratio, M for an antisymmetrically laminated cross-ply square plates of graphite/epoxy and carbon/epoxy materials. The essential features are the same as those observed in the case of plates with free edges.

It is now desirable to study the effect of various boundary conditions on the variation of buckling load with different parameters. Figure 5.30 shows the variation of buckling load with fibre orientation for various boundary conditions. It is seen that the buckling load falls progressively from $\theta = 0^\circ$ to $\theta = 90^\circ$ for all number of layers (2, 4 and 6) for (a) plates with loaded edges simply supported and the remaining edges free and for (b) plates with loaded edges simply supported, one side clamped and the remaining side free. The fundamental mode shape for each of these cases occurs at $m = 1$. The variation of buckling load with fibre orientation for plates with two loaded edges simply supported and the remaining edges clamped is, however, quite

different. The buckling loads rise continuously upto the fibre orientation of 40° and progressively fall thereafter for four- and six-layered plates. For a two-layered plate, however, the minimum values occur around $\theta = 20°$ and 70° approximately. The distinct change in trend in the variation of buckling load with fibre orientation for this type of boundary condition may be attributed to the Poisson's effect which appears to be predominant at these edge conditions. The effect of boundary conditions on the variation of buckling load with thickness ratio for a four-layered plate at various fibre orientations is shown in Figure 5.31. It can be seen easily that the change in buckling load with thickness ratio is more sensitive for plates with two loaded edges simply supported and the remaining edges clamped than for other types of boundary conditions. This effect is, however, found to be least for plates with unloaded edges free.

- o -

TABLE 5.1. PERCENTAGE REDUCTION IN BUCKLING LOAD BETWEEN DIFFERENT LAYERS OF AN ANTISYMMETRIC CFRP ANGLE-PLY SQUARE PLATE AS A FUNCTION OF FIBRE ORIENTATIONS (FREE EDGES)

Fibre Orientation in Degrees	Percentage Reduction in Buckling Load Between N = 4 and N = 2	Percentage Reduction in Buckling Load Between N = 6 and N = 4
15	6.73	-
20	18.93	3.24
25	22.39	3.90
30	23.92	4.32
35	23.97	4.20
40	22.39	3.93
45	19.67	3.34
50	16.18	-
55	12.27	2.23
60	8.37	1.63
65	5.36	1.14
70	3.63	0.98
75	1.29	0.40

TABLE 5.2. PERCENTAGE REDUCTION IN BUCKLING LOAD BETWEEN DIFFERENT LAYERS OF AN ANTISYMMETRIC CFRP ANGLE-PLY SQUARE PLATE AS A FUNCTION OF FIBRE ORIENTATIONS (CLAMPED EDGES)

Fibre Orientation in Degrees	Percentage Reduction in Buckling Load Between N = 4 and N = 2	Percentage Reduction in Buckling Load Between N = 6 and N = 4
15	9.82	-
20	15.73	2.20
25	18.94	4.04
30	23.30	3.74
35	27.03	5.13
40	28.57	4.80
45	30.05	5.27
50	29.31	5.23
55	-	4.98
60	24.63	4.42
65	20.98	3.77
70	16.34	2.60
75	10.33	2.05

TABLE 5.3. PERCENTAGE REDUCTION IN BUCKLING LOAD BETWEEN DIFFERENT LAYERS OF AN ANTISYMMETRIC CFRP ANGLE-PLY SQUARE PLATE AS A FUNCTION OF FIBRE ORIENTATIONS (CLAMPED-FREE EDGES)

Fibre Orientation in Degrees	Percentage Reduction in Buckling Load Between N = 4 and N = 2	Percentage Reduction in Buckling Load Between N = 6 and N = 4
15	12.40	3.22
20	17.57	3.84
25	21.96	4.41
30	24.78	4.66
35	26.66	4.79
40	27.39	4.82
45	27.26	4.50
50	26.24	4.15
55	24.35	-
60	21.53	3.23
65	17.76	2.98
70	14.05	2.12
75	7.07	-

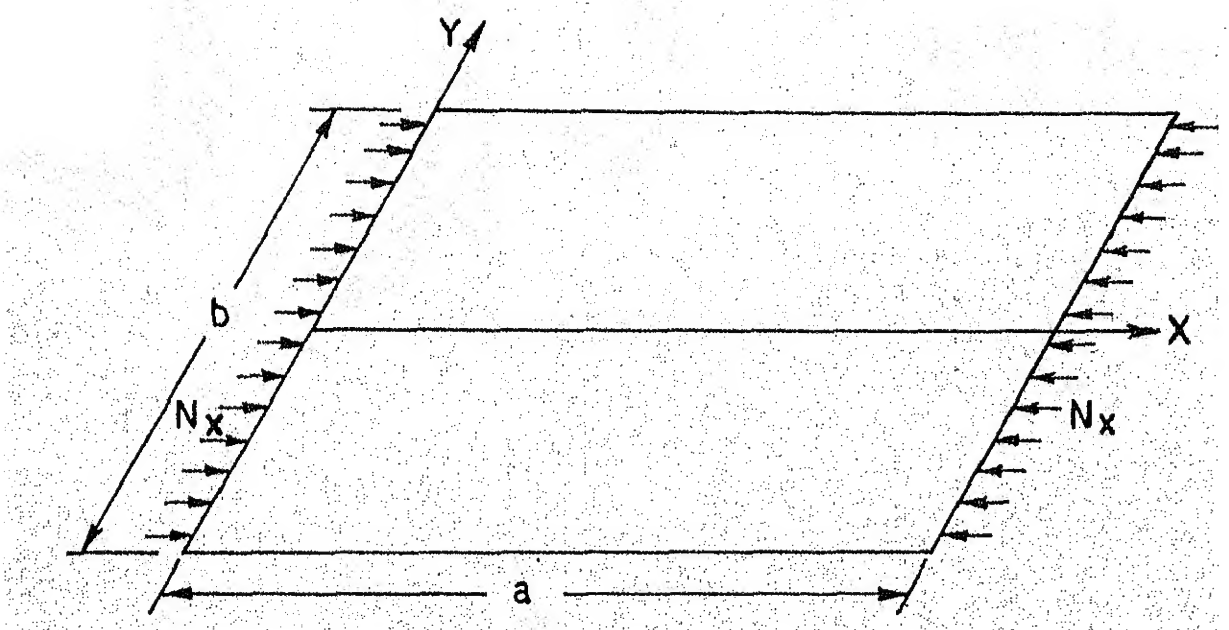

FIG. 5.1: COORDINATES OF THE PLATE

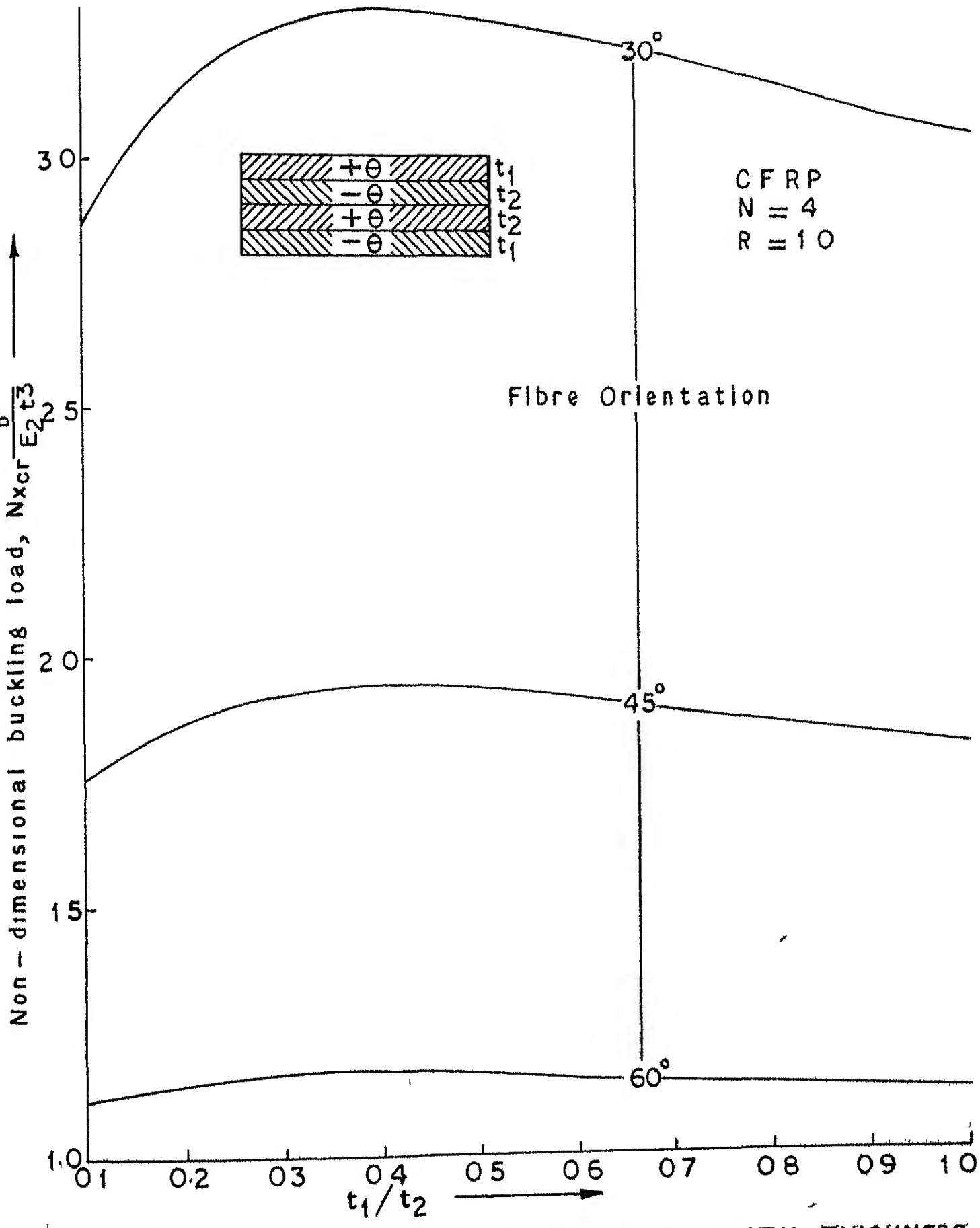

FIG. 5 2 VARIATION OF BUCKLING LOAD WITH THICKNESS RATIO FOR AN ANTISYMMETRIC ANGLE-PLY SQUARE PLATE.

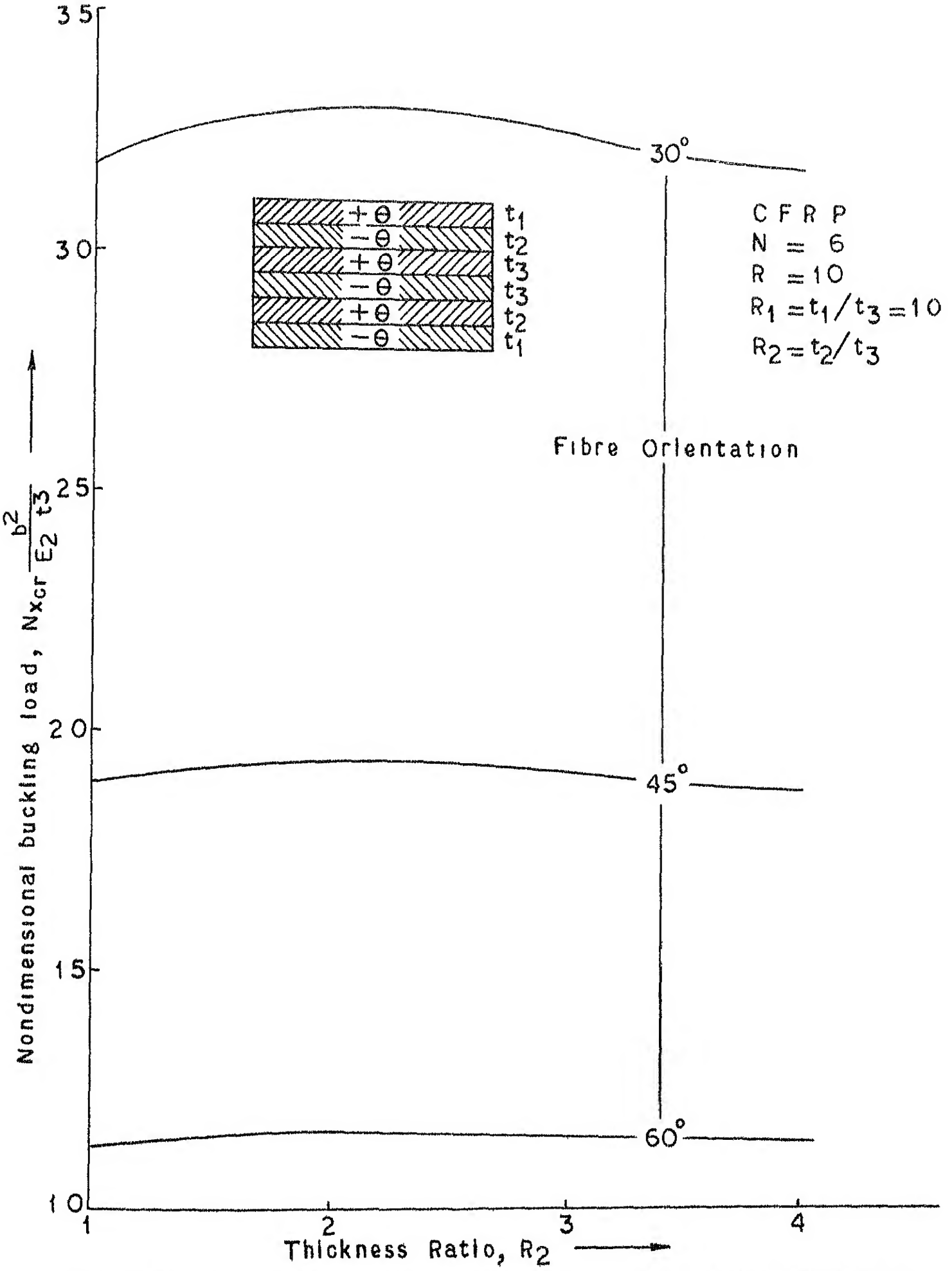

FIG 53 VARIATION OF BUCKLING LOAD WITH THICKNESS RATIO FOR AN ANTISYMMETRIC SQUARE PLATE

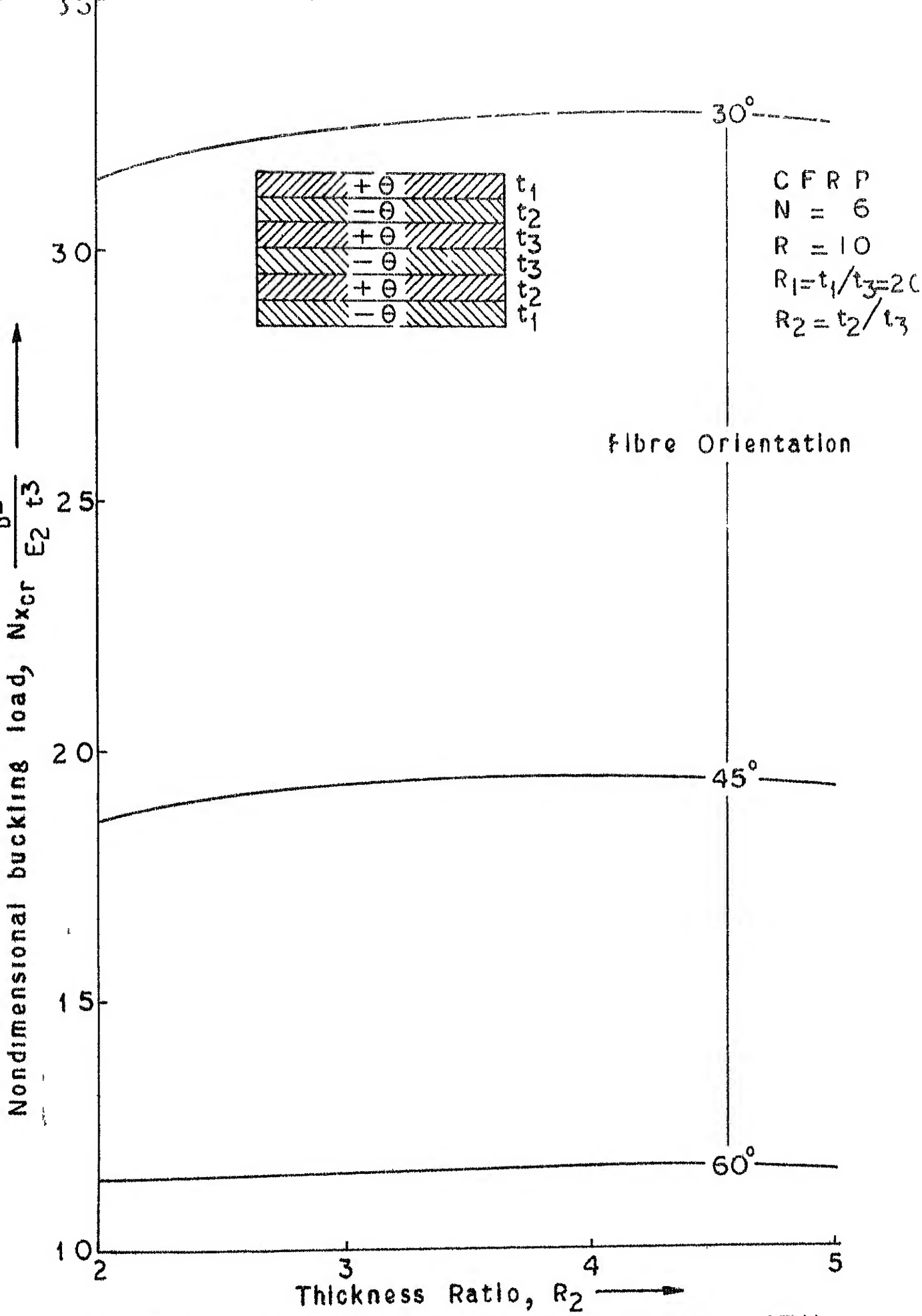

FIG 5 4 VARIATION OF BUCKLING LOAD WITH THICKNESS RATIO FOR AN ANTISYMMETRIC ANGLE-PLY SQUARE PLATE

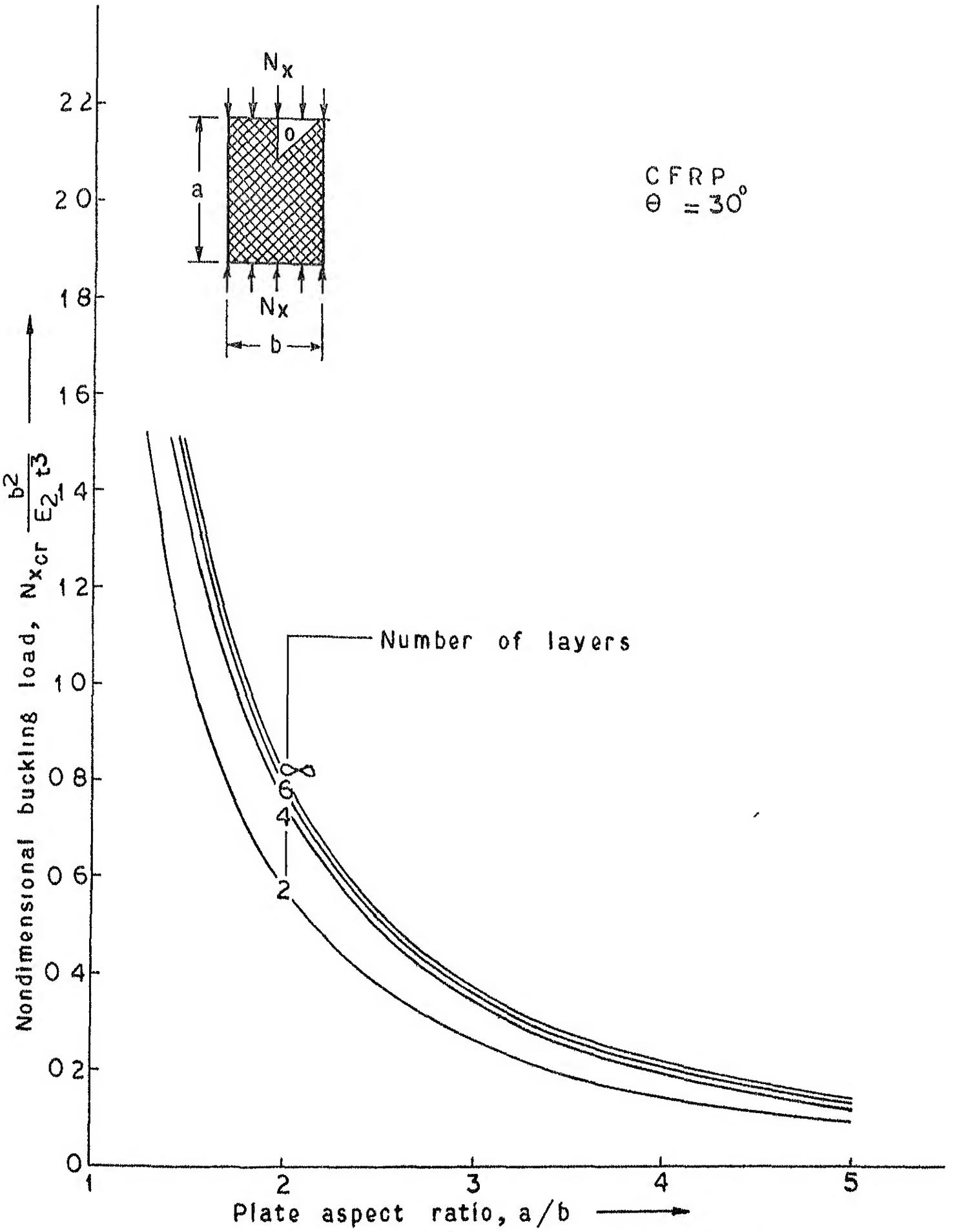

FIG 55 VARIATION OF BUCKLING LOAD WITH ASPECT RATIO

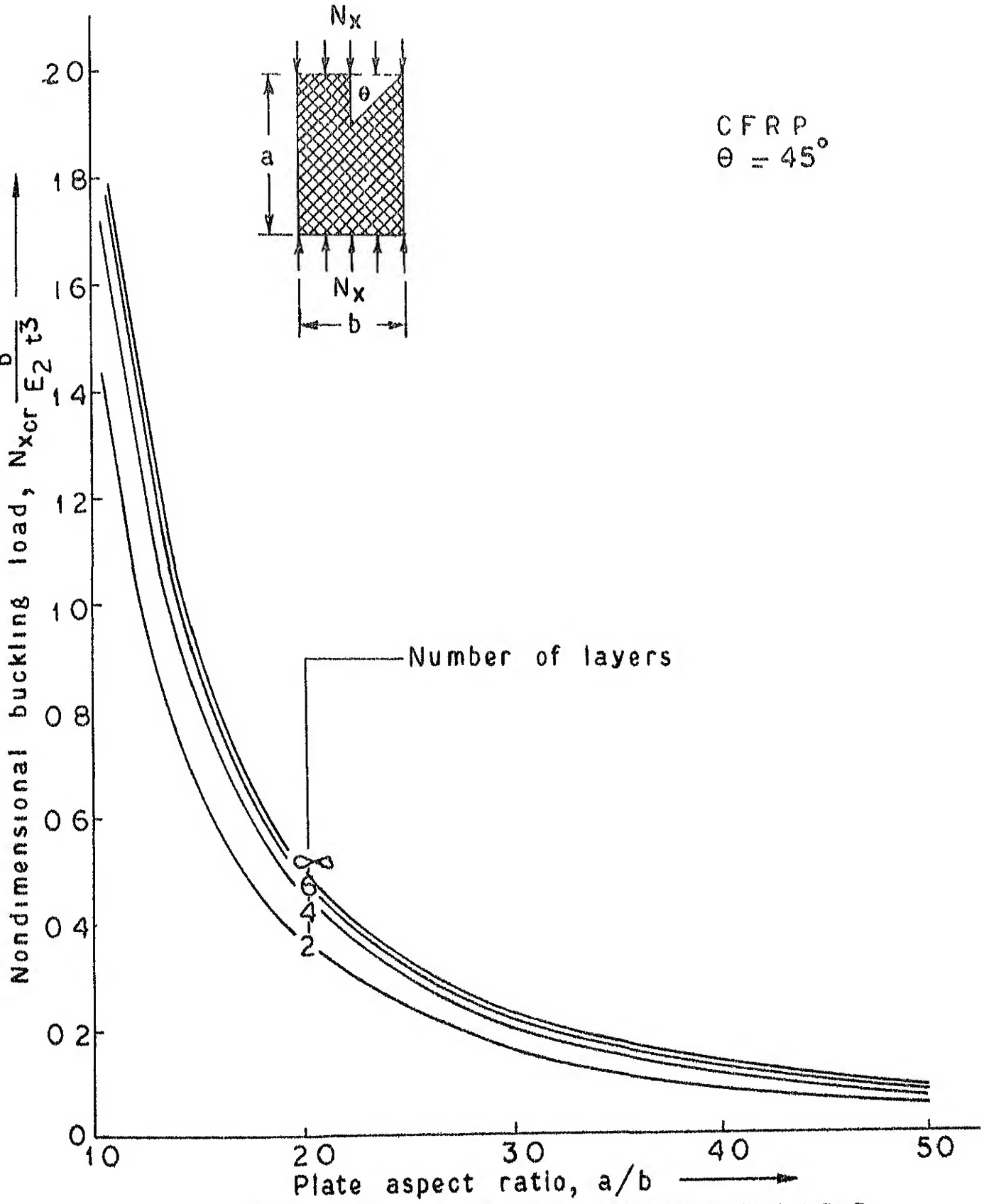

FIG 56 VARIATION OF BUCKLING LOAD WITH ASPECT RATIO

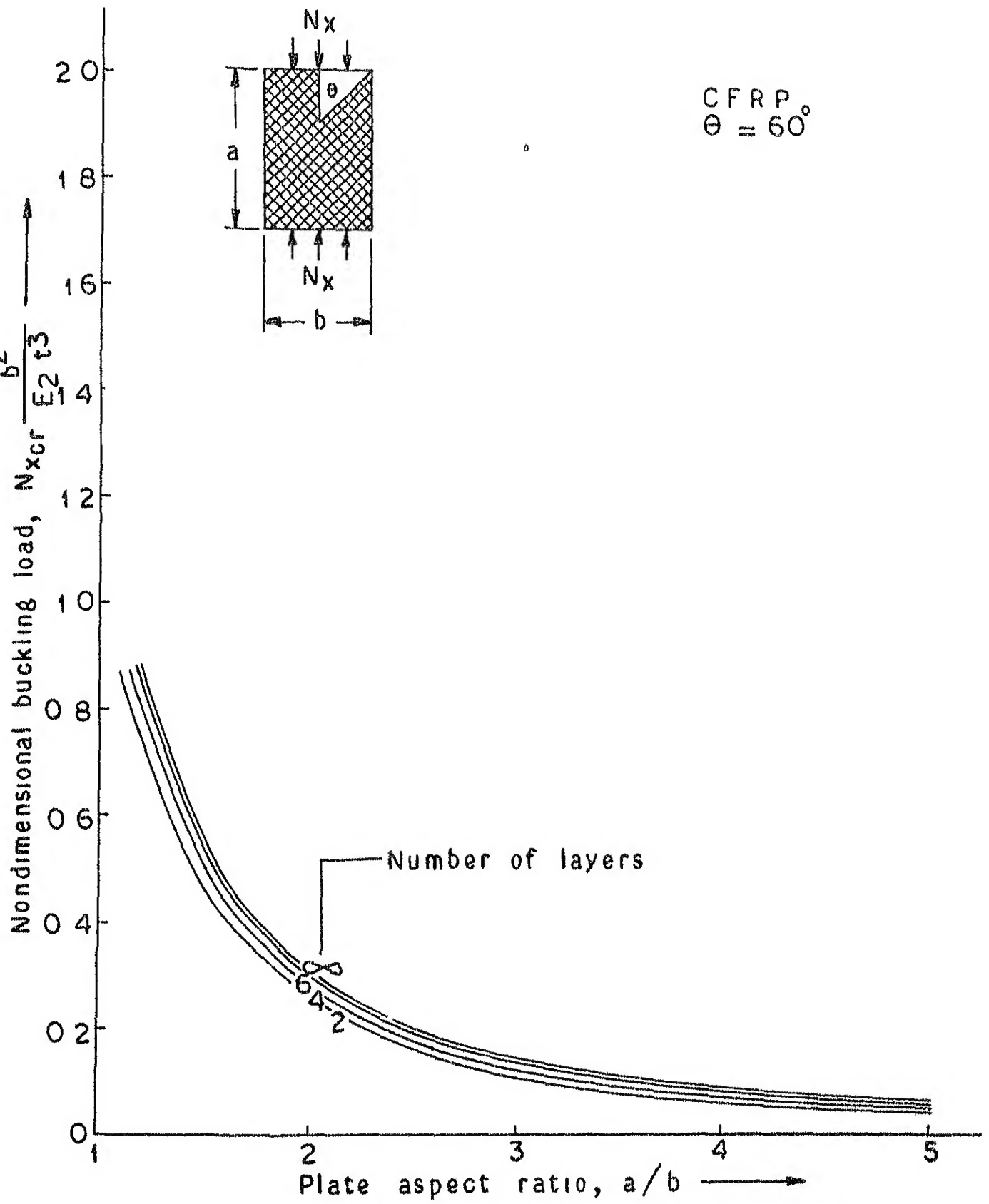

FIG 5 7 VARIATION OF BUCKLING LOAD WITH ASPECT RATIO

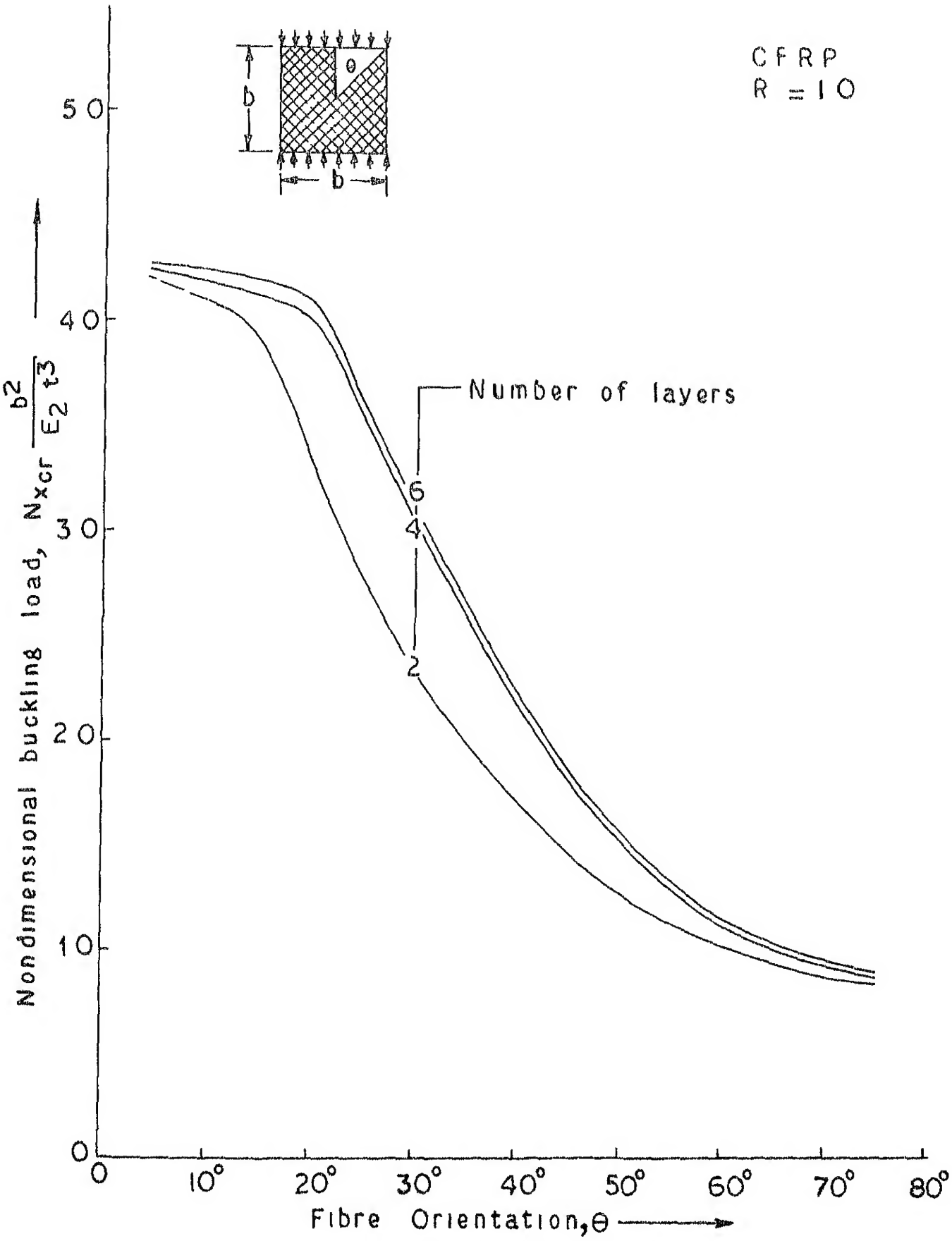

FIG 5 8 VARIATION OF BUCKLING-LOAD WITH FIBRE ORIENTATION

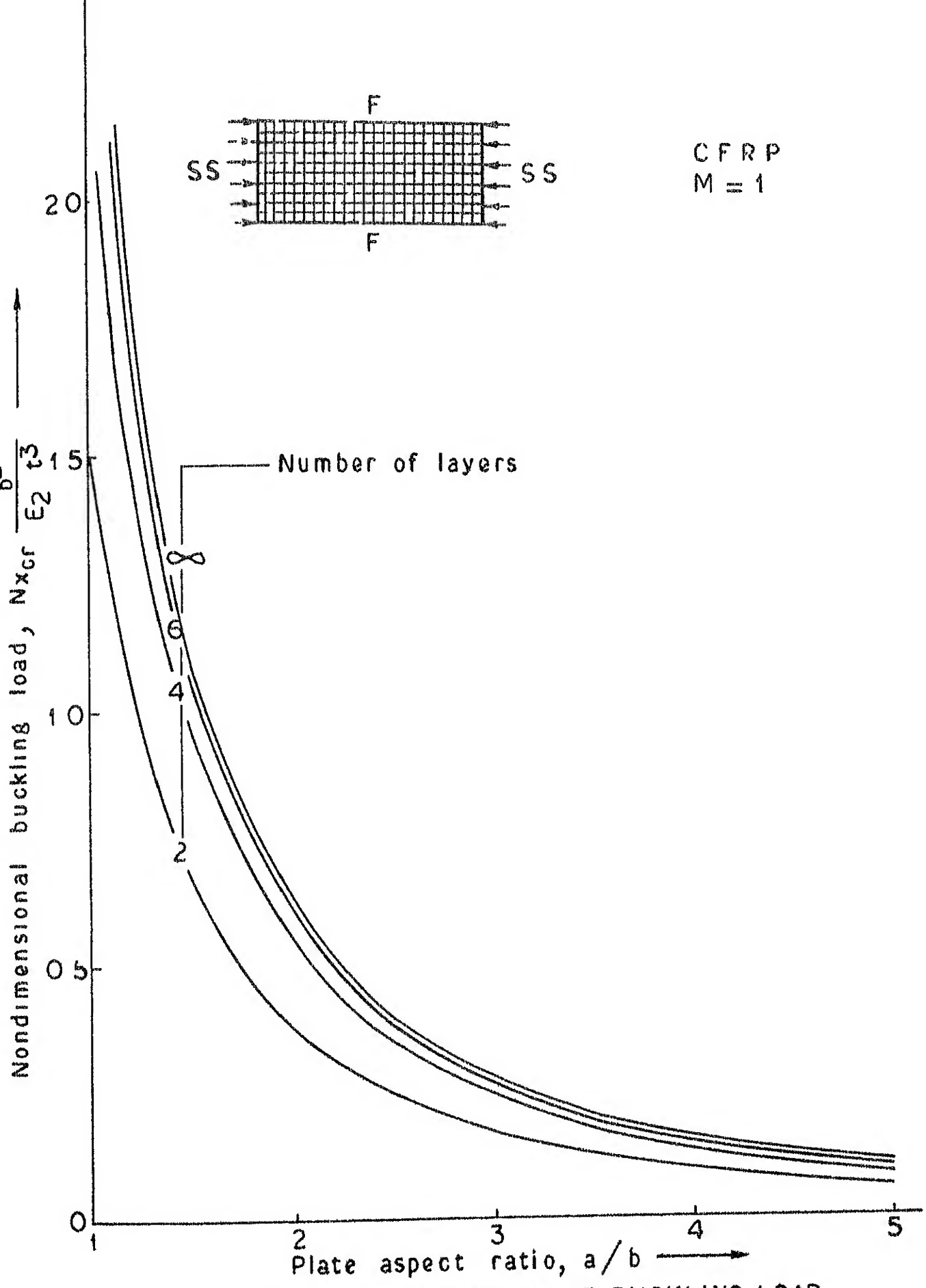

FIG 5 9 VARIATION OF BUCKLING LOAD WITH PLATE ASPECT RATIO OF AN ANTISYMMETRIC CROSS-PLY PLATE

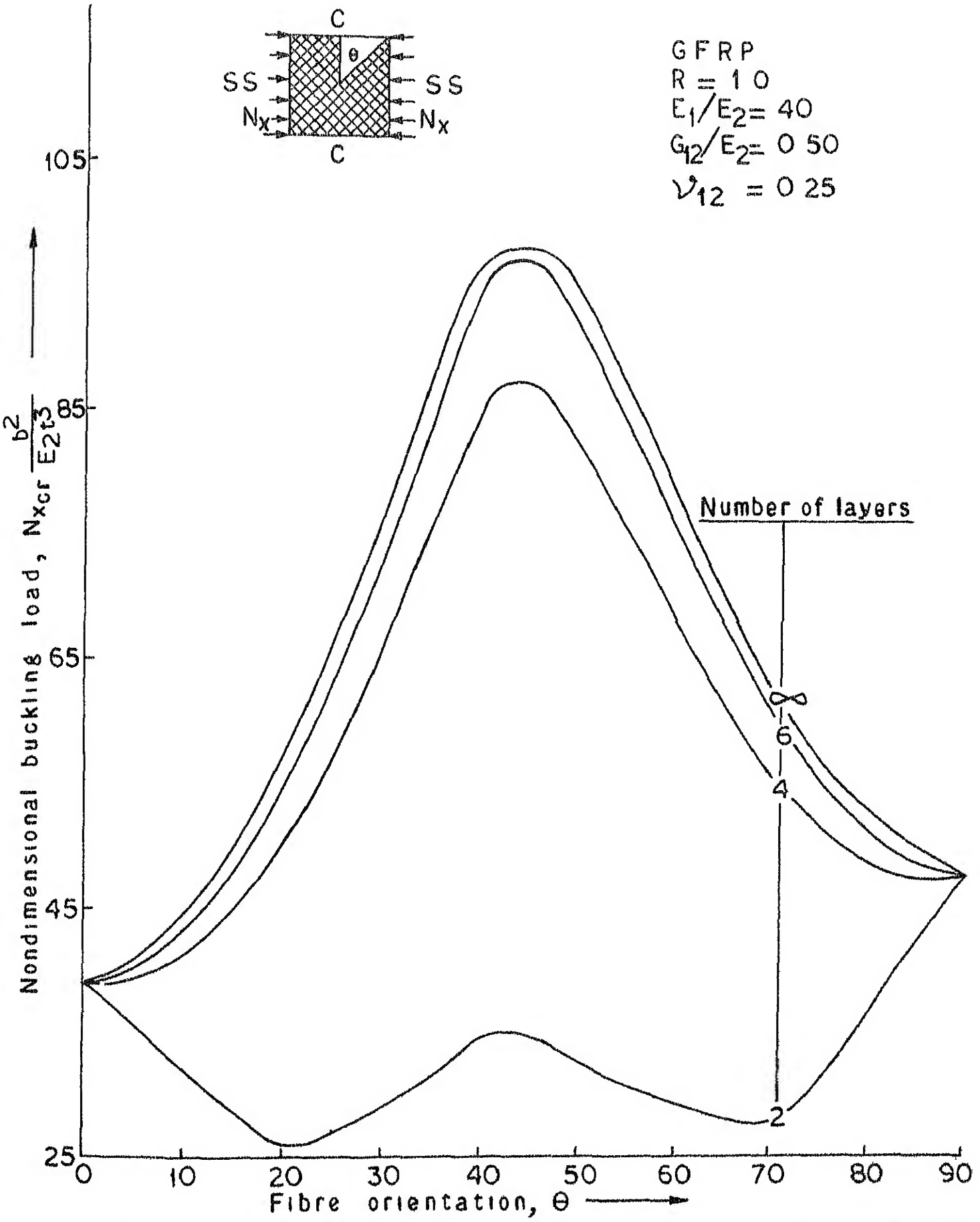

FIG 5 11 VARIATION OF BUCKLING LOAD WITH FIBRE ORIENTATION

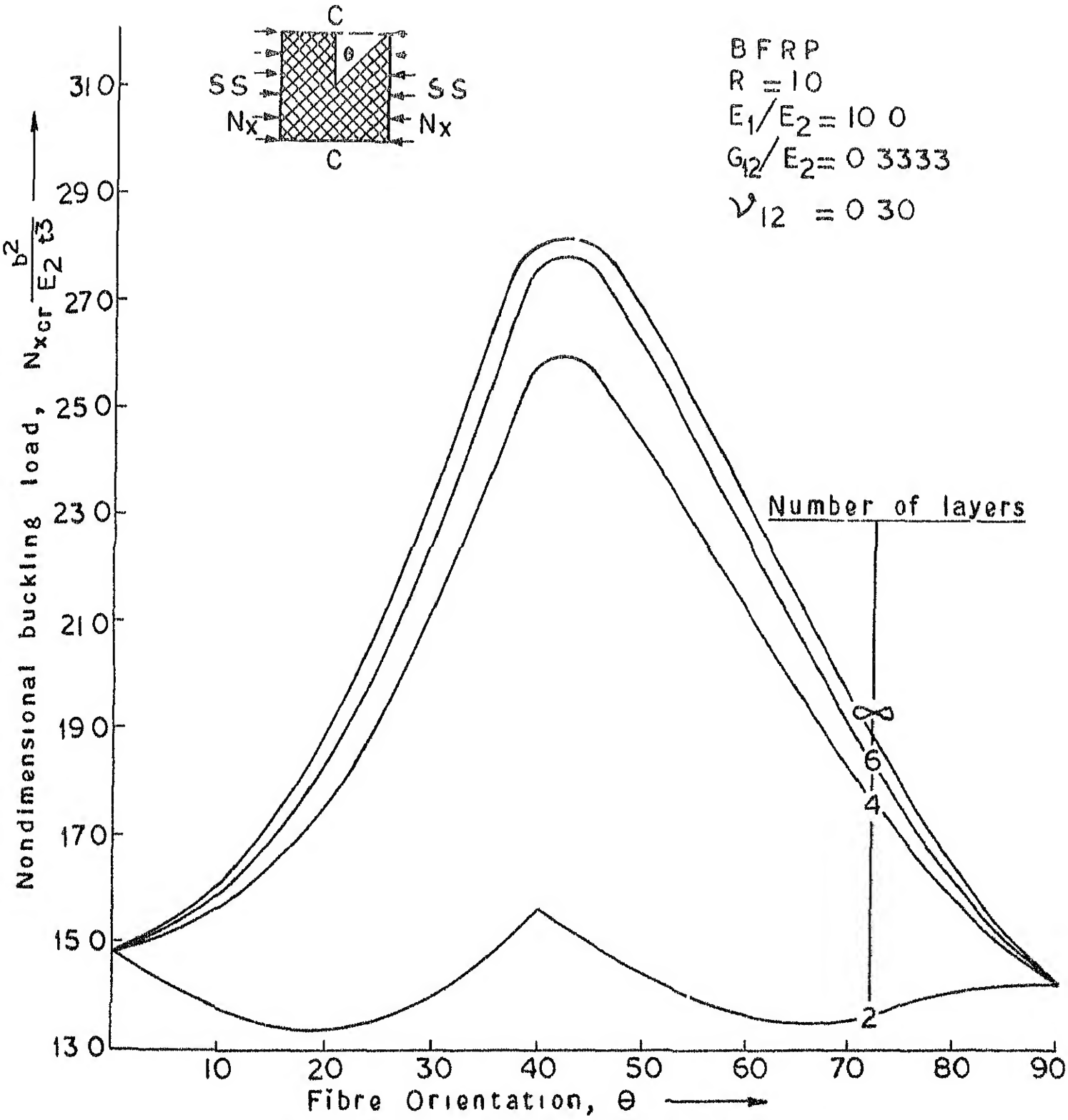

FIG 5 12 VARIATION OF BUCKLING LOAD WITH FIBRE ORIENTATION

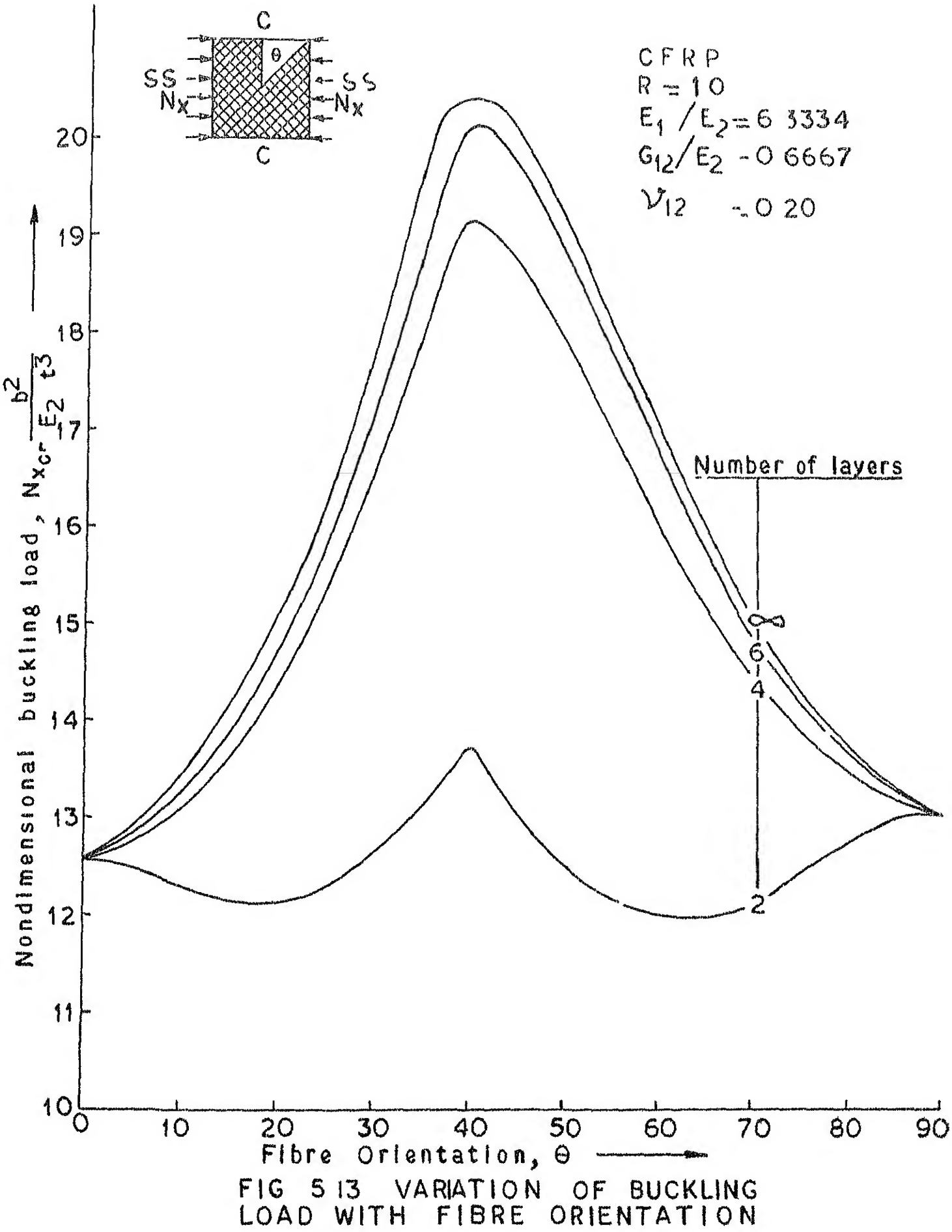

FIG 5 13 VARIATION OF BUCKLING LOAD WITH FIBRE ORIENTATION

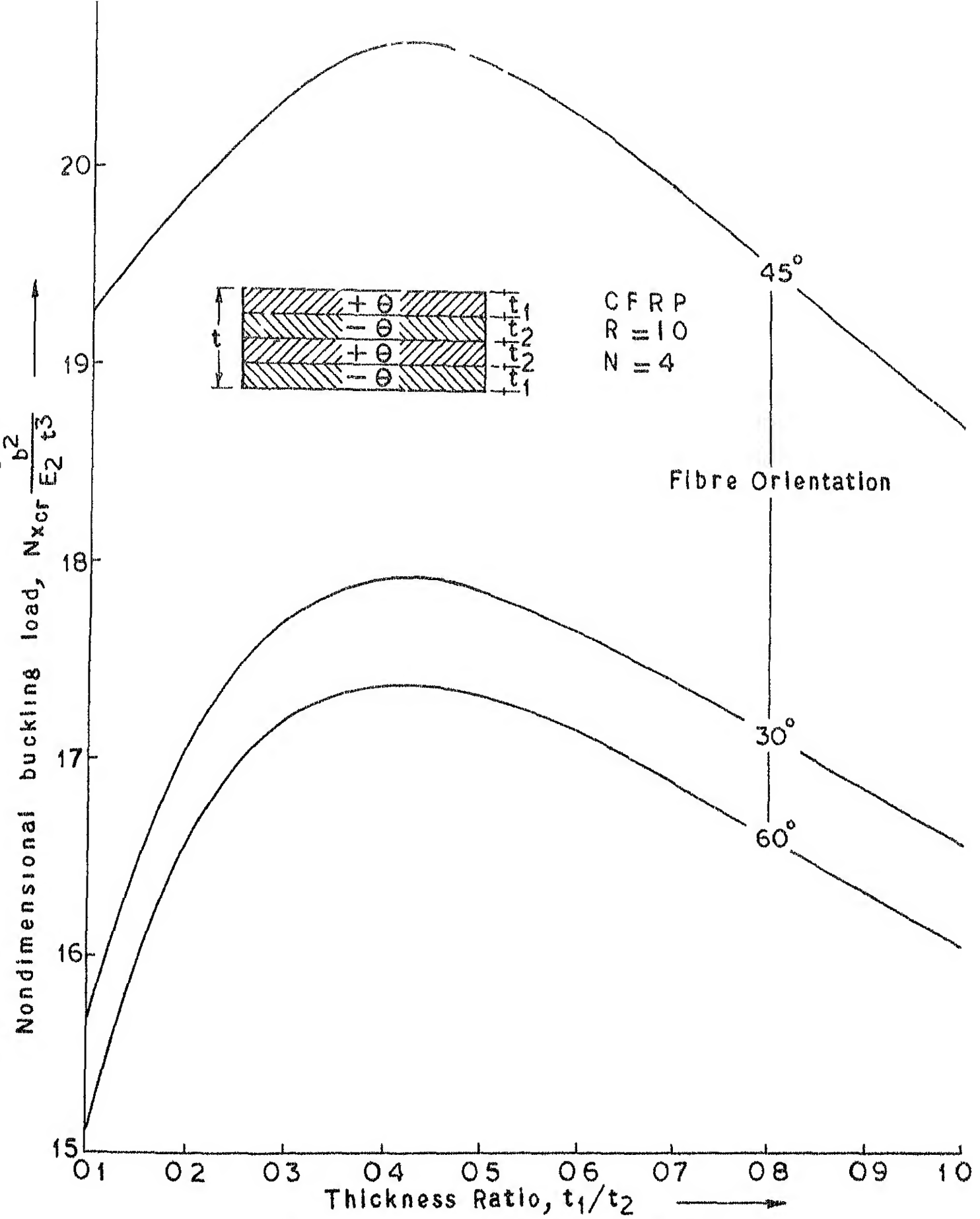

FIG 5 14 VARIATION OF BUCKLING LOAD AS A FUNCTION OF THICKNESS RATIO

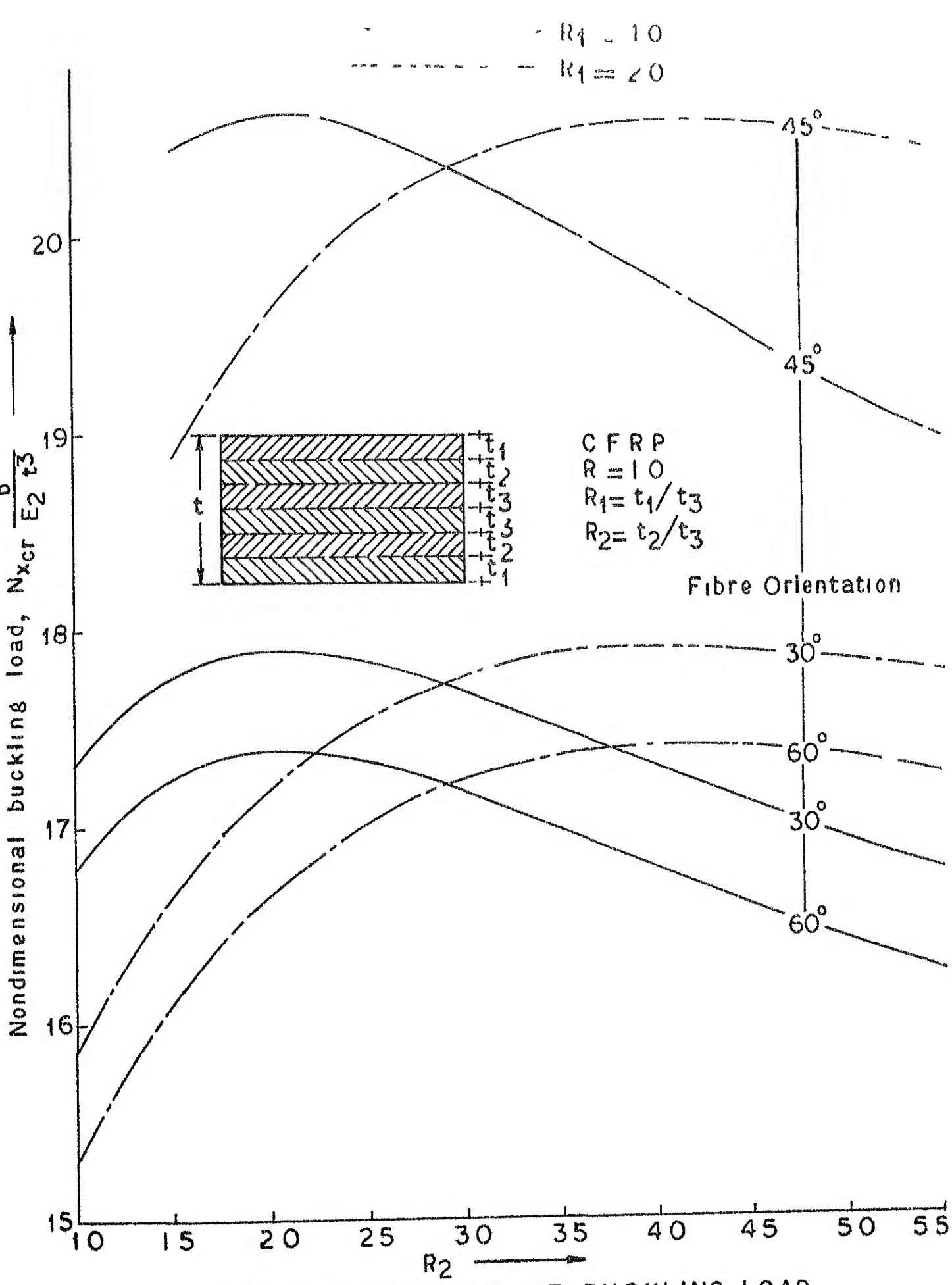

FIG 5.15 VARIATION OF BUCKLING LOAD AS A FUNCTION OF THICKNESS RATIO

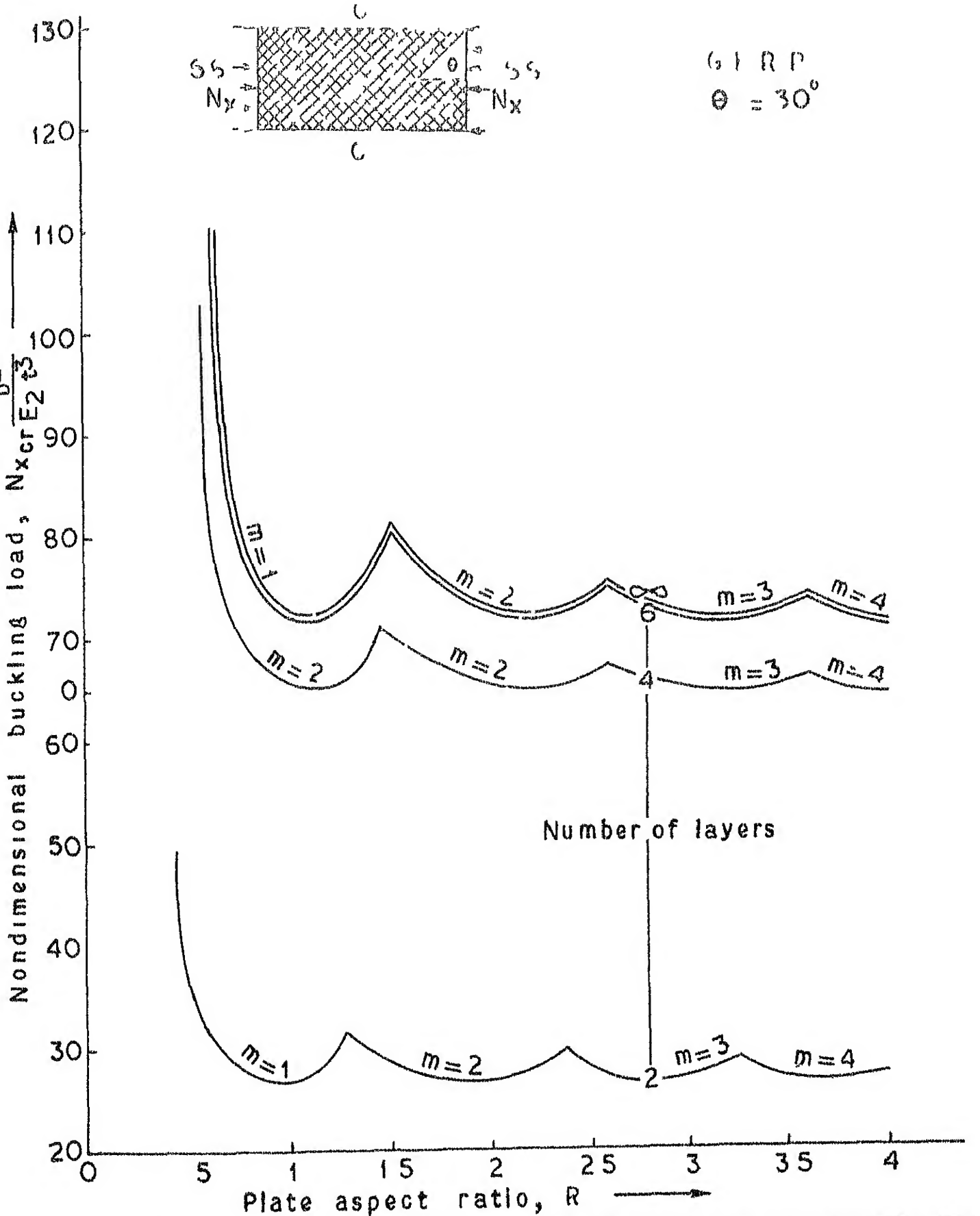

FIG 5 16 VARIATION OF BUCKLING LOAD WITH ASPECT RATIO

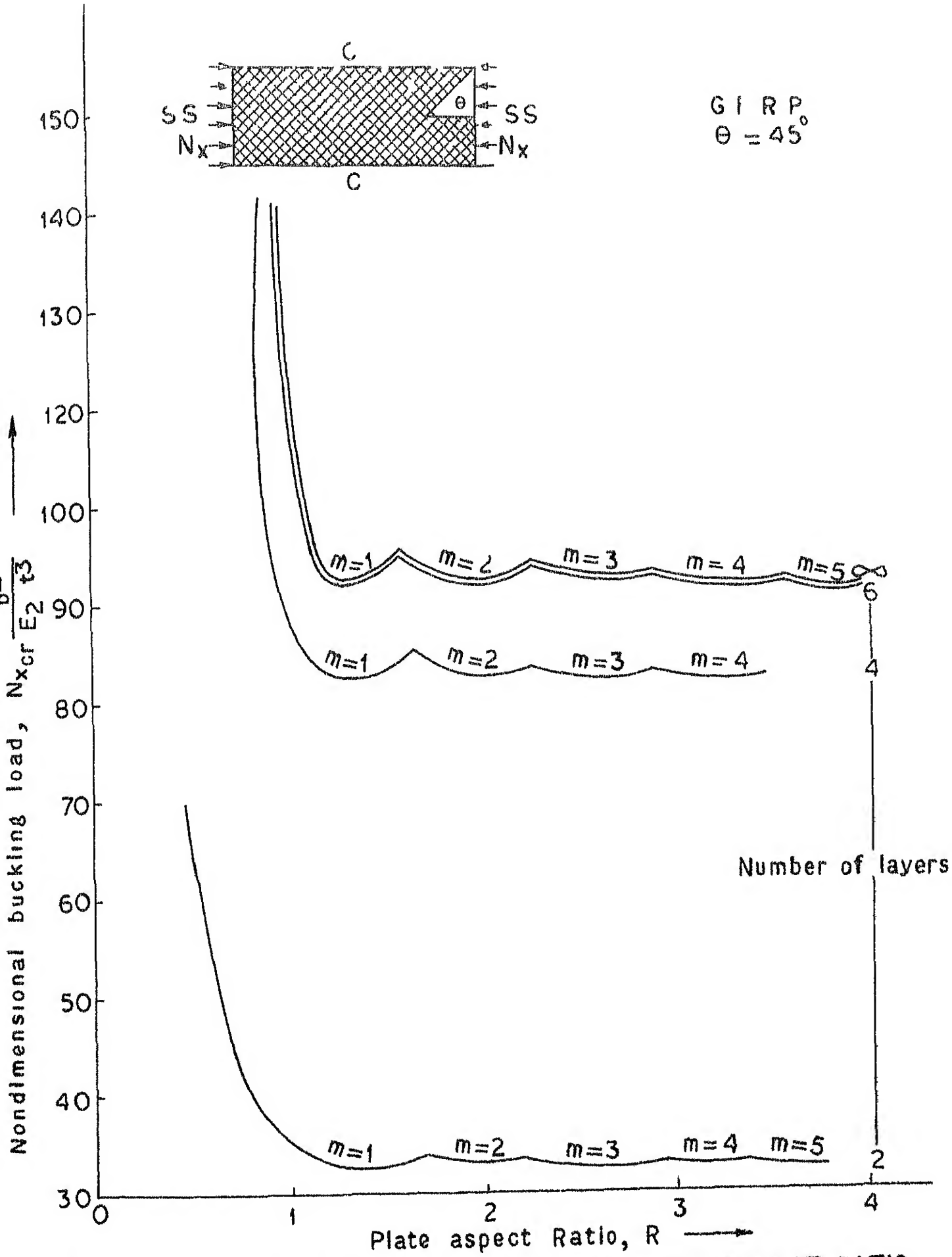

FIG 517 VARIATION OF BUCKLING LOAD WITH ASPECT RATIO

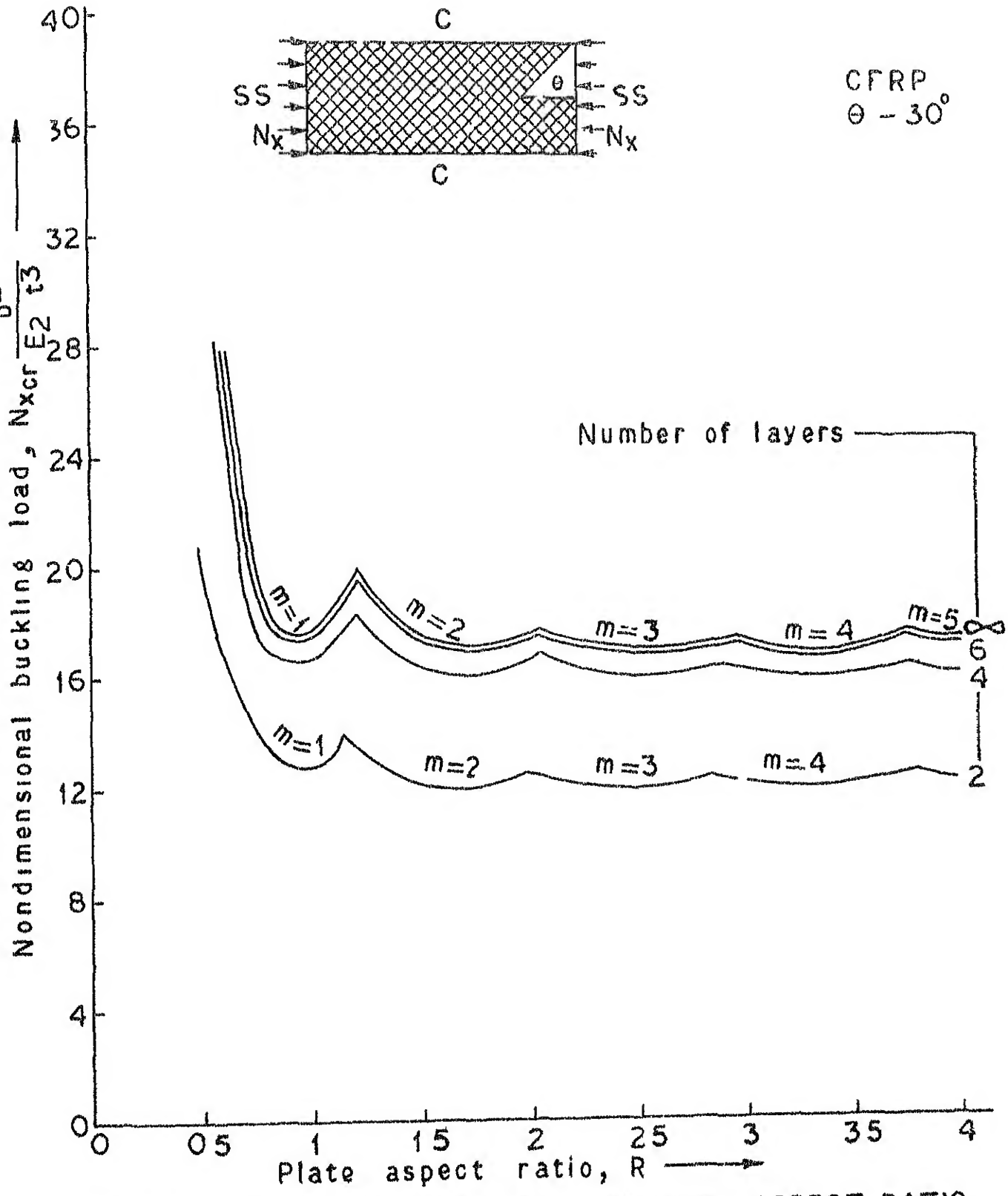

FIG 518 VARIATION OF BUCKLING LOAD WITH ASPECT RATIO

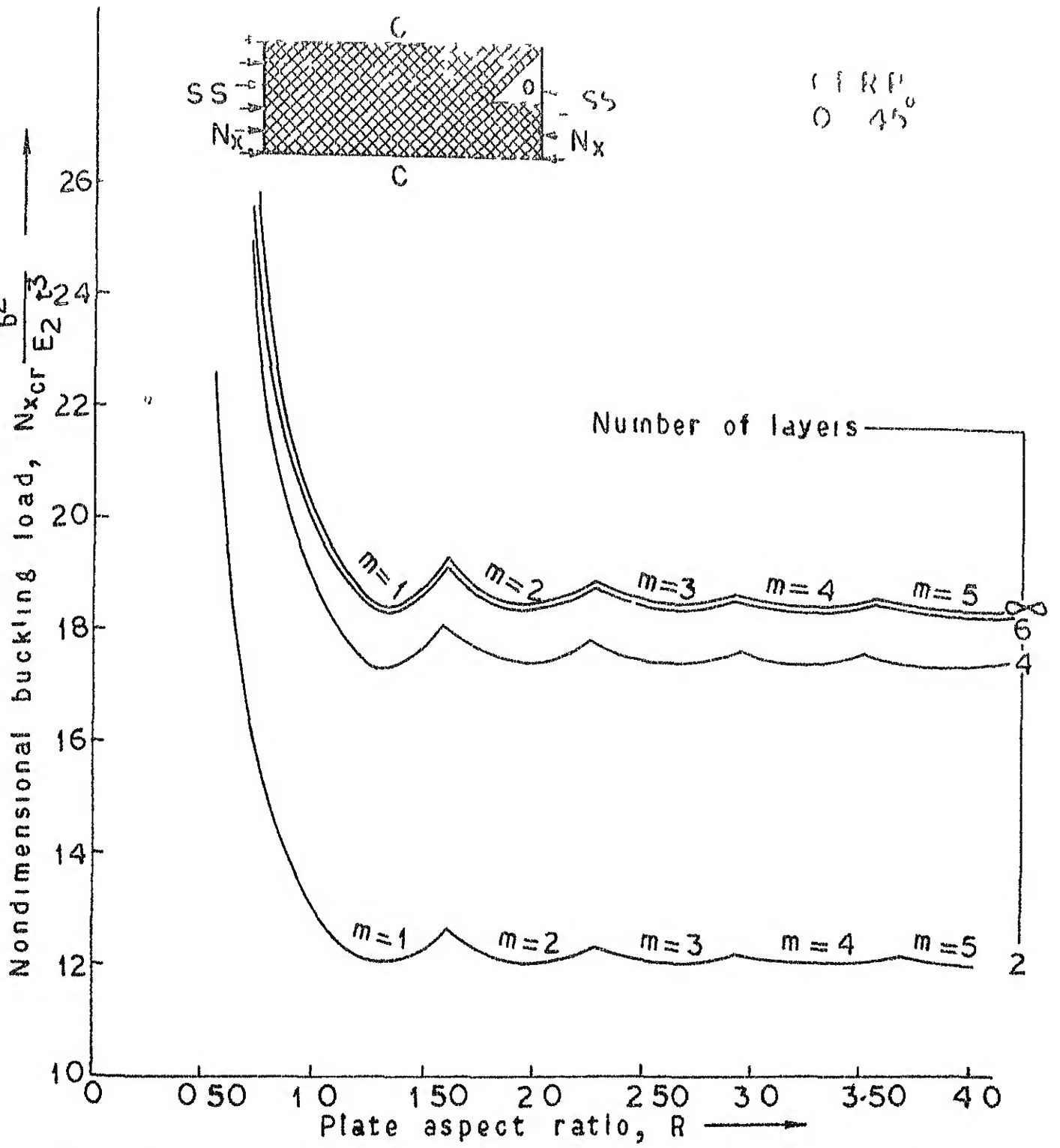

FIG 5 19 VARIATION OF BUCKLING LOAD WITH ASPECT RATIO

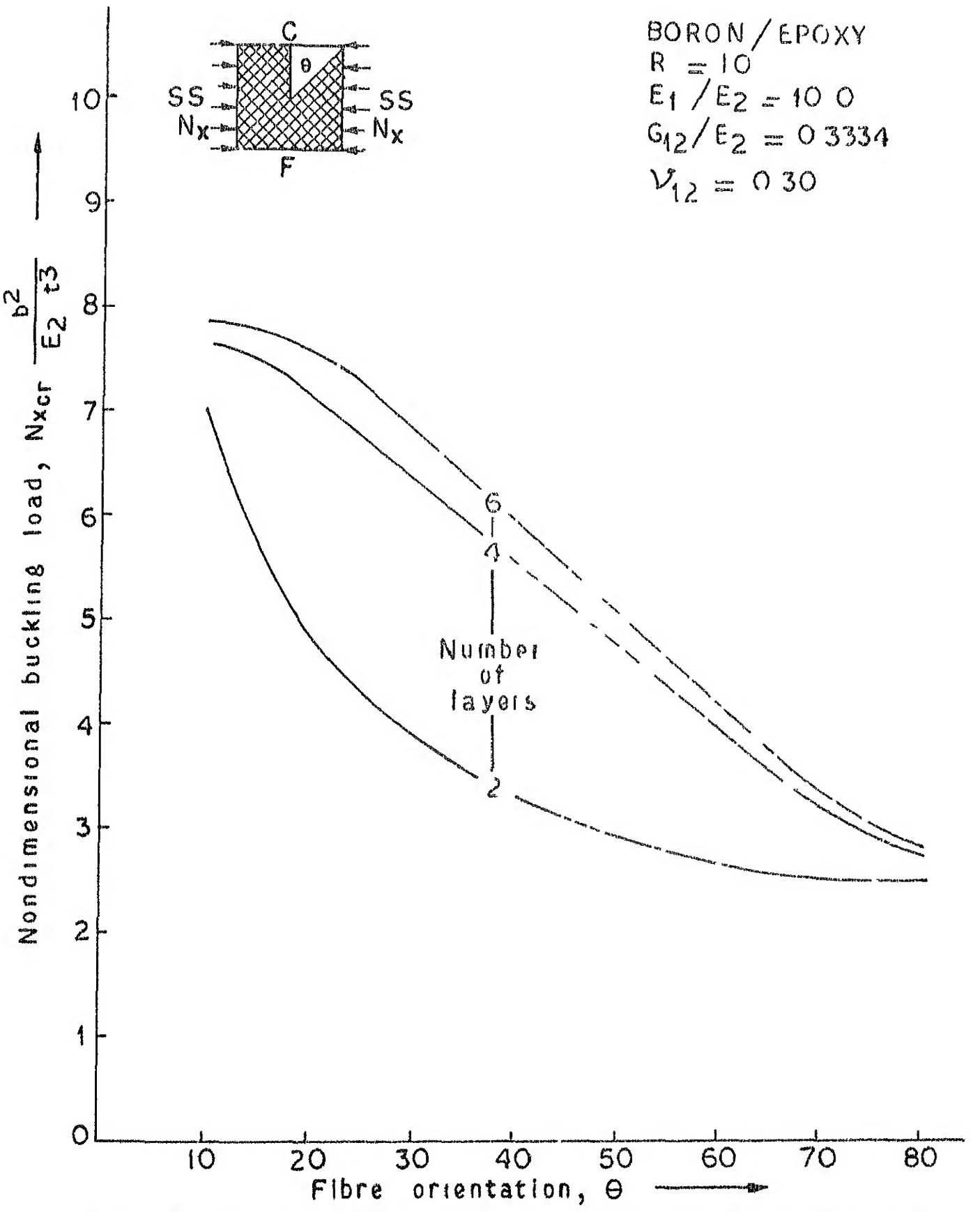

FIG 5 20 BUCKLING LOAD AS A FUNCTION OF ANGLE-PLY ORIENTATION FOR A SQUARE PLATE UNDER UNIFORM UNIAXIAL COMPRESSION

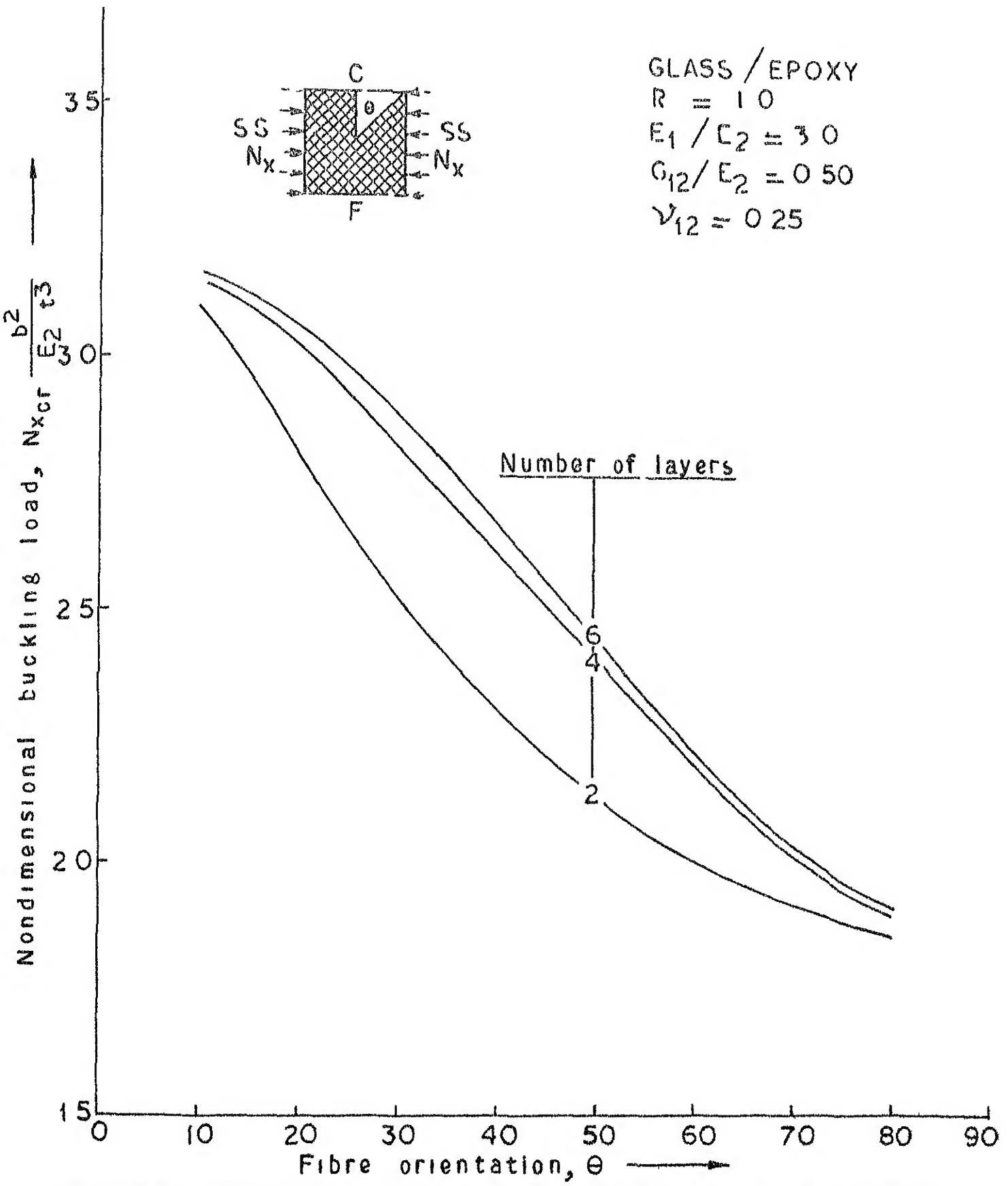

FIG 5.21 BUCKLING LOAD AS A FUNCTION OF ANGLE-PLY ORIENTATION FOR A SQUARE PLATE UNDER UNIFORM UNIAXIAL COMPRESSION

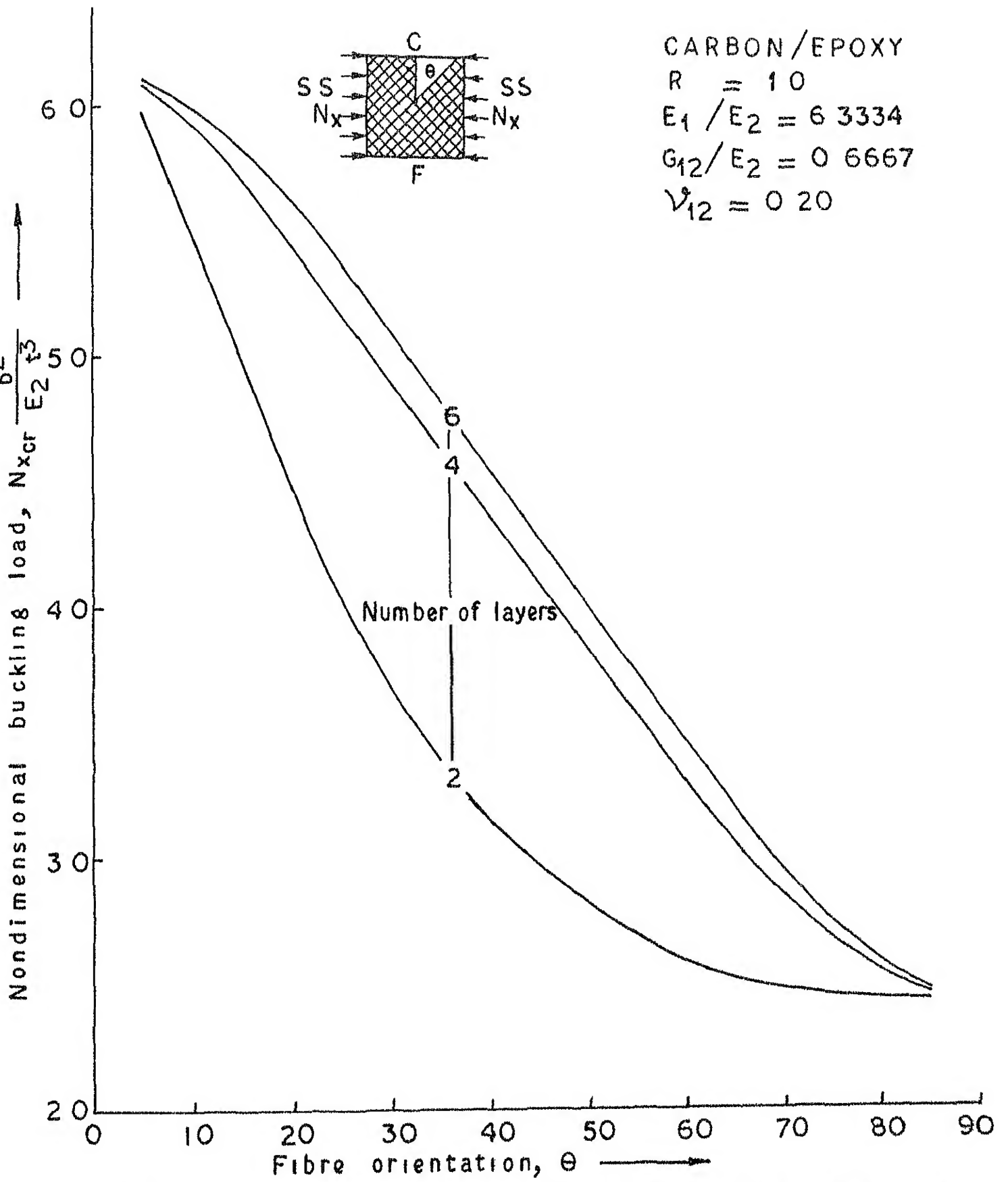

FIG 5 22 BUCKLING LOAD AS A FUNCTION OF ANGLE-PLY ORIENTATION FOR A SQUARE PLATE UNDER UNIFORM UNIAXIAL COMPRESSION

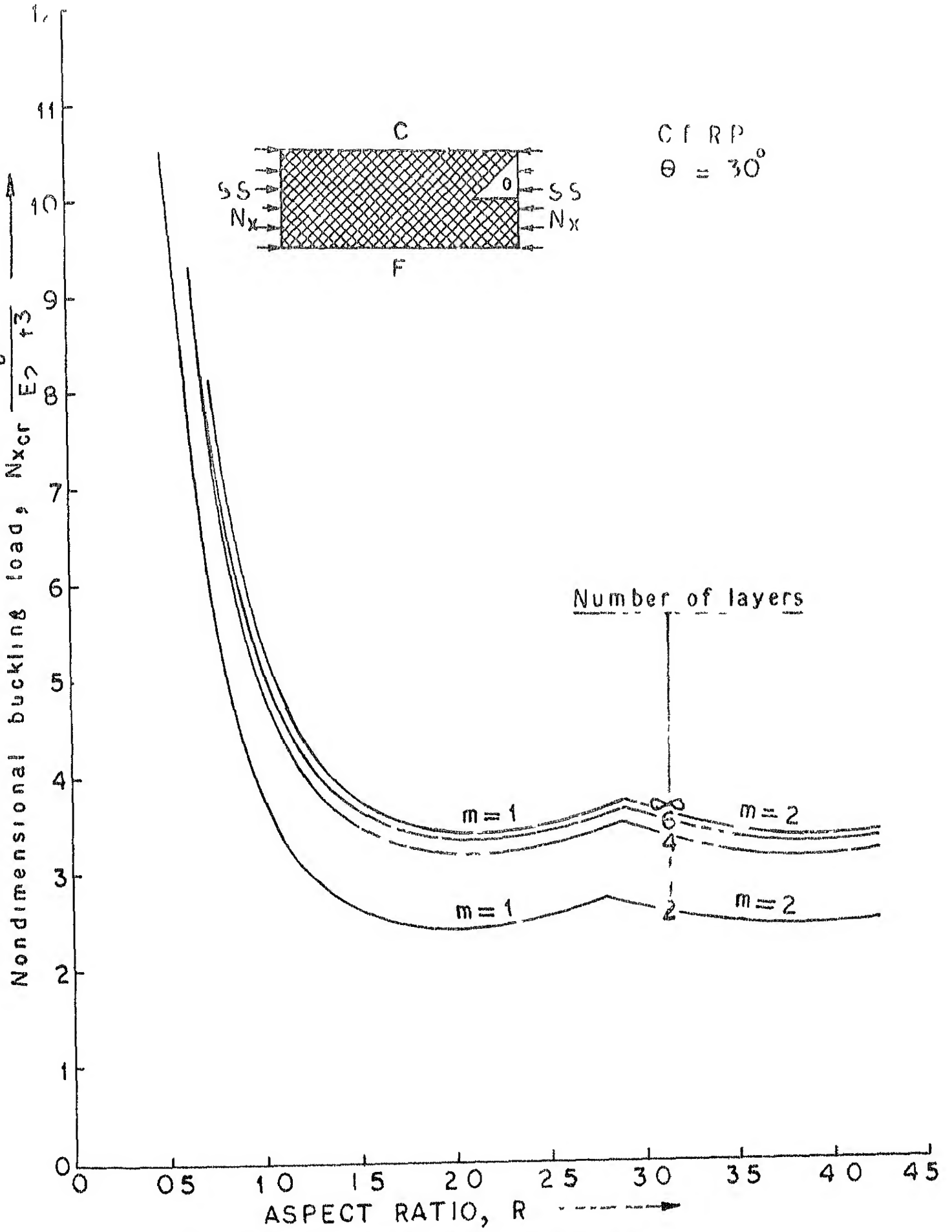

FIG 5 23 BUCKLING LOAD AS A FUNCTION OF ASPECT RATIO

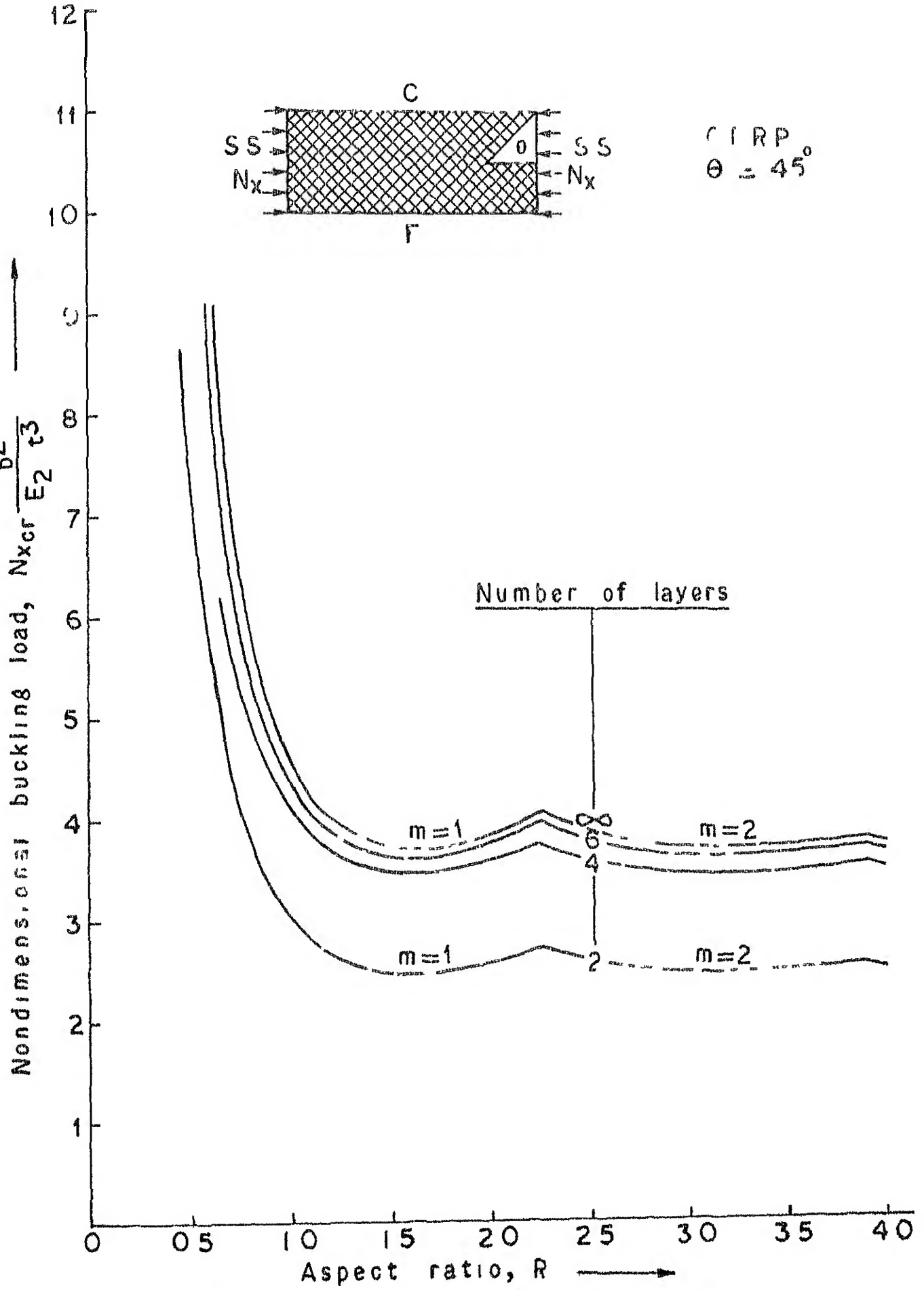

FIG 5 24 BUCKLING LOAD AS A FUNCTION OF ASPECT RATIO

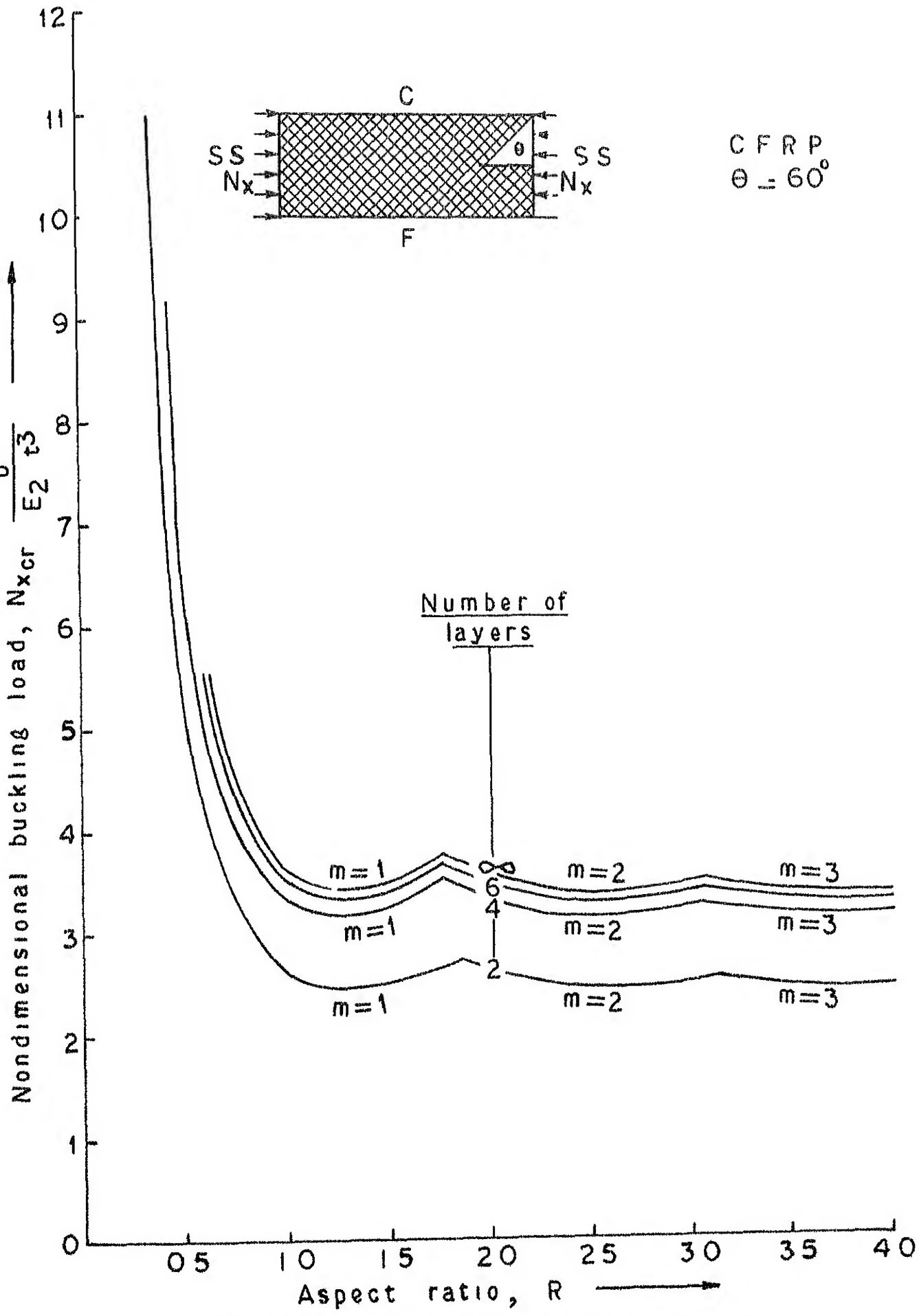

FIG 5 25 BUCKLING LOAD AS A FUNCTION OF ASPECT RATIO

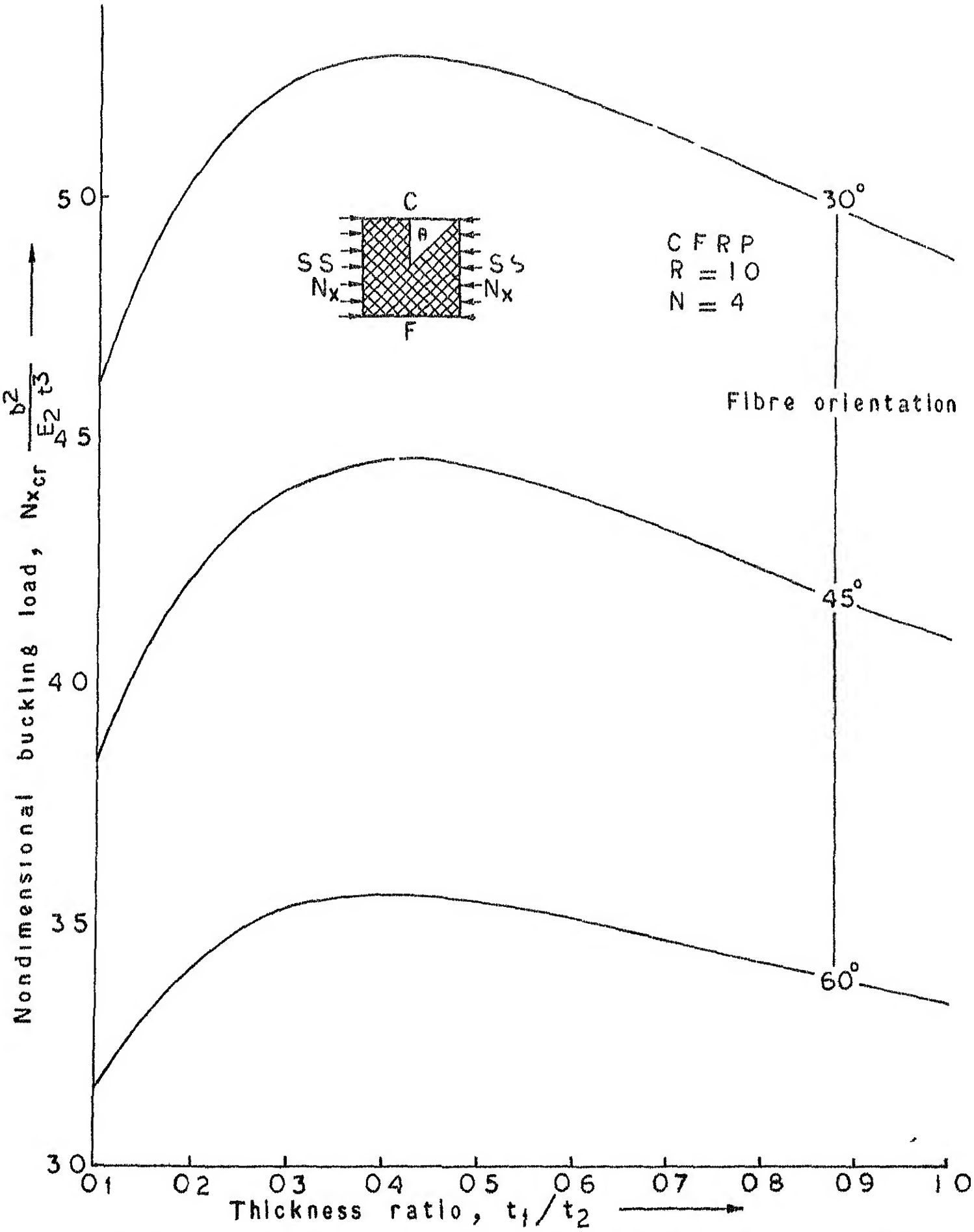

FIG 5 26 BUCKLING LOAD AS A FUNCTION OF THICKNESS RATIO FOR A FOUR - LAYERED LAMINATE

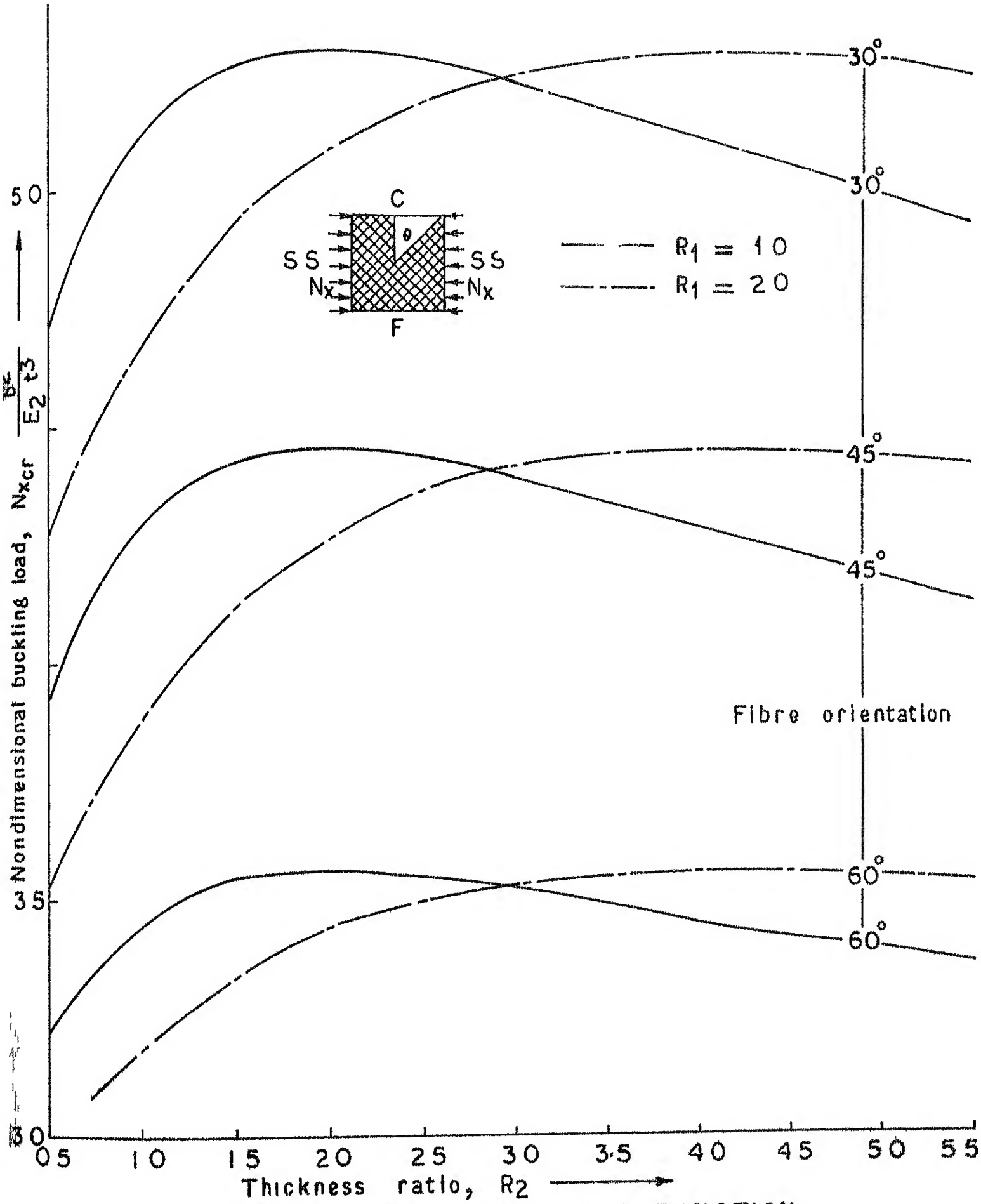

FIG 5.27 BUCKLING LOAD AS A FUNCTION OF THICKNESS RATIO FOR A SIX-LAYERED LAMINATE

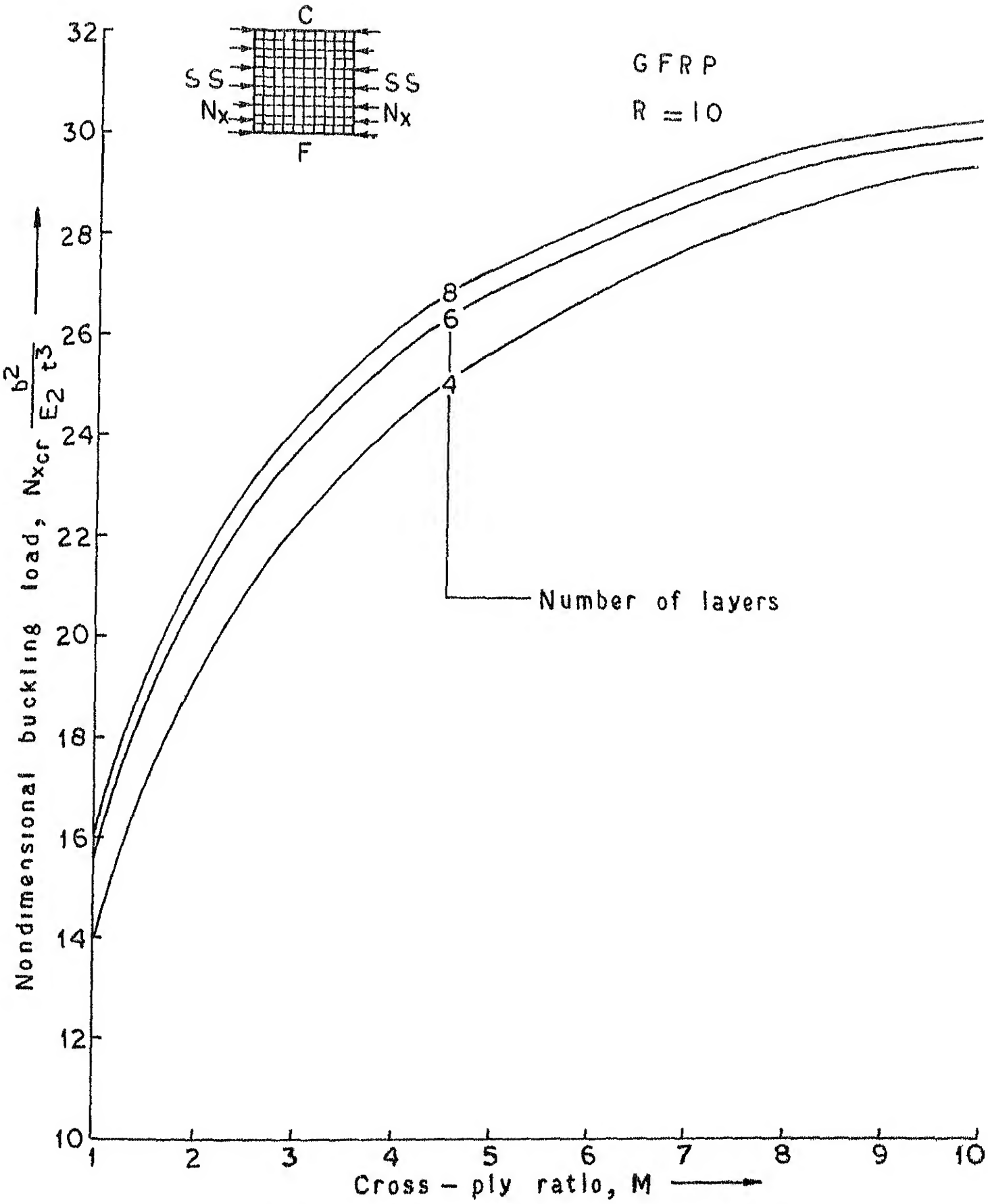

FIG 5.28 VARIATION OF BUCKLING LOAD AS A FUNCTION OF CROSS-PLY RATIO

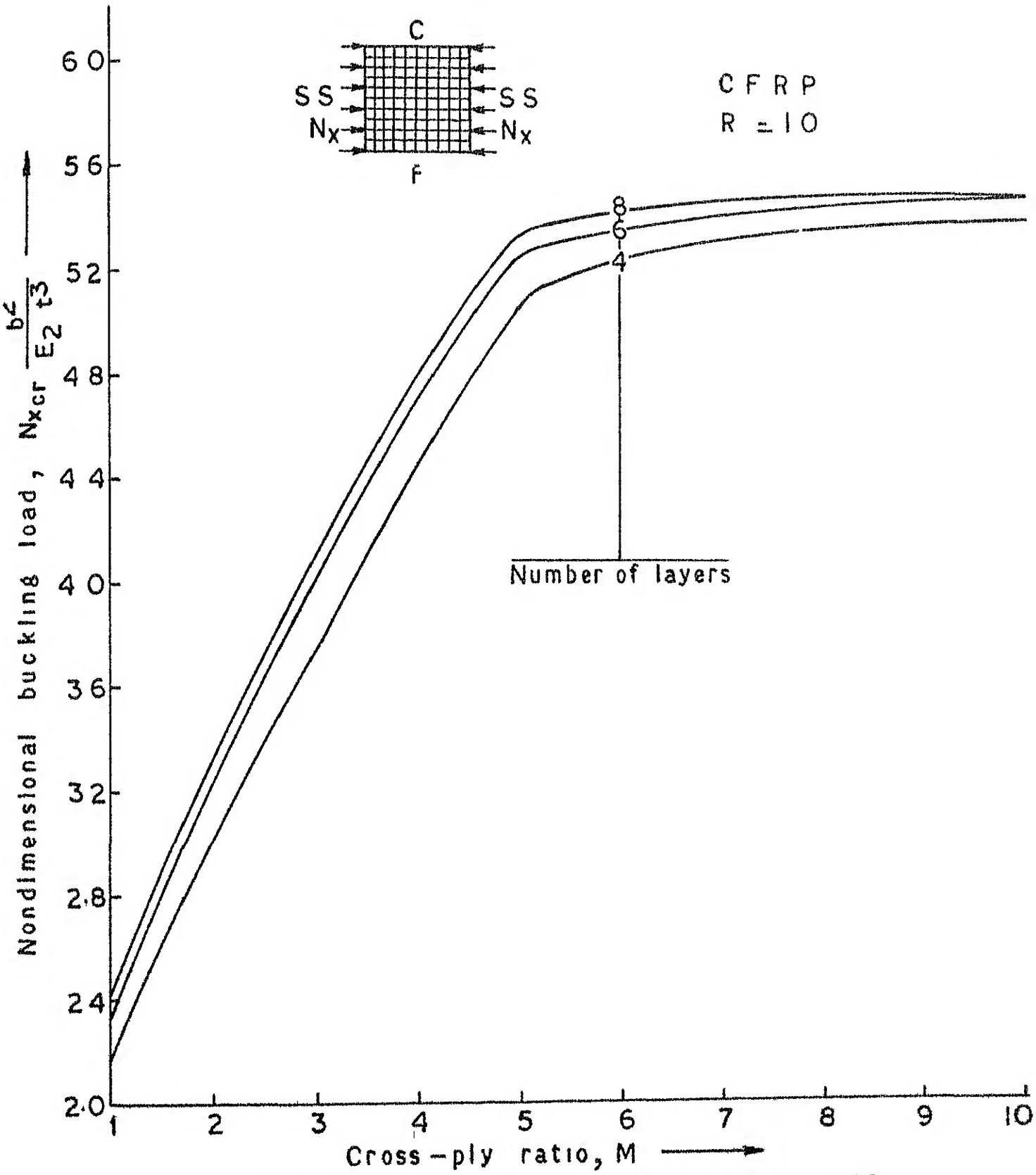

FIG 5 29 VARIATION OF BUCKLING LOAD AS A FUNCTION OF CROSS-PLY RATIO, M

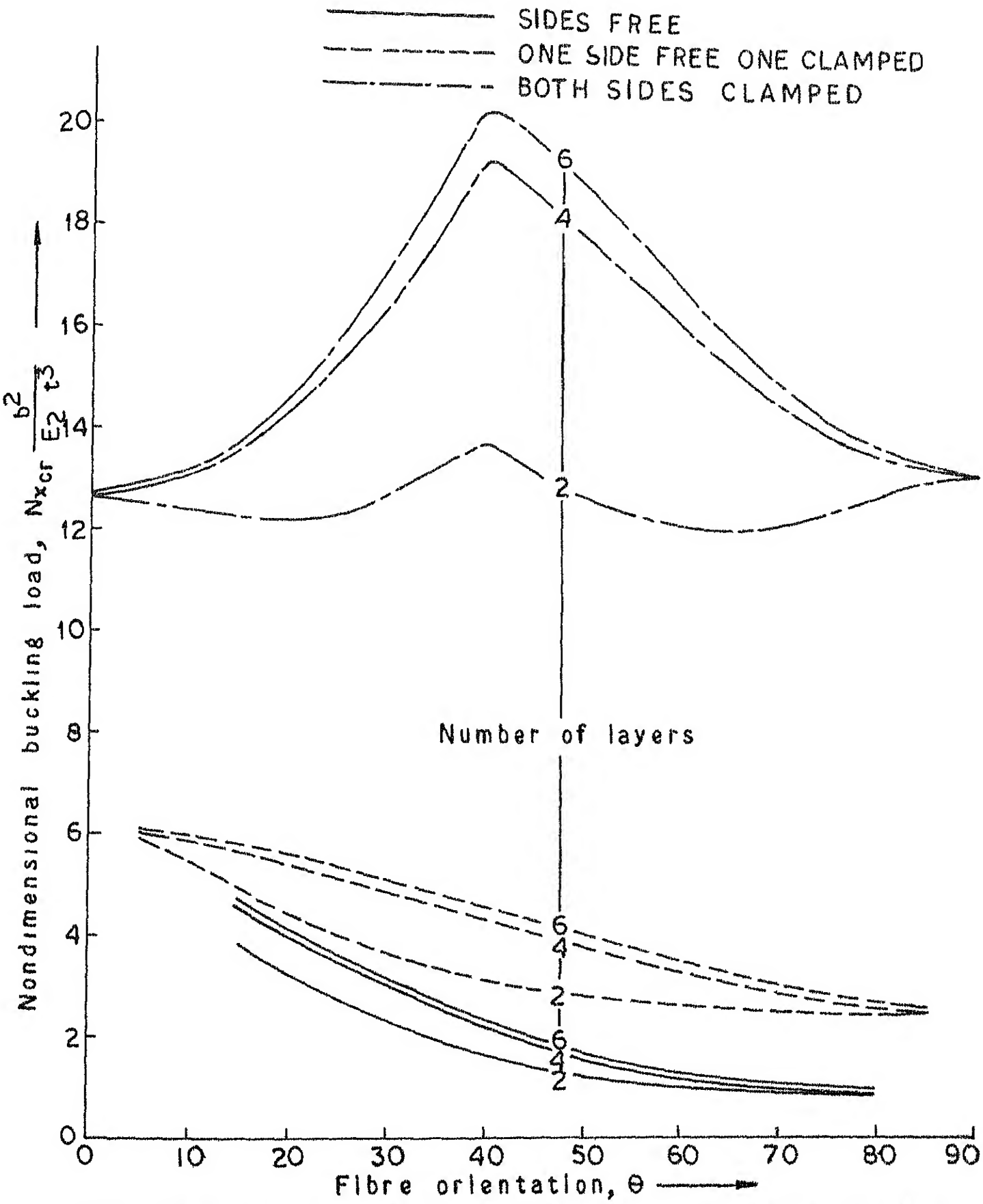

FIG 5 30 VARIATION OF BUCKLING LOAD WITH FIBRE ORIENTATION WITH NUMBER OF LAYERS AND BOUNDARY CONDITIONS AS PARAMETERS

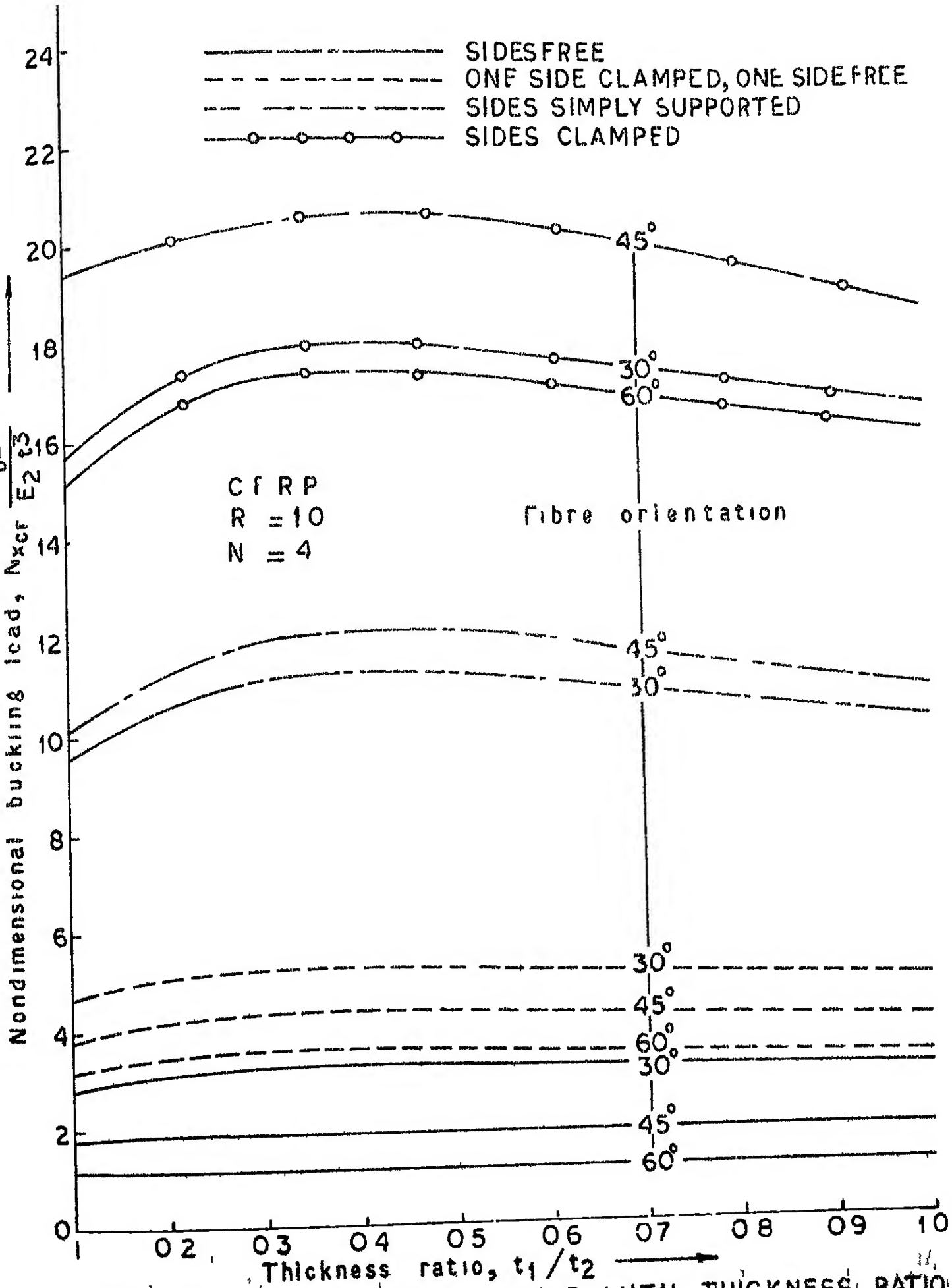

FIG. 5.31 VARIATION OF BUCKLING LOAD WITH THICKNESS RATIO WITH FIBRE ORIENTATION & BOUNDARY CONDITIONS AS PARAMETERS

CHAPTER 6

BUCKLING OF ANTISYMMETRICALLY LAMINATED, RECTANGULAR PLATES ON A WINKLER-PASTERNAK FOUNDATION

6.1 INTRODUCTION

Till now we have considered the buckling behaviour of laminated plates under uniaxial compressive edge loads. In this chapter we propose to consider the behaviour of similar plates under both uniaxial and lateral loads dependent of transverse displacements. A similar practical problem of great interest is a laminated plate on Winkler-Pasternak foundation. The behaviour of a soil performing the support function as a foundation has been modelled by Winkler and Pasternak as shown in Figure 6.1. A considerable amount of work has already been done regarding the elastic behaviour of isotropic plates resting on elastic foundation.[29-43] It is, however, only recently that an attempt has been made to combine the coupling effects common with laminated plates in the presence of an elastic foundation.[44-45]

Turvey[44] presented simple, exact solutions for uniformly loaded, simply supported and antisymmetrically laminated cross- and angle-ply plate strip resting on Winkler-Pasternak foundation. In a recent paper,[45] he presented the analysis for a uniformly loaded, simply supported, anti-symmetrically laminated, cross- and angle-ply rectangular

plates resting on a similar elastic foundation. The deflections and stress couples are evaluated as a function of material coupling and foundation stiffnesses. However, it seems that there is no study on the buckling response of composite plates resting on Winkler-Pasternak foundation. The purpose of this chapter is, therefore, to fill this gap. The plates are assumed to be simply supported on the two opposite loaded edges and various boundary conditions on the remaining two edges are considered. The influence of the foundation, material coupling and boundary conditions on the buckling response of anti-symmetrically laminated cross- and angle-ply plates is studied.

6.2 BUCKLING ANALYSIS

6.2.1 Antisymmetric Angle-ply Plates

The governing eighth order partial differential equation (3.22) as derived in Chapter 3 can be written as

$$A_1 \frac{\partial^8 \phi}{\partial x^8} + A_3 \frac{\partial^8 \phi}{\partial x^6 \partial y^2} + A_5 \frac{\partial^8 \phi}{\partial x^4 \partial y^4} + A_7 \frac{\partial^8 \phi}{\partial x^2 \partial y^6} + A_9 \frac{\partial^8 \phi}{\partial y^8} = q(x, y) \qquad (3.22)$$

For an antisymmetric angle-ply plate resting on Winkler-Pasternak foundation and subjected to an in-plane load N_x per unit width as shown in Figure 6.1, the loading term $q(x, y)$ in the above equation can be written as

$$q(x, y) = -N_x \frac{\partial^2 w}{\partial x^2} - kw + g\left(\frac{\partial^2 w}{\partial x^2} + \frac{\partial^2 w}{\partial y^2}\right) \tag{6.1}$$

where

k = Winkler foundation stiffness

g = Pasternak foundation stiffness.

Substituting the expression for w from Eq. (3.25) into Eq. (3.22), the resulting eighth order polynomial in is

$$\begin{aligned}
&\lambda^8 + [-A_7/A_9 - GD_{11}a_9/\beta^2 A_9]\lambda^6 \\
&+ [A_5/A_9 - \mu a_9/A_9 + G(a_8 + a_9)D_{11}/\beta^2 A_9 + KD_{11}a_9/\beta^4 A_9]\lambda^4 \\
&+ [-A_3/A_9 + \mu a_8/A_9 - G(a_7 + a_8)D_{11}/\beta^2 A_9 - KD_{11}a_8/\beta^4 A_9]\lambda^2 \\
&+ [A_1/A_9 - \mu a_7/A_9 + GD_{11}a_7/\beta^2 A_9 + KD_{11}a_7/\beta^4 A_9] = 0
\end{aligned} \tag{6.2}$$

where

$K = kb^4/D_{11}$

$G = gb^2/D_{11}$

$\beta = m\pi/R$

Equation (6.2) can now be solved by the method as discussed in Chapter 3.

6.2.2 Antisymmetric Cross-ply Plates

An eighth order polynomial in λ for an antisymmetric cross-ply plate corresponding to Eq. (6.2) developed for an antisymmetric angle-ply plate is obtained by replacing a_7, a_8

and a_9 in Eq. (6.2) by b_7, b_8 and b_9 given by relations (3.75-3.77) respectively. The coefficients A_1, A_3, A_5, A_7 and A_9 in Eq. (6.2) are replaced by those of antisymmetric cross-ply plates. These are given by relations (3.35) to (3.39).

The coefficients of Eq. (6.2) for given values of K and G contain two unknowns N_x and m. m corresponds to number of half waves that the plate buckles. In fact m is an integer and takes on the values 1, 2 etc., depending on the mode of buckling. The estimation of buckling loads for given boundary conditions is then carried out by the procedure outlined in Chapter 5.

The following sets of boundary conditions have been considered:

(a) Two loaded edges simply supported and the other two edges free.

(b) Two loaded edges simply supported and the other two edges clamped.

(c) Two loaded edges simply supported, one edge clamped and the remaining edge free.

6.3 RESULTS AND DISCUSSION

The numerical computations are carried out for the following data of carbon fibre reinforced plastics:

$E_1/E_2 = 6.33$; $G_{12}/E_2 = 0.667$; $\nu_{12} = 0.20$

The variation of buckling load as a function of nondimensional Winkler foundation stiffness K for three different fibre orientations (30°, 45° and 60°) of angle-ply square plates with two loaded edges simply supported and the remaining sides free are shown in Figures 6.2, 6.3 and 6.4 respectively with nondimensional Pasternak foundation stiffness, G and number of layers, N as parameters. It is seen that a small change in the value of the Pasternak foundation stiffness results in a greater change in the values of buckling loads than does an equal change in the values of the Winkler foundation stiffness. The percentage change in the buckling loads for a two-layered configuration, for example, between G = 2.0 and G = 4.0 at K = 2.0 is of the order of twenty whereas the corresponding figure between K = 2.0 and K = 4.0 at G = 0 is only of the order of three percent for a 30° fibre oriented plate. The order of these changes appears to be fairly independent of the fibre orientations. Further the buckling load increases linearly with K. Figure 6.5 shows the variation of buckling load with Winkler foundation stiffness for an antisymmetrically laminated cross-ply square plate with two loaded edges simply supported and the remaining sides free with G and N as parameters. It is observed that the buckling load for a two-layered laminate at G = 5.0 approaches that for a four-layered laminate at G = 3.0. This may be attributed to the general increase of overall stiffness of the plate with increases in

K, G and N. However, the effect of coupling rapidly diminishes as the number of layers in the laminate is increased.

The variations of buckling load with Winkler stiffness, K for an antisymmetric square plate are shown in Figures 6.6, 6.7 and 6.8 for three different fibre orientations, $\theta = 30°$, $45°$ and $60°$ respectively with loaded edges simply supported and the remaining sides clamped. Here the buckling load for a $30°$ oriented, two-layered laminate at Pasternak foundation stiffness values of 6.0 and 8.0 are seen to approach those for a six-layered laminate of the corresponding foundation stiffness values of 0.0 and 2.0 respectively. However, no such overlapping of buckling loads is observed for $45°$ and $60°$ oriented plates. Thus changes in buckling loads for given changes in Pasternak stiffness values or in Winkler stiffness appear to be dependent upon fibre orientation for this type of boundary conditions. The percentage change in buckling load, for example, for a two-layered laminate between G of 2.0 and 4.0 at K = 2.0 is of the order of eleven for $\theta = 30°$, five for $\theta = 45°$ and 2.5 for $\theta = 60°$. The corresponding changes in buckling loads due to changes in Winkler stiffness values from K = 2.0 to K = 4.0 at G = 0 are of the order of 0.55 percent for $\theta = 30°$, 0.10 percent for $\theta = 45°$ and 0.05 percent for $\theta = 60°$. Thus the changes in buckling loads for given changes in Winkler or Pasternak stiffness values are dependent upon the fibre orientation for a plate with loaded edges simply

supported and the remaining edges clamped, though the earlier observation of dominance of Pasternak stiffness in comparison to Winkler stiffness remains valid even in this case. Further, for a given value of G, there is very little change in the buckling load with K.

Figures 6.9 through 6.11 show respectively the variations of buckling loads with Winkler stiffness, K for an antisymmetric square plate with two loaded edges simply supported, one side fixed and the remaining side free for three fibre orientations, $\theta = 30°$, $45°$ and $60°$ and with number of layers (N) and Pasternak shear stiffness (G) as parameters. An examination of these figures reveals that in addition to the general dominance of Pasternak stiffness over Winkler stiffness (in terms of increase in buckling loads), the changes in buckling loads appear to be dependent upon fibre orientations. The percentage increase in buckling load for a two-layered laminate, for example, between G = 2.0 and 4.0 at K = 2 is of the order of fifteen for $\theta = 30°$, twelve for $\theta = 45°$ and nine for $\theta = 60°$. The corresponding figures between K = 2.0 and 4.0 at G = 0 for a two-layered laminate are 1.9, 1.5 and 1.2 percent for $\theta = 30°$, $45°$ and $60°$ respectively.

The variations of buckling load with fibre orientation, θ is shown in Figure 6.12 for a square anti-symmetric angle-ply plate with two opposite edges simply

supported and the remaining edges fixed and with number of layers, Winkler and Pasternak foundation stiffnesses as parameters. It is of interest to note that both foundation stiffnesses (K and G) exert greater influence on buckling load in the fibre orientation range of 5° to 25° than at other fibre orientations. The variation of buckling load for a two-layered laminate at K = 10.0 and G = 5.0 follows partly a different trend than when the Pasternak foundation is absent. However, as expected, the solutions at different foundation stiffnesses tend to become independent of the number of layers at extreme values of fibre orientations. The variation of buckling load with fibre orientation for a square antisymmetric angle-ply plate with two loaded edges simply supported, one side clamped and the remaining side free is shown in Figure 6.13 with number of layers (N), Winkler stiffness (K) and Pasternak stiffness (G) as parameters. The general observations for these variations appear to be common with those discussed above.

A comparison of Figures 6.2 - 6.13 for different boundary conditions reveal that the increments in buckling load levels for given increments of K, G and N are maximum for free-free boundary conditions and minimum for clamped-clamped boundary conditions. For other boundary conditions, the values lie in between. Furthermore, the effect of fibre orientation on the buckling load is quite significant for some types of boundary conditions.

It can be concluded from the above study that both material coupling and foundation stiffnesses affect the buckling response of the antisymmetric cross- and angle-ply plates significantly. The effect is more significant for plates with free edges than for those with fixed edges. The changes in buckling loads due to changes in foundation stiffnesses also appear to be dependent upon fibre orientations for certain types of boundary conditions. It is further observed that a change in the Pasternak foundation stiffness exerts a far greater change in the buckling load than does a similar change in the Winkler foundation stiffness.

- o -

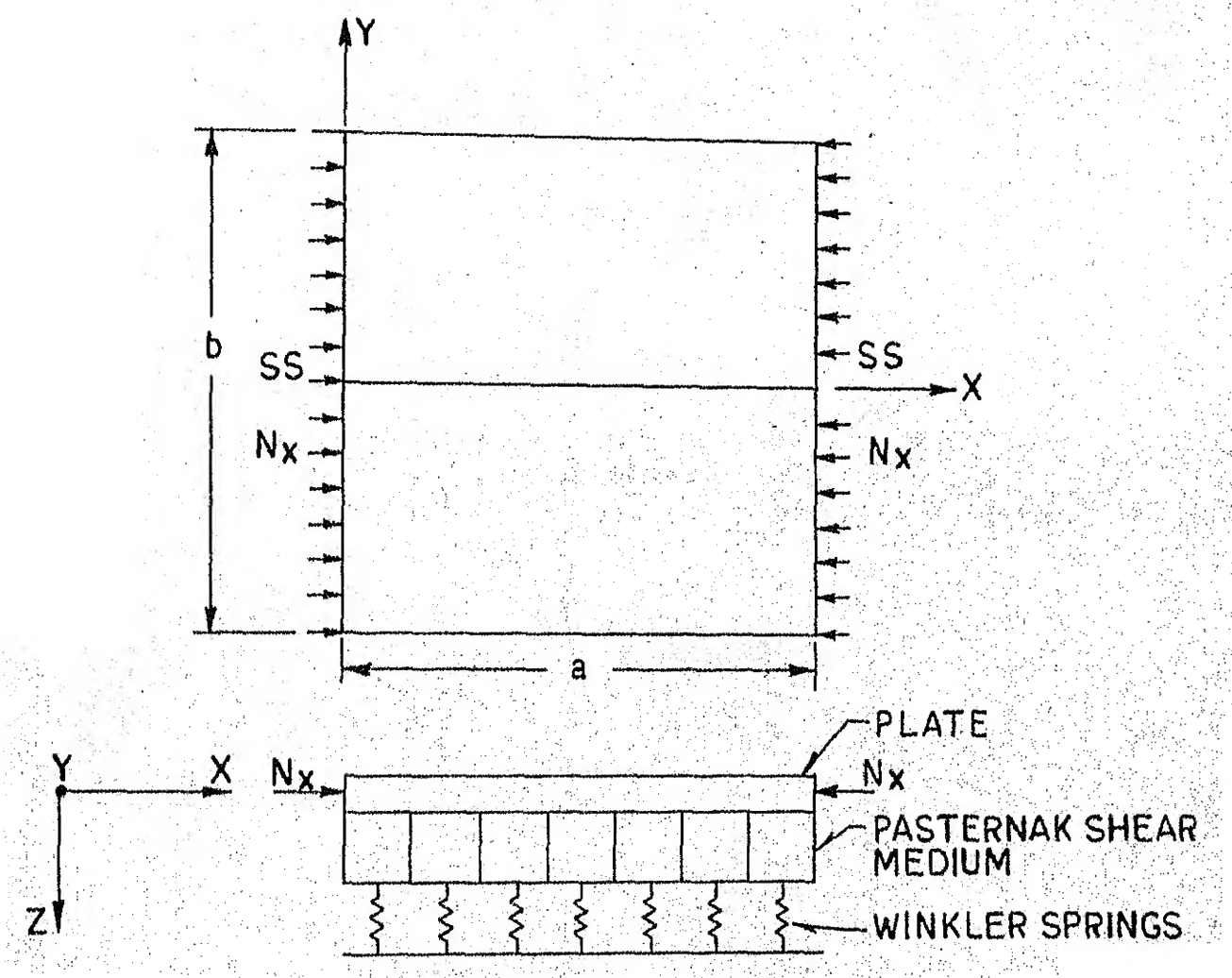

FIG. 6.1: GEOMETRY OF THE PLATE RESTING ON WINKLER-PASTERNAK FOUNDATION.

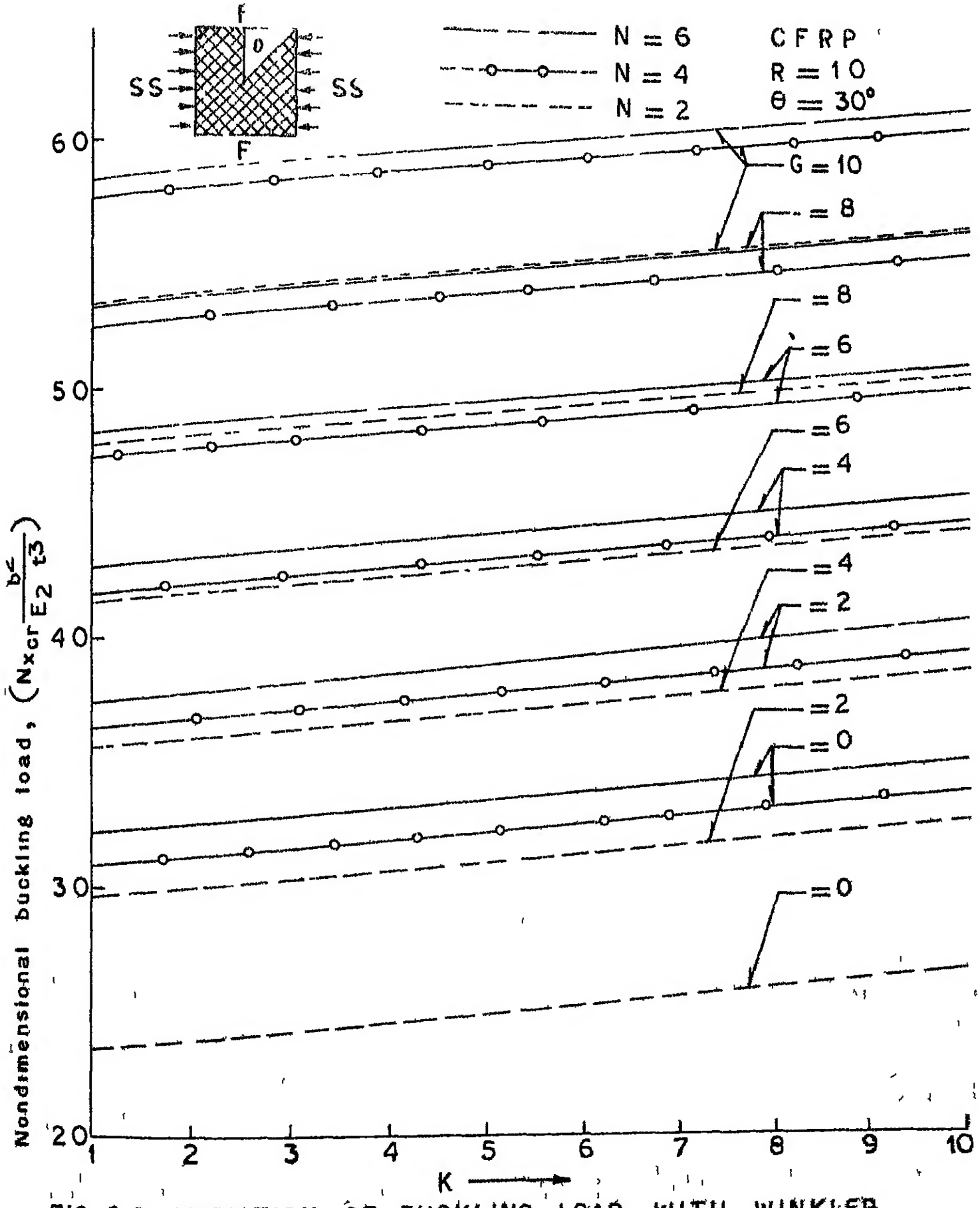

FIG 6.2 VARIATION OF BUCKLING LOAD WITH WINKLER STIFFNESS, K FOR A SQUARE ANTISYMMETRIC ANGLE-PLY PLATE.

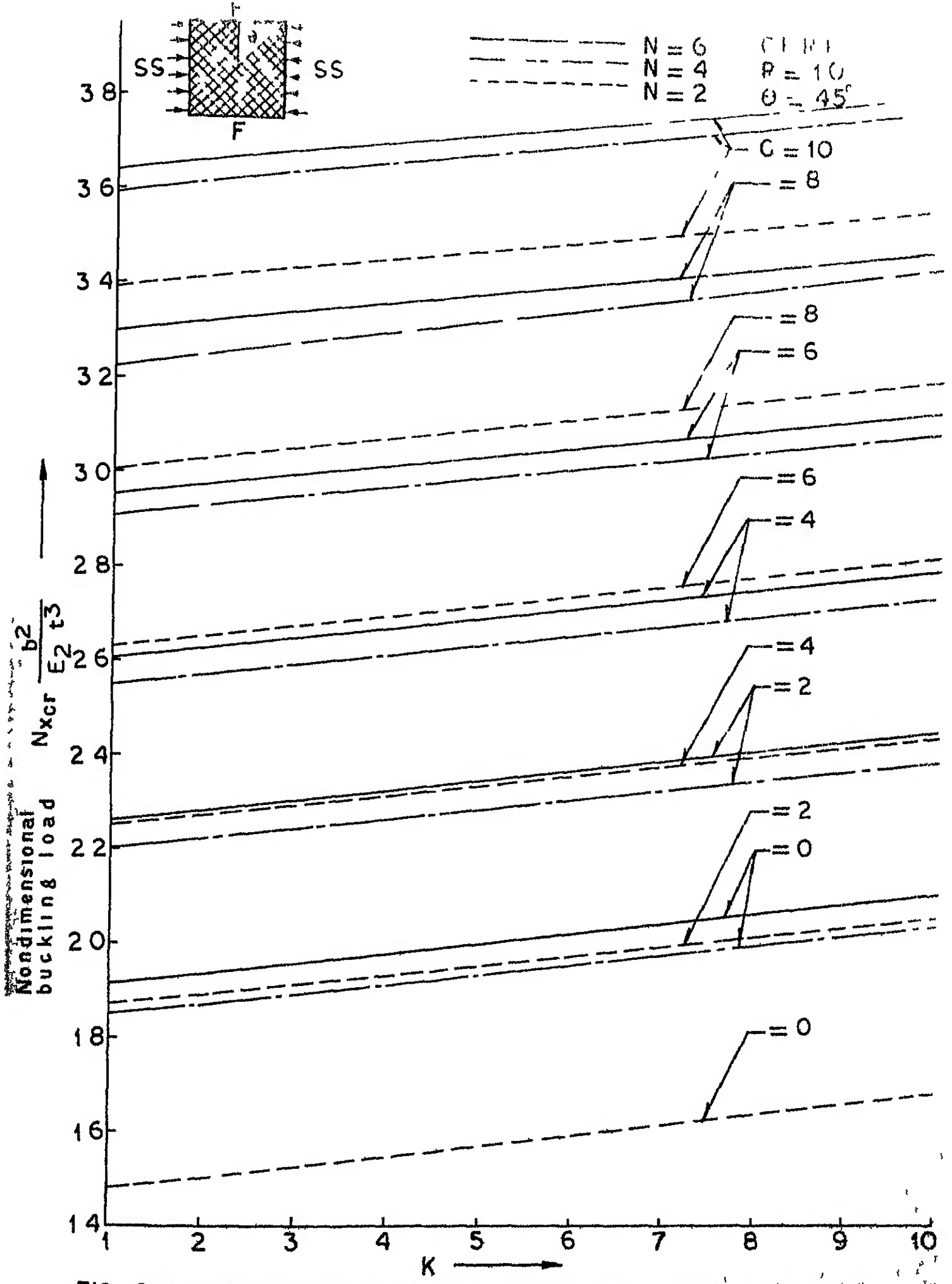

FIG 63 VARIATION OF BUCKLING LOAD WITH WINKLER STIFFNESS, K FOR A SQUARE ANTISYMMETRIC ANGLE-PLY PLATE

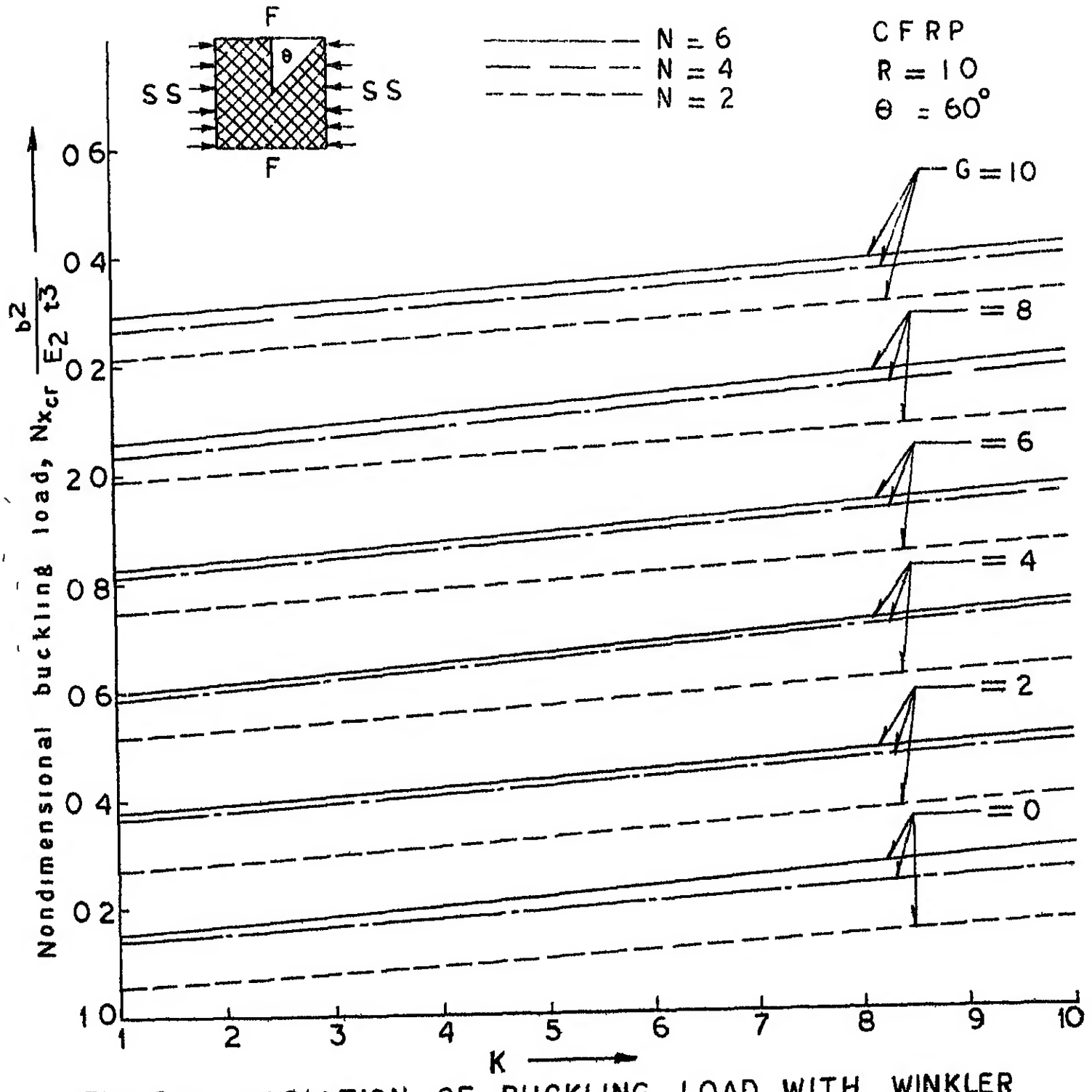

FIG 6 4 VARIATION OF BUCKLING LOAD WITH WINKLER STIFFNESS, K FOR A SQUARE ANTISYMMETRIC ANGLE-PLY PLATE

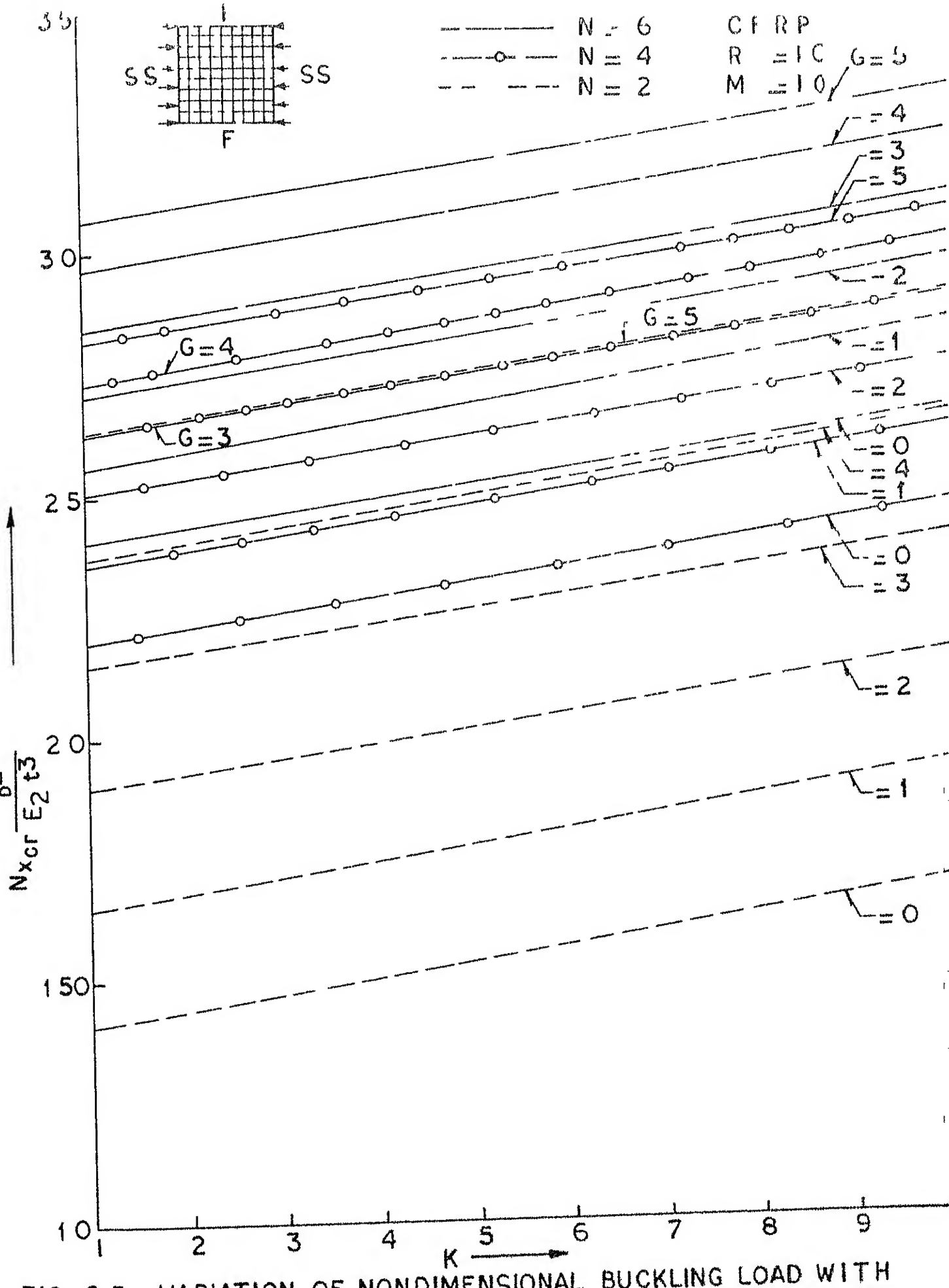

FIG 6 5 VARIATION OF NONDIMENSIONAL BUCKLING LOAD WITH WINKLER STIFFNESS FOR AN ANTISYMMETRIC CROSS-PLY PLATE WITH NUMBER OF LAYERS (N) AND PASTERNAK SHEAR STIFFNESS

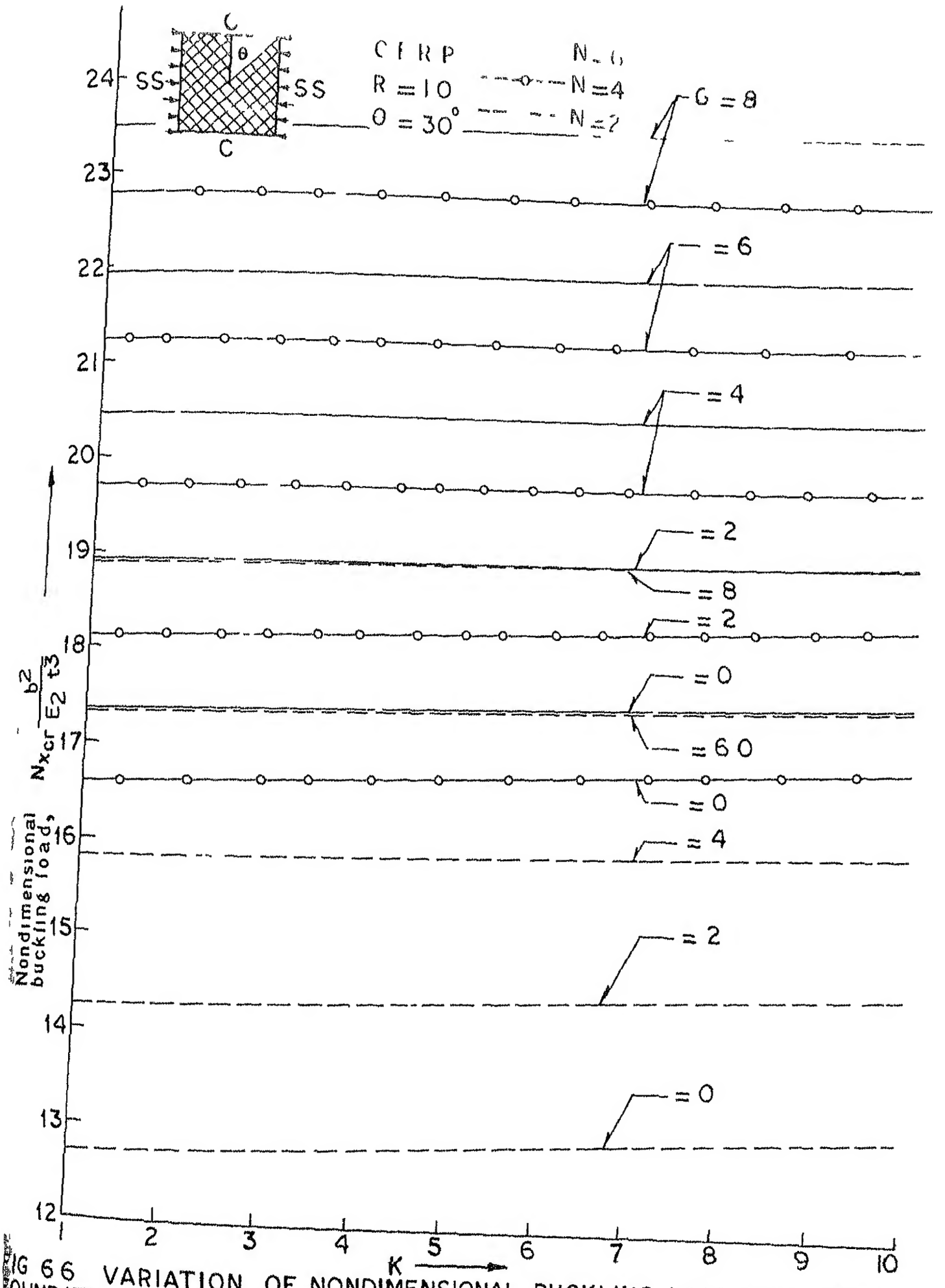

FIG 66 VARIATION OF NONDIMENSIONAL BUCKLING LOAD WITH WINKLER FOUNDATION STIFFNESS FOR AN ANTISYMMETRIC ANGLE-PLY SQUARE PLATE WITH NUMBER OF LAYERS (N) AND PASTERNAK SHEAR STIFFNESS(G) AS PARAMETERS

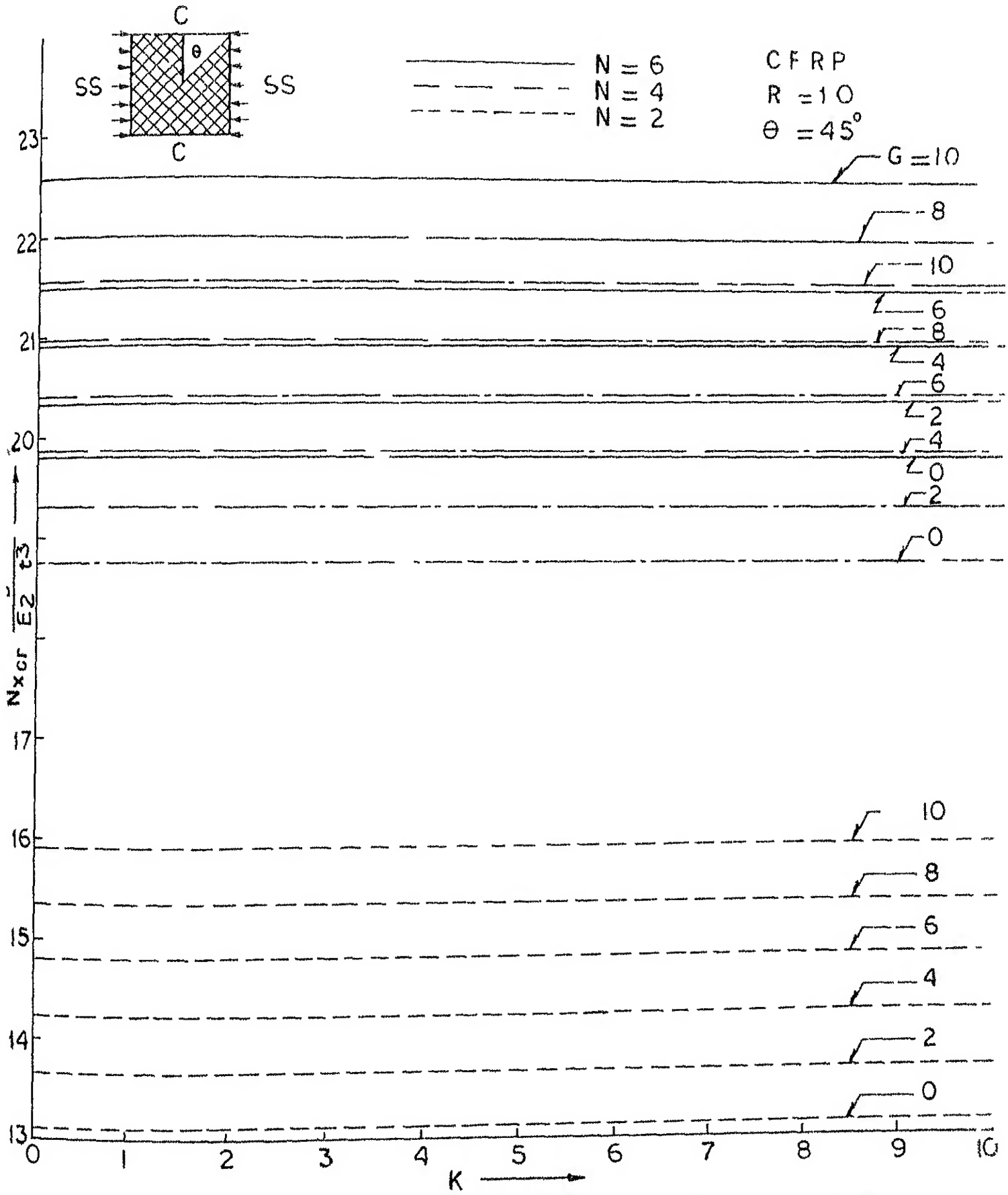

FIG 6 7 VARIATION OF NONDIMENSIONAL BUCKLING LOAD WITH WINKLER FOUNDATION STIFFNESS FOR AN ANTISYMMETRIC ANGLE-PLY SQUARE PLATE WITH NUMBER OF LAYERS (N) & PASTERNAK STIFFNESS (G) AS PARAMETERS

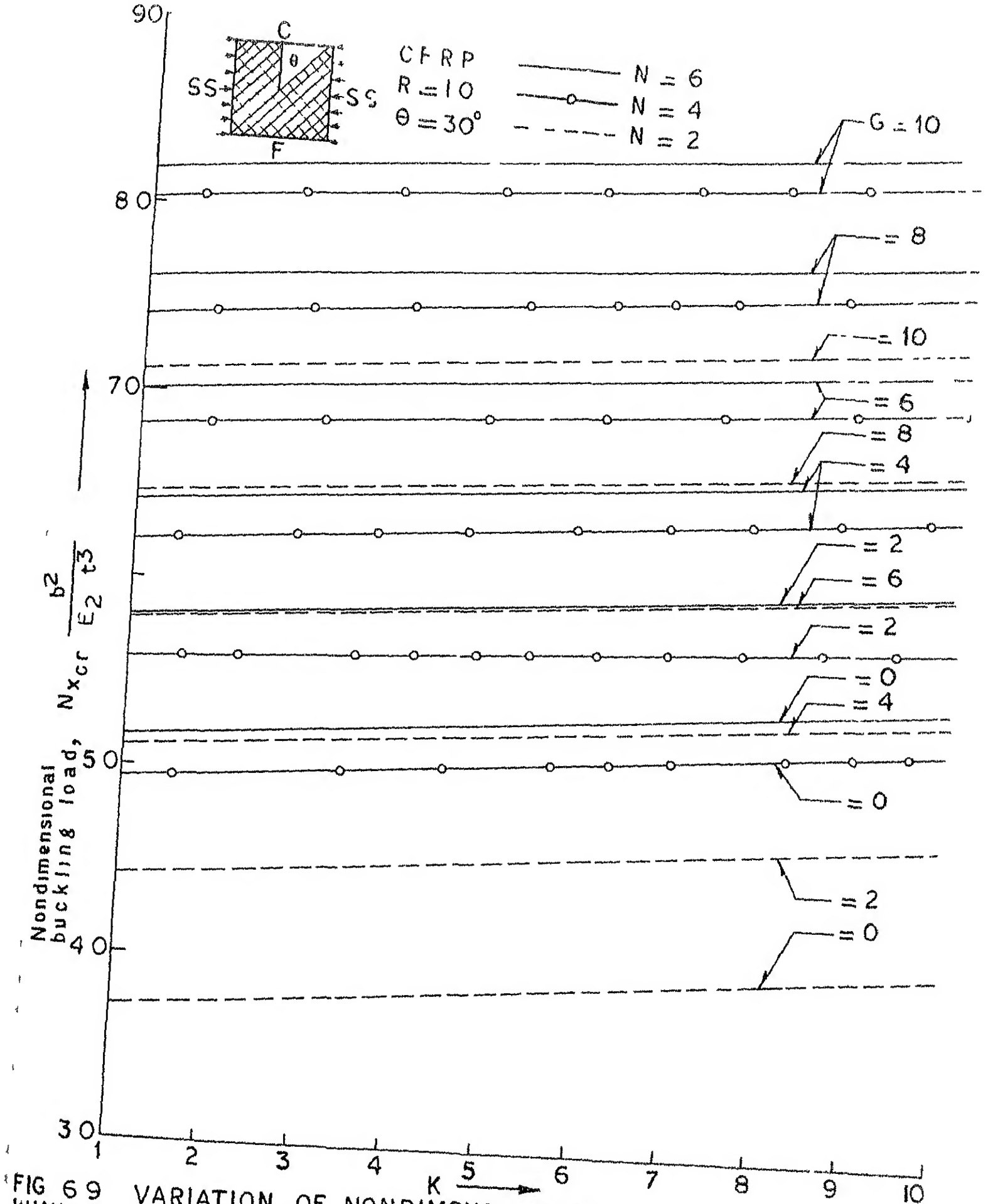

FIG 69 VARIATION OF NONDIMENSIONAL BUCKLING LOAD WITH WINKLER FOUNDATION STIFFNESS FOR A SQUARE ANTISYMMETRIC ANGLE-PLY PLATE WITH NUMBER OF LAYERS (N) AND PASTERNAK SHEAR STIFFNESS (G) AS PARAMETERS

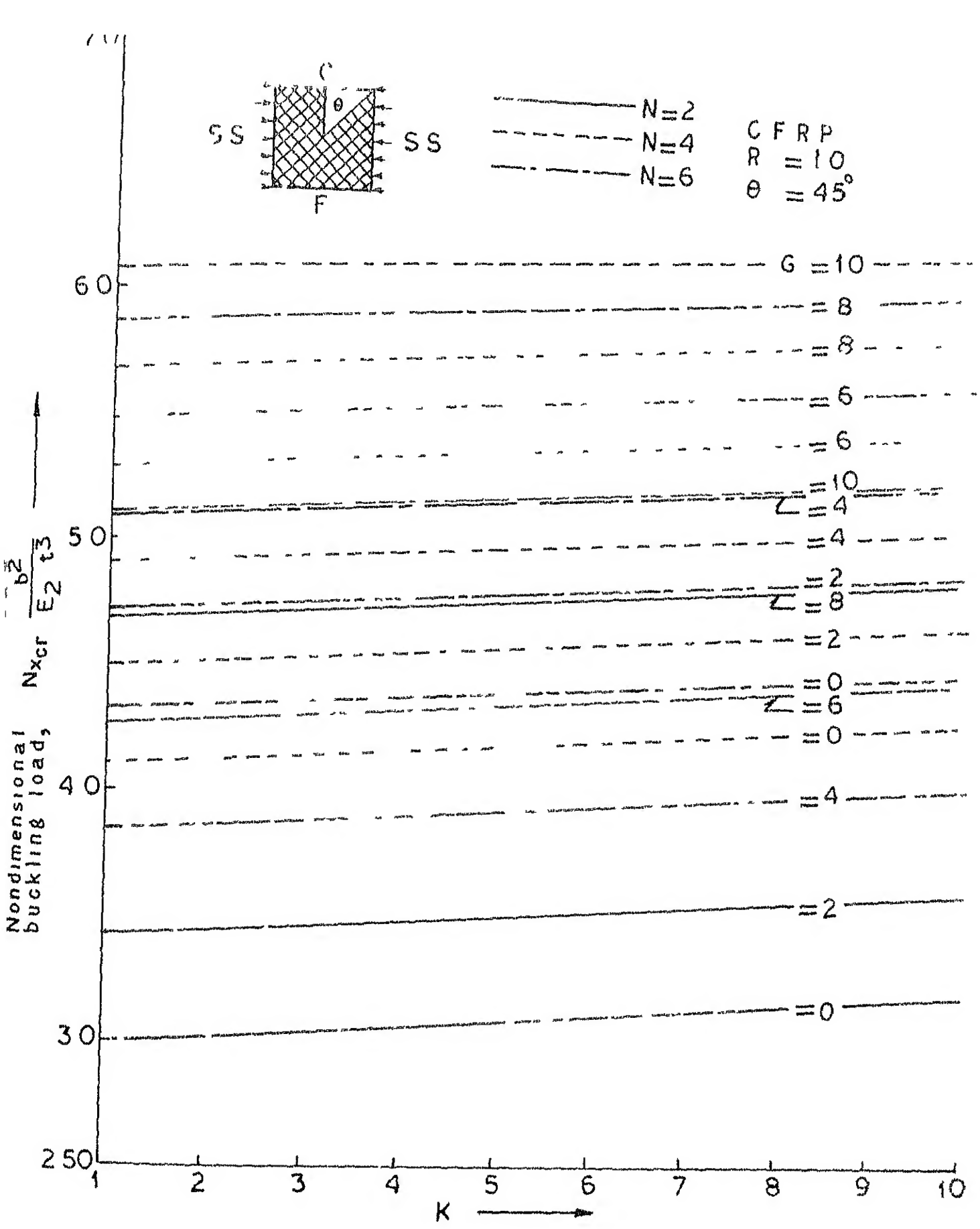

FIG 6.10 VARIATION OF NONDIMENSIONAL BUCKLING LOAD WITH WINKLER FOUNDATION STIFFNESS FOR A SQUARE ANTISYMMETRIC ANGLE-PLY PLATE WITH NUMBER OF LAYERS (N) & PASTERNAK SHEAR STIFFNESS (G) AS PARAMETERS

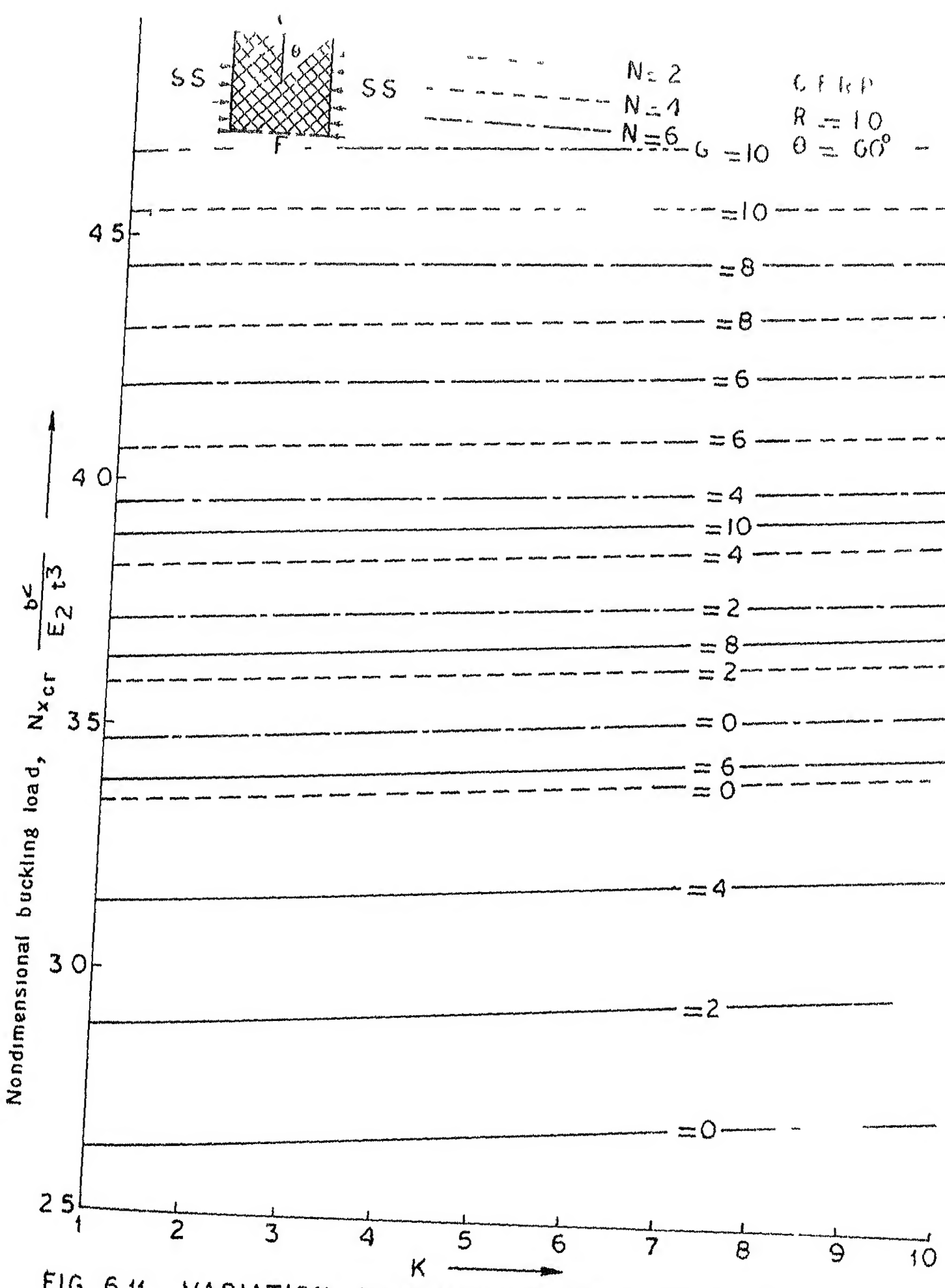

FIG 6 11 VARIATION OF NONDIMENSIONAL BUCKLING LOAD WITH WINKLER FOUNDATION STIFFNESS FOR A SQUARE ANTISYMMETRIC ANGLE-PLY PLATE WITH NUMBER OF LAYERS (N) & PASTERNAK SHEAR STIFFNESS (G) AS PARAMETERS

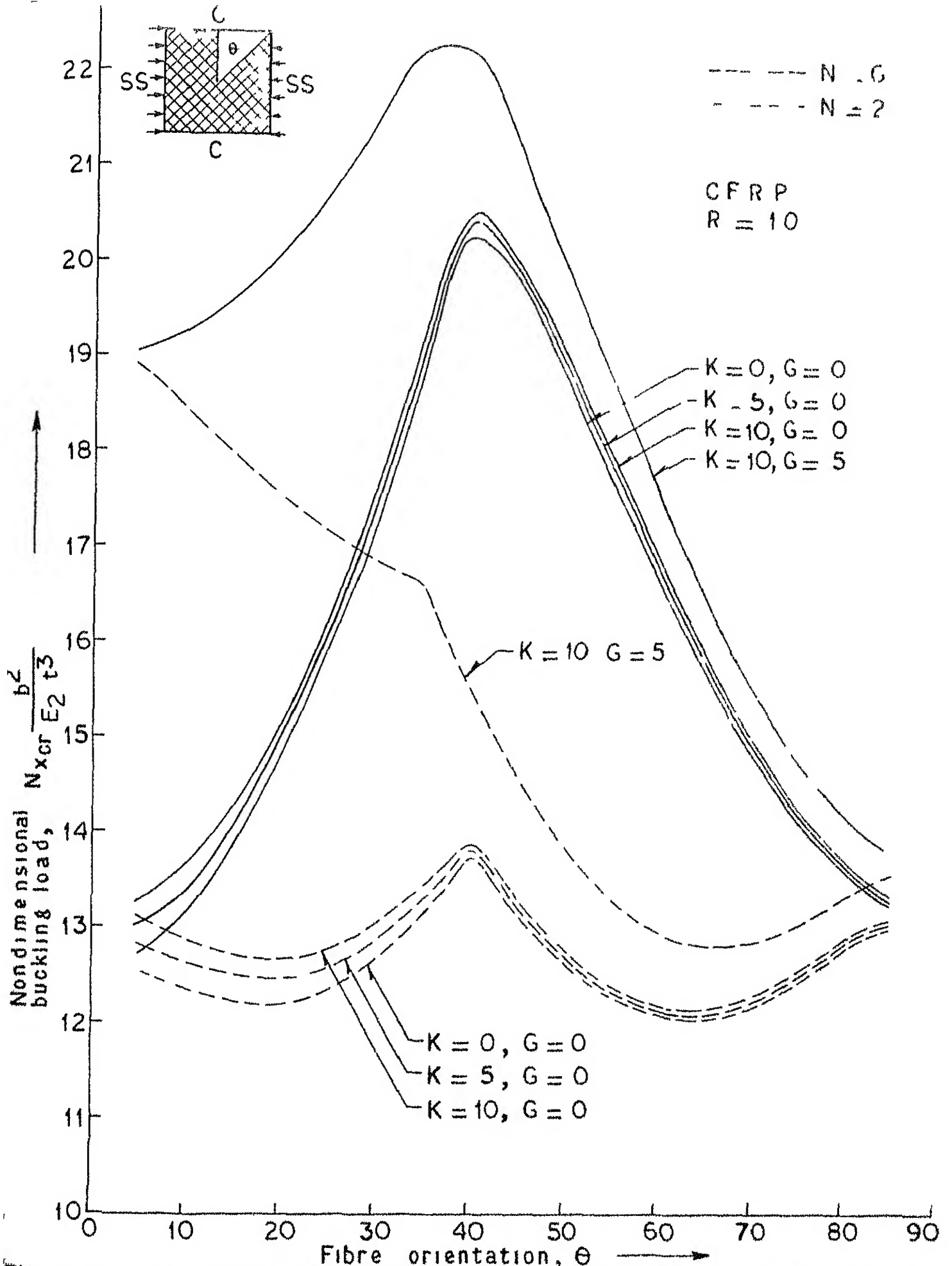

FIG 6.12 VARIATION OF NONDIMENSIONAL BUCKLING LOAD WITH ANGLE OF FIBRE ORIENTATION FOR A SQUARE ANTISYMMETRIC PLATE WITH NUMBER OF LAYERS (N), WINKLER STIFFNESS (K) AND PASTERNAK SHEAR STIFFNESS (G) AS PARAMETERS

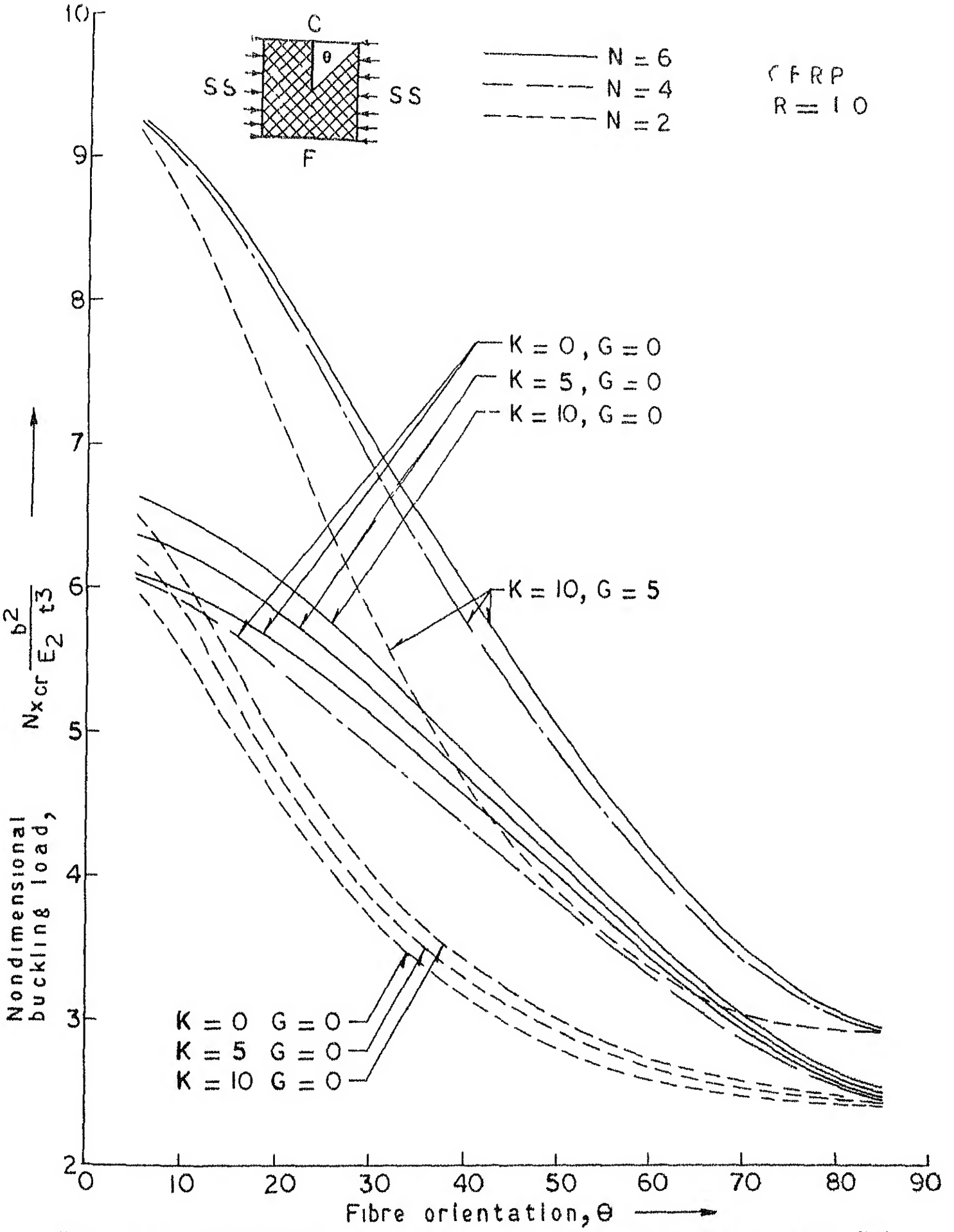

FIG 6 13 VARIATION OF NONDIMENSIONAL BUCKLING LOAD WITH ANGLE OF FIBRE ORIENTATION FOR A SQUARE ANTISYMMETRIC ANGLE-PLY PLATE WITH NUMBER OF LAYERS (N), WINKLER STIFFNESS (K) AND PASTERNAK SHEAR STIFFNESS (G) AS PARAMETERS

CHAPTER 7

BUCKLING OF ANTISYMMETRIC CROSS- AND ANGLE-PLY COMPOSITE PLATES SUBJECTED TO VARYING UNI-AXIAL LOADS

7.1 INTRODUCTION

The next logical set of studies on buckling of laminated plates will be to extend the analysis to combined and varying edge loads. Study of literature shows that Chamis[13] analyzed the buckling of simply supported anisotropic plates under combined loading: membrane, normal and shear loads. He also investigated the effects of the various coupling responses on the buckling load. There seems to be no information on the buckling of anisotropic laminated plates subjected to varying in-plane loads. The purpose of this chapter is, therefore, to develop an efficient formulation to predict the buckling response of laminated plates subjected to varying in-plane loads at the edges. It is somewhat difficult to attempt a closed form solution directly from the differential equation due to the fact that it is difficult to satisfy the boundary conditions on the loaded edges. One may, however, get a closed form solution, in principle, by expanding the edge loads in the form of a series and matching it with the series solution of Eq. (3.22). This, however, leads to an infinite set of equations and consequently a characteristic matrix of infinite size. For

numerical computations one is, therefore, forced to make a choice of the number of terms and limit the size of the matrix for a viable solution consistent with the needs of convergence. Consequently it turns out to be like any other approximate technique. In this study, the well-known Galerkin technique was, therefore, chosen to study the problem. The numerical solution is obtained for a particular case of variable loading, namely pure bending by the well-known Power method.[74,75] The formulation leads to an iterative convergence which approximates the buckling loads as closely as desired.

7.2 ANALYSIS

7.2.1 Antisymmetric Angle-ply Laminates

Let a simply supported rectangular plate as shown in Figure 7.1 be subjected to a system of distributed forces, acting in the middle plane of the plate. The distribution of these applied forces may be expressed by the relation

$$N_x = N_o (1 - \alpha y/b) \qquad (7.1)$$

where N_o is the intensity of compressive force at the edge $y = 0$ and α is a numerical factor. It can be seen that by changing α, various particular cases of practical interest are obtained. $\alpha = 2$, for example, corresponds to the case of pure bending.

The governing differential equation for an anti-symmetric angle-ply plate is given by (Chapter 3)

$$A_1 \frac{\partial^8 \phi}{\partial x^8} + A_3 \frac{\partial^8 \phi}{\partial x^6 \partial y^2} + A_5 \frac{\partial^8 \phi}{\partial x^4 \partial y^4} + A_7 \frac{\partial^8 \phi}{\partial x^2 \partial y^6} + A_9 \frac{\partial^8 \phi}{\partial y^8} = q(x, y) \tag{3.22}$$

For the plate loading shown in Figure 7.1, Eq. (3.22) becomes

$$A_1 \frac{\partial^8 \phi}{\partial x^8} + A_3 \frac{\partial^8 \phi}{\partial x^6 \partial y^2} + A_5 \frac{\partial^8 \phi}{\partial x^4 \partial y^4} + A_7 \frac{\partial^8 \phi}{\partial x^2 \partial y^6} + A_9 \frac{\partial^8 \phi}{\partial y^8} + N_x \frac{\partial^2 w}{\partial x^2} = 0 \tag{7.2}$$

Substituting the expression for N_x from Eq. (7.1) and w from Eq. (3.25) into Eq. (7.2), we have

$$A_1 \frac{\partial^8 \phi}{\partial x^8} + A_3 \frac{\partial^8 \phi}{\partial x^6 \partial y^2} + A_5 \frac{\partial^8 \phi}{\partial x^4 \partial y^4} + A_7 \frac{\partial^8 \phi}{\partial x^2 \partial y^6} + A_9 \frac{\partial^8 \phi}{\partial y^8}$$
$$+ a_7 N_o (1 - \alpha y/b) \frac{\partial^6 \phi}{\partial x^6} + a_8 N_o (1 - \alpha y/b) \frac{\partial^6 \phi}{\partial x^4 \partial y^2}$$
$$+ a_9 N_o (1 - \alpha y/b) \frac{\partial^6 \phi}{\partial x^2 \partial y^4} = 0 \tag{7.3}$$

The present problem is solved for the following set of simply supported edge boundary conditions:

$$\left.\begin{aligned} w &= 0, & M_x &= 0 \\ u^o &= 0, & N_{xy} &= 0 \end{aligned}\right\} \quad x = 0, a$$

$$\left.\begin{aligned} w &= 0, & M_y &= 0 \\ v^o &= 0, & N_{xy} &= 0 \end{aligned}\right\} \quad y = 0, b \tag{7.4}$$

By the choice of

$$\phi = \sum_{m=1}^{\infty} \sum_{n=1} a_{mn} \sin m\pi x/a \sin n\pi y/b \tag{7.5}$$

the boundary conditions (7.4) are identically satisfied. This can be verified by the expressions of displacements and stress resultants in terms of ϕ, which are given by relations (3.23) through (3.31).

Now applying the Galerkin technique and substituting for ϕ from Eq. (7.5) into Eq. (7.3), we get

$$\int_o^a \int_o^b \left[\sum_m \sum_n A_{mn} a_{mn} \sin \frac{m\pi x}{a} \cdot \sin \frac{n\pi y}{b} \right] \sin \frac{p\pi x}{a} \cdot \sin \frac{q\pi y}{b} \, dxdy$$

$$- N_o \int_o^a \int_o^b \left[\sum_m \sum_n B_{mn} a_{mn} \sin \frac{m\pi x}{a} \cdot \sin \frac{n\pi y}{b} \right] \sin \frac{p\pi x}{a} \cdot$$

$$\sin \frac{q\pi y}{b} \, dxdy + N_o \frac{\alpha}{b} \int_o^a \int_o^b \left[\sum_m \sum_n B_{mn} a_{mn} y \sin \frac{m\pi x}{a} \cdot \right.$$

$$\left. \sin \frac{n\pi y}{b} \right] \sin \frac{p\pi x}{a} \cdot \sin \frac{q\pi y}{b} \, dxdy = 0 \tag{7.6}$$

$$p, q = 1, 2, \ldots$$

where

$$A_{mn} = A_1 \left(\frac{m\pi}{a}\right)^8 + A_3 \left(\frac{m\pi}{a}\right)^6 \left(\frac{n\pi}{b}\right)^2 + A_5 \left(\frac{m\pi}{a}\right)^4 \left(\frac{n\pi}{b}\right)^4$$

$$+ A_7 \left(\frac{m\pi}{a}\right)^2 \left(\frac{n\pi}{b}\right)^6 + A_9 \left(\frac{n\pi}{b}\right)^8$$

and

$$B_{mn} = a_7\left(\frac{m\pi}{a}\right)^6 + a_8\left(\frac{m\pi}{a}\right)^4\left(\frac{n\pi}{b}\right)^2 + a_9\left(\frac{m\pi}{a}\right)^2\left(\frac{n\pi}{b}\right)^4$$

Equation (7.6) yields a set of mxn equations to determine a_{mn}.

Making use of the identity

$$\int_0^a \sin\frac{i\pi x}{a} \cdot \sin\frac{j\pi x}{a}\,dx = 0 \quad \text{for } i \neq j$$

$$= a/2 \quad \text{for } i = j$$

the first term of Eq. (7.6) can be written as

$$\int_0^a \sum_m \left[\int_0^b \left\{\sum_n A_{mn}a_{mn} \sin\frac{m\pi x}{a} \sin\frac{n\pi y}{b}\right\} \sin\frac{q\pi y}{b}\,dy\right] \cdot \sin\frac{p\pi x}{a}\,dx$$

$$= \int_0^a \sum_m \left[\frac{b}{2} A_{mq}a_{mq} \sin\frac{m\pi x}{a} \sin\frac{p\pi x}{a}\right] dx$$

$$= \frac{b}{2}\left[\int_0^a \sum_m A_{mq}a_{mq} \sin\frac{m\pi x}{a} \cdot \sin\frac{p\pi x}{a}\,dx\right]$$

$$= \frac{b}{2} \cdot \frac{a}{2} \cdot A_{pq}a_{pq}$$

Applying this simplification to Eq. (7.6), the result is

$$\frac{ab}{4} A_{pq}a_{pq} - N_o\left(\frac{ab}{4} B_{pq}a_{pq}\right) + N_o \frac{\alpha}{b} \int_0^a \int_0^b \left[\sum_m \sum_n B_{mn} \cdot a_{mn}y \sin\frac{m\pi x}{a} \cdot \sin\frac{n\pi y}{b}\right] \sin\frac{p\pi x}{a} \sin\frac{q\pi y}{b}\,dxdy = 0 \qquad (7.7)$$

The last term in Eq. (7.7) can be further simplified as

$$N_o \frac{\alpha}{b} \int_o^a \int_o^b \Big[\sum_m \sum_n B_{mn} a_{mn} y \sin \frac{m\pi x}{a} \sin \frac{n\pi y}{b} \Big] \cdot \sin \frac{p\pi x}{a} \sin \frac{q\pi y}{b} \, dx dy$$

$$= \int_o^b \sum_n \Big[\int_o^a \Big(\sum_m B_{mn} a_{mn} \sin \frac{m\pi x}{a} \sin \frac{p\pi x}{a} \, dx \Big] y \sin \frac{n\pi y}{b} \cdot \sin \frac{q\pi y}{b} \, dy$$

$$= \frac{a}{2} \int_o^b \sum_n B_{pn} a_{pn} y \sin \frac{n\pi y}{b} \sin \frac{q\pi y}{b} \, dy$$

$$= \frac{a}{2} \sum_n B_{pn} a_{pn} \int_o^b y \sin \frac{n\pi y}{b} \sin \frac{q\pi y}{b} \, dy$$

$$= \frac{a}{2} \sum_n B_{pn} a_{pn} I_{qn}$$

where $I_{qn} = \int_o^b y \sin \frac{n\pi y}{b} \sin \frac{q\pi y}{b} \, dy$

$= \frac{b}{2}$, $q = n$

$= 0$, $q \neq n$; $q \pm n$ is an even number

$= -\frac{4b^2}{\pi^2} \frac{nq}{(n^2 - q^2)^2}$; $q \neq n$, $q \pm n$ is an odd number

Thus Eq. (7.7) can be written as

$$\frac{ab}{4} A_{pq} a_{pq} - N_o \frac{ab}{4} B_{pq} a_{pq}$$

$$+ N_o \frac{\alpha}{b} \frac{a}{2} \left(\sum_{i=1} B_{pi} a_{pi} I_{qi} \right)$$

$$= 0 ; \qquad p = 1, 2, \ldots m, \ldots \qquad (7.8)$$

$$q = 1, 2, \ldots n, \ldots$$

This leads to an infinite set of homogeneous equations for a_{pq}. It is assumed that this has a solution. The corresponding matrix say A can be solved by a process of iteration to determine N_o. The determination of eigen values of the matrix A is made by the well-known Power method.[74,75]

7.3 NUMERICAL COMPUTATIONS

Numerical computations are carried out for two different materials, namely carbon fibre reinforced plastics (CFRP) and graphite fibre reinforced plastics (GFRP) with the following data:

CFRP

$E_1/E_2 = 6.333$; $G_{12}/E_2 = 0.667$; $\nu_{12} = 0.20$

GFRP

$E_1/E_2 = 40.0$; $G_{12}/E_2 = 0.50$; $\nu_{12} = 0.25$

A generalized computer programme is written with a provision for consideration of different values of α. However, in view of the multiplicity of parameters that characterize the present problem for a given loading condition, only the case of pure bending corresponding to $\alpha = 2$ is considered for antisymmetric angle-ply and cross-ply plates.

7.4 RESULTS AND DISCUSSION

The variation of buckling load with fibre orientation is shown in Figure 7.2 for a square antisymmetric graphite/epoxy angle-ply plate with number of layers as a parameter. These are reduced to uniaxial uniform compressive case for comparison with Whitney and Leissa[1]. It can be seen that the coupling tends to reduce the buckling load. The results for an infinite number of layers in this figure are the same as the orthotropic solution in which all coupling between bending and extension is ignored. For a square two-layered plate, the actual results are about 65% below the six-layered results at $\theta = 45°$. A similar phenomenon was also observed by Jones[26] for antisymmetric cross-ply square plates of the same material (GFRP). It is also observed that as the number of layers increases beyond two, the buckling loads rapidly approach the orthotropic solution. This shows that the coupling between bending and extension rapidly dies out as the number of layers increases. The percentage difference

in the buckling loads between a six-layered plate and a four-layered one, for example, is only of the order of 10 as against 61 between four- and two-layered square plates at $\Theta = 45°$. Figure 7.3 shows similar results for a square anti-symmetric carbon/epoxy plate.

Figures 7.4 through 7.6 show the variations of buckling load with aspect ratio for a carbon/epoxy anti-symmetric angle-ply plate for three different fibre orientations of 30°, 45° and 60° respectively. The cusps in these figures occur because of the changes in the mode shape as the plate aspect ratio changes. It can be noted that the location of the cusps occurs at an aspect ratio which is a function of the fibre orientation and number of layers. The first change in mode shape for a 30° fibre orientation occurs between aspect ratios of 1.10 and 1.20 for a two-layered laminate whereas the corresponding change in mode shape occurs between aspect ratios of 1.20 and 1.30 for both the four-layered and six-layered laminates. However, because of symmetry of fibre orientation at $\Theta = 45°$, the first change in mode shape occurs between aspect ratios of 0.90 and 1.0 for all the number of layers ($N = 2, 4, 6$). For a 60° fibre oriented plate, the above figures are approximately between 0.70 and 0.80 for all the number of layers considered. Regarding the effect of coupling between bending and extension, it can be seen that this is constant irrespective of aspect ratio for a given

number of layers which means that the curves in these figures have the same relation to one another. The variation of buckling load with aspect ratio for a regular anti-symmetric carbon/epoxy cross-ply plate are shown in Figures 7.7 and 7.8 for two different loadings, namely $\alpha = 2$ (pure-bending) and $\alpha = 0$ (uniform uniaxial compression). The comparison of these two figures reveals another interesting feature, namely that the location of cusps besides being dependent upon fibre orientation and number of layers (as noted in the case of antisymmetric angle-ply plates above), also depends upon the in-plane loading. The first change in mode shape, for example, for $\alpha = 2$ occurs between aspect ratios of 0.90 and 1.0 whereas the corresponding figures for $\alpha = 0$ lie between 1.4 and 1.5 for all number of layers considered. The number of changes in mode shape is also more for $\alpha = 2$ case than for $\alpha = 0$ case.

Figures 7.9 through 7.12 depict the variations of buckling loads with thickness ratios of the laminae constituting a laminate of a given thickness for two different in-plane loading conditions ($\alpha = 0, 2$). The variation of buckling load with thickness ratio, t_1/t_2 is shown in Figure 7.9 for three different fibre orientations 30°, 45° and 60° for the case of pure bending. The percentage increase in buckling load for a 45° oriented plate between an equal thickness laminate ($t_1/t_2 = 1.0$) and a critical one ($t_1/t_2 =$

0.4142) is of the order of 10.5 whereas for 30° and 60° plates, these figures are of the order of 8.7. Thus the use of critical thickness ratio laminates from the design point of view is quite advantageous, considering the substantial increase of buckling loads that such laminates accrue to the designers. The maximum advantage for a 45° oriented plate is obvious from the maximum coupling effects associated with this fibre orientation. The variation of buckling load with thickness ratio for a six-layered laminate for the case of pure bending is shown in Figure 7.10 for three different fibre orientations and for R_1 = 1.0 and 2.0. It is seen that the maximum buckling load for R_1 = 1.0 curve occurs at R_2 = 2.0 whereas for R_1 = 2.0, the maximum load is obtained at R_2 = 4.4162 (see Chapter 2). Figures 7.11 and 7.12 show the variations of buckling load with thickness ratio for the case of uniform uniaxial loading (α = 0) for four- and six-layered plates respectively at two different fibre orientations of 30° and 45°. A comparison of Figure 7.9 for uniform uniaxial compression loading with that of Figure 7.10 for pure bending shows that the maximum increase in buckling load in both the cases occurs at fibre orientation of 45°. However, the percentage increase in the former case is marginally more than in the latter case.

The variations of buckling load with cross-ply ratio, M for an antisymmetric square cross-ply plate are

shown in Figures 7.13 and 7.14 for two different materials namely CFRP and GFRP respectively for the case of uniform uniaxial loading. It is observed that the increase in buckling load may also depend upon the material and therefore the degree of anisotropy. The percentage increase in buckling load, for example, between cross-ply ratios of 1.0 and 10.0 is of the order of seven for CFRP whereas it is 14 percent for GFRP for a four-layered plate.

- o -

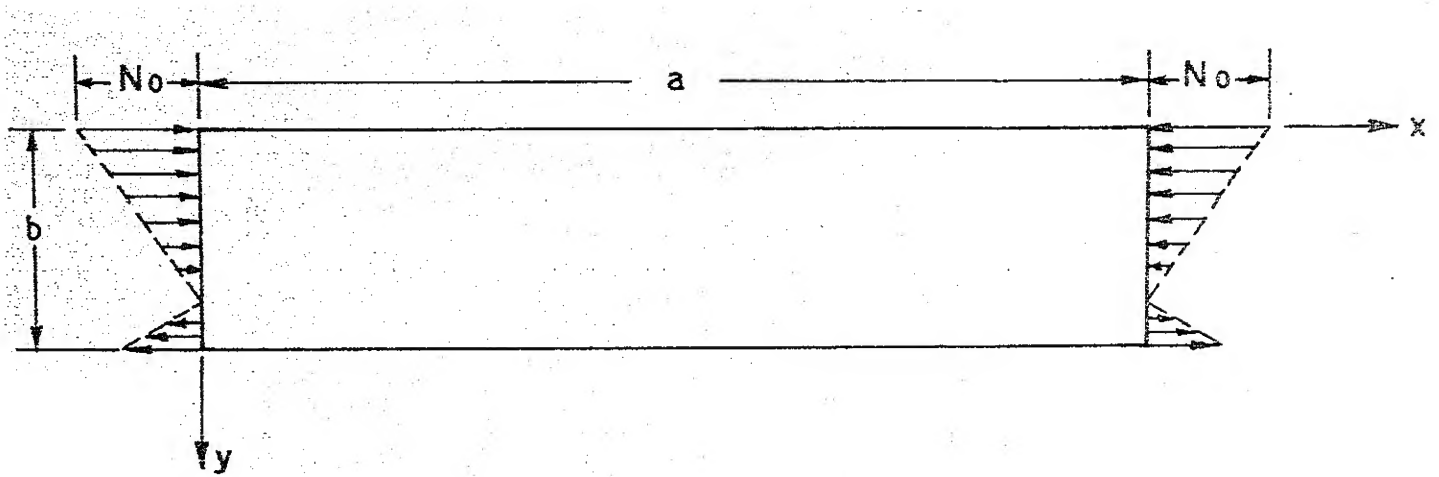

FIG. 7-1: GEOMETRY AND LOADING OF THE PLATE.

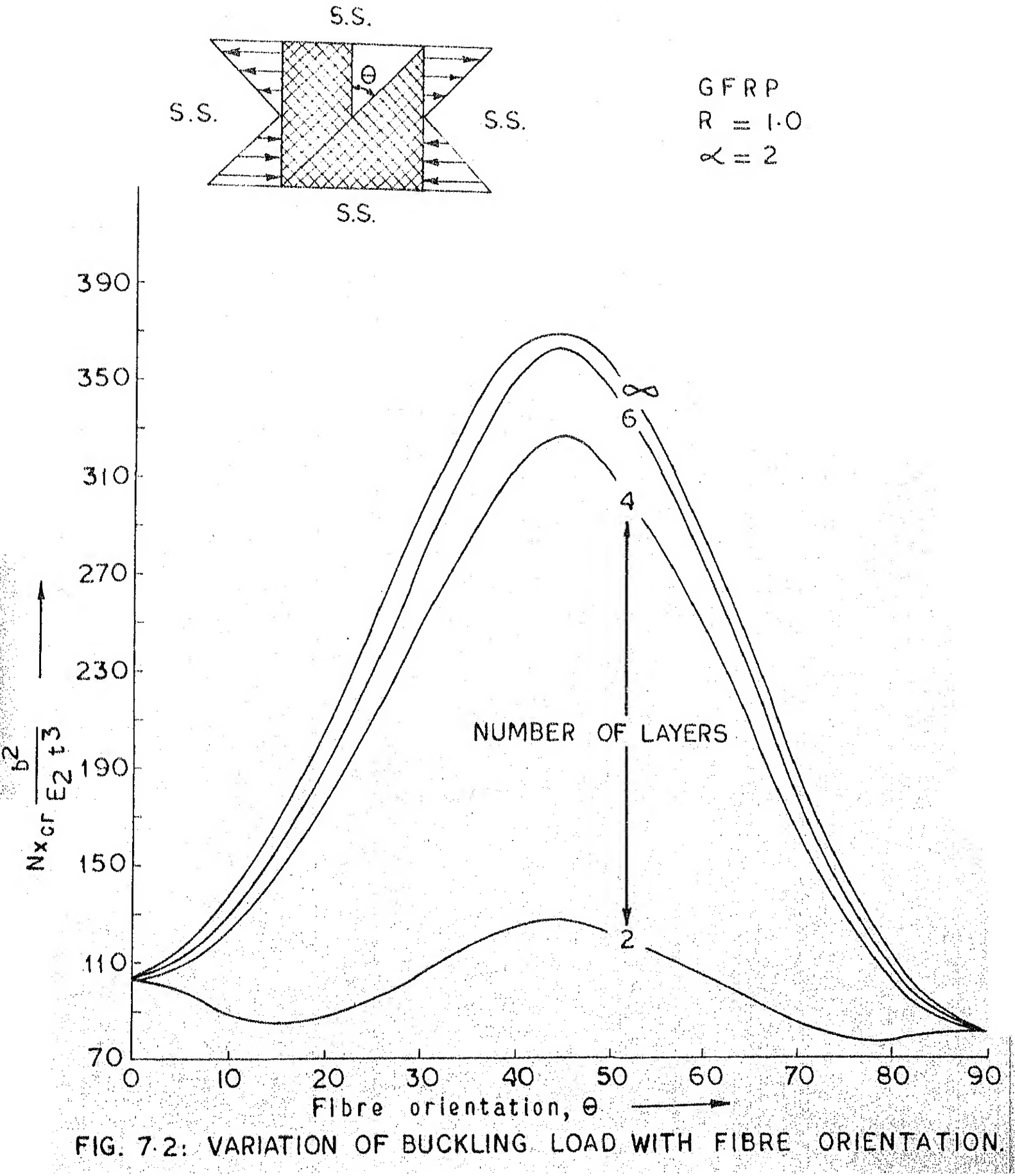

FIG. 7·2: VARIATION OF BUCKLING LOAD WITH FIBRE ORIENTATION.

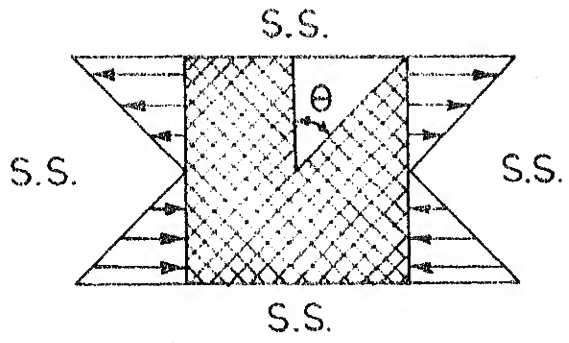

CFRP
R = 1.0
$\alpha = 2$

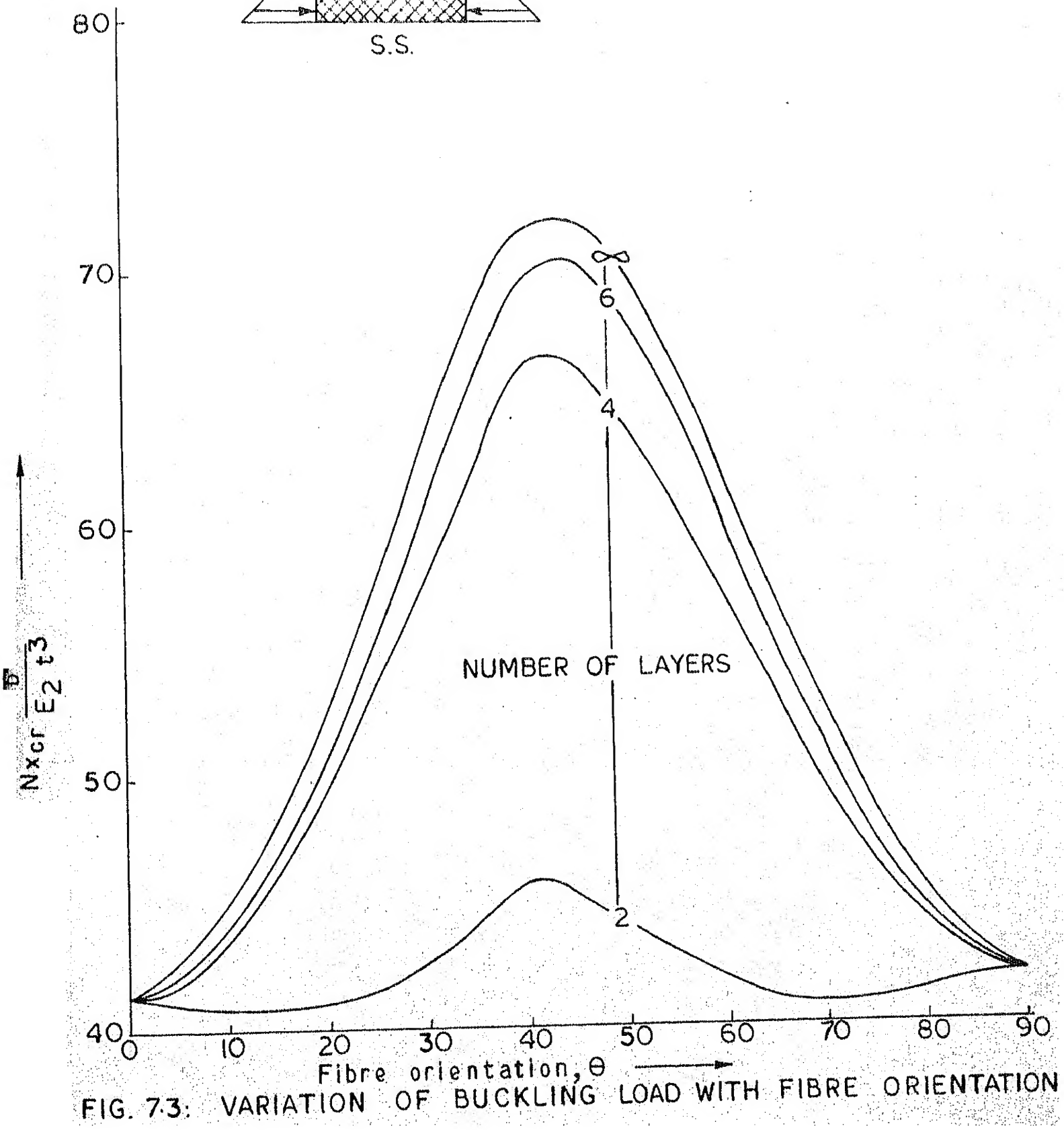

FIG. 7.3: VARIATION OF BUCKLING LOAD WITH FIBRE ORIENTATION

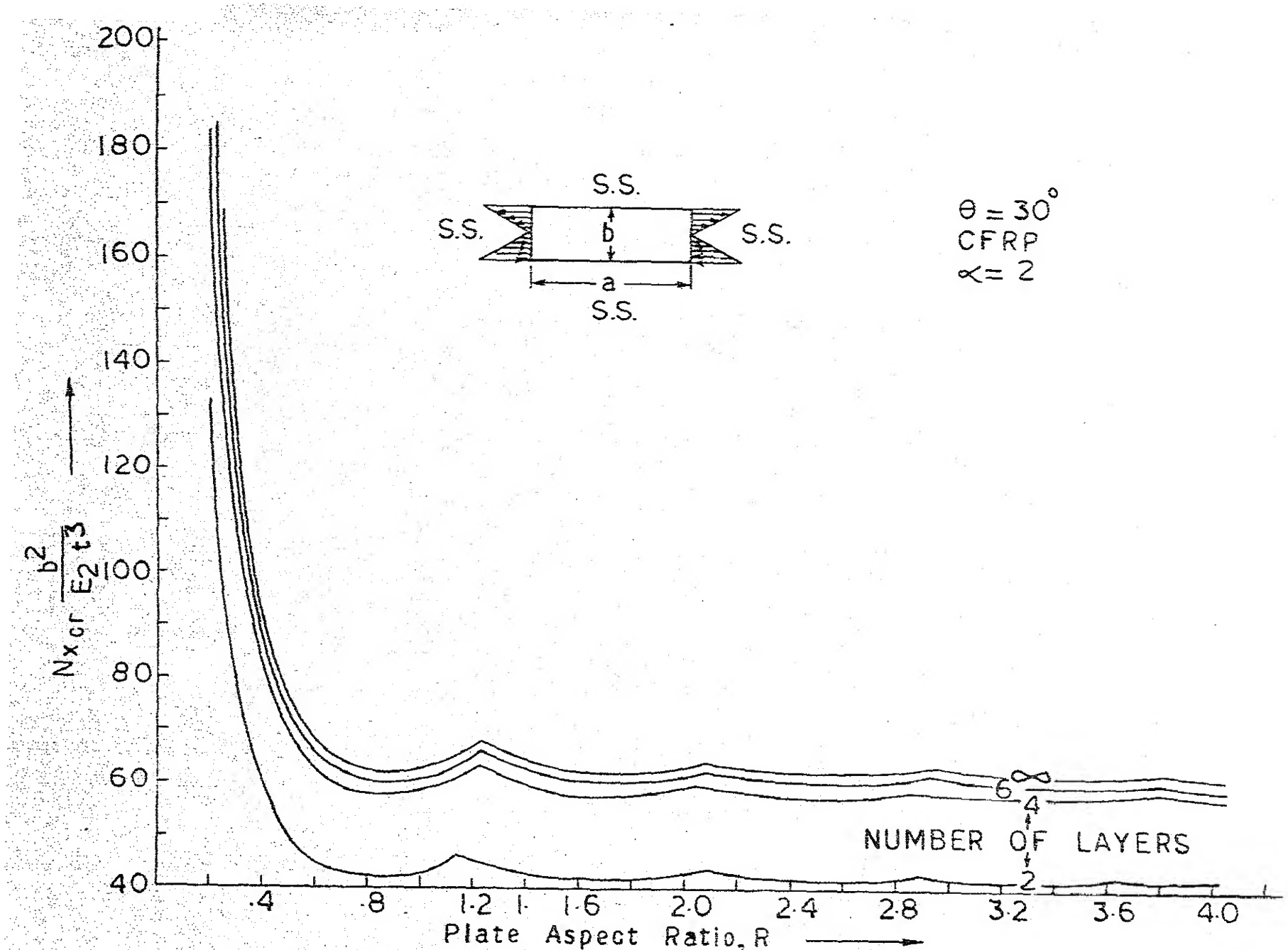

FIG. 7·4: VARIATION OF BUCKLING LOAD WITH ASPECT RATIO.

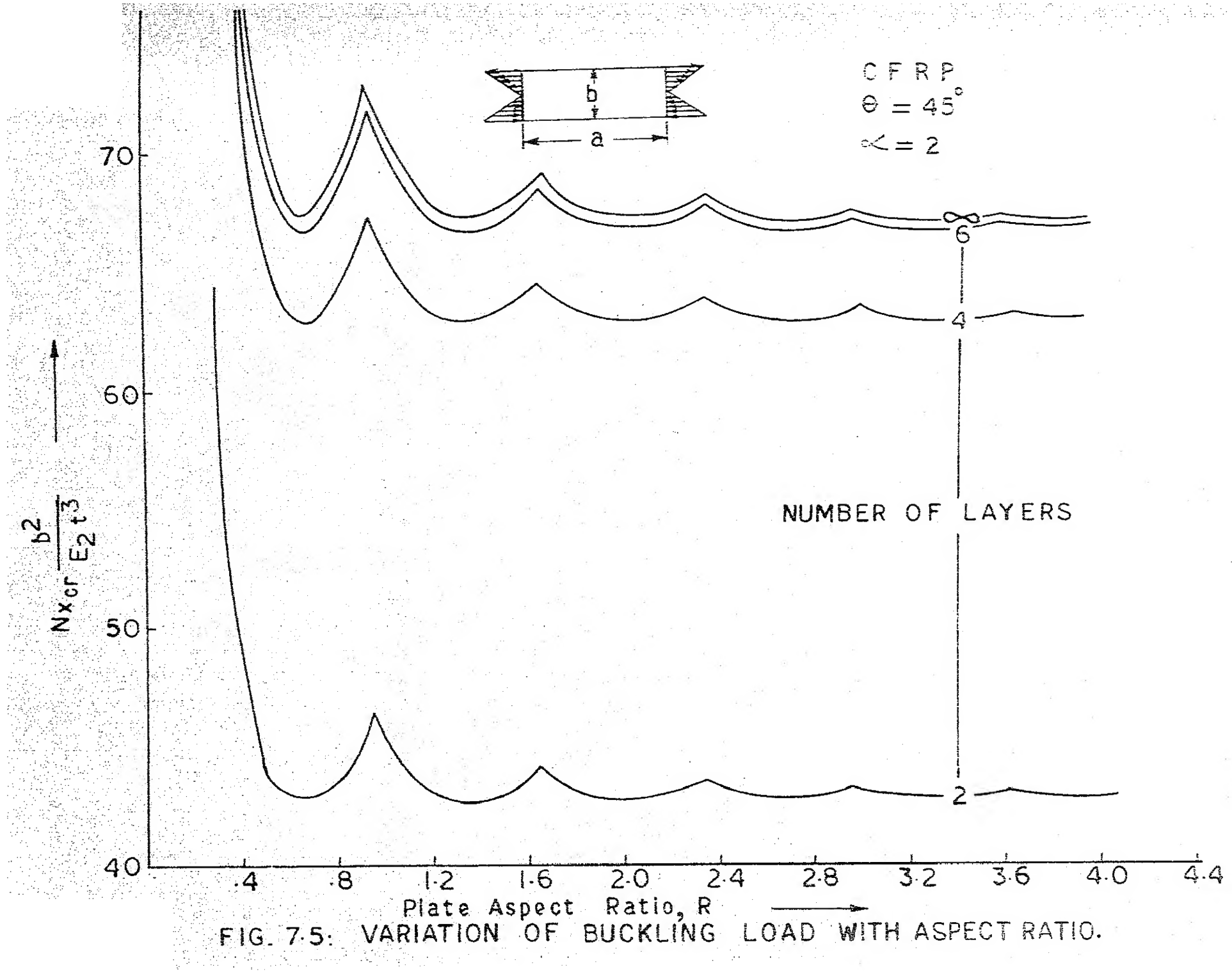

FIG. 7.5: VARIATION OF BUCKLING LOAD WITH ASPECT RATIO.

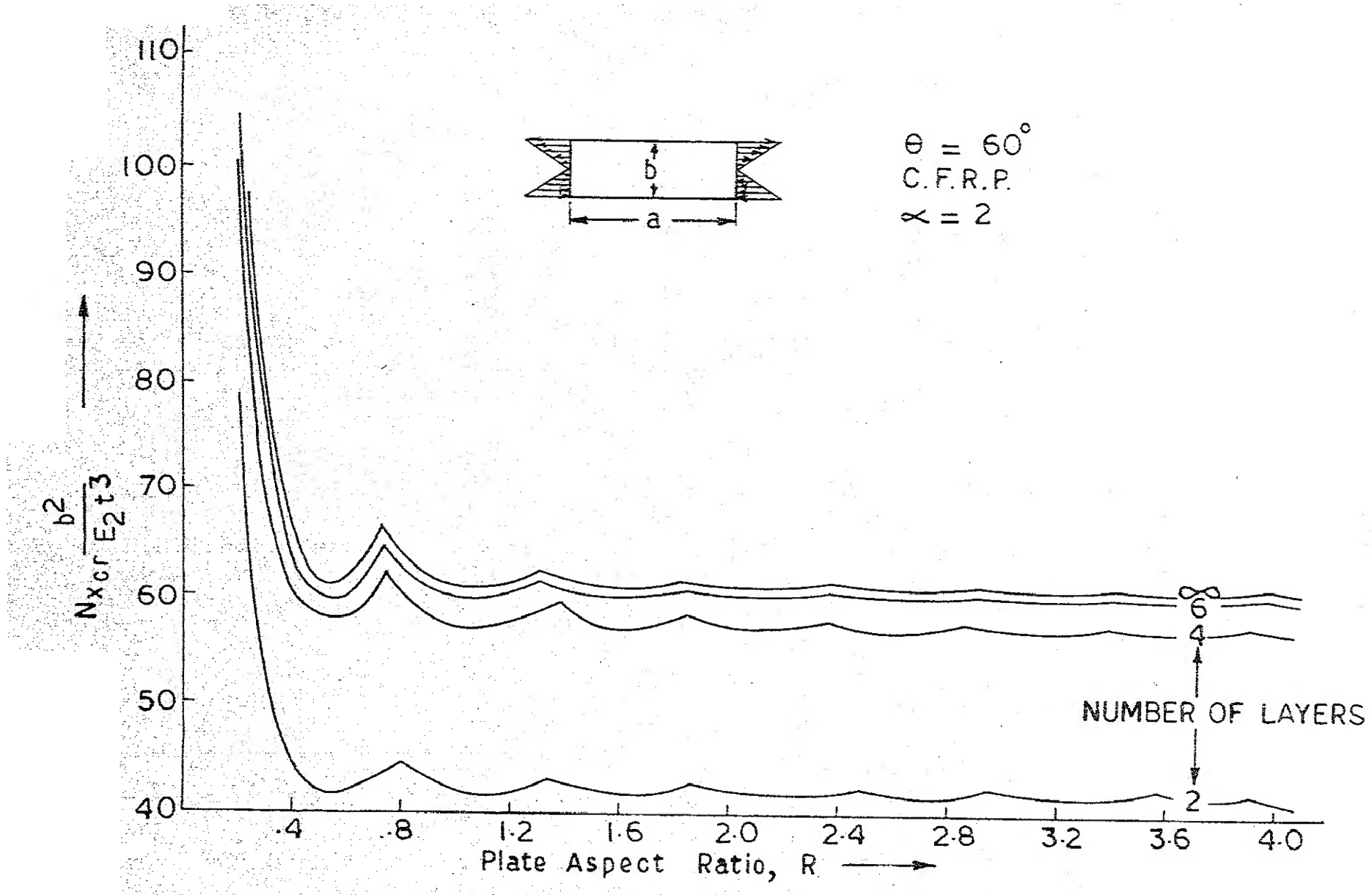

FIG. 7·6: VARIATION OF BUCKLING LOAD WITH ASPECT RATIO.

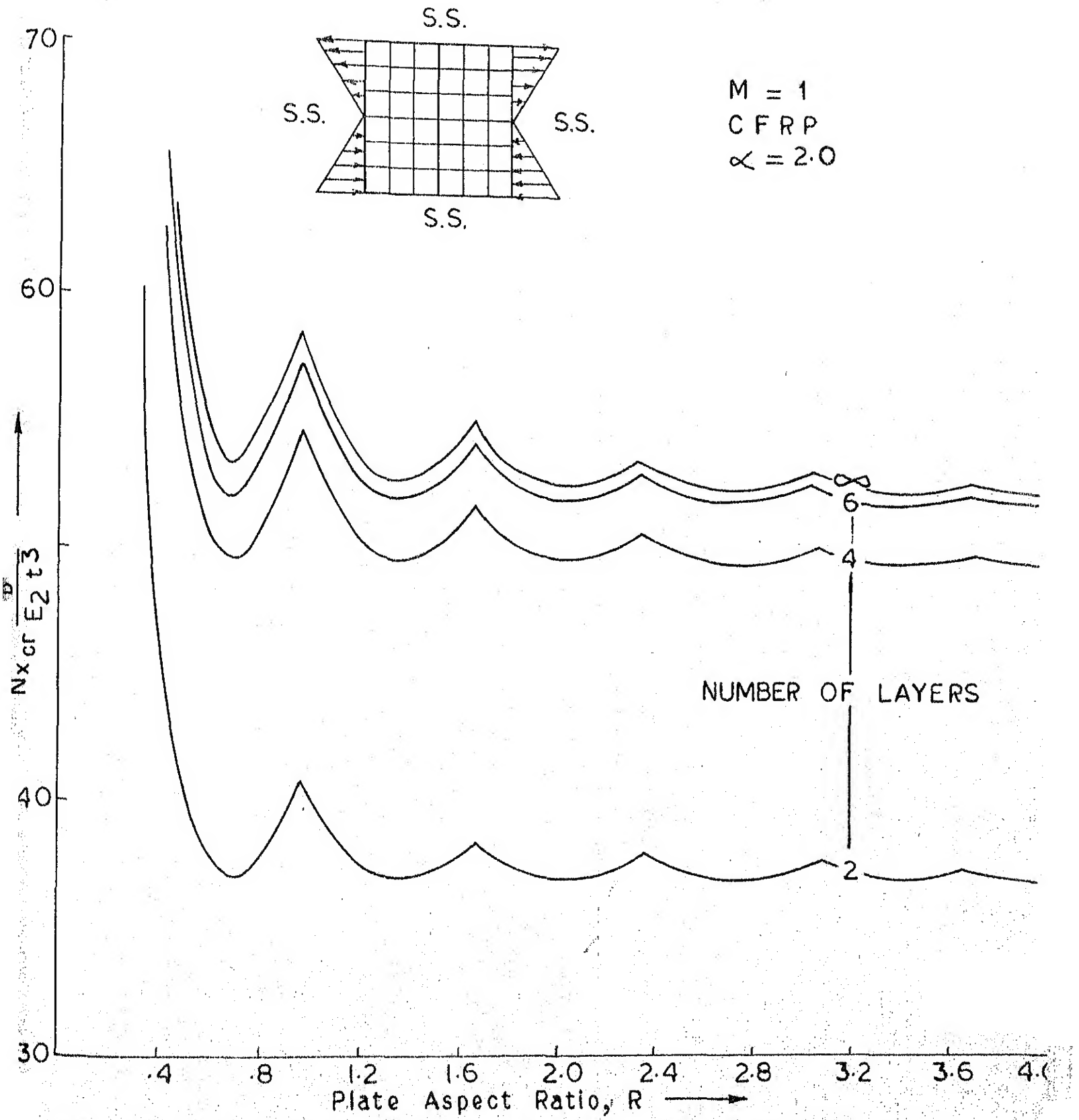

FIG. 7·7: VARIATION OF BUCKLING LOAD WITH ASPECT RATIO.

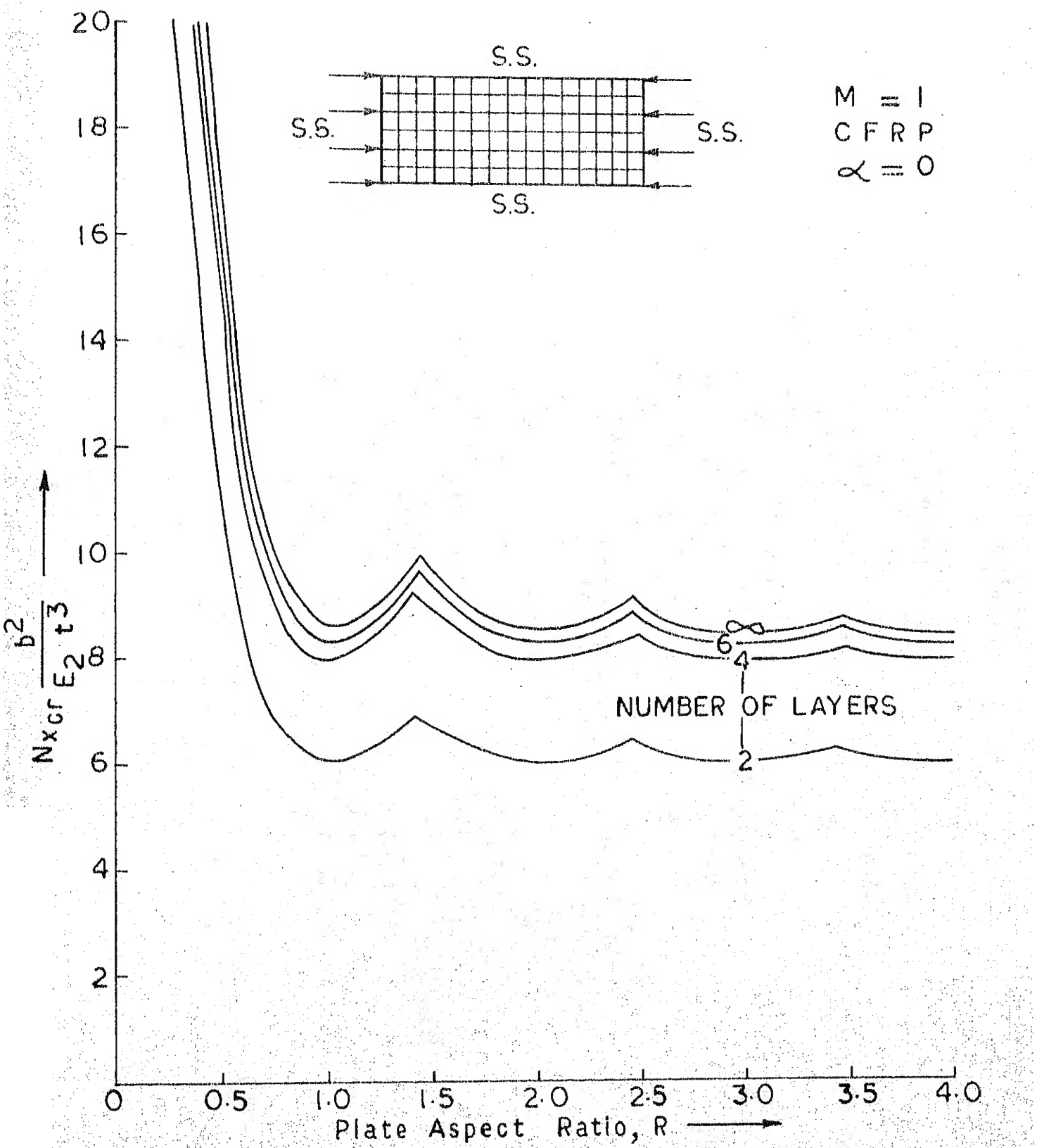

FIG. 7.8: VARIATION OF BUCKLING LOAD WITH ASPECT RATIO.

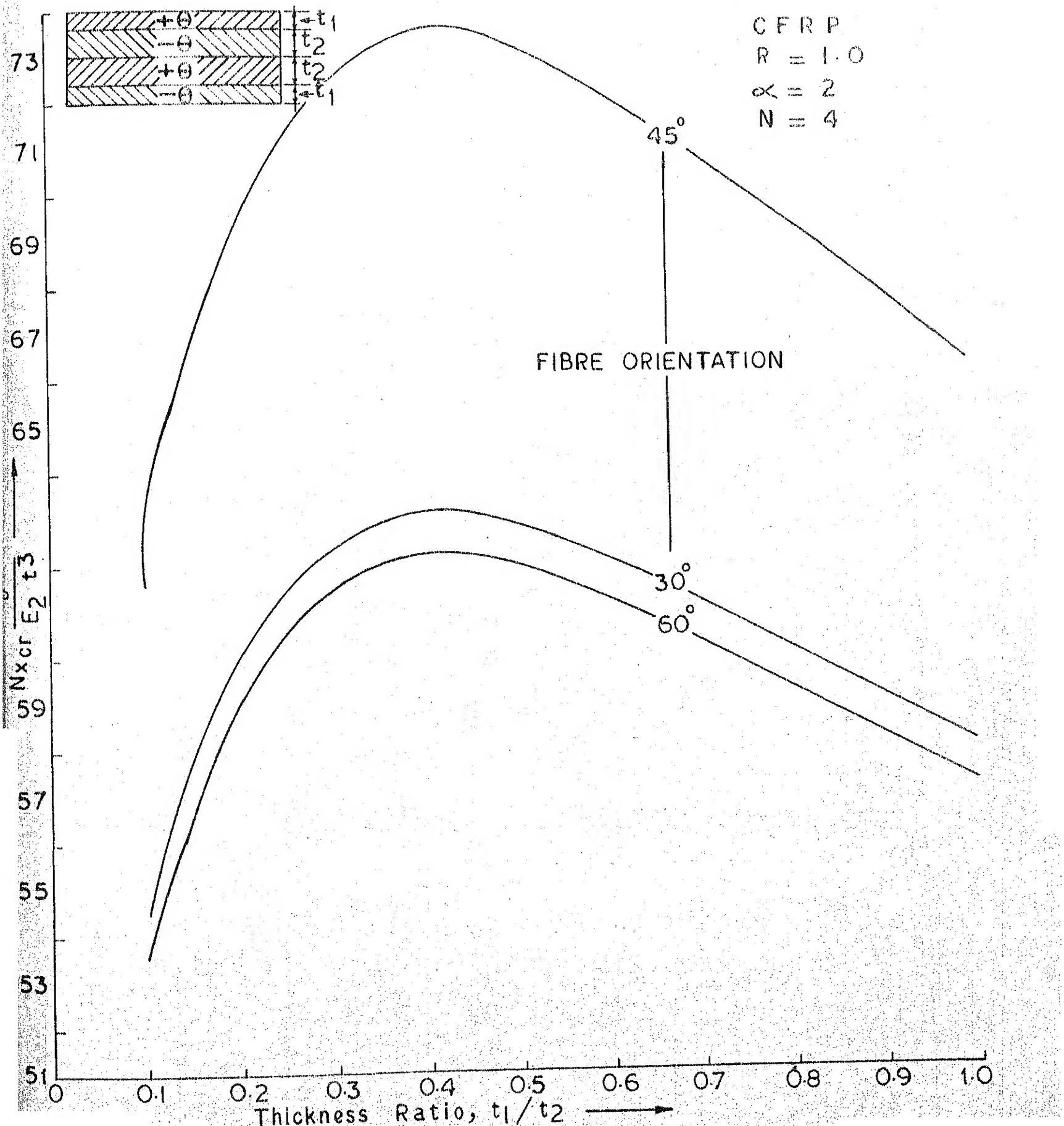

FIG. 7·9: VARIATION OF BUCKLING LOAD WITH THICKNESS RATIO FOR A FOUR LAYERED SQUARE PLATE.

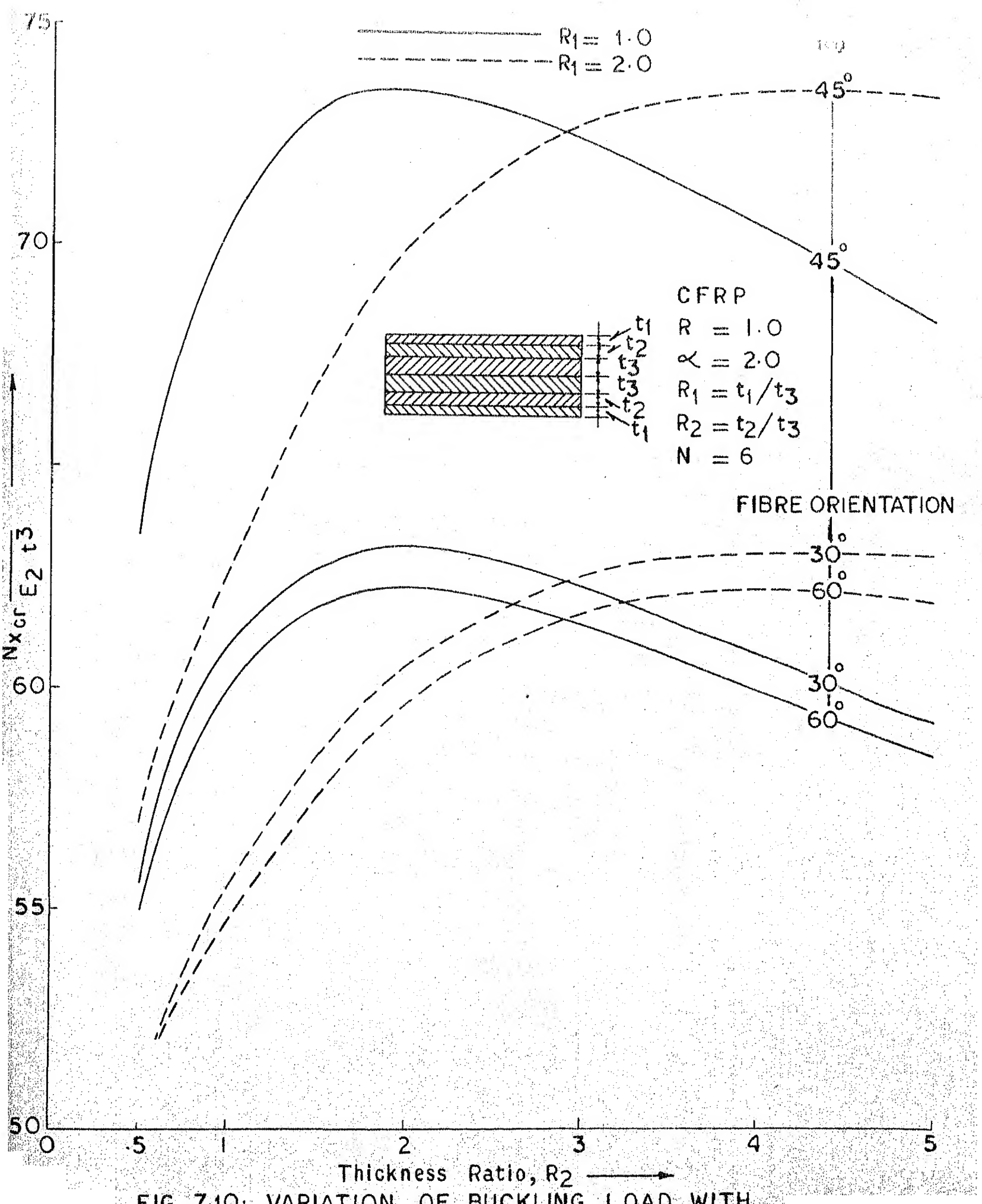

FIG. 7.10: VARIATION OF BUCKLING LOAD WITH THICKNESS RATIO FOR A SIX LAYERED P L A T E.

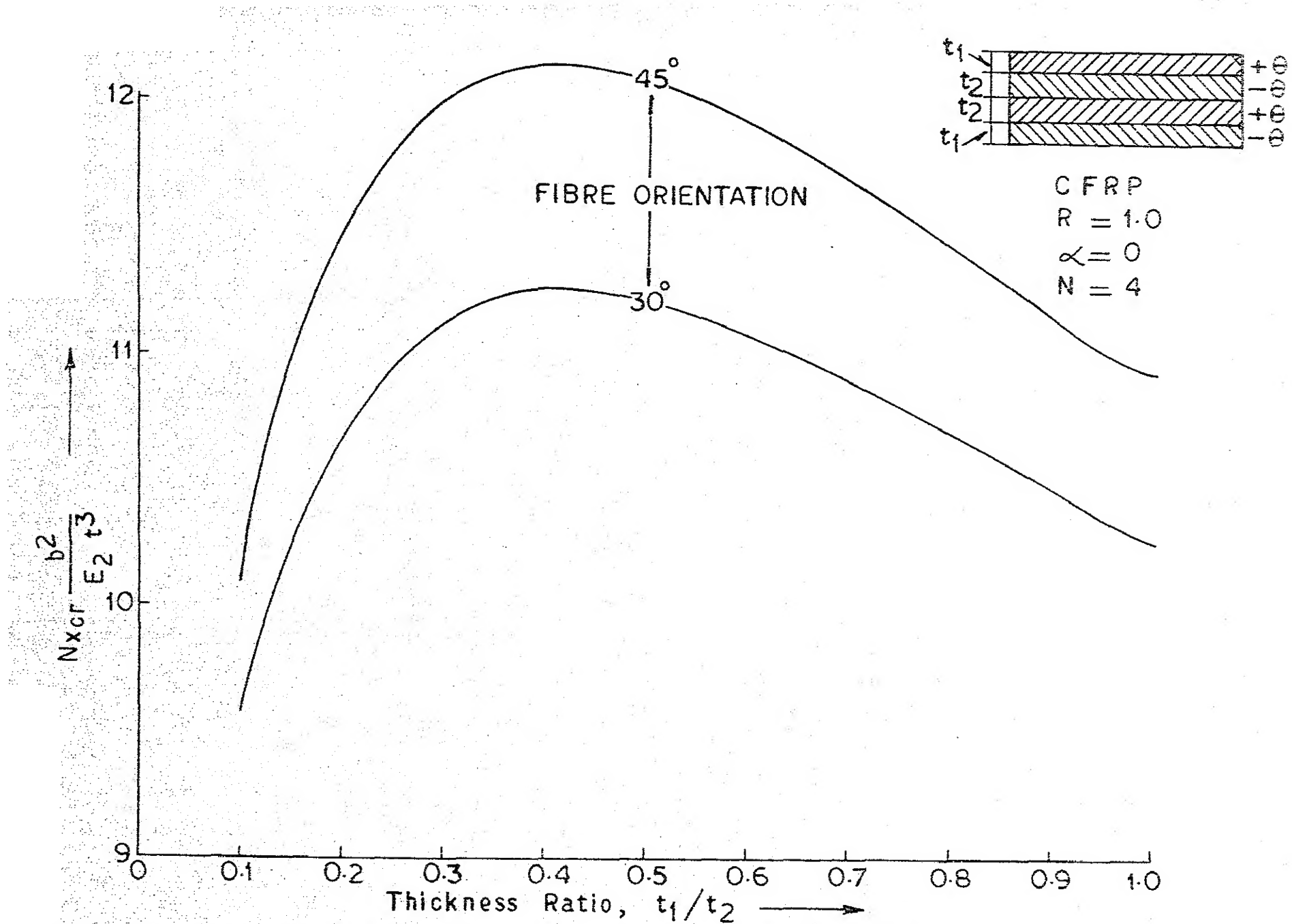

FIG. 7·11: VARIATION OF BUCKLING LOAD WITH THICKNESS RATIO FOR A FOUR LAYERED PLATE.

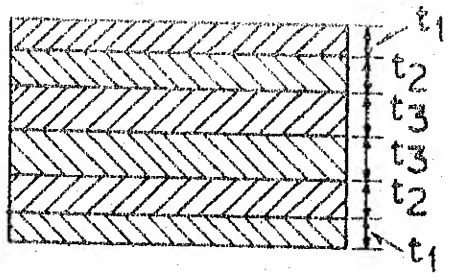

CFRP
R = 1·0
α = 0

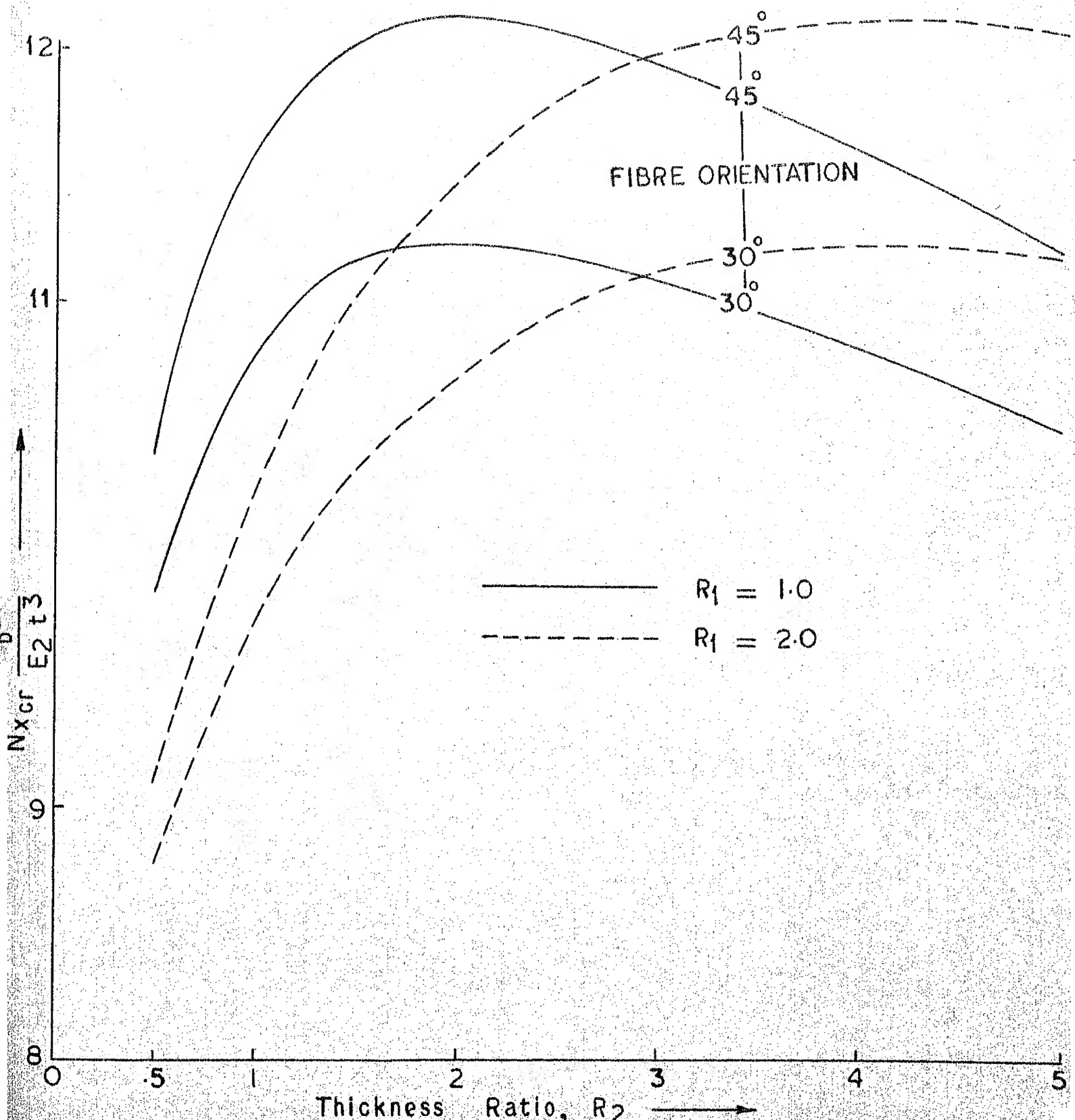

FIG. 7·12: VARIATION OF BUCKLING LOAD WITH THICKNESS RATIO FOR A SIX LAYERED PLATE.

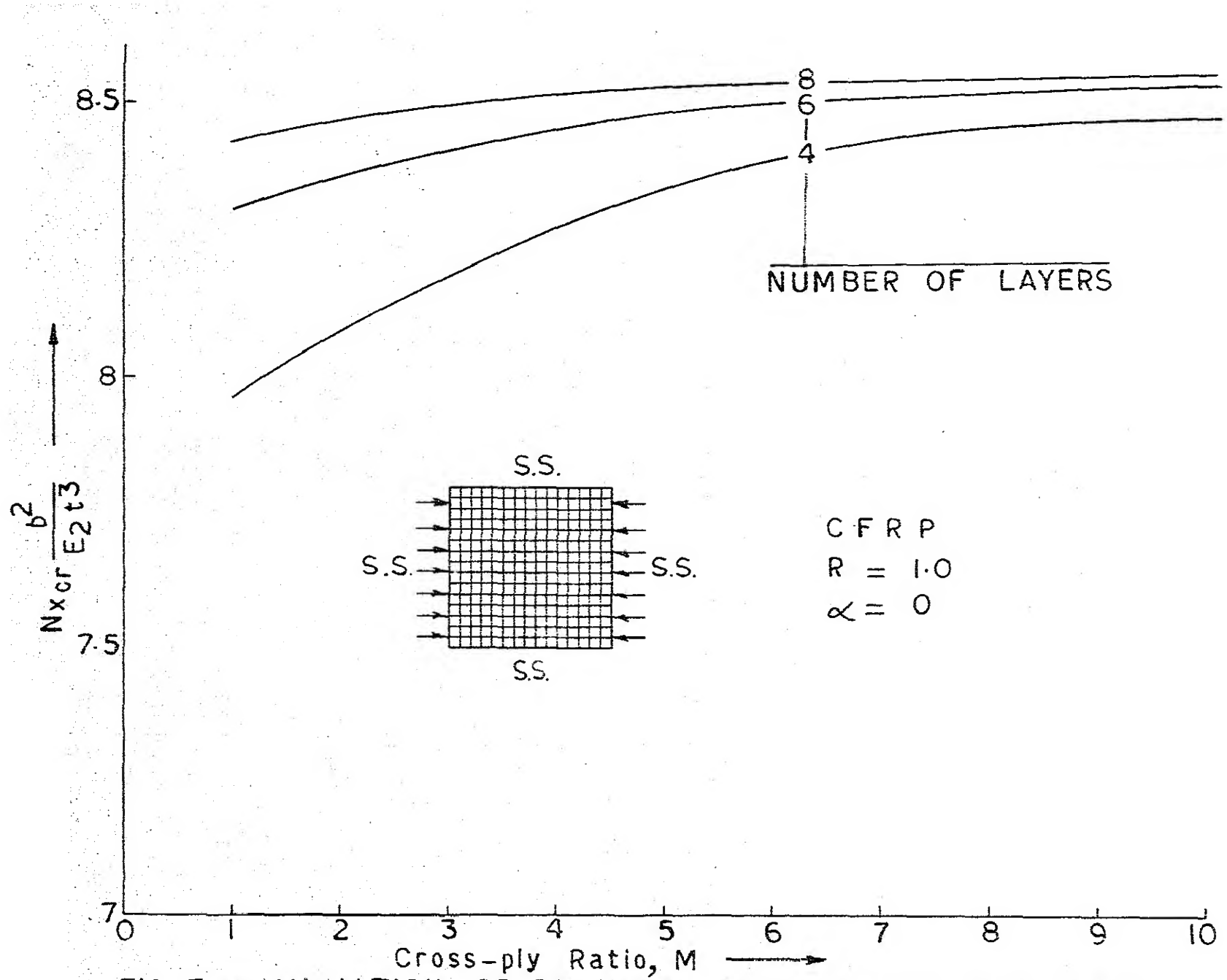

FIG. 7·13: VARIATION OF BUCKLING WITH CROSS-PLY RATIO.

CHAPTER 8

RESULTS AND CONCLUSIONS

8.1 GENERAL CONCLUSIONS

Two aspects of composite plates namely (i) characterisation of composites and (ii) buckling of composite plates with various boundary conditions subjected to uniform uniaxial and varying in-plane loads with or without lateral loads have been considered in this thesis.

An attempt has been made to eliminate the effect of coupling between in-plane extension and out-of-plane bending of composite plates by a choice of suitable thickness ratios of the laminae of a given laminate and thereby reduce the degradation in the overall stiffness of the laminate. It is shown that for a four-layered antisymmetric angle-ply laminate there exists a thickness ratio (t_1/t_2) of 0.4142 at which the coupling between in-plane extension and out-of-plane bending is completely eliminated. This unique thickness ratio is further shown to be independent of fibre orientations and material properties. For other types of laminates, it is shown that the degrading coupling effect can in general be alleviated or partly reduced. However, for a particular case of stacking sequence of $(\pi/4 \pm \theta)$, it is shown that there exists a thickness ratio for a six-layered laminate at

which the coupling is entirely eliminated. On the other hand, for six-layered antisymmetric angle-ply laminates, it is shown that there exist infinite combinations of R_1 ($= t_1/t_3$) and R_2 ($= t_2/t_3$) which lead to special orthotropic conditions (complete elimination of coupling stiffnesses).

The static and buckling analyses of composite plates are based upon the solution of governing eighth order partial differential equation which is obtained from the three governing equations of composite plates. Both antisymmetric, cross- and angle-ply plates are considered. In order to confirm the validity of the proposed analysis, a specimen problem on the static response of antisymmetric angle-ply plate subjected to transverse line loads is solved and the results are compared with those existing in literature. Moments and reactions are found to increase with increase in fibre orientation upto $\theta = 45°$ whereafter the trend is reversed. This is attributed to the coupling between bending and extension which increases continuously from $\theta = 0°$ to $\theta = 45°$ and decreases progressively from $\theta = 45°$ to $\theta = 90°$.

The variations of buckling loads of antisymmetric angle-ply plates with fibre orientations for various boundary conditions reveal an interesting features. The buckling loads decrease continuously from $\theta = 0°$ to $\theta = 90°$ for plates with two loaded edges simply supported and the unloaded edges (a) either both free or one edge clamped and the

remaining edge free. However, for plates with two loaded edges simply supported and the unloaded edges (b) both clamped, the buckling loads increase continuously from $\theta = 0°$ to $\theta = 40°$ approximately whereafter the trend is reversed for four- and six-layered and orthotropic laminates. The variation for a two-layered laminate shows additional minima approximately at $\theta = 20°$ and $70°$. The difference in the response of buckling load between boundary conditions (a) and (b) can be attributed to the difference in the conditions on in-plane displacements. u^o and v^o, in addition to Poisson's effect which assumes predominance in the latter case. Another important observation for the type (b) boundary condition is that the buckling load at $\theta = 90°$ is higher or lower than at $\theta = 0°$. This can be due to the occurrence of higher mode shape (i.e., $m = 2$ as compared to $m = 1$ at $\theta = 0°$) and/or the effect of E_1/E_2 ratio. It may be noted that the buckling mode in the x-direction changes from $m = 1$ to $m = 2$ at $\theta \geqslant 40°$. This feature of the type (b) boundary conditions is distinctly different from type (a) boundary conditions wherein the buckling mode always retains the single wave shape, for the aspect ratios considered.

The designer may also be interested in the optimal thickness ratio of the laminae leading to maximum buckling loads. To this effect, the variations of buckling loads with thickness ratio for four- and six-layered laminates under

various boundary conditions are studied. In all cases the buckling loads are found to be maximum at the optimal thickness ratios derived in Chapter 2 for various configurations of the laminates. However, it is of interest to note that the buckling loads are much more sensitive to thickness ratios for plates with clamped edges than for those with free edges. The use of optimal thickness ratios may, therefore, be more meaningful for plates with maximum restraints at the edges. The variations of buckling loads with cross-ply ratio, M for antisymmetric cross-ply plates with free edges, one edge free and one clamped and those with all edges simply supported are also considered. It is found that the increase in buckling load with increase in cross-ply ratio is maximum for plates with free sides than for plates with all edges simply supported. The maximum increase in buckling load is, however, limited to the cross-ply ratio range of M = 1 to 5. For a designer, this may indicate the optimal cross-ply ratios beyond which the increase in the ratio becomes unnecessary to achieve a given buckling load.

An important aspect of the variations of buckling loads with plate aspect ratio for various boundary conditions is also considered. It is found that for plates with two loaded edges simply supported and the remaining edges free, the buckling load per unit width of the plate is fairly constant with aspect ratio and the buckling mode shape in the

x-direction always occurs at m = 1 for all aspect ratios. This is distinctly different from the other types of boundary conditions considered in this thesis. The cusps in these variations occur because of the change in mode shape and their location with respect to aspect ratio is found to be dependent upon (i) the number of layers (ii) the fibre orientations and (iii) the boundary conditions. For a symmetric 45° oriented plate, however, the location of cusps is found to be independent of number of layers.

The buckling of composite plates under the action of both the in-plane and lateral loads and with two loaded edges simply supported and various other boundary conditions on the remaining edges is also investigated. The lateral loads are represented by the well-known Winkler-Pasternak medium. It is observed that both the material coupling and Winkler-Pasternak foundation stiffnesses effect the buckling response of the antisymmetric cross- and angle-ply plates significantly. However, the change in the Pasternak foundation stiffness exerts a far greater change in the buckling load than does a similar change in the Winkler foundation stiffness. Furthermore, these effects are more significant for plates with two loaded edges simply supported and the remaining edges free than for plates with other boundary conditions.

The problem of the buckling of antisymmetric cross- and angle-ply plates under the action of pure bending and

with all edges simply supported is solved employing the Galerkin technique. The variations of buckling load with aspect ratio, number of layers, fibre orientation and thickness ratio of the laminae of a laminate ore studied. The general observations on the buckling response made with this type of loading are common with those of uniform uniaxial loads. However, the symmetry of buckling loads at $\theta = 30^{\circ}$ and 60° obtained for uniform uniaxial load with all edges simply supported is absent for the corresponding case of pure bending.

8.2 SCOPE FOR FURTHER WORK

The optimal thickness ratios leading to special orthotropy of antisymmetric angle-ply laminates have been derived in this thesis. However, for general unsymmetric angle-ply laminates, partial reduction of coupling is shown to be possible with certain thickness ratios assuming an arbitrary ply stacking sequence. It may, therefore, be possible to work out the suitable combinations of ply stacking sequence and thickness ratios that may lead to complete elimination of coupling stiffnesses even for more general types of laminates. Such combinations will give additional choice of optimal thickness ratio and ply stacking sequence to the designer who may be interested in the optimization.

It is seen that for antisymmetric cross- and angle-ply laminates considered in this thesis, it is possible to obtain the closed form solution to the various problems of buckling in view of coefficients A_2, A_4, A_6 and A_8 of the governing eighth order partial differential equation (3.14) becoming zero. However, for more general types of laminates, this analytical simplification is not possible and full stiffness matrices (A_{ij}, B_{ij} and D_{ij}) accompanying such laminates can make the analysis more complicated. Finite difference or finite element techniques can be conveniently used to yield an approximate numerical solution to such problems.

Equation (3.22) can be used to study the buckling of laminates under combined normal and shear loads which is of direct practical interest to the designer. Interaction curves can be prepared from these results. Equation (3.22) can also be applied with suitable modifications to study the vibration of laminated plates with benefit.

The study of the influence of conditions on u^o and v^o on the buckling load variation with orientation in the case of free edges can also be of interest to reveal the relative importance of the various end conditions in determining the buckling loads.

- o -

REFERENCES

1. Whitney, J.M. and Leissa, A.W., "Analysis of Heterogeneous Anisotropic Plates", Journal of Applied Mechanics, Vol. 36, 2, 1969, 261-266.

2. Bartholomew, P., "Ply Stacking Sequence for Laminated Plates Having Inplane and Bending Orthotropy", Royal Aircraft Establishment, TR-76003, 1976.

3. Gerard, G. and Becker, H., "Hand Book of Structural Stability, Part I - Buckling of Plates", NACA, TN-3781, 1957.

4. Timoshenko, S.P. and Gere, J.M., Theory of Elastic Stability, 2nd ed., McGraw-Hill Co., 1961.

5. Hearmon, R., An Introduction to Applied Anisotropic Elasticity, Oxford University Press, 1961.

6. Lekhnitskii, S.G., "Contributions to Metallurgy of Steel", American Iron and Steel Institute, No. 50, 1956.

7. MIL-HDBK-17, Plastics for Flight Vehicles, Part I - Reinforced Plastics, 1959.

8. Thielemann, W., "Contributions to the Problem of Buckling of Orthotropic Plates, with Special Reference to Plywood", NACA, TM-1263, 1950.

9. Ashton, J.E., "Anisotropic Plate Analysis -- Boundary Conditions", Journal of Composite Materials, Vol. 4, 2, 1970, 162-171.

10. Mandell, J.F., "An Experimental Investigation of the Buckling of Anisotropic Plates", Ph.D. Thesis, presented to Case Western Reserve University, Ohio, 1968.

11. Monforton, G., "Discrete Element Finite Displacement Analysis of Anisotropic Sandwich Shells", Ph.D. Thesis, Case Western Reserve University, Ohio, 1969.

12. Sarkisian, V.A. and Movsisian, L.A., "Methods for Determining Critical Loads of Anisotropic Plates", in Russian, Inzhenernyi Zhurnal, Vol. 5, 4, 1965, p. 777.

13. Chamis, C.C., "Buckling of Anisotropic Composite Plates", J. Str. Div., Proc. ASCE, Vol. 95, ST 10, 1969, 2119-2139.

14. Chiu, K.D., "Stability of Orthotropic Stiffened Composite Plates", J. Engg. Mech. Div., Proc. ASCE, Vol. 98, EM 5, 1972, 1253-1271.

15. Massey, C., "The Elastic Buckling of Orthotropic Rectangular Plates", Institution of Engineers, Australia, Civil Engineering Transactions CE 13, 1, 1971, 63-65.

16. Harris, G.Z., "The Buckling of Orthotropic Rectangular Plates Including the Effect of Lateral Edge Restraint", International Journal of Solids and Structures, Vol. 1, 7/8, 1975, 877-885.

17. Ashton, J.E. and Waddoups, M.E., "Analysis of Anisotropic Plates", J. of Composite Materials, Vol. 3, 1, 1969, 148-165.

18. Ashton, J.E., "An Analogy for Certain Anisotropic Plates", J. of Composite Materials, Vol. 3, 2, 1969, 355-358.

19. Wang, J.T.S., "On the Solution of Plates of Composite Materials", J. of Composite Materials, Vol. 3, 3, 1969, 590-592.

20. Holston, A., Jr., "Buckling of Orthotropic Plates with One Free Edge", AIAA Journal, Vol. 8, 7, 1970, 1352-1354.

21. Kicher, T.P. and Mandell, J.F., "A Study of the Buckling of Laminated Composite Plates", AIAA Journal, Vol. 9, 4, 1971, 605-613.

22. Reissner, E. and Stavsky, Y., "Bending and Stretching of Certain Types of Heterogeneous Aeolotropic Elastic Plates", Journal of Applied Mechanics, Vol. 28, 3, 1961, 402-408.

23. Whitney, J.M. and Leissa, A.W., "Analysis of a Simply Supported Laminated Anisotropic Rectangular Plate", AIAA Journal, Vol. 8, 1, 1970, 28-33.

24. Whitney, J.M., "Bending Extensional Coupling in Laminated Plates under Transverse Loads", J. of Composite Materials, Vol. 3, 1, 1969, 20-28.

25. Turvey, G.J., "Biaxial Buckling of Moderately Thick Laminated Plates", J. of Strain Analysis, Vol. 12, 2, 1977, 89-96.

26. Jones, R.M., "Buckling and Vibration of Unsymmetrically Laminated Cross-Ply Rectangular Plates", AIAA Journal, Vol. 11, 12, 1973, 1626-1632.

27. Chamis, C.C., "Theoretical Buckling Loads of Boron/Aluminium and Graphite/Resin Fibre Composite Anisotropic Plates", NASA TND-6572, 1971.

28. Bert, C.W. and Francis, P.H., "Composite Materials Mechanics: Structural Mechanics", AIAA Journal, Vol. 12, 9, 1974, 1173-1186.

29. Kerr, A.D., "Elastic Plates on a Liquid Foundation", J. Engg. Mech. Div., Proc. ASCE, Vol. 89, EM 3, 1963, 59-71.

30. Kerr, A.D., "Elastic and Viscoelastic Foundation Models", Journal of Applied Mechanics, Vol. 31, 3, 1964, 491-498.

31. Hetenyi, M., Beams on Elastic Foundations, University of Michigan Press, Ann Arbor, 1946,

32. Malter, H., "Numerical Solutions for Beams on Elastic Foundation", Journal of the Structural Division, Proc. ASCE, 1958, Vol. 84, ST 2, 1958.

33. Lee, S.L. et al., "Continuous Beam-Columns on Elastic Foundations", J. Engg. Mech. Div., Proc. ASCE, EM 2, 1961, 55-70.

34. Essenburg, F., "Shear Deformation in Beams on Elastic Foundation", Journal of Applied Mechanics, Vol. 29, 2, 1962, 313-317.

35. Hetenyi, M., "Series Solutions for Beams on Elastic Foundations", Journal of Applied Mechanics, Vol. 38, 2, 1971, 507-514.

36. Murthy, G.K.N., "Buckling of Continuously Supported Beams", Journal of Applied Mechanics, Vol. 40, 2, 1973, 546-552.

37. Tsai, N. and Westmann, R.A., "Beams on Tensionless Foundation", J. Engg. Mech. Div., Proc. ASCE, Vol. 93, EM 5, 1967, 1-12.

38. Vlasov, V.Z. and Leont'ev, U.N., "Beams, Plates and Shells on Elastic Foundations", Israel Program for Scientific Translations, Jerusalem, 1966.

39. Rao, N.S.V.K., "Variational Approach to Beams and Plates on Elastic Foundations", Ph.D. Thesis, I.I.T. Kanpur, 1969.

40. Livesley, R.K., "Some Notes on the Mathematical Theory of a Loaded Elastic Plate Resting on an Elastic Foundation", Quarterly Journal of Mechanics and Applied Mathematics, Oxford, March, 1953.

41. Hess, M.S., "Eigen Function Solution for Beams on Elastic Foundation", Journal of Applied Mechanics, Vol. 36, 4, 1969, 799-802.

42. Reissner, E., "A Note on Deflection of Plates on a Visco-elastic Foundation", Journal of Applied Mechanics, Vol. 25, 1, 1958, 144.

43. Iyengar, N.G.R. and Valsangkar, A.J., "Note on the Bending of Clamped Plates on Elastic Foundation Under Combined Inplane and Lateral Load", J. Struct. Mech., Vol. 4, 1976, 227-234.

44. Turvey, G.J., "Uniformly Loaded, Simply Supported, Antisymmetrically Laminated, Cross- and Angle-ply Strips on a Winkler-Pasternak Foundation", Aero. J., Vol. 80, 1976, 222-226,

45. Turvey, G.J., "Uniformly Loaded, Simply-Supported, Antisymmetrically Laminated, Rectangular Plate on a Winkler-Pasternak Foundation", Int. J. Solids Structures, Vol. 13, 5, 1977, 437-444.

46. Ambartsumyan, S.A., "Theory of Anisotropic Shells", TTF-118, May 1964, NASA.

47. Reissner, E., Private communication, as quoted in the review article; Bert, C.W., and Francis, P.H., "Composite Materials Mechanics: Structural Mechanics", AIAA Journal, Vol. 12, 9, 1974, 1173-1186.

48. Timoshenko, S. and Woinowsky-Krieger, S., Theory of Plates and Shells, 2nd ed., McGraw-Hill, New York, 1959.

49. Werren, F. and Norris, C.B., "Mechanical Properties of a Laminate Designed to be Isotropic", Rept. 1841, May 1953, Forest Products Lab., Madison, Wis.

50. Abrams, J.I. and Scheyning, E.R., "Thin Laminates with Homogeneous Elastic Properties", J. Engg. Mech. Div., Proc. ASCE, Vol. 96, EM 6, 1970, 847-866.

51. Tsai, S.W., "Structural Behaviour of Composite Materials", NASA CR-71, July, 1964.

52. Hoff, N.J., "The Strength of Laminated and Sandwich Structural Elements", in Engineering Laminates, Edited by A.G.H. Dietz, Wiley, New York, 1949.

53. Smith, C.B., "Some New Types of Orthotropic Plates Laminated of Orthotropic Material", Journal of Applied Mechanics, Vol. 20, 2, 1953, 286-288.

54. Stavsky, Y., "Bending and Stretching of Laminated Aeolotropic Plates", J. Engg. Mech. Div., Proc. ASCE, Vol. 87, EM 6, 1961, 31-56.

55. Ashton, J.E. and Whitney, J.M., Theory of Laminated Plates, Technomic Publishing Co., Westport, Conn., 1970.

56. Almorth, B.O., "Influence of Edge Conditions on the Stability of Axially Compressed Cylindrical Shells", AIAA Journal, Vol. 4, 1, 1966, 134-140.

57. Jones, R.M., Mechanics of Composite Materials, McGraw-Hill Book Co., 1975.

58. Uspensky, J.V., Theory of Equations, McGraw-Hill, New York, 1948.

59. Ashton, J.E., "Approximate Solutions for Unsymmetrically Laminated Plates", J. of Composite Materials, Vol. 3, 1, 1969, 189-191.

60. Sun, C.T., "Double Fourier Series Solution to General Anisotropic Plates", Journal of Mathematical and Physical Sciences, Vol. 6, 2, 1972, 205-223.

61. Kan, Y.R. and Ito, Y.M., "Analysis of Unbalanced Angle-ply Rectangular Plates", Int. J. Solids Structures, Vol. 8, 11, 1972, 1283-1297.

62. Whitney, J.M., "Analysis of Anisotropic Rectangular Plates", AIAA Journal, Vol. 10, 10, 1972, 1344-1345.

63. Keays, R.H., "Analysis of an Orthotropic Plate with Two Opposite Edges Simply Supported and the Other Two Free", Department of Supply, Australian Defence Scientific Service, Aeronautical Research Laboratories, Structures and Materials Note 398, Sept. 1973.

64. Dong, S.B., Pister, I.D. and Taylor, R.L., "On the Theory of Laminated Anisotropic Shells and Plates", J. of Aerospace Sciences, Vol. 29, 8, 1962, 969-975.

65. Vinson, J.R. and Chou, T., Composite Materials and Their Uses in Structures, Applied Science Publishers Ltd., London, 1975.

66. Southwell, R.V. and Skan, S.W., "On the Stability Under Shearing Forces of a Flat Elastic Strip", Proc. of the Royal Society, Series A, Vol. 105, 1924, 582-607.

67. Batdorf, S.B. and Houbolt, J.C., "Critical Combinations of Shear and Transverse Direct Stress for an Infinitely Long Flat Plate with Edges Elastically Restrained Against Rotation", NACA, R. No. 84, 7, 1946.

68. Stein, M. and Neff, J., "Buckling Stresses of Simply Supported Rectangular Flat Plates in Shear", NACA, TN 1222, March 1947.

69. Batdorf, S.B. and Stein, M., "Critical Combinations of Shear and Direct Stress for Simply Supported Rectangular Flat Plates", NACA, TN 1223, March 1947.

70. Johnson, A.E., Jr., and Buchert, K.P., "Critical Combinations of Bending, Shear and Transverse Compressive Stresses for Buckling of Infinitely Long Flat Plates", NACA, TN 2536, Sept. 1951.

71. Johnson, J.H., Jr., "Critical Buckling Stresses of Simply Supported Flat Rectangular Plates Under Combined Longitudinal Compression, Transverse Compression and Shear", J. of Aero. Sciences, Vol. 21, 6, 1954, 411-416.

72. Johns, D.J., "Shear Buckling of Isotropic and Orthotropic Plates — A Review", R & M No. 3677, Aeronautical Research Council, Oct. 1970.

73. Whitney, J.M., "The Effect of Boundary Conditions on the Response of Laminated Composites", J. of Composite Materials, Vol. 4, 2, April 1970, 192-203.

74. Faddeev, D.K. and Faddeeva, V.M., Computational Methods of Linear Algebra, W.H. Freeman, San Francisco, California, 1963.

75. Froberg, C.E., An Introduction to Numerical Analysis, Addison-Wesley Company, Inc., 1965.

List of papers accepted for Publication based on the work reported in the thesis:

1. "Buckling of Antisymmetrically Laminated Cross- and Angle-ply Rectangular Plates on Winkler-Pasternak Foundation", Accepted for Publication in Journal of Engineering Mechanics, Proceedings of ASCE.

2. "The Buckling of Antisymmetrically Laminated Angle-ply and Cross-ply Plates", Accepted for Publication in the Journal of Fibre Science and Technology.

3. "Some Comments on the Coupling Effects of Angle-ply Laminates", Accepted for Publication in Journal of Structural Mechanics.

4. "Static Analysis of Anisotropic Composite Plates", Submitted for Publication to Journal of the Aeronautical Society of India.

- o -

AE-1979-D-SHA-BUC